Performance of Hot-Mix Asphalt Mixtures for a Balanced Mix Design

By

Mahmoud Rizk

A Thesis submitted to the Faculty of Graduate Studies of

The University of Manitoba

in partial fulfillment of the requirements of the degree of

DOCTOR OF PHILOSOPHY

Department of Civil Engineering

University of Manitoba

Winnipeg

Abstract

The essential goal of all highway agencies around the world is to construct safe and durable mixtures for road users as well as to prevent the occurrence of premature failures in asphalt pavements. Despite the development of the Superpave mix design method, several highways are still a victim of long-term pavement defects. This means that volumetric mix design procedure, which is currently relied on for acceptance or rejection of the final mix design, is not sufficient to secure acceptable long-term pavement performance. Consequently, the integration of suitable laboratory performance tests to current volumetric mix design methods as well as quality control and quality assurance activities became an essential step to validate asphalt mixtures and mitigate potential pavement defects. In essence, a balanced mix design (BMD) method, which integrates two or more performance tests into the Superpave mix design method, was developed to produce asphalt mixtures that are more resistant to specific types of pavement distresses such as cracking and rutting. The primary objective of this thesis was to develop a BMD framework for asphalt mixtures and implement preliminary performance-based specifications (PBS) for the mix design process. Additionally, it aims to investigate ways of optimizing mix performance for moving towards a BMD through the assessment of various mix design parameters as well as application of reclaimed asphalt pavement (RAP) fractionation technology. Finally, it aims to validate the proposed rutting criteria in the BMD framework via testing and analyzing rutting performance of local in-service asphalt mixtures.

This thesis is divided into three studies to fulfill its objectives. The first study involved testing and analyzing cracking and rutting performance of five laboratory-produced fractionated RAP mixtures. RAP fractionation, which divides RAP into at least two sizes to control its finer proportions, is one processing method that overcomes the restriction of high RAP contents in asphalt mixtures while minimizing issues related with mixture performance which might overall contribute to pavement sustainability. The mixtures consisted of a virgin mix and 10% RAP mix with unprocessed RAP as well as three mixtures with 30%, 40% and 50% coarse RAP (i.e., larger than 4.75 mm). The second study involved testing and analyzing cracking and rutting performance of six plant-produced asphalt mixtures containing different mix design properties. The mixtures consisted of virgin materials, RAP, recycled asphalt shingles (RAS), straight binders, polymer-modified binders, and gradations with two nominal maximum aggregate sizes (NMAS), 12.5 mm and 19 mm. The third study involved testing and analyzing rutting performance of four in-service asphalt mixtures that contained several rutted wheel paths in the field. Rutting performance was evaluated using Hamburg wheel-tracking test (HWTT) and cracking performance was evaluated using Illinois flexibility index test (I-FIT) for the three studies.

The outcome of this thesis deduced that fractionated RAP mixtures showed improvements in at least one performance measure in comparison to virgin and unprocessed RAP mixtures. All RAP mixtures had better rutting performance than the virgin mix while 30% and 40% coarse RAP mixes had better cracking performance than the 10% unprocessed RAP mix. Performance test results of plant-produced mixtures concluded that mixtures with limestone aggregates and/or RAS had unacceptable cracking performance. On the other hand, 12.5 mm NMAS mixtures with 0% and 10% RAP content had acceptable cracking and rutting performance. Therefore, reduction of NMAS and unprocessed RAP content as well as application of RAP fractionation technology for high RAP contents were proved to be strategies that support the BMD. In-service mixtures had acceptable rutting performance in the HWTT test which proved that poor rutting performance in the field can be related to factors other than improper mix design. They also passed the suggested

preliminary HWTT test criteria (i.e., maximum 10 mm rut depth at 15,000 passes) which proved the validity of these criteria as threshold values for adequate rutting performance. Overall, this research recommended integrating suitable performance tests to accept final mix designs as well as to correlate laboratory and field performance for a better assessment of PBS. Furthermore, it recommended identifying the root cause of rutting in the field to decide the appropriate maintenance action that will lead to longer service life of the pavement.

Acknowledgements

First, I would like to express my deepest thanks to the thesis advisor, Prof. Ahmed Shalaby, for his absolute support, technical guidance, and encouragement during the entire period of the study. My sincere gratitude to the advisory committee members, Dr. Babak Mehran and Dr. Ahmed Ghazy, for their comments and taking the time to review this thesis. Special thanks to the technical staff, Daniel Szara and Scott Sparrow, for their assistance with conducting laboratory tests and experiments involved in this thesis.

I would also like to acknowledge Manitoba Transportation and Infrastructure as well as City of Winnipeg Public Works Department for their support with providing materials and mixtures required for testing in this thesis. My appreciation goes to Gordon McNabb for his assistance with sample preparation in the experimental phase of this thesis. Special thanks are also dedicated to my colleagues in the Pavement Research Group.

Finally, I am grateful to my parents, my sisters, and other family members for their love, support, and encouragement.

Table of Contents

List of Tables

List of Figures

List of Abbreviations

AASHTO	American Association of State Highway and Transportation Officials
ANOVA	Analysis of Variance
AV	Air Voids
BMD	Balanced Mix Design
BSG	Bulk Specific Gravity
C.O.V	Coefficient of Variation
COW	City of Winnipeg
DMT	Dynamic Modulus Test
DOE	Design of Experiment
DOT	Department of Transportation
$\lvert E^* \rvert$	Dynamic Modulus
FAA	Fine Aggregate Angularity
FHWA	Federal Highway Administration
HMA	Hot-Mix Asphalt
HSD	Honestly Significant Difference
HWTT	Hamburg Wheel-Tracking Test
I-FIT	Illinois Flexibility Index Test
JMF	Job Mix Formula
MTI	Manitoba Transportation and Infrastructure
NCHRP	National Cooperative Highway Research Program
NMAS	Nominal Maximum Aggregate Size
OAC	Optimum Asphalt Content
PBS	Performance-Based Specifications
PG	Performance Grade

PSD	Performance Space Diagram
QA	Quality Assurance
QC	Quality Control
R	Coefficient of Correlation
R^2	Coefficient of Determination
RAP	Reclaimed Asphalt Pavement
RAS	Recycled Asphalt Shingles
RRI	Rutting Resistance Index
S.D.	Standard Deviation
SIP	Stripping Inflection Point
TSR	Tensile Strength Ratio
VFA	Voids Filled with Asphalt
VMA	Voids in Mineral Aggregate

Chapter 1. Introduction

1.1 Background

Currently, asphalt pavements are preferred over other pavement types because they facilitate construction as well as maintenance and rehabilitation of highways. Therefore, it is critical for transportation agencies to ensure that asphalt pavements are designed to provide adequate performance during their service life to improve safety for road users. In addition, it is vital to consider the economic use of pavement materials and mitigate the negative aspects on the environment during construction. Moreover, asphalt pavement design must account for the future increase in traffic loading as well as the impacts of climate change. Overall, asphalt pavements should be designed, produced, laid, and compacted to provide desirable properties such as stability, durability, and skid resistance (Salehi-Ashani, 2021).

Asphalt pavements are prone to several types of distresses during their service life. Cracking and rutting are two of the most common distresses that can impact asphalt pavements. Cracking can occur in various types on the pavement surface such as alligator (fatigue) cracking, thermal cracking, edge cracking and reflective cracking (West et al., 2018). In addition to affecting the structural integrity and durability of an asphalt pavement, cracks allow for the infiltration of air and water into the pavement structure causing accelerated aging and stripping which can lead to other serious distresses such as raveling and potholes. Rutting is permanent deformation that happens on the pavement surface under the wheel path. It is due to densification of the asphalt mixture mainly at high temperatures when it continues to compact under traffic loading (Brown et al., 2009). Rutting is a serious safety concern especially in wet conditions as it causes loss of skid resistance between the tires and pavement surface which minimizes safety of road users.

Consequently, transportation agencies started increasing their budgets on maintenance and rehabilitation programs to overcome challenges associated with cracking and rutting. Also, they are currently investigating ways to address cracking and rutting issues of the pavement from the mix design stage (Grobler et al., 2018).

One of the primary developments by the Strategic Highway Research Program in 1993 was the Superpave mix design method. It was initially designed to include three components in the mix design system. Firstly, asphalt binder specification system which classifies asphalt binder according to its performance response to high and low temperatures as well as aging characteristics. Secondly, a system that accounts for traffic levels and climatic conditions in the selection of aggregates and asphalt binder. Thirdly, asphalt mixture specification system which incorporates performance testing and analysis into the mix design system for predicting long-term pavement performance. The first two components were successfully implemented in the Superpave mix design method; however, asphalt mixture performance testing had not yet been established in the system due to its cost and complexity. Therefore, the Superpave method is still incapable of measuring distresses such as cracking and rutting nor predicting long-term pavement performance (Brown et al., 2009). It is mainly dependent on characteristics of aggregate and asphalt binder as well as volumetric properties for acceptance of mix design which were proved to not correlate well with long-term performance of asphalt mixtures (Salehi-Ashani, 2021). Additionally, the introduction of polymer modified binders, fibers, recycling agents and anti-stripping additives into asphalt mixtures led to difficulties with the Superpave mix design method and uncertainty regarding future field performance (Newcomb and Zhou, 2018). As a result, performance testing became an essential step to validate asphalt mixtures produced using the Superpave mix design method to mitigate rutting and premature cracking issues. In essence, a balanced mix design (BMD) approach, which integrates at least two performance tests to the Superpave mix design method, had been investigated to produce asphalt mixtures that can better resist different modes of distresses such as fatigue cracking, thermal cracking, stripping, and permanent deflection.

The use of reclaimed asphalt pavement (RAP) is highly recommended in pavement construction as it conserves natural resources, reduces asphalt waste disposal, and mitigates construction costs. However, there are constraints to using high quantities of RAP (i.e., more than 25%) due to mix design challenges and performance issues. RAP possesses a high proportion of aged and stiff binder which makes RAP mixtures more resistant to permanent deformation, but more vulnerable to premature fatigue and thermal cracking. Moreover, RAP comes from variable sources; thus, inconsistencies of aggregate and binder type as well as gradation can lead to difficulties in achieving the desired volumetric properties. In addition, the excessive amount of fine material in RAP generated from crushing and milling operations increases dust binder ratios. A processing method called RAP fractionation screens the RAP stockpile into at least two sizes, usually coarse and fine RAP, to control their proportions within a mix. Coarse RAP (RAP aggregates larger than 4.75 mm) and fine RAP (RAP aggregates smaller than 4.75 mm) were proved to have different properties of RAP binder (Saliani et al., 2019). Therefore, RAP fractionation facilitates the volumetric mix design procedure via enhancing RAP consistency and mix gradation properties as well as adjusting dust binder ratios (West, 2015). This leads to a more efficient BMD which is a crucial approach to determine the validity of fractionated RAP mixtures.

1.2 Problem Statement

Currently, Superpave and Marshall mix design methods are the two most common asphalt mix design methods around the world. Most transportation agencies in Canada still consider the volumetric properties of as-built asphalt pavements as the main element of quality control (QC) and quality assurance (QA). Subsequently, it has been proved that relying solely on volumetric properties as quality acceptance criteria does not guarantee adequate long-term performance of as-built asphalt pavements (Newcomb and Zhou, 2018). In Manitoba, most asphalt mixtures are designed using the volumetric-based Superpave mix design method and roads still suffer from rutting and premature cracking issues. Therefore, transportation agencies across Canada are examining ways to implement cracking and rutting performance tests with their mix design methods as well as to develop performance-based specifications according to local conditions (Grobler et al., 2018).

The use of RAP is a growing practice in pavement design and construction as it aligns with sustainability goals of most jurisdictions. Nevertheless, its application in high contents remains a constraint due to volumetric mix design difficulties and unpredictable performance. Research has proved that RAP fractionation allowed for the consumption of higher RAP proportions via better control of air void contents and dust binder ratios (Hossain et al., 2012). However, the long-term performance of fractionated RAP mixtures had not yet been investigated in detail, neither compared to the performance of unfractionated RAP mixtures. Consequently, laboratory performance testing is required to evaluate fractionated RAP mixtures and determine whether they contribute to a successful BMD.

1.3 Research Objectives

It is evident that the volumetric mix design procedure does not secure adequate long-term pavement performance and the use of RAP is still limited due to uncertainties regarding future field performance. The major objective of this thesis is to explore various asphalt mix design parameters through performance testing of plant-produced mixtures to result in the creation of durable asphalt mixes that are cracking and rutting resistant. Also, it aims to explore the modern RAP processing technology called "RAP fractionation" through the balanced mix design procedure to result in the creation of more sustainable asphalt mixes that have comparable performance to virgin mixes. The overall objectives of this thesis are as follows:

- Evaluate the performance of fractionated RAP mixtures that meet current Superpave mix design requirements.
- Evaluate the performance of plant-produced asphalt mixtures to validate traditional mix design methods.
- Develop preliminary performance-based specifications for cracking and rutting performance tests according to local conditions in Manitoba.
- Develop a BMD framework and discover strategies to optimize cracking and rutting performance of asphalt mixtures.
- Determine the impact of standard long-term aging protocol on cracking performance of plant-produced asphalt mixtures.
- Evaluate rutting performance of in-service asphalt mixtures to validate the adopted criteria and improve rehabilitation guidelines.

1.4 Research Methodology

To fulfill the objectives, the experimental program of this thesis was divided into three phases. In the first phase, five hot-mix asphalt mixtures with RAP contents ranging from 0 to 50% were produced in the laboratory. High RAP mixtures were fractionated to remove fine RAP material from the mix design process. The mixtures were compacted to meet Superpave volumetric mix design requirements for the city of Winnipeg. The Illinois flexibility index test (I-FIT) and Hamburg wheel-tracking test (HWTT) were conducted on test specimens from each mix to assess cracking and rutting resistance, respectively. Dynamic modulus test (DMT) was used to characterize stiffness of mixtures.

In the second phase, six loose plant-produced asphalt mixtures were compacted in the laboratory to produce test specimens for laboratory performance testing. Mixtures comprised of different mix design properties such as aggregate type and gradation, binder type as well as RAP and recycled asphalt shingles (RAS) contents. A BMD approach was conducted to correlate mix design properties to cracking and rutting performance. Moreover, a comparison between I-FIT test results of short-term and long-term aged specimens was conducted to determine aging resistance of plant-produced mixtures. Finally, a database of HWTT and I-FIT performance tests results was developed to estimate preliminary threshold criteria for each performance measure.

During the third phase, visual field inspection investigated early-age deterioration on some city of Winnipeg (COW) roads. As part of forensic investigations, field cores were extracted from four regional roads to measure rutting resistance and stiffness modulus of in-service surface layers. Asphalt content and aggregate gradation of in-service mixtures were determined using ignition oven test and sieve analysis procedure, respectively, to examine whether they follow COW specifications (City of Winnipeg, 2020). Additionally, rutting test results were used to validate the adopted preliminary HWTT test criteria and DMT test results at high temperature were correlated with HWTT test output parameters to explore the reasonability of elastic modulus values of field specimens.

1.5 Significance of Research

This research investigates the performance of hot-mix asphalt mixtures that fulfill the desired volumetric mix design requirements and establishes initial acceptance criteria for various performance tests. This will enable transportation agencies to integrate suitable performance tests to QC and QA specifications as well as to construct more durable asphalt pavements that require fewer maintenance and rehabilitation programs; thus, reduce life cycle costs. This research also investigates the performance of fractionated RAP mixtures that did not undergo any other mix design modifications. This will allow for higher RAP consumption without sacrificing hot-mix asphalt performance and facilitate volumetric mix design procedure of high RAP mixtures. Finally, the findings of this research could provide a tool to inspect the performance of in-service asphalt mixtures for forensic investigations and design improvements.

1.6 Thesis Organization

This thesis is divided into seven chapters and three appendices as follows:

- Chapter 1 illustrates the background and problem statement, the objectives and importance of this study.
- Chapter 2 represents a comprehensive literature review of the balanced mix design and its approaches as well as its applications in recent research. In addition, it represents a review of the history of RAP, its advantages, and disadvantages as well as Superpave mix design considerations for high RAP contents. Furthermore, the chapter summarizes main asphalt pavement distresses and includes a review of applications of RAP and fractionated RAP in pavement research.
- Chapter 3 presents the research methodology which includes properties of materials, sample preparations and laboratory performance testing procedures.
- Chapter 4 presents the results and discussions of the performance of five fractionated hot-mix asphalt RAP mixtures produced in the laboratory. The chapter includes the outcome of HWTT, I-FIT and DMT tests as well as demonstrates a BMD approach.

- Chapter 5 presents the results and discussions of the performance of six plant-produced hot-mix asphalt mixtures. The chapter includes the outcome of HWTT, I-FIT and DMT tests as well as demonstrates a BMD approach. It also involves an approach to propose initial acceptance criteria of various performance tests.
- Chapter 6 presents the results and discussions of laboratory tests performed on four in-service asphalt mixtures. The chapter includes the outcome of sieve analysis procedure as well as bulk specific gravity, ignition oven, HWTT and DMT tests.
- Chapter 7 involves a summary and the research conclusions as well as recommendations for future work.
- Appendix A comprises the I-FIT test output parameters and dynamic modulus values of individual samples evaluated in Chapter 4.
- Appendix B comprises the I-FIT test output parameters and dynamic modulus values of individual samples evaluated in Chapter 5.
- Appendix C comprises the bulk specific gravity, ignition oven test and sieve analysis procedures as well as dynamic modulus values of individual samples evaluated in Chapter 6.

Chapter 2. Literature Review

This chapter provides a detailed summary of common asphalt pavement distresses that are evaluated in this thesis. It also provides current state of knowledge on the balanced mix design concept and its approaches. Lastly, it provides a comprehensive literature review of all the concepts pertaining to the application of reclaimed asphalt pavement in hot-mix asphalt.

2.1 Asphalt Pavement Distresses

Asphalt pavements consist of bound (wearing surface and binder course), and unbound (granular base and subbase) layers placed above the subgrade. They are also called flexible pavements as they tend to deflect under traffic loads. The main function of flexible pavements is to distribute stresses from vehicle tires safely onto a wider area on the underlying subgrade to prevent subgrade deformation under repeated loading (Baghaee Moghaddam, 2019). The top bound layers are usually the strongest layers in the pavement structure; however, they are susceptible to major types of distresses due to traffic loading, climatic changes, and moisture. The most common types of flexible pavement distresses are explained in the following sections.

2.1.1 Rutting

Rutting or permanent deformation are longitudinal surface depressions that occur under the wheel path due to irrecoverable strains that accumulated from repeated traffic loading as shown in Figure 2.1a. It usually occurs at high temperatures and is common in locations of slow-moving traffic such as intersections and bus stops. Rutting can pose several challenges associated with driving due to complicated vehicle handling and the risk of hydroplaning during wet conditions which threatens road safety (Kafi Farashah, 2023). Hence, it is significant to identify the rutting performance of asphalt mixtures via suitable performance tests to secure driving conditions.

There are two main causes of permanent deformation. The first cause is deflection in any of the underlying layers (base, subbase, or subgrade) which leads to deformation in the whole pavement structure. The second cause is insufficient stability or lack of shear strength in the asphalt mixture which appears as rutted wheel paths on the wearing surface. Mixture instability can result from inadequate aggregate interlock or lack of cohesion by asphalt binder (Salehi-Ashani, 2021). Aggregate interlock is governed by aggregate texture, gradation, shape, and angularity. Various studies agreed that aggregates with a high degree of angularity and rough texture produce more rut-resistant asphalt mixtures (Kalcheff and Tunnicliff, 1982; Kandhal and Mallick, 2001). On the other hand, cohesion is governed mainly by stiffness of asphalt binder. Mahboub and Little (1988) deduced that more viscous asphalt binders have greater stiffness and produce more rut-resistant asphalt mixtures. As a result, good aggregate interlock and cohesion are necessary for asphalt mixtures to resist shear stresses generated by vehicles during braking, turning, and maneuvering.

2.1.2 Fatigue Cracking

Fatigue cracking is mainly a result of repetitive stresses or strains induced into the asphalt layer by traffic loading or debonding between any two layers in the pavement structure (Zhou, 2017). It usually occurs at intermediate temperatures and takes the shape of an alligator skin as shown in Figure 2.1b. Fatigue cracking can be divided into two types based on its point of initiation (Salehi-Ashani, 2021). If cracks initiate at the bottom of asphalt layer (i.e., the point of maximum tensile strain) and propagate upwards, they are called bottom-up cracking. The second type is called top-down cracking and occurs when longitudinal cracks initiate at the top of asphalt layer outside the wheel path (i.e., the point where tensile strains occur away from the tire) and propagate downwards (see Figure 2.1c). In general, cracking at intermediate temperatures relies on the concept of crack initiation at a particular point followed by its propagation across the asphalt layer. Thus, laboratory tests to evaluate fatigue cracking resistance are conducted on notched specimens to simulate the same concept where a crack initiates at the tip of a notch and propagates across the sample.

2.1.3 Thermal Cracking

Thermal or low temperature cracking is a type of cracking associated with cold climatic regions such as Canada and Northern United States. It occurs due to contraction of asphalt layer at low temperatures which induces tensile stresses. If the tensile strength of asphalt layer fails to withstand the induced tensile stresses during contraction, thermal cracking occurs and appears as transverse cracks on the pavement surface as shown in Figure 2.1d (Zhou, 2017). In addition to cold climate, there are other factors that influence low temperature cracking including asphalt binder performance grade, aging, and type of subgrade (i.e., cohesive or non-cohesive). Hence, it is significant to assess thermal cracking of asphalt mixtures during the mix design process.

a) Rutting (permanent deformation)

b) Alligator crack (fatigue cracking)

c) Longitudinal crack (top-down cracking)

d) Transverse crack (thermal cracking)

Figure 2.1 Common asphalt pavement distresses

2.1.4 Moisture Damage

Moisture damage, also known as stripping, is a type of asphalt pavement failure that leads to costly maintenance and rehabilitation actions. It is mainly a result of three main mechanisms (Tavassoti and Baaj, 2020). The first mechanism is adhesion loss between aggregates and asphalt binder which happens when water gets absorbed by aggregates and starts replacing the asphalt film coating. The second mechanism is called hydraulic scouring which is the hydraulic pressure induced within water-filled air voids due to traffic movement. The third mechanism is the number of freezing-thawing cycles which happen due to temperature variations. When entrapped water freezes at low temperatures, it expands and breaks the bond within the asphalt pavement. Tensile strength ratio has been the most common method used to evaluate moisture damage in North America. Nevertheless, research had proved a weak correlation between this technique and field performance (Tavassoti and Baaj, 2020). Therefore, transportation agencies have been recently relying on more advanced testing methods such as Moisture Induced Stress Tester to evaluate moisture damage.

2.2 Balanced Mix Design

The oldest mix design method is called the Hveem method and was developed in the late 1920's (Coleri et al., 2020). In the beginning of 1940's, the Marshall method was developed to design airport asphalt mixtures. This method became dominant until the beginning of the 1990's when the Superpave mix design method was brought to light. Presently, intensive research is taking place to incorporate performance assessment of mixes to the Superpave volumetric mix design procedure. This approach became known as "balanced mix design (BMD)" which relies on current methods and procedures as well as predicts long-term pavement performance. A comprehensive literature review of BMD is represented in the following sections.

2.2.1 Definition and Approaches

BMD is an approach that integrates two or more performance tests such as rutting test and cracking test to assess the mixture's ability to resist different forms of distress for a given traffic level, climate, and pavement structure (Al-Qadi et al., 2015). The main objective of a BMD is to accomplish the proportions and quality of materials which will create asphalt mixes that are resistant to cracking, rutting and moisture damage (Newcomb and Zhou, 2018). In 2015, a BMD Expert Task Group created by Federal Highway Administration (FHWA) defined BMD as "asphalt mix design using performance tests on appropriately conditioned specimens that address multiple modes of distress taking into consideration mixture aging, traffic, climate and location within the pavement structure" (FHWA, 2016).

Cracking and rutting performance are two desirable properties of asphalt mixes that are inversely related. This means that the increase in value of one parameter will lead to the decrease in value of the other parameter and vice versa. This is represented by Figure 2.2 which shows that an increase in asphalt content leads to a decrease in cracking potential, but an increase in rutting potential. The first approach to BMD was implemented at the Texas A&M Transportation Institute in 2006 (Zhou et al., 2006). This approach relied on the concept of determining an acceptable range of asphalt content that meets both cracking and rutting criteria as shown in Figure 2.2. A minimum value of asphalt content was set corresponding to minimum criteria for cracking resistance, while a maximum value of asphalt content was set corresponding to minimum criteria for rutting resistance. Any value of asphalt content that lies within that range is deemed to fulfill the requirements of BMD. Other State Departments of Transportation also followed the same concept of BMD, yet cracking and rutting criteria ought to vary depending on climate and traffic level at the project location.

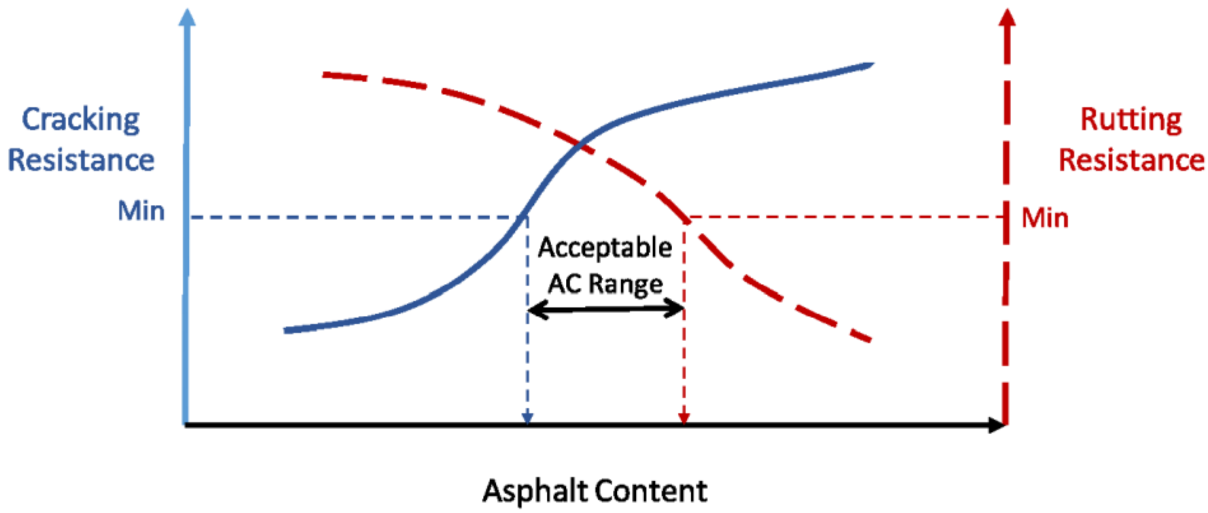

Figure 2.2 Concept of BMD (Newcomb and Zhou, 2018)

The BMD Expert Task Group defined three different approaches to conduct BMD based on how volumetric and performance analysis are associated with one other (FHWA, 2016). The three approaches are illustrated in a flowchart in Figure 2.3 and summarized as follows:

1) <u>Volumetric Design with Performance Verification:</u> This is the most common approach currently implemented by State Departments of Transportation. The mix is initially designed to meet the desired volumetric properties and determine the optimum asphalt content using Superpave mix design method. The mix is then subjected to the specified performance tests to verify its cracking and rutting resistance. The mix must meet the performance criteria for the job mix formula to be confirmed; or else, the complete mix design procedure must be repeated. The mix can undergo any modification (e.g., aggregate source or gradation, binder source or grade, material proportions, use of additives, etc.) until it meets both volumetric and performance criteria. Finally, the mix must pass a moisture susceptibility test to ensure durability and subsequently confirm the start of production.

2) <u>Performance-Modified Volumetric Mix Design:</u> In this method, the mix is designed to meet the desired volumetric properties using Superpave mix design method to determine a preliminary aggregate combination and asphalt content. The mix is then subjected to the specified cracking and rutting performance tests. If the mix fails the performance criteria, modifications are made until performance criteria are met, regardless of the volumetric criteria. In other words, volumetric requirements in this approach act as a starting point to the mix design, and the job mix formula is confirmed based only on satisfying performance criteria. Finally, the mix must pass a moisture susceptibility test to ensure durability and subsequently confirm the start of production.

3) <u>Performance Design:</u> This approach relies completely on satisfying performance criteria to confirm the job mix formula with minimum or no intervention for volumetric requirements. Nevertheless, volumetric requirements might act as a guideline in the mix design process, but not as design criteria that should be obeyed. Since there is no knowledge regarding the efficiency of this method, it has not yet been implemented by any State Department of Transportation. It was developed to promote innovations in mix designs and to mitigate mixture costs while satisfying failure criteria for cracking, rutting, and moisture damage. Hence, it could be a feasible alternative in the future for BMD.

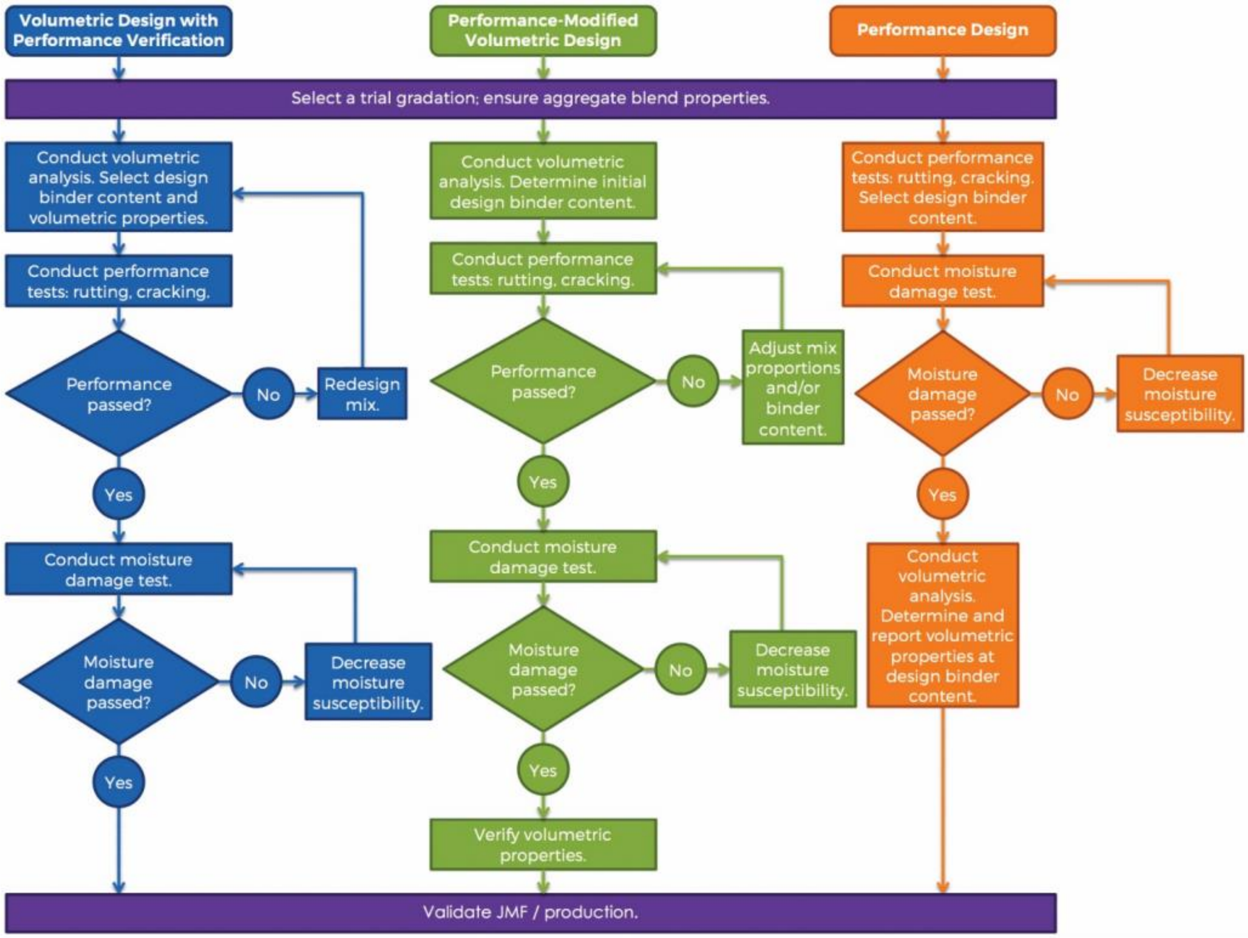

Figure 2.3 Illustration of BMD approaches (West et al., 2018)

2.2.2 Performance Tests

When performance assessment became a crucial stage in the validation of asphalt mixtures, researchers started developing several performance tests to evaluate mixture rutting and cracking resistance as well as moisture susceptibility. Cracking tests were further divided into various categories based on the mechanism of crack initiation and propagation (West et al., 2018). Table 2.1 represents the performance tests that are commonly used by highway agencies along with the type of distress that suits the function of each test. Table 2.1 also indicates whether performance criteria are available for each test as well as test practicality for mix design and quality assurance (QA). Practicality for mix design and QA is rated based on several factors including test complexity and variability, testing time, equipment cost and correlation to field performance (West et al., 2018). Few of these performance tests are quick and simple, hence they can easily become a part of the ordinary mix design procedure. Other tests are more complex and emphasize distinguishing the essential properties of asphalt mixtures. Performance criteria must initially be established for the test to become a part of the BMD procedure, while at the same time considering the factors affecting test practicality for mix design and QA (West et al., 2018).

Table 2.1 Common performance tests of asphalt mixtures (West et al., 2018)

Performance test	Type of distress	Test standard	Test output	Criteria available	Practicality for mix design and QA
Disc-Shaped Compact Tension (DCT) Test	Thermal and reflective cracking	ASTM D7313	Fracture energy	Yes	Good
Semi-Circular Bend (SCB) Test	Thermal cracking	AASHTO TP 105	Fracture energy	Yes	Fair
Texas Overlay (OT) Test	Reflective cracking	Tex-248-F	Cycles to failure	Yes	Good
Illinois Flexibility Index Test (I-FIT)	Bottom-up fatigue cracking	AASHTO T 124	Flexibility index	Yes	Good
Indirect Tensile Asphalt Cracking Test (IDEAL-CT)	Fatigue, thermal and reflective cracking	Not Available	Cracking test index	No	Good
Indirect Tensile (IDT) Creep Compliance and Strength Test	Thermal cracking	AASHTO T 322	Tensile strength	No	Fair
Flexural Bending Beam Fatigue (BBF) Test	Bottom-up fatigue cracking	AASHTO T 321	Cycles to failure	No	Poor
Indirect Tensile (IDT) Energy Ratio Test	Top-down fatigue cracking	Not Available	Energy ratio	Yes	Good
Hamburg Wheel Tracking Test (HWTT)	Rutting and moisture susceptibility	AASHTO T 324	Rut depth & stripping behavior	Yes	Good

Table 2.1 (Cont'd) Common performance tests of asphalt mixtures (West et al., 2018)

Performance test	Type of distress	Test standard	Test output	Criteria available	Practicality for mix design and QA
Asphalt Pavement Analyzer (APA)	Rutting	AASHTO T 340	Rut depth	Yes	Good
Flow Number (FN) Test	Rutting	AASHTO TP 79	FN	Yes	Fair
Superpave Shear Tester	Rutting	AASHTO T 320	Permanent shear strain	No	Poor
Moisture Induced Stress Tester (MIST)	Moisture susceptibility	ASTM D7870	Changes in bulk specific gravity	No	Good
Tensile Strength Ratio (TSR) Test	Moisture susceptibility	AASHTO T 283	TSR	Yes	Good

2.2.3 State of Practice

Table 2.2 lists the state of practice of BMD for some State Departments of Transportation that started to follow BMD approaches and explore performance tests to include in the BMD procedure. To date, no highway agency in Canada has adopted the BMD approach despite a few research (mainly in Ontario) that investigated the method and developed preliminary criteria for some performance tests.

Table 2.2 State of practice of BMD for some State Departments of Transportation (West et al., 2018)

State	Approach	Cracking test criteria	Rutting test criteria
Illinois	Volumetric Design with Performance Verification	I-FIT Acceptance criteria: Flexibility Index ≥ 8	HWTT @ 50°C Acceptance criteria: At 12.5 mm rut depth, no. of passes > 5,000; 7,500; 15,000 & 20,000 for PG 58-xx; PG 64-xx; PG 70-xx and PG 76-xx binders, respectively
Oklahoma	Research is ongoing	I-FIT	HWTT @ 50°C Acceptance criteria: At 12.5 mm rut depth, no. of passes > 10,000; 15,000 & 20,000 for PG 64-xx; PG 70-xx and PG 76-xx binders, respectively
Texas	Volumetric Design with Performance Verification	OT Test Acceptance criteria: No. of cycles ≥ 200 for Stone Matrix Asphalt	HWTT @ 50°C Acceptance criteria: At 12.5 mm rut depth, no. of passes > 10,000; 15,000 & 20,000 for PG 64-xx; PG 70-xx and PG 76-xx binders, respectively
Minnesota	Research is ongoing	DCT Test @ Low PG+10°C Acceptance criteria: Fracture energy (J/m^2) ≥ 690, 460 & 400 for 30M, 10-30M and 10M ESALs, respectively	Research is ongoing
Utah	Research is ongoing	I-FIT	HWTT @ 54°C, 50°C and 46°C for PG 70-xx, PG 64-xx and PG 58-xx binders, respectively Acceptance criteria: Maximum 10 mm rut depth at 20,000 cycles

2.2.4 Recent Research

Newcomb and Zhou (2018) conducted Performance-Modified Volumetric BMD to determine optimum asphalt content (OAC) of mixes based on three cracking tests and one rutting test.

Cracking tests included the I-FIT, DCT and IDEAL-CT tests, while HWTT test was the only rutting test considered. Materials obtained from four construction projects in Minnesota were designed for three OAC's at 0.5% increment. A maximum AC was assigned for each of the four mixes based on rutting criteria. Three asphalt contents were then determined based on each cracking test criteria. The AC that meets the three cracking tests criteria and abides by the maximum AC of rutting criteria was selected as OAC of the mix. Results showed that OAC's obtained from BMD method were lower than OAC's obtained from volumetric analysis, but this deduction is not necessary to take place in all cases. The study also recommended re-defining cracking and rutting criteria based on site-specific conditions such as climate and traffic level.

A study was conducted by West et al. (2018) to determine the effect of regressing air voids from 4% to 3% on the performance of six mixes containing RAP/RAS in Wisconsin. The I-FIT test and DCT test were used to evaluate resistance to fatigue cracking and thermal cracking, respectively. The HWTT test was used to evaluate both rutting resistance and moisture susceptibility. Results showed that 1% regression in air voids led to higher optimum asphalt contents by about 0.3% to 0.4%. Despite a decrease in rutting resistance due to higher asphalt contents, HWTT test results met the minimum requirements for all mixes. On the other hand, thermal and fatigue cracking resistance improved for all mixes at 3% air voids as shown in Figure 2.4. Assuming a flexibility index value of 8 as minimum criteria, 1% regression in air voids caused four mixes to pass the I-FIT test. Overall, the study concluded that regression of air voids led to a more efficient BMD of RAP/RAS mixes via enhancing thermal and fatigue cracking performance while maintaining rutting performance that fulfilled minimum requirements.

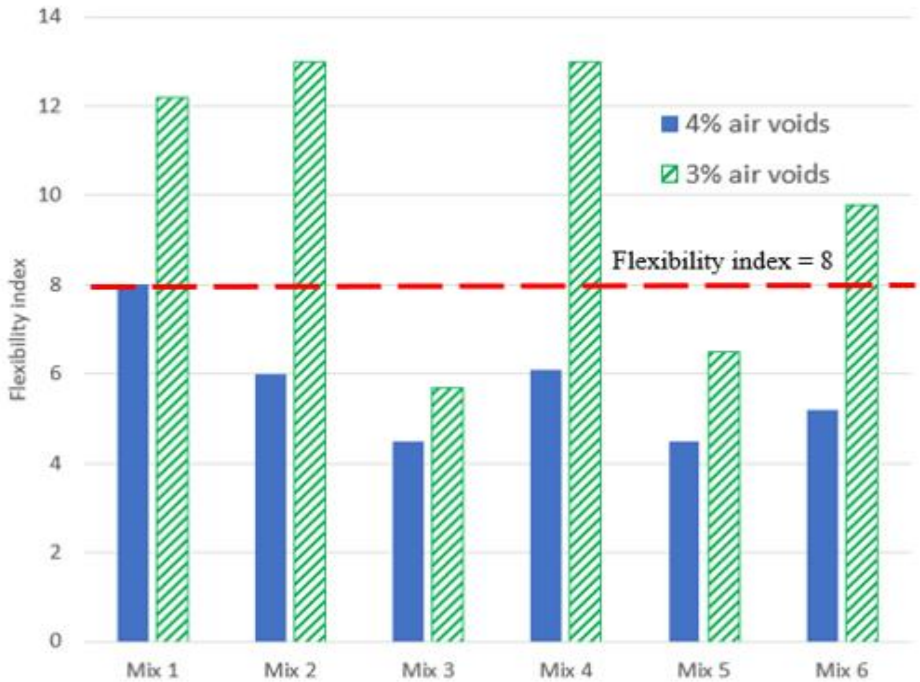

a) I-FIT test results

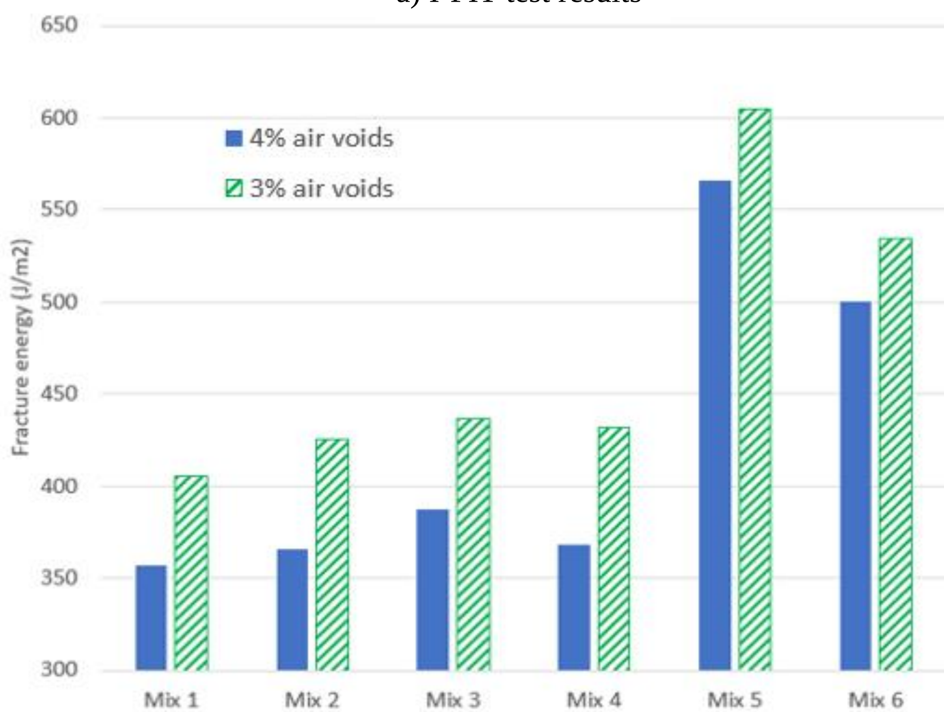

b) DCT test results

Figure 2.4 I-FIT and DCT tests results of RAP/RAS mixes after 1% regression in air voids (West et al., 2018)

Another study by Noorvand et al. (2021) evaluated the impact of aramid fibers with three different lengths (10, 19 and 38 mm) on the BMD of asphalt mixtures. Two cracking tests and one rutting test were conducted on fiber-reinforced asphalt mixes at four binder contents (5.4, 5.8, 6.2 and 6.6%). The uniaxial fatigue test and IDEAL-CT test were used to evaluate cracking performance, while the FN test was used to evaluate rutting performance. Results showed that addition of aramid fibers, in general, enhanced both cracking and rutting performance of asphalt mixtures especially at higher binder contents. Mixtures with 19 mm fibers demonstrated the best performance among all tested mixes. Furthermore, inclusion of aramid fibers widened the acceptable range of asphalt content which meets cracking and rutting requirements in the BMD as shown in Figure 2.5. This provides greater flexibility to mix designers to alter asphalt contents to monitor cracking and rutting performance.

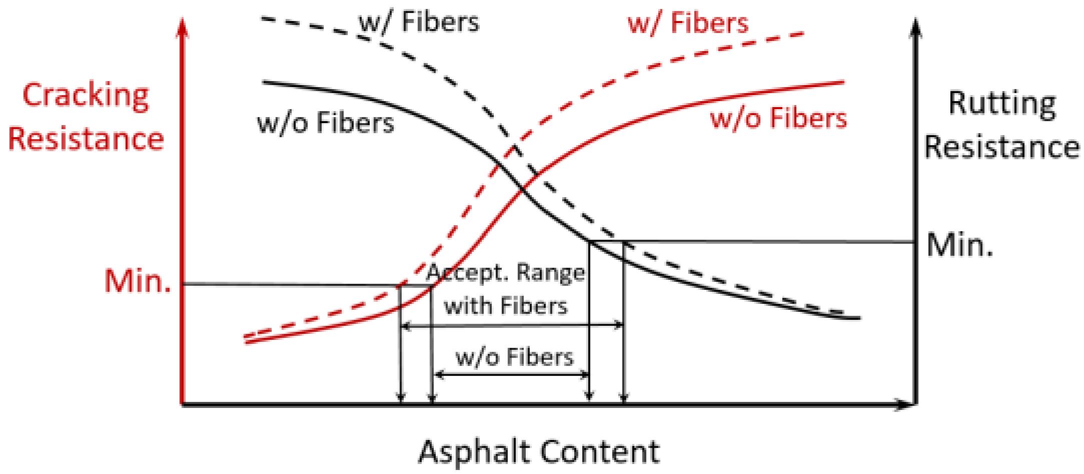

Figure 2.5 Effect of aramid fibers on BMD (Noorvand et al., 2021)

Salehi-Ashani (2021) performed a BMD study to characterize asphalt mixtures in Ontario as well as develop performance-related specifications for cracking and rutting performance. The study also aimed to determine the most feasible cracking and rutting tests for integration in BMD approach. HWTT test was the only test selected to evaluate rutting performance, whereas several cracking tests were included; namely, DCT, I-FIT, IDEAL-CT and SCB tests. Results showed that fracture energy values of SCB test had no statistically significant difference with fracture energy values of DCT test at three low testing temperatures (-18°C, -24°C and -30°C). In addition, DCT and I-FIT test results were not sensitive to different long-term mix aging methods, but mixtures with stiff binders produced I-FIT test results that are more sensitive to testing temperatures. Finally, stone mastic asphalt mixtures were the only mixtures that required a higher threshold cracking value, while rutting criteria was, in general, highly dependent on asphalt binder grade.

2.3 Reclaimed Asphalt Pavement

Reclaimed asphalt pavement (RAP) is a combination of aggregate materials and asphalt binder removed from a demolished pavement. It consists of the original constituents of the mix design for the old pavement. Similar to current mix design procedures, the material composition of the old pavement had to meet the requirements of the specified mix design procedure (such as aggregate gradation and source, quality of binder, mix volumetrics, etc.) prior to construction. Therefore, RAP materials are expected to possess homogenous properties with virgin materials that are being used in current mix design procedures. In other words, if RAP materials are properly crushed, screened, stockpiled, and characterized, they can be combined with regular virgin materials to create pavement designs that will still meet the requirements of current mix design standards (Shannon, 2012). A comprehensive literature review of RAP is represented in the following sections.

2.3.1 History and Sources

The concept of recycling asphalt pavements started over more than a century ago in 1915, but it remained a rare practice until the beginning of the 1970's because the cost of demolishing existing asphalt was higher than that of using virgin material (Kandhal and Mallick, 1997). When asphalt binder prices surged during mid 1970's, asphalt industries started developing advanced recycling technologies (many of which are still used regularly today) to reduce the cost burden of demolishing existing asphalt and to favor the notion of recycling asphalt pavements. In addition, several studies have been initiated to analyze the performance of RAP pavements and these studies deduced that RAP pavements can provide a comparable performance to virgin pavements (Al-Qadi et al., 2012).

RAP has a variety of sources, but the main source of RAP is through milling of distressed and aged pavement layers by a milling machine (West, 2015). Milling machines strike the pavement using a system of blades mounted on a rotating drum that continuously crushes the material leading some aggregate particles to break. As a result, the RAP would have a finer gradation than the original constructed pavement layer.

2.3.2 Advantages and Disadvantages

The main advantages of utilizing RAP in asphalt mixes are the economic and environmental benefits. The use of RAP reduces the cost of transporting virgin materials since fewer amounts of virgin binder and virgin aggregate are expected to be used in asphalt mixes. It was reported that using 20% - 50% RAP can save about 34% of total cost (Kandhal and Mallick, 1997). Also, the use of RAP decreases the amounts of asphalt waste disposal which leads to a reduction in the overall eco-burden. Finally, it was proved that RAP usage has some positive impacts on pavement field performance. RAP increases the relative stiffness of the asphalt mix because it increases the performance grade of blended binder. Therefore, RAP mixes are more rut-resistant (i.e., resist permanent deformation) which makes them favorable options for pavement locations that are expected to withstand higher stresses such as intersections, bus stops and parking lots (Hill, 2011).

On the other hand, the disadvantages of utilizing RAP in asphalt mixes are mainly associated with variability of RAP. RAP obtained from different construction projects experiences high variability in aggregate gradation as well as binder stiffness and content. Thus, obtaining RAP from a single source might help to minimize variability. Increased variability of RAP leads to inconsistent asphalt mixes and less reliable field performance. Solaimanian and Tahmoressi (1996) noticed that RAP stockpiles with a high variation in binder stiffness and content produced plant mixes with a high variation in total asphalt content. The difficulties in estimating total asphalt content can also be attributed to unknown degree of blending between aged and virgin binder. In addition to RAP binder stiffness and content, degree of blending is also affected by virgin binder grade and mixing/compaction temperatures (Faheem et al., 2018). Hence, achieving the desired mix design volumetrics is another challenge pertinent to RAP usage. Al-Qadi et al. (2009) investigated that voids in mineral aggregate did not have a specific trend with increasing RAP content. Finally, cracking performance of RAP mixes is always a major point of concern. Due to the reaction with atmospheric oxygen, RAP binder becomes very stiff and causes blended binder to become more brittle; thus, reducing the mix's cracking resistance at low temperatures (Hill, 2011). Xiao et al. (2007) investigated that 15% RAP is enough to stiffen the mixture and diminish its cracking performance.

2.3.3 Characterization

Integration of RAP in HMA mixtures is contingent on maintaining equivalent performance to mixtures created from only virgin materials. Therefore, laboratory tests must be conducted on RAP materials to determine their properties and establish an accurate mix design. RAP binder content is the first property of RAP that needs to be investigated as it participates in total asphalt content of the mix. RAP binder content is determined by extracting binder from aggregate and calculating the percentage weight loss of binder. The extraction process is done by either burning off binder from aggregates in an ignition oven or using a solvent in a centrifuge or vacuum. The ignition test method provides accurate results of binder content but causes a significant loss of fine aggregate material due to excessive heat (can reach 1 - 2% for some aggregate types such as dolomite) which might alter RAP gradation (West, 2015). Solvent extraction test method does not significantly alter RAP gradation as well as retains RAP binder which might be needed for further testing. However, it provides lower binder content than actual as it does not remove all the binder absorbed by aggregate (West, 2015).

RAP gradation is another property of RAP that needs to be determined for aggregate blending purposes. There are two common types of RAP gradation; namely, black gradation and white gradation (Saliani et al., 2019). Black gradation is the gradation of RAP aggregate prior to binder extraction, whereas white gradation is the gradation of extracted and recovered RAP aggregate. Despite being the same material, these two gradations are completely different from each other. Black gradation tends to represent lower amounts of fine material in RAP, while white gradation represents the opposite outcome. Thus, the use of black gradation might result in an unanticipated amount of extra fine material in the mix. As a result, white gradation is the primary gradation of RAP in all testing standards and is much more common in practice. However, it must be noted that both black gradation and white gradation do not represent actual RAP gradation which is believed to be somewhere in between.

Bulk specific gravity (G_{sb}) of RAP is a property required to calculate voids in mineral aggregate (VMA) of a mix. VMA is a fundamental parameter in mix design to ensure durability; therefore, G_{sb} of extracted RAP aggregate must be accurately determined. Nevertheless, it is difficult to accurately determine G_{sb} of extracted RAP aggregates due to modification of aggregate properties caused by the extraction process as well as changes in aggregate gradation (Al-Qadi et al., 2012). A sample of extracted RAP aggregate is separated on sieve no. 4 (4.75 mm or 3/16 in) and the bulk specific gravity test is conducted via a simple lab procedure on coarse and fine aggregate portions individually. G_{sb} value of the RAP sample is then calculated by combining the G_{sb} values of coarse and fine aggregate portions based on their composition within the sample. In addition, NCHRP Report 452 (McDaniel and Anderson, 2001) mentioned that G_{sb} value of RAP can be estimated from effective specific gravity (G_{se}) value of RAP. The maximum theoretical specific gravity test must be conducted on a loose sample of RAP to determine its G_{se} value as shown in Equation 2.1:

$$G_{se} = \frac{100 - P_b}{\frac{100}{G_{mm}} - \frac{P_b}{G_b}} \tag{2.1}$$

Where G_{se} = effective specific gravity of RAP aggregate, P_b = binder content of RAP, G_{mm} = maximum theoretical specific gravity of loose RAP sample, and G_b = specific gravity of RAP binder.

G_{sb} value is then determined based on G_{se} value using Equation 2.2:

$$G_{sb} = \frac{G_{se}}{\left(\frac{P_{ba} * G_{se}}{100 * G_b} + 1\right)} \tag{2.2}$$

Where G_{sb} = bulk specific gravity of RAP aggregate, and P_{ba} = percentage of absorbed binder by weight of aggregate.

P_{ba} value is usually assumed based on experience or historical records of mixes created from the same raw materials. The reliability of estimating G_{sb} value of RAP from its G_{se} value depends predominantly on the accuracy of assumed P_{ba} value, since small errors in P_{ba} can lead to considerable errors in VMA (West, 2015). Therefore, using this method to estimate G_{sb} of RAP is not recommended, especially for high RAP mixes.

Finally, the properties of extracted RAP aggregate and recovered RAP binder are only required when dealing with high RAP mixes. RAP aggregate properties such as Los Angeles abrasion, sand-equivalent and soundness are crucial to determine the validity of aggregate. Furthermore, critical temperatures of recovered RAP binder should be determined using Superpave binder performance grading (PG) process. Recovered RAP binder grade is important as it aids in the selection of an appropriate virgin binder grade. Also, it might impose limits on the maximum allowable amount of RAP to be used in the mix. According to NCHRP Report 752 (West et al., 2013), recovered RAP binder (which is already aged) should be conditioned only in the rolling thin-film oven prior to grading to simulate aging in the pressure-aging vessel. The high and intermediate temperature PG grades are then determined using dynamic shear rheometer, while the low temperature PG grade is determined using bending beam rheometer.

2.3.4 Fractionation

Milling of aged pavement layers was found to break down significant amounts of aggregate leading to excessive fine RAP material and high dust contents. Characterization of RAP materials proved that properties of coarse and fine RAP binder are nonidentical (Saliani et al., 2019). In addition, fine RAP possesses higher binder content than coarse RAP since asphalt binder coats a larger surface area on fine aggregate (Saliani et al., 2019). Thus, the contribution of fine RAP to a higher proportion of aged binder as well as existence of high dust content causes complexity in meeting volumetric mix design requirements, especially for high RAP mixes (Shannon, 2012). Consequently, RAP processing is essential to control different RAP particle sizes and ensure efficient utilization of high RAP contents in asphalt mixes.

A RAP processing method called “RAP fractionation” is currently gaining popularity in high RAP mix design to provide greater flexibility in adhering to mix design requirements. RAP fractionation is a process in which the RAP stockpile is screened into three sizes, typically +9.5 mm (+3/8 in), 4.75 mm – 9.5 mm (3/16 in – 3/8 in), and -4.75 mm (-3/16 in) as shown in Figure 2.6 (West, 2015).

In mixes with nominal maximum aggregate size (NMAS) of 12.5 mm (0.5 in) or less, only sieve no. 4 (4.75 mm or 3/16 in) can be used to separate between coarse and fine RAP sizes. Mechanically splitting RAP into coarse and fine stockpiles allows to control the amounts of different RAP particle sizes within the mix which enhances gradation properties, dust-binder ratios, and binder content adjustments. In conclusion, variability of RAP is reduced, and its consistency is improved which leads to higher RAP utilization in asphalt mixes while simultaneously meeting the desired volumetrics and maintaining acceptable performance.

Figure 2.6 Typical fractionated RAP samples (West, 2015)

Although RAP fractionation had improved consistency of high RAP mixes, it is the least considered RAP processing method in practice (West, 2015). Other methods such as crushing all RAP into a single size or using millings without further processing are more commonly used. RAP fractionation is a more expensive processing method and requires at least one additional screening/fractionation unit. Moreover, it requires more space to accommodate storage of RAP stockpiles with different particle sizes. Finally, it was found to be mechanically impractical with some of the equipment available with contractors. Therefore, RAP fractionation should be considered when designing high RAP mixes only and the decision should only be made according to the mix producer’s choice (i.e., the decision whether to fractionate RAP must not become a specification). If there is reluctance to fractionate RAP due to its cost or impracticality, then agencies must impose limits on the variability of RAP stockpiles to ensure consistency in high RAP mixes (West, 2015).

2.4 Superpave Mix Design Considerations of RAP Mixtures

RAP mixtures have the same mix design procedure as virgin mixtures. After RAP characterization, aggregate blending is conducted using extracted RAP gradation and the selected blend must abide by the specification limits. Furthermore, the proportion of asphalt binder in RAP must be accounted for when determining total asphalt content of the mix. Prior to mixing, RAP heating time should be limited to a maximum of three hours at mixing temperature (West et al., 2013). Another approach is to heat RAP at a much lower temperature (as low as 60°C) while super-heating virgin aggregates, so that the desired mixing temperature of the combined material is reached during mixing (Hossain et al., 2012). In brief, constraints to RAP heating must be considered in the mix design procedure to prevent additional aging of RAP binder. Finally, the recycled HMA must meet the desired volumetric properties (like virgin mixes) such as VMA, voids filled with asphalt (VFA), dust to binder ratio, and density at 4% air voids at design number of gyrations.

2.4.1 Virgin Binder Grade

RAP binders are stiffer than virgin binders; thus, the inclusion of RAP will inevitably lead to stiffer mixtures. Stiffer mixtures were proved to have adverse effects on field performance such as reduced cracking and raveling resistance (West et al., 2013). One method to mitigate the stiffening effect of aged RAP binder is to adjust the virgin binder grade that will be used in the mix; however, this will require knowledge of the corresponding RAP binder grade (Al-Qadi et al., 2012). Table

2.3 shows the three recommended levels of virgin binder grade adjustments according to current guidelines for using RAP in Superpave mixtures.

In general, Table 2.3 shows that softer RAP binders will lead to higher RAP contents being utilized in the mix. The first level shows the maximum RAP content that can be used for three RAP binder grade categories without the need to change the standard virgin binder grade. The second level shows the range of RAP content that can be used in each RAP binder grade category when the virgin binder grade is bumped by only one grade (6°C) on both high and low critical temperatures. The third level shows that for higher RAP percentages, the virgin binder grade should be determined based on dedicated equations or blending charts. The three approaches for blending with high RAP contents are described concisely in the next subsections.

Table 2.3 Guidelines for virgin binder grade selection of RAP mixes (McDaniel and Anderson, 2001)

Recommended virgin asphalt binder grade	RAP Percentage Recovered RAP Grade		
	PG xx-22 or lower	PG xx-16	PG xx-10 or higher
No change in binder selection	< 20%	< 15%	< 10%
Select virgin binder one grade softer than normal (e.g., select a PG 58-28 instead of a PG 64-22)	20% - 30%	15% - 25%	10% - 15%
Follow recommendations from blending charts	> 30%	> 25%	> 15%

2.4.1.1 Blending with a Known Percentage of RAP

This approach requires the knowledge of RAP content, recovered RAP binder critical temperatures and desired final blended binder critical temperatures to determine the desired properties of virgin binder grade (Hossain et al., 2012). Equation 2.3 shows how to calculate the required high, intermediate, and low critical temperatures of the virgin binder separately.

$$T_{virgin} = \frac{T_{blend} - (\%RAP * T_{RAP})}{1 - \%RAP} \quad (2.3)$$

Where T_{virgin} = critical temperature of virgin binder, T_{blend} = desired critical temperature of final blended binder, %RAP = RAP percentage expressed as a decimal, and T_{RAP} = critical temperature of recovered RAP binder.

2.4.1.2 Blending with a Known Grade of Virgin Binder

Sometimes agencies select to fix the virgin binder grade to abide by the specifications or due to lack of funding as softer binders are more expensive than stiffer binders (Al-Qadi et al., 2012). In this case, the allowable RAP content (of known RAP binder properties) that can be used with a fixed virgin binder grade and abide by the desired final blended binder properties should be determined using Equation 2.4:

$$\%RAP = \frac{T_{blend} - T_{virgin}}{T_{RAP} - T_{virgin}} \quad (2.4)$$

The allowable RAP content should be calculated at high, intermediate, and low critical temperatures separately; and the RAP content that meets all requirements of the three critical temperatures should be chosen (Hossain et al., 2012).

2.4.1.3 Blending Charts

Blending charts are plotted separately for high and low critical temperatures. It is a rough estimation of the impact of RAP content on the PG grade of virgin binder (Copeland, 2011). The PG grades of different RAP binders recovered from different RAP samples across a certain region (e.g., province, state, city, etc.) are tested. These RAP binders are assumed to have reached maximum stiffness; therefore, their high and low critical temperatures are plotted corresponding to 100% RAP content on two separate charts. The high and low critical temperatures of the standard virgin binder within the same region are also plotted on the two charts corresponding to

0% RAP content. Eventually, a straight line is drawn to connect the two points on each chart forming two blending charts (one for each critical temperature). Figure 2.7 shows an example of a blending chart for both high and low PG grades.

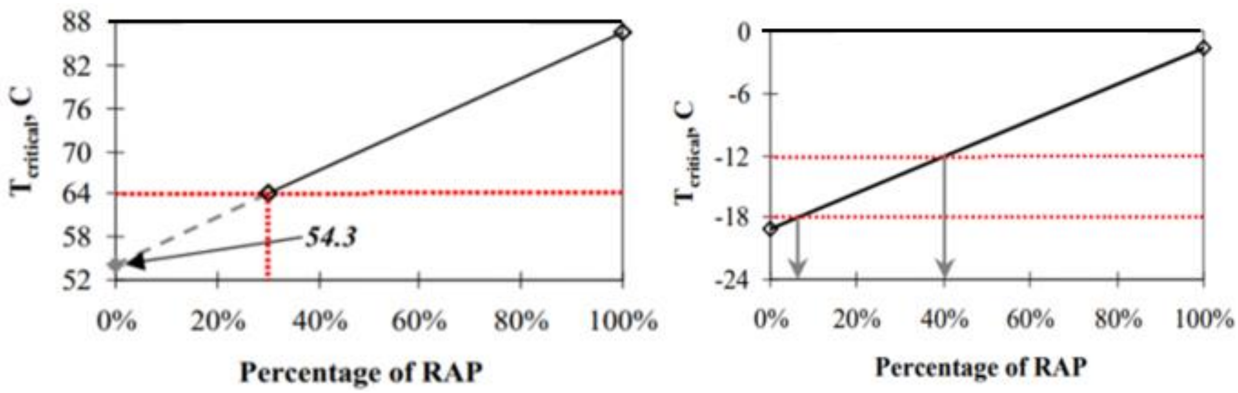

a) High PG grade b) Low PG grade

Figure 2.7 Blending Charts (McDaniel, 2011)

2.4.2 Use of Rejuvenators

The chemical composition and original properties of RAP binders change due to aging during plant mixing, construction, and pavement service life. Therefore, rejuvenators (or recycling agents) are sometimes added to RAP mixtures to retrieve the chemical composition and original properties of RAP binders (Lu et al., 2019). Rejuvenators introduce maltenes into RAP binders as the quantity of maltenes in RAP binders is reduced due to oxidation. The required dosage of rejuvenator is highly dependent on the viscosity of RAP binder. Rejuvenators sustain the cracking property of RAP mixtures while preventing grade bumping of virgin binder. Despite that use of rejuvenators remains a cost-effective approach that allows higher RAP utilization in asphalt mixtures, they are still not considered in any Superpave mix design guidelines. The asphalt mixing plant may require major modifications to integrate rejuvenators into the mixing process. Additionally, rejuvenators affect properties of asphalt mixtures; thus, it is significant to know the severity of their impact on asphalt mixture performance prior to their use in mix design.

2.5 RAP Binder Replacement

Historically, most highway agencies expressed RAP content as the proportion of RAP material to total mix by weight (Copeland, 2011). Nevertheless, the main objective of utilizing RAP in asphalt mixtures is to make the most of aged binder and decrease the need for virgin binder. Therefore, an increasing number of highway agencies are currently shifting towards the concept of expressing RAP content based on the amount of RAP binder that contributes to total binder content in the mix. This concept is called "RAP binder replacement" or "RAP binder ratio" and was found to change the significance of how RAP binders might impact mix properties and performance. The percentage of total binder that is superseded by RAP binder can be calculated using Equation 2.5:

$$\text{RAP Binder Ratio } (\%) = \frac{\text{A}*\text{B}}{\text{C}} \quad (2.5)$$

Where A = RAP binder content (%), B = RAP content in mixture (%), and C = Total binder content in mixture (%).

The RAP binder replacement concept sets limits on the amount of binder that might come from RAP and these limits will aid in initiating the mix design as well as determining optimum binder content of the mix (Copeland, 2011). For example, if a highway agency specifies a minimum virgin binder content of 70% for high RAP mixes, then a RAP binder replacement value of 30% can be used to determine optimum asphalt content of the mix at the desired RAP content.

2.6 Blending of RAP and Virgin Binder

A primary concern of using RAP in HMA mixes is uncertainty regarding the amount of RAP binder expected to diffuse into virgin binder during mixing and become part of the composite binder coating the aggregates (Zhao et al., 2015). There are three possible views for RAP and virgin binder blending (Gottumukkala et al., 2018). The first view is when RAP is treated as black rock in which no blending takes place between RAP and virgin binders. The second view is opposite of the first view in which full blending occurs between RAP and virgin binders. In this scenario, properties of the composite binder can be estimated proportionally from the properties of RAP and virgin binder. The third view is incomplete blending between RAP and virgin binders in which a portion of RAP binder diffuses into virgin binder, while the remaining portion becomes part of the black rock. Figure 2.8 shows a sketch of the three blending scenarios.

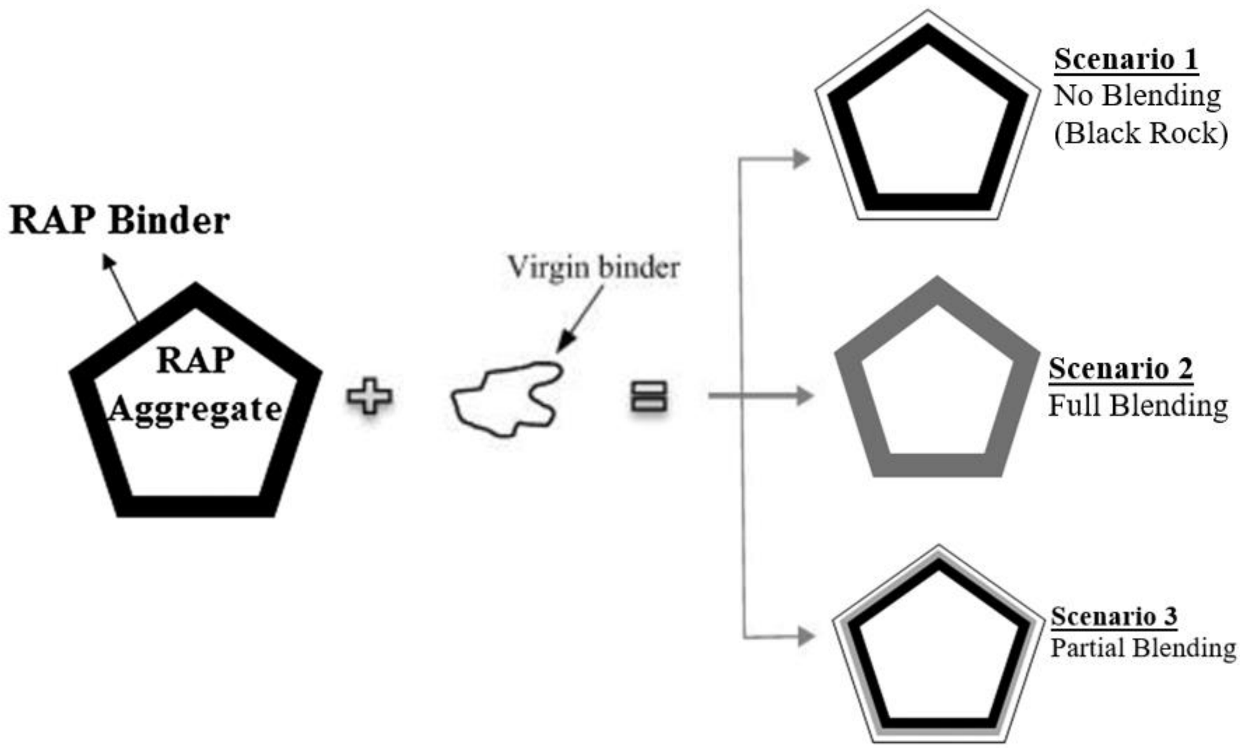

Figure 2.8 Blending scenarios of RAP and virgin binder (Kadhim, 2019)

The second scenario (i.e., full blending) is applied by most highway agencies due to the simplicity of estimating composite binder properties as well as the belief that RAP binder gains enough energy during the production process to completely blend with virgin binder (Zhao et al., 2015). For this reason, blending charts are plotted as a linear relationship between RAP content and critical Superpave temperatures of blended binder. However, the assumption of 100% degree of blending became controversial among highway agencies due to the stiffer nature of RAP binders.

Soleymani et al. (2000) deduced that blended binder properties remain very close to virgin binder properties only when low RAP contents are included in the mix. Zhao et al. (2015) proved that RAP binder requires much more energy (i.e., heat) to drain completely from aggregate and then mingle with virgin binder which is a condition impossible to achieve in a normal asphalt plant mix. Zaumanis and Mallick (2015) proved that the assumption of complete blending produces mixes with insufficient asphalt content which results in undesirable properties such as higher cracking and raveling potential as well as early pavement moisture damage. All these concerns are expected to exacerbate with higher RAP contents in the mix which made the full blending assumption a less reliable scenario to consider in high RAP mix design.

The assumption of partial (or incomplete) blending gradually became a more realistic scenario and recent research attempted to study the actual degree of blending between RAP and virgin binders. Gottumukkala et al. (2018) evaluated the degree of blending of 20% and 35% RAP mixes via determining the properties of blended binder. Each RAP mix was created with two virgin binders (one soft and one stiff virgin binder). Table 2.4 shows the blending ratio results corresponding to each binder property for all RAP mixes. In essence, Table 2.4 proves that degree of blending is highly dependent on stiffness of virgin binder used as well as RAP proportion. Mixes with high RAP proportion and stiff virgin binder represented least blending ratios and vice versa.

Table 2.4 Blending ratio of RAP mixes (Gottumukkala et al., 2018)

Binder property	RAP content (%)	Blending ratio with soft virgin binder (%)	Blending ratio with stiff virgin binder (%)
$G^*/\sin\delta$ (Pa)	20	84.4	66.4
	35	70.8	15.9
Penetration (dmm)	20	87.1	84.0
	35	73.3	54.6
Softening point (°C)	20	82.8	65.8
	35	78.3	33.2

Huang et al. (2005) studied the amount of RAP binder that transferred from RAP aggregate to virgin aggregate in mixes with RAP contents ranging from 10% to 30%. RAP aggregates passing sieve no. 4 were mixed at 190°C with virgin aggregates retained on the same sieve for three minutes (i.e., fine RAP aggregates were mixed with coarse virgin aggregates). Mixes were then short-term conditioned and split again into coarse and fine fractions. Subsequently, binder was extracted and recovered from the two fractions and its properties were evaluated. Results showed that only 11% of RAP binder had been transported to the virgin aggregates. Additionally, more than 50% of RAP binder remained inactive or as part of the original black rock and did not interact with virgin binder. Finally, Zhao et al. (2015) evaluated the degree of blending in mixes with a variety of RAP contents starting from 10% and up to 80%. Results showed that almost full blending took place at 10% and 20% RAP contents, whereas degree of blending decreased from 73% to 24% when RAP contents increased from 30% to 80% as shown in Figure 2.9.

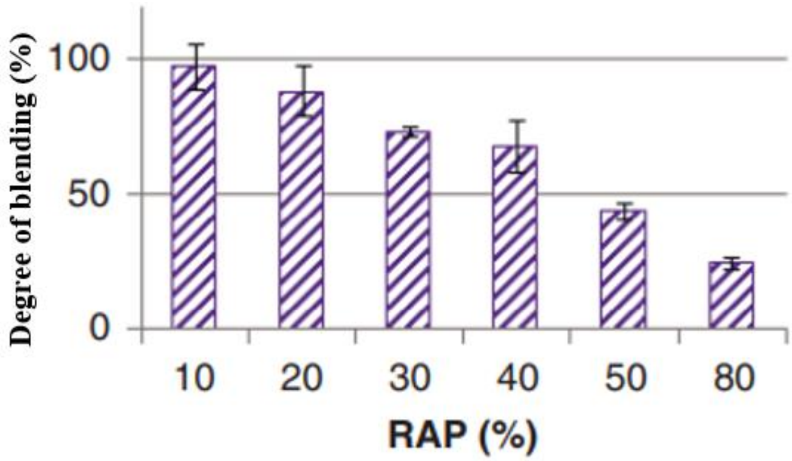

Figure 2.9 Degree of blending at various RAP contents (Zhao et al., 2015)

2.7 RAP and Volumetric Properties

Mix volumetrics such as air voids, voids in mineral aggregate (VMA) and voids filled with asphalt (VFA) are all significant properties used in determining the validity of HMA mix design. Most highway agencies require RAP mixes to have similar criteria for volumetric properties as virgin mixes. However, stiffer binder and more fines as well as incomplete blending are all factors that make the adherence of RAP mixes to similar volumetric criteria more challenging. The purpose of this section is to highlight these challenges and focus on the issues of high RAP mixes with VMA via reviewing the literature on the effect of RAP and fractionated RAP on volumetric properties.

In the experimental procedure of NCHRP project 752 (West et al., 2013), materials collected from State of Utah were used to design three RAP mixes (0%, 25% and 55%) using two virgin binders (PG 58-34 and PG 64-34). All mixes had a nominal maximum aggregate size (NMAS) of 12.5 mm and gradations were kept as close to each other as possible. Table 2.5 shows the volumetric properties of the three RAP mixes designed using PG 58-34 and PG 64-34 virgin binders.

Table 2.5 Volumetric properties of RAP mixes in Utah (West et al., 2013)

Property	PG 58-34 virgin binder			PG 64-34 virgin binder		
	RAP content (%)			RAP content (%)		
	0	25	55	0	25	55
Optimum asphalt content (OAC, %)	5.50	5.70	6.50	5.90	6.10	6.20
Air voids (%)	3.90	3.70	3.70	4.20	4.00	3.80
VMA (%)	14.0	14.1	15.1	15.2	15.3	15.4
VFA (%)	72.2	73.8	75.4	71.9	73.3	75.3

Table 2.5 shows that higher RAP contents led to higher VMA as well as higher OAC to reach an acceptable range of air voids at design gyrations. When mixing with PG 58-34, a minor increase in OAC (only 0.2%) was required at low RAP content (25%), whereas an additional 1% of asphalt was required at high RAP content (55%). On the other hand, the increase in OAC was minor at both RAP contents when mixing with PG 64-34. This can be attributed to the increasing trend of VMA with RAP content. The greater the VMA compared to the virgin mix means a greater amount of additional binder is required to fill the extra air voids caused by inclusion of RAP. This assumption can also be interpreted by the increasing trend of VFA with RAP content.

In the same experimental procedure of NCHRP project 752 (West et al., 2013), volumetric properties of fractionated RAP mixes were compared. Materials collected from New Hampshire were used to design two 55% RAP mixes with different coarse and fine RAP fractions using PG 58-28 virgin binder. One mix had a high fine RAP content of 24% and the other mix had no fine RAP. Similarly, mixes had a 12.5 mm NMAS and close gradations to each other. Table 2.6 shows the characteristics and volumetric properties of the two fractionated RAP mixes.

Table 2.6 Characteristics and volumetric properties of fractionated RAP mixes in New Hampshire (West et al., 2013)

Property	RAP content (%)	
	55	55
% Coarse RAP (AC = 3.20%)	55.0	31.0
% Fine RAP (AC = 6.05%)	0.00	24.0
Optimum asphalt content (OAC, %)	5.20	6.10
AC from virgin binder (%)	3.40	3.70
AC from RAP (%)	1.76	2.44
RAP binder replacement (%)	34.0	40.0
Air voids (%)	4.00	4.00
VMA (%)	14.4	15.5
VFA (%)	73.0	74.2

Table 2.6 shows that asphalt content in fine RAP is nearly double the asphalt content in coarse RAP. This caused the two mixes to have completely different properties despite having the same total RAP content. The high binder content in fine RAP led to a higher OAC and RAP binder ratio in the 24% fine RAP mix. Furthermore, volumetric properties of VMA and VFA showed a noticeable increase with more fine RAP content. The increase in VMA can be attributed to higher aged binder content in fine RAP aggregates. Accordingly, fine RAP binder is subject to lower degree of blending which causes fine RAP aggregates to possess a coarser gradation than their actual (extracted) gradation used in the mix design because of binder that became part of the black rock. Therefore, VMA and OAC increased to compensate for the extra air voids created by fine RAP.

Another comparison of volumetric properties was performed on fractionated RAP mixes in the same NCHRP project 752 (West et al., 2013), but with materials collected from Florida. Two groups of mixes were designed with different NMAS, 9.5 mm and 19 mm. One virgin mix and one 40% RAP mix were created in each group using a PG 67-22 virgin binder. Gradations in each group were kept similar, but the two 40% RAP mixes had different coarse and fine RAP fractions. One mix had a high fine RAP content of 20%, while the other mix had a low fine RAP content of 5%. Table 2.7 shows the characteristics and volumetric properties of the four mixes.

Table 2.7 Characteristics and volumetric properties of virgin and fractionated RAP mixes in Florida (West et al., 2013)

Property	NMAS = 9.5 mm		NMAS = 19.0 mm	
	RAP content (%)		RAP content (%)	
	0	40	0	40
% Coarse RAP (AC = 5.27%)	0.00	35.0	0.00	20.0
% Fine RAP (AC = 5.95%)	0.00	5.00	0.00	20.0
Optimum asphalt content (OAC, %)	5.40	5.60	4.50	5.10
AC from virgin binder (%)	5.40	3.50	4.50	2.90
AC from RAP (%)	0.00	2.10	0.00	2.20
RAP binder replacement (%)	0.00	38.0	0.00	44.0
Air voids (%)	3.80	4.20	4.1	4.1
VMA (%)	15.1	15.0	13.5	13.6
VFA (%)	72.6	71.8	70.3	70.4

Table 2.7 represents approximately similar AC values in coarse and fine RAP fractions; thus, amount of AC from RAP is nearly equal in the two 40% RAP mixes regardless of different RAP particle size divisions. In addition, the mix with a higher fine RAP content led to a greater increase in OAC in comparison to virgin mix. This is due to lower degree of blending of fine RAP binder which forced additional virgin binder into the mix to compensate for the inactive binder portion.

VMA is a volumetric property that has no relationship to the amount of RAP. As shown in Table 2.7, inclusion of 40% RAP led to a negligible difference in VMA compared to the virgin mix in both groups which contradicts the increase in VMA at higher RAP contents represented in Table

2.5. Kim et al. (2009) demonstrated an opposite trend where VMA decreased with an increase in RAP content. Conflicting outcomes are due to inaccuracy in determining bulk specific gravity value of RAP which leads to inevitable error in VMA. Consequently, some highway agencies increase their minimum VMA requirements, while others do not rely on VMA in the acceptance or rejection of volumetric properties for high RAP mixes (Al-Qadi et al., 2012).

Lachance (2006) studied the effect of RAP heating time on VMA. RAP heating time was proved to control the degree of blending between RAP and virgin binder which is a primary factor affecting VMA. 19 mm NMAS mixtures with 25% and 40% RAP contents were designed using a PG 58-28 virgin binder. RAP heating times prior to mixing were 2, 3.5 and 8 hours at 150°C. Results indicated that VMA dropped by 0.5% when RAP heating time increased from 2 to 3.5 hours, whereas VMA experienced a 3% increase at 8 hours of heating time. This means that 3.5 hours was the optimum RAP heating time which enabled the greatest degree of blending and led to minimum VMA. Therefore, RAP heating time is a parameter that should be monitored to control VMA. Short heating times mean that not enough energy is acquired to drain off RAP binder which increases VMA, while long heating times mean that RAP binder experiences additional aging which decreases blending degree with virgin binder leading to greater increase in VMA. As a result, there is a need to determine the optimum RAP heating time which differentiates between increasing and decreasing trend of VMA.

2.8 Laboratory Performance of RAP in HMA

Numerous researchers examined the performance of HMA mixtures with RAP to determine the eligibility of such mixes. Li et al. (2008) investigated the impact of RAP content and source on complex modulus and SCB test results of laboratory-produced specimens. HMA samples with three RAP contents (0%, 20% and 40%) from two different RAP sources (A and B) were prepared using PG 58-28 and PG 58-34 virgin binders. Results showed that mixes with higher RAP contents and stiffer binders had higher complex modulus values. Also, RAP source did not affect complex modulus results at low temperatures, while it was an influential factor on stiffness at high temperatures. SCB test results showed that low temperature cracking resistance decreased at higher RAP contents; thus, 40% RAP mixes had the least fracture energy values as shown in Table 2.8. In addition, RAP source did not have a significant effect on SCB test results. Finally, the relationship between fracture energy and complex modulus was not statistically significant.

Table 2.8 Fracture energy values of virgin and RAP mixes (Li et al., 2008)

RAP source	SCB test temperature (°C)	Fracture energy (J/m^2)					
		PG 58-28 virgin binder			PG 58-34 virgin binder		
		RAP content (%)			RAP content (%)		
		0	20	40	0	20	40
A	-12	742.3	530.3	511.0	1104.3	1009.5	697.6
	-24	275.9	266.0	217.9	440.3	381.9	263.6
	-36	225.3	246.5	166.1	298.0	252.6	197.4
B	-12	742.3	577.4	446.9	1104.3	792.8	527.9
	-24	275.9	281.4	250.5	440.3	328.9	280.0
	-36	225.3	215.3	165.0	298.0	244.6	219.6

Shah et al. (2007) investigated the impact of RAP content on complex modulus and indirect tensile strength of plant-produced mixtures. One virgin mix (no RAP) and three RAP mixes (15%, 25% and 40%) produced with a PG 64-22 virgin binder were collected and tested. Results showed that complex modulus (i.e., stiffness) of the virgin mix did not increase when only 15% RAP was added, whereas 25% and 40% RAP mixes showed a noticeable increase in stiffness. Furthermore, indirect tensile strength results were directly proportional with mix stiffness; thus, 40% RAP mix had the highest indirect tensile strength value.

Willis et al. (2013) investigated the eligibility of virgin binder grade bumping to enhance durability of asphalt mixtures containing average and high contents of RAP. Two virgin binder grades (i.e., PG 67-22 and PG 58-28) were used to create 9.5 mm NMAS Superpave mixtures comprising 25% and 50% RAP. A virgin mix was produced with a base virgin binder of PG 67-22. Three laboratory tests were included; namely, IDT Energy Ratio Test to assess top-down cracking resistance, OT test to assess reflective cracking resistance, and APA to assess rutting resistance. OT test results showed that cracking resistance decreased for RAP mixes produced with both virgin binders. However, virgin binder grade bumping could improve cracking resistance of RAP mixes (see Figure 2.10). IDT Energy Ratio test results represented a similar outcome to OT test results. APA results showed that rutting resistance increased at higher RAP contents. Nevertheless, virgin binder grade bumping led to reduced rutting resistance (less than the virgin mix) even at high RAP contents as shown in Figure 2.10.

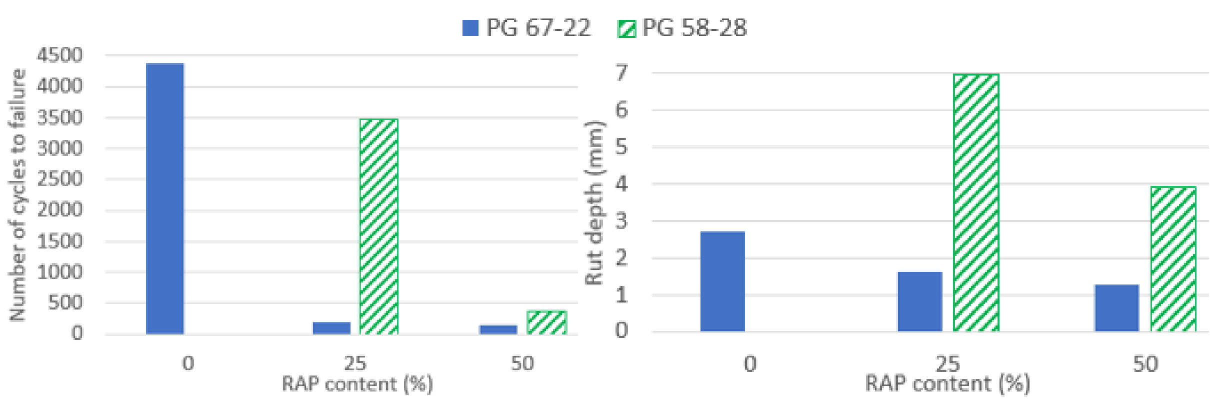

a) OT test results b) APA test results

Figure 2.10 OT and APA test results of RAP mixes with different virgin binders (Willis et al., 2013)

Al-Qadi et al. (2012) studied the impact of RAP content and virgin binder grade bumping on volumetric properties and performance of HMA mixtures. One virgin mix and three high RAP mixes (30%, 40% and 50%) were designed using three virgin binder grades; namely, PG 64-22 (base binder), PG 58-22 (single-bumped) and PG 58-28 (double-bumped). A comprehensive laboratory testing program was conducted to characterize performance of the various RAP mixtures. Five laboratory tests were included in the program; namely, TSR test to evaluate moisture susceptibility, FN test and HWTT test to evaluate rutting resistance, DMT test to evaluate stiffness, and SCB test to evaluate thermal cracking resistance. Results showed that RAP had to be fractionated to control gradation of mixes and facilitate volumetric mix design procedure. TSR test results indicated that high RAP mixtures are less susceptible to moisture due to better adhesion between RAP binder and RAP aggregate. DMT test results showed that complex modulus values increased at higher RAP contents indicating greater stiffness, whereas SCB test results indicated that high RAP mixtures are more prone to thermal cracking. Results of FN test and HWTT test indicated that high RAP mixtures are less susceptible to rutting as shown in Figure 2.11. Finally, both single and double grade bumping of virgin binder caused RAP mixes to have closer performance results to virgin mixes. Hence, virgin binder grade bumping was recommended to enhance durability of high RAP mixtures.

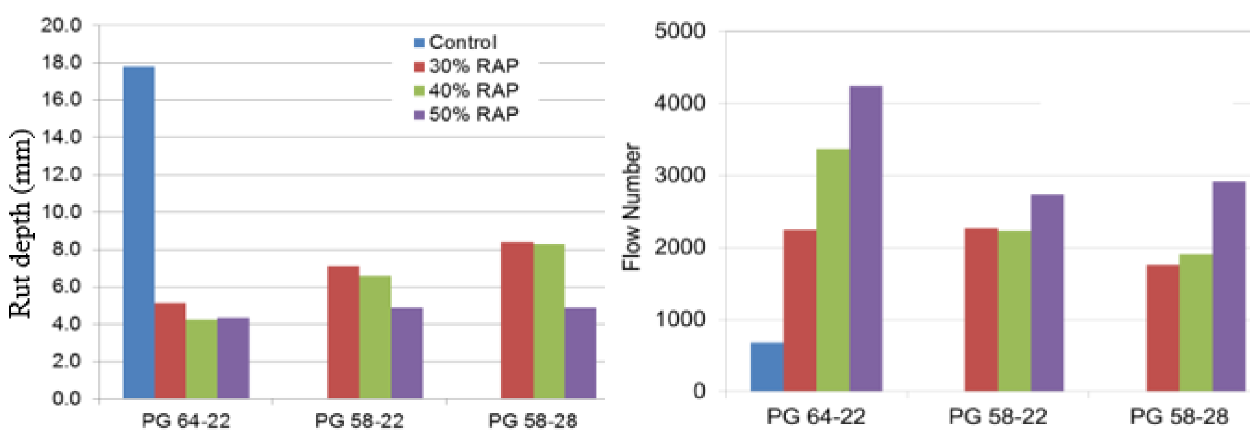

a) HWTT test results b) FN test results

Figure 2.11 HWTT and FN tests results of RAP mixes with different virgin binders (Al-Qadi et al., 2012)

West et al. (2009) conducted a laboratory study to evaluate the performance of asphalt mixtures containing 0%, 20% and 45% RAP. Three laboratory tests were included; namely, APA to assess rutting resistance, BBF test to assess fatigue cracking resistance, and Dynamic Modulus Test (DMT) to assess stiffness. APA results showed that rutting resistance increased at higher RAP contents. DMT results showed that stiffness also increased at higher RAP contents. Conversely, BBF test results showed that fatigue cracking resistance decreased at higher RAP contents.

Arshad et al. (2018) conducted a laboratory study in Malaysia to evaluate volumetric properties, rutting resistance and moisture susceptibility of asphalt mixtures containing low, average, and high RAP contents. Mixes were designed using Marshall mix design procedure with 0%, 15%, 25% and 35% RAP contents. HWTT test and TSR test were used to assess rutting resistance and moisture susceptibility, respectively. Marshall properties proved that all mixes achieved the desired volumetric properties, but higher RAP mixes had lower optimum binder contents due to RAP binder replacement phenomenon. TSR test results met the minimum criteria (i.e., TSR ≥ 80%) for all mixes indicating an adequate level of moisture resistance as shown in Figure 2.12. Figure 2.12 also shows that HWTT test results met the minimum criteria (i.e., minimum 8,000 passes at 20 mm rut depth) for all mixes, while the difference in final rut depth between the most and least rut-resistant mixture was negligible (less than 1 mm).

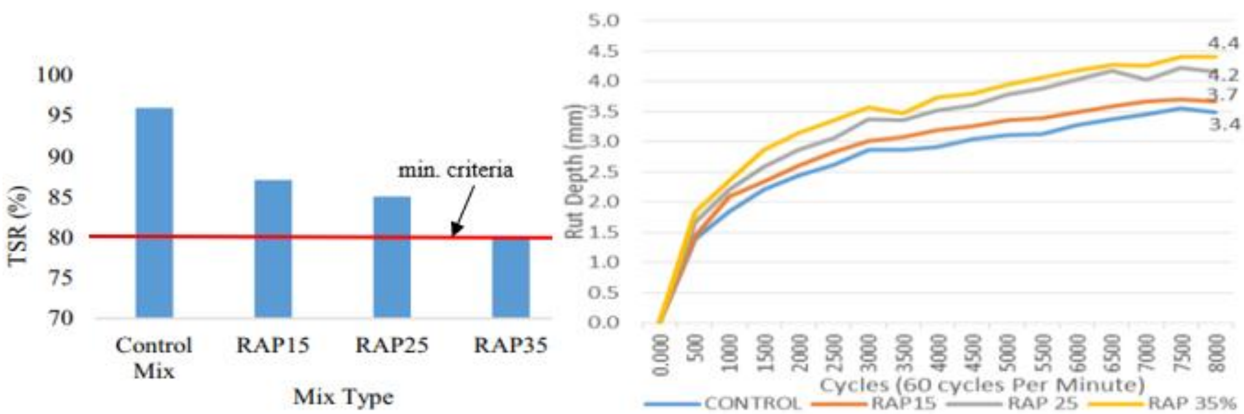

a) TSR test results

b) HWTT curves

Figure 2.12 TSR test results and HWTT curves of RAP mixes (Arshad et al., 2018)

2.9 Laboratory Performance of Fractionated RAP in HMA

This section summarizes the basic outcome of some studies that investigated the performance of fractionated RAP mixtures. Han et al. (2019) characterized the performance of high RAP mixtures containing different fine RAP contents. Three mix categories of high RAP content (30%, 40% and 50%) were included in the study as well as one virgin mix designed only for comparative purposes. Each RAP category had three mixes of different fine RAP content (10%, 15% and 20%) to make up a total of nine high RAP mixes. The ten mixes were characterized with respect to their resistance to moisture, fatigue cracking and thermal cracking. Results showed that thermal cracking resistance decreased with the increase of both total and fine RAP content. Fatigue cracking results matched with thermal cracking results, but it was recommended that fine RAP content should not exceed 15% to maintain acceptable fatigue cracking performance. Finally, TSR test results showed that moisture resistance was sensitive to total RAP content, but not to fine RAP content.

Saliani et al. (2019) characterized the performance of high RAP mixtures created with a single RAP fraction, either coarse RAP or fine RAP. Three mixes were designed for this study including a virgin mix, a 54% coarse RAP mix, and a 35% fine RAP mix. RAP percentage in each of the coarse and fine RAP mix was determined based on maintaining constant total binder content in the three mixes as well as maintaining constant recycled binder ratio in the two RAP mixes. In other words, the amount of RAP binder acquired from 54% coarse RAP and 35% fine RAP was equal when full blending conditions were assumed, and virgin binder was added as residual to balance their total binder content to that of the virgin mix. These three mixes were characterized with respect to their rutting resistance using the French rutting test and fatigue cracking resistance using the uniaxial tension-compression test. Results showed that the virgin mix had better rutting performance than both fractionated RAP mixes as represented in Table 2.9, but the three mixes met the minimum rutting criteria (i.e., < 10% rut depth). On the other hand, Table 2.9 shows that the two fractionated RAP mixes had higher fatigue cracking potential than the virgin mix, but the coarse RAP mix still had better fatigue life than the fine RAP mix. Overall, the coarse RAP mix performed better or at least equivalent to the fine RAP mix despite having a higher total RAP content. Therefore, it is necessary to consider RAP fractionation as an effective processing method to enhance the performance of high RAP mixtures.

Table 2.9 Rut depth and fatigue life of virgin and fractionated RAP mixes (Saliani et al., 2019)

Mix	Average rut depth (%)	Average number of cycles to failure (fatigue life)
Virgin mix	3.0	2,420,715
54% coarse RAP	4.0	1,165,318
35% fine RAP	4.0	25,611

Overall, most research that investigated RAP fractionation presented an outcome in favor of the approach. For example, Shannon (2012) proved that fractionated RAP facilitates the achievement of desired mix volumetrics if fine RAP material is eliminated or reduced in high RAP mixes. On the contrary, some research presented a negative outcome regarding the approach. For instance, Hossain et al. (2012) proved that fractionated RAP mixes do not perform better than traditional RAP mixes in terms of fatigue cracking, rutting and moisture resistance. To sum up, RAP fractionation is still an evolving concept in RAP research and more work is needed to confirm its eligibility in mix design and performance.

2.10 Summary, Research Gaps and Needs

Transportation agencies in Manitoba rely on achieving the desired volumetric properties for acceptance of asphalt mix design. However, Manitoba roads are a victim of major pavement distresses such as rutting due to plastic deformation in low traffic areas as well as cracking due to repetitive traffic stresses and cold weather. This proves the incapability of volumetric mix design procedure to predict adequate long-term pavement performance. In addition, transportation agencies in Manitoba use the two common methods (Marshall and Superpave) to design their asphalt mixes as well as they use a variety of mix design constituents such as type of aggregate (granite, gravel, and limestone), type of binder (straight and polymer-modified binders) and proportions of RAP/RAS. All these mix design considerations and variations impose challenges to predict long-term performance of asphalt pavements. To date, no studies have been conducted to evaluate cracking and rutting performance of asphalt mixtures that meet current mix design requirements in Manitoba. Hence, the primary goal of this thesis is to develop a performance testing program and implement preliminary specifications based on one rutting and one cracking test to accommodate local conditions in Manitoba.

The use of RAP in asphalt mixes is of wide-ranging interest among agencies and practitioners due to its major cost savings and environmental benefits. However, transportation agencies in Manitoba limit the use of RAP to 10% and 20% for top and bottom lift mixes, respectively, due to uncertain performance. A processing method called RAP fractionation divides RAP aggregate into different sizes to facilitate volumetric mix design procedure of high RAP mixes while reducing the need for other mix design modifications. Despite the dependence on volumetric properties as End Results Specification, the concept of RAP fractionation was never implemented in Manitoba to encourage high RAP consumption and save costs. As a result, another goal of this thesis is to design fractionated RAP mixes and test their performance to determine the eligibility of this processing method in producing high RAP mixes that meet current Superpave volumetric mix design requirements in Manitoba without sacrificing pavement performance.

Chapter 3. Methodology, Materials, and Testing Program

3.1 Introduction

The goal of this thesis was to develop a laboratory performance testing program for plant-produced asphalt mixtures and conduct a balanced mix design (BMD) approach to optimize cracking and rutting resistance. Another goal was to evaluate the performance of fractionated RAP mixtures that meet current Superpave mix design requirements to determine the eligibility of RAP fractionation in pavement design and construction.

To fulfill the goals of this thesis, the experimental program was divided into three major sections. Firstly, five HMA-RAP mixtures including 0, 10, 30, 40 and 50% RAP content were designed to abide by city of Winnipeg (COW) specifications (City of Winnipeg, 2020). The 10% RAP mix comprised of unfractionated (unprocessed) RAP, whereas the 30, 40 and 50% RAP mixes were fractionated RAP mixes that included coarse RAP only. The five mixtures were characterized according to rutting performance using the Hamburg wheel-tracking test (HWTT), cracking performance using the Illinois flexibility index test (I-FIT) and elastic modulus using the dynamic modulus test (DMT). Secondly, six plant-produced loose asphalt mixtures were compacted in the lab to produce specimens for performance testing. The six mixtures comprised of various mix design characteristics including type of aggregate (granite, gravel, and limestone), type of binder (straight and polymer-modified binders) and proportions of RAP/RAS. The six mixtures were characterized according to rutting performance using the HWTT test, cracking performance using the I-FIT test and elastic modulus using the DMT test to investigate the factors that contribute to a more efficient BMD. Thirdly, field cores were extracted from regional highways in the city of Winnipeg to investigate possible causes of early pavement deterioration of in-service asphalt mixtures. The main aim of this section of the experimental program was to examine whether in-service mixtures meet COW specifications in terms of bulk density, asphalt content and aggregate gradation as well as to conduct some laboratory testing to evaluate their performance. Therefore, bulk specific gravity and ignition oven tests as well as sieve analysis were conducted to compare properties of in-service mixtures to the specification limits, whereas HWTT and DMT tests were conducted to evaluate rutting performance and elastic modulus, respectively. Performance tests results of the three sections were then analyzed. In addition, preliminary threshold criteria for the HWTT and I-FIT tests were established for the plant-produced asphalt mixtures according to local conditions in Manitoba.

3.2 Design of Experiments

Tables 3.1 and 3.2 show the Design of Experiments (DOEs) used for the research conducted on laboratory produced fractionated HMA-RAP mixtures. Table 3.3 shows the DOEs used for the research conducted on plant-produced asphalt mixtures. Table 3.4 shows the DOEs used for the research conducted on in-service asphalt mixtures. Figure 3.1 shows the outline of research methodology.

Table 3.1 DOE used to characterize RAP material

Research variable	Number of levels	Levels [Number of specimens per experiment]
Laboratory test	3	Ignition oven [2]
		Sieve analysis [2]
		Specific gravity [2]
RAP material	2	Coarse RAP
		Fine RAP

Table 3.2 DOE used for laboratory produced fractionated HMA-RAP mixtures

Research variable	Number of levels	Levels [Number of specimens per experiment]
Advanced performance test	3	HWTT [2]
		I-FIT [8]
		DMT [2]
HMA-RAP mixture	5	Virgin mix
		10% RAP
		30% Coarse RAP
		40% Coarse RAP
		50% Coarse RAP

Table 3.3 DOE used for plant-produced asphalt mixtures

Research variable	Number of levels	Levels [Number of specimens per experiment]
Advanced performance test	3	HWTT [2]
		I-FIT [8]
		DMT [3]
Asphalt mixture	6	Mix 1 (19, 58, 0, 0)
		Mix 2 (12.5, 58 P, 0, 0)
		Mix 3 (12.5, 64 P, 10, 0)
		Mix 4 (12.5, 64 P, 10, 3)
		Mix 5 (19, 58, 0, 0)
		Mix 6 (12.5, 58 P, 0, 0)

Table 3.4 DOE used for in-service asphalt mixtures

Research variable	Number of levels	Levels [Number of specimens per experiment]
Laboratory test	3	Bulk density [2]
		Ignition oven [1]
		Sieve analysis [1]
Advanced performance test	2	HWTT test [2]
		DMT test [2]
In-service mixture	4	Street 1
		Street 2
		Street 3
		Street 4

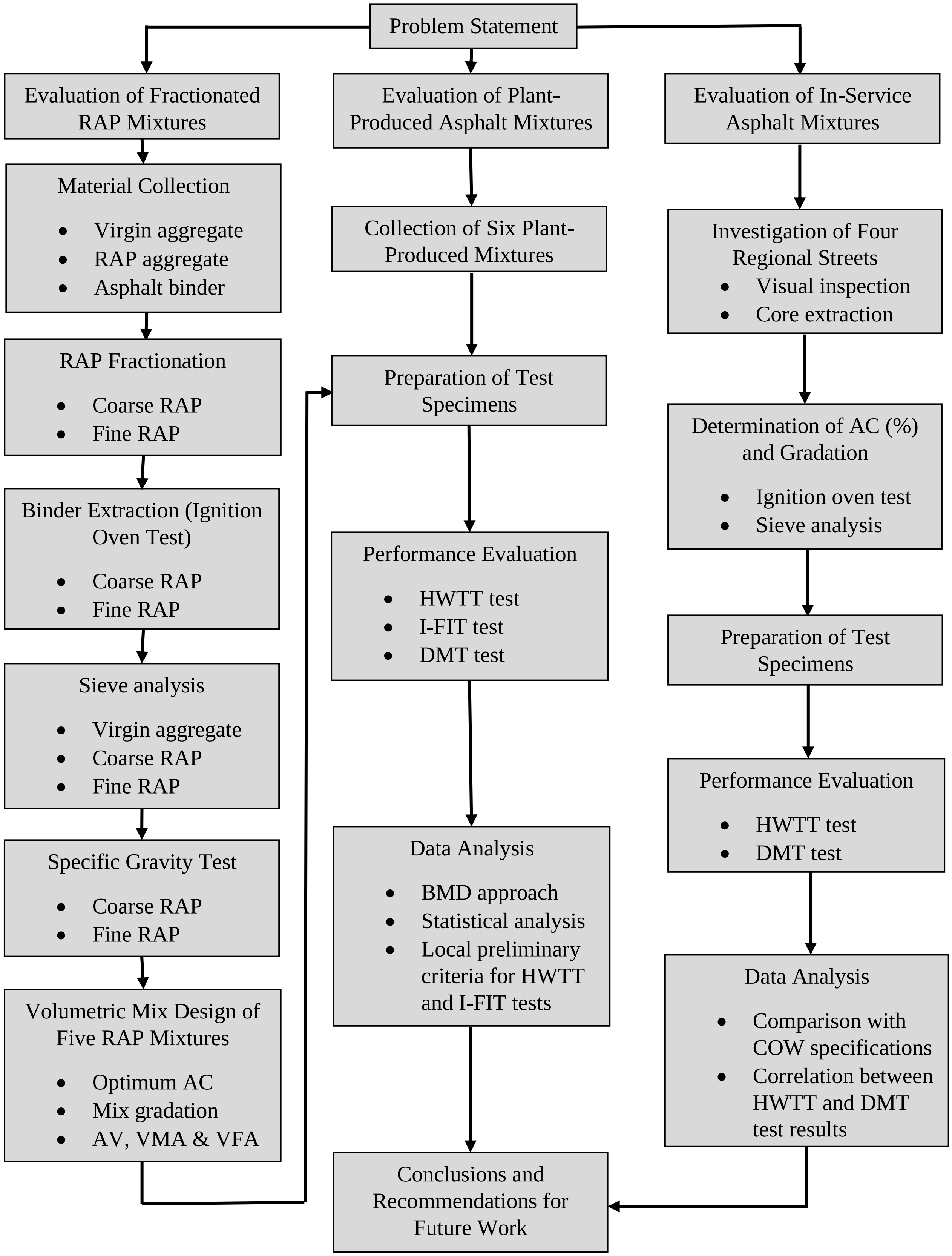

Figure 3.1 Research Methodology Outline

3.3 Materials

3.3.1 Fractionated RAP Mixtures

Five fractionated HMA-RAP mixtures including 0, 10, 30, 40 and 50% RAP content were designed by Manitoba Transportation and Infrastructure (MTI) central labs using the Superpave mix design method (AASHTO R 35, 2022). In this study, four stockpiles of virgin aggregate material and a single stockpile of RAP material were obtained from an ongoing pavement construction project. The project is resurfacing a major highway in Manitoba. Virgin materials included limestone coarse aggregates, sand, crushed and natural fines. RAP material was collected from a single source to minimize variability of RAP properties. Table 3.5 shows the gradations and specific gravities of virgin and RAP materials used to create the fractionated RAP mixes.

Table 3.5 Gradations and specific gravities of virgin and RAP aggregate stockpiles

Sieve size (mm)	Percent passing				
	Coarse aggregates	Crushed fines	Natural fines	Sand	RAP aggregates[1]
19	100.0	100.0	100.0	100.0	100.0
12.5	78.0	100.0	100.0	100.0	93.6
9.5	45.0	100.0	100.0	100.0	87.8
4.75	6.0	87.0	81.0	100.0	70.6
2.36	3.0	60.0	64.0	100.0	59.0
1.18	3.0	37.0	55.0	100.0	49.4
0.60	3.0	18.0	33.0	94.0	40.5
0.30	2.0	10.0	12.0	49.0	27.1
0.15	2.0	7.0	8.0	8.0	13.8
0.075	2.0	5.0	6.0	3.0	10.5
Specific gravity	2.639	2.614	2.606	2.631	2.630

1. RAP asphalt content is 4.50%

The obtained RAP aggregates were then fractionated (divided) through sieve no. 4 (4.75 mm) to produce two different sized RAP aggregates: coarse RAP and fine RAP as shown in Figure 3.2. The ignition test method (AASHTO T 308, 2022) was conducted on two samples from each RAP aggregate size to determine its asphalt content as well as to prepare extracted RAP aggregate samples for sieve analysis and specific gravity tests. The specific gravity test was conducted according to AASHTO T 85 (2022) and AASHTO T 84 (2022) for coarse RAP and fine RAP, respectively. The high and low performance grade (PG) of fine RAP and combined RAP binder were determined by MTI central labs. Due to the low asphalt content of coarse RAP aggregate and its significantly lower proportion in the RAP stockpile, there was not enough coarse RAP binder to test its PG grade. Therefore, coarse RAP binder PG grade was estimated by interpolation between the PG grades of fine RAP and combined RAP binder based on their proportions in the RAP stockpile. Table 3.6 shows the basic properties of coarse and fine RAP.

a) Coarse RAP (> 4.75 mm) b) Fine RAP (< 4.75 mm)

Figure 3.2 Fractionated RAP aggregates

Table 3.6 Properties of coarse and fine RAP

Sieve size (mm)	Percent passing	
	Coarse RAP	Fine RAP
19	100.0	100.0
12.5	85.0	100.0
9.5	72.2	100.0
4.75	35.0	100.0
2.36	27.3	84.2
1.18	23.8	69.2
0.60	20.5	55.7
0.30	15.0	37.4
0.15	8.0	18.5
0.075	5.5	12.8
Asphalt content (%)	3.00	5.50
Specific gravity	2.599	2.639
RAP binder true PG grade[1]	81-15.1	86-22.4
RAP binder PG grade[2]	76-10	82-22

1. Combined RAP binder true PG grade is 84.5-20.2, 2. Combined RAP binder PG grade is 82-16

In the experimental procedure of this project, the five fractionated HMA-RAP mixtures were designed to meet the volumetric requirements of COW specifications (City of Winnipeg, 2020). Gradations of the five mixtures were selected to match wearing surface gradations of current pavement construction projects in Manitoba. Hence, all mixtures were fine graded mixtures with a nominal maximum aggregate size (NMAS) of 12.5 mm. In addition, gradations of the five mixtures were kept as close to each other as possible (i.e., within maximum allowable deviation limit from the job mix formula according to COW specifications) to eliminate the impact of change in gradation on mix performance. In other words, performance of mixtures had to vary due to RAP content only. The 10% RAP mix was designed using unfractionated (unprocessed) RAP due to low RAP content. On the other hand, 30, 40 and 50% RAP mixtures were designed using coarse RAP material only. The high amount of dust content in fine RAP material led to the rejection of mix volumetrics at high RAP contents; thus, it had to be omitted from the mix design of high HMA-RAP mixtures. Table 3.7 shows gradations of the five fractionated HMA-RAP mixtures as well as gradation limits and maximum allowable deviation from job mix formula (JMF) according to COW specifications (City of Winnipeg, 2020). Figure 3.3 represents the 0.45 power gradation curves of the five mixtures.

Table 3.7 Aggregate gradations of fractionated HMA-RAP mixtures

Sieve size (mm)	Percent passing					Specification limits (%)	Maximum deviation from JMF (%)
	Virgin mix	10% RAP	30% Coarse RAP	40% Coarse RAP	50% Coarse RAP		
19	100.0	100.0	100.0	100.0	100.0	100	± 5.0
12.5	92.7	92.6	92.0	92.0	91.8	90 – 100	± 4.0
9.5	81.9	81.8	82.8	83.9	84.4	76 – 90	
4.75	59.7	59.1	57.3	57.6	56.9	48 – 71	± 3.0
2.36	47.9	47.4	45.9	46.2	45.5	28 – 58	
1.18	40.8	40.4	39.2	39.3	38.5	19 – 41	
0.60	28.6	28.2	28.1	28.5	27.9	13 – 30	± 2.0
0.30	13.2	13.5	14.4	15.1	15.2	8 – 21	
0.15	5.9	6.6	6.9	7.4	7.7	4 – 15	
0.075	4.1	4.8	4.7	4.9	5.1	2 – 10	± 1.0

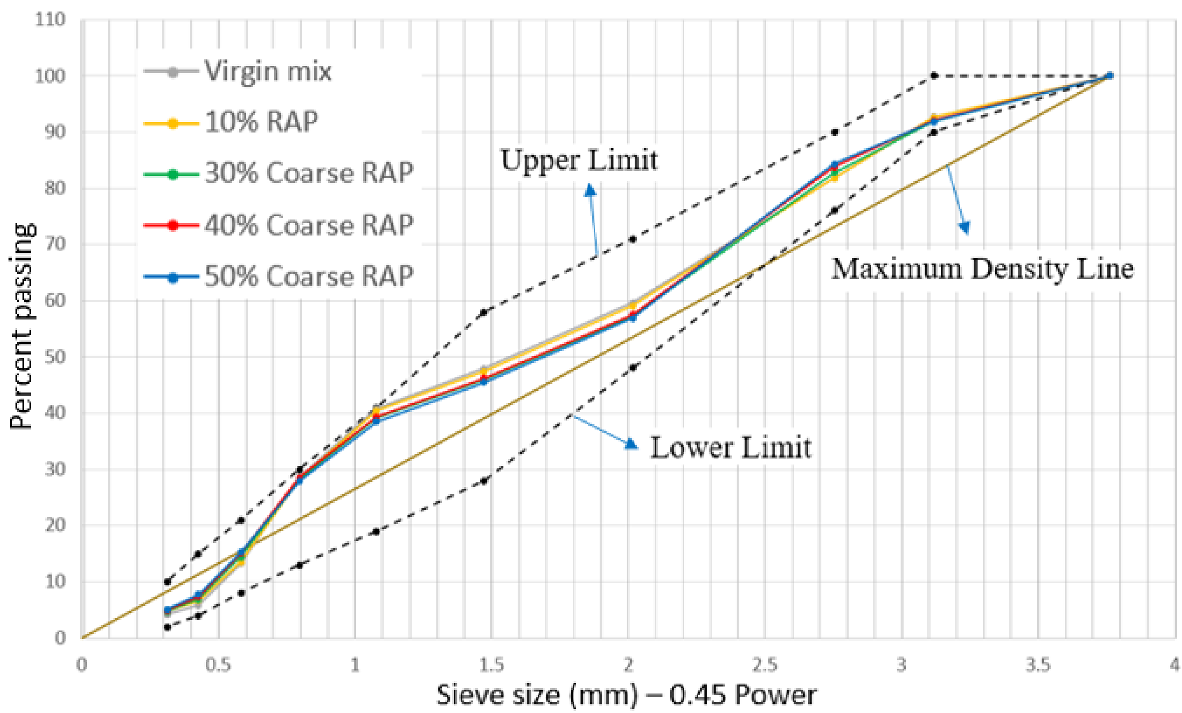

Figure 3.3 0.45 power gradation curves of fractionated HMA-RAP mixtures

A single virgin binder of performance grade 58-34 was used for the five fractionated HMA-RAP mixtures since it is the most common type of binder used in Manitoba mixes. In the mix design of high RAP mixtures, neither bumping of virgin binder grade nor use of recycling agent (rejuvenator) were taken into consideration. This was to eliminate the impact of any factor related to asphalt binder properties on mix performance. Additionally, full blending efficiency between aged and virgin binder was assumed for all RAP mixtures. Virgin and RAP aggregates were mechanically mixed with virgin binder for 120 seconds at 155ºC. The mixture was then conditioned in an oven for 2 hours at 140ºC prior to compaction. Finally, the optimum binder content of mixtures was selected at a target air void range of 4 ± 0.5% at 75 design gyrations in a Superpave gyratory compactor.

3.3.2 Plant-Produced Mixtures

To carry out performance tests for enabling more effective characterization of asphalt mixtures, six loose plant-produced asphalt mixtures were collected from three different pavement construction projects across the province of Manitoba. The six mixtures consisted of virgin mixtures, mixtures containing RAP/RAS, mixtures with straight and polymer-modified binders, mixtures having different NMAS, and mixtures designed using Marshall and Superpave mix design methods. The properties and aggregate gradation of the six plant-produced asphalt mixtures are shown in Table 3.8. Each mix was given a specific ID consisting of four numbers to represent its main design parameters. The first number indicates NMAS, while the second number indicates high temperature PG grade of virgin binder (accompanied by a letter “P” if it’s a polymer-modified binder). The third number indicates the proportion of RAP, and fourth number indicates proportion of RAS. Mixes 1 and 2 are binder coarse and surface coarse layers, respectively, of a single project. Similarly, mixes 5 and 6 are binder coarse and surface coarse layers, respectively, of another project. Mixes 3 and 4 are two surface coarse layers of a third project that were used to pave different road sections. The only difference between these two mixtures is that mix 4 contains an additional 3% RAS.

Table 3.8 Aggregate gradation and properties of plant-produced mixtures

Sieve size (mm)	Percent passing					
	Mix 1 (19, 58, 0, 0)	Mix 2 (12.5, 58 P, 0, 0)	Mix 3 (12.5, 64 P, 10, 0)	Mix 4 (12.5, 64 P, 10, 3)	Mix 5 (19, 58, 0, 0)	Mix 6 (12.5, 58 P, 0, 0)
25	100.0	100.0	100.0	100.0	100.0	100.0
19	93.0	100.0	100.0	100.0	100.0	100.0
12.5	75.9	93.8	92.8	92.9	85.1	94.0
9.5	68.3	80.4	79.5	79.7	74.2	85.4
4.75	51.6	52.8	61.3	61.1	55.3	65.9
2.36	42.4	39.1	50.3	48.9	42.5	47.3
1.18	32.6	27.3	42.4	38.9	32.0	34.2
0.60	22.0	18.1	33.3	28.7	16.3	17.8
0.30	11.8	10.0	18.9	16.8	7.5	8.2
0.15	5.1	4.9	7.4	8.5	4.7	5.5
0.075	3.2	3.1	4.5	5.8	4.0	4.5
Mix design method	Superpave	Superpave	Marshall	Marshall	Superpave	Superpave
NMAS (mm)	19	12.5	12.5	12.5	19	12.5
% RAP	–	–	10	10	–	–
% RAS	–	–	–	3	–	–
Type of aggregate	Granite	Granite	Gravel	Gravel	Limestone	Limestone
Binder PG grade[1]	58-34	58-37 P	64-37 P	64-37 P	58-34	58-34 P

1. "P" indicates polymer modified binder.

The six loose plant-produced asphalt mixtures were compacted in a Superpave gyratory compactor by MTI central labs to produce asphalt briquettes that were used to prepare specimens for laboratory performance testing. To produce specimens at the desired air void content for performance testing (i.e., 7 ± 0.5%), bulk specific gravity values of gyratory compacted briquettes had to be approximately equal to 93% of the maximum theoretical specific gravity value specified in the mix design report of the corresponding loose mixture. Consequently, a certain mass of loose mixture was compacted to produce an asphalt briquette having an air void range of 7 ± 0.5% at a known final height. Two categories of briquette heights (150 mm and 170 mm) were considered, and each category was used to fabricate specimens for different performance tests. Prior to compaction, the loose mixture and a 150 mm diameter compaction mould were heated in an oven to the compaction temperature stipulated in the mix design report. Afterwards, the loose mixture was poured into the compaction mould via a slump cone placed above the mould. The slump cone was needed to ensure that the loose mixture was poured directly to the center of the compaction mould. Finally, the compaction mould was placed into a gyratory compactor and gyrations were applied immediately to compact the loose mixture according to AASHTO T 312 procedure (AASHTO T 312, 2019). Figure 3.4 shows the Superpave gyratory compaction procedure of loose asphalt mixtures as well as final compacted asphalt briquettes at the two height categories.

a) Loose mixture after heating to compaction temperature

b) Slump cone above compaction mould prepared for pouring of loose mixture

c) Extracted specimen after superpave gyratory compaction

d) Gyratory compacted cylinders at two different compaction heights

Figure 3.4 Superpave gyratory compaction procedure of loose asphalt mixtures to two compaction heights

3.3.3 In-Service Mixtures

To conduct advanced laboratory tests for understanding the probable causes of early-age deterioration on recently constructed regional roads in the city of Winnipeg, four streets were investigated in this analysis based on visual inspection that identified the type and extent of pavement defects. A total of eight 150 mm diameter intact core specimens were extracted from each street, either from the wheel path or near the defect area. Six cores were used for the purpose of performance testing including rut resistance and dynamic modulus testing. The remaining two cores were used for the purpose of relative density and binder content evaluation as well as gradation of recovered aggregates. Table 3.9 represents the characteristics of the four in-service mixtures as well as a sample photo of field cores extracted from each street.

Table 3.9 Site characteristics of selected in-service mixtures

Street number	1	2	3	4
Annual average daily traffic	9,200	12,800	9,550	11,700
Type of pavement	Asphalt over concrete	Asphalt	Asphalt over concrete	Asphalt
Asphalt binder penetration grade	150 – 200 (A)	150 – 200 (A)	150 – 200 (A)	150 – 200 (A)
Type of aggregate	Natural gravel	Natural gravel	Natural gravel	Natural gravel
Sample photo				

For density evaluation, the bulk specific gravity (BSG) of the compacted wearing surface layer was determined for each in-service mixture according to AASHTO T 166 procedure (AASHTO T 166, 2022). The wearing surface was sawed from the top of two field cores at a visible compaction line to produce two BSG samples for each in-service mixture. The dry weight of the sample and its weight under water after being submerged for 4-5 minutes were measured. After removal from water, the sample was quickly surface-dried using a damp cloth to record its saturated surface dry weight. The BSG of each sample was then calculated using Equation 3.1 and the average value of the two samples represented the relative density of the wearing surface for each in-service mixture.

$$\text{Bulk Specific Gravity} = \frac{A}{B-C} \tag{3.1}$$

Where A = mass of dry sample (g), B = mass of saturated surface-dry sample (g), and C = mass of sample submerged in water (g).

The BSG testing procedure is shown in Figure 3.5. All BSG samples were then preserved for the determination of asphalt binder content and gradation of each in-service mixture subsequently.

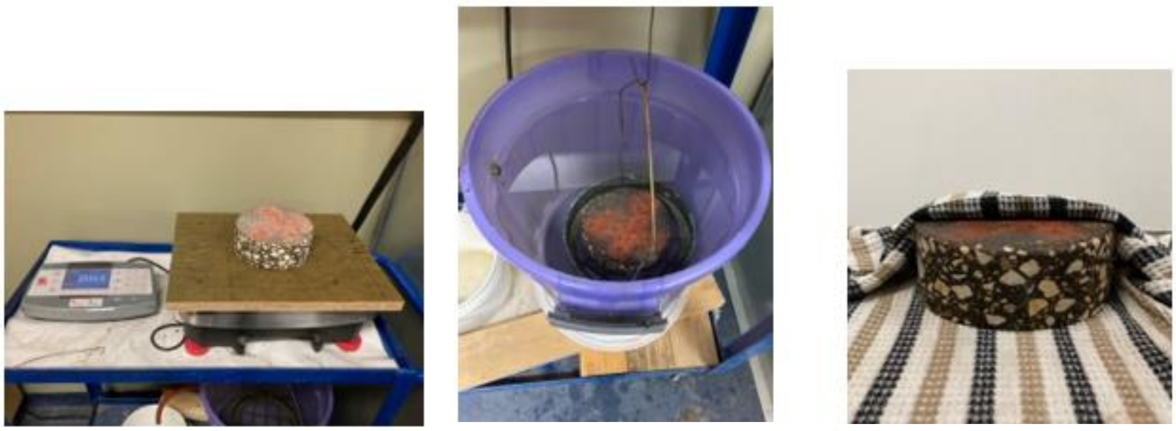

a) Measuring dry weight of field core

b) Measuring submerged weight of field core in water

c) Surface-drying the field core using a damp towel

Figure 3.5 Bulk specific gravity testing procedure of in-service mixtures

3.4 Laboratory Test Procedures

3.4.1 Hamburg Wheel-Tracking Test

The Hamburg wheel-tracking test (HWTT) was used to assess the rutting potential of fractionated RAP, plant-produced, and in-service mixtures considered in this study. It was conducted according to AASHTO T 324 procedure (AASHTO T 324, 2023). To simulate field conditions, the HWTT equipment tracks two steel wheels, each applying a load of 703 ± 4.5 N (158 ± 1.0 lb) approximately on the underlying specimen. The wheels travel back and forth over the specimen at a constant speed of 26 cycles/minute (52 passes/minute) which is equivalent to a frequency of 0.87 Hz. Eventually, the specimen deformation (i.e., rut depth) along the wheel pass is measured using linear displacement transducers throughout the test.

The HWTT test was also used to assess moisture performance of specimens; therefore, it was conducted by immersing specimens in water within the equipment tank at a designated temperature. The test temperature is not specified in AASHTO T 324 procedure; however, some Departments of Transportation (DOTs) in the United States had selected their test temperature based on the asphalt binder performance grade (West et al., 2018). Other State DOTs defined a single test temperature and altered the test criteria. The degree of stiffness of asphalt binder is very sensitive to heat; hence, the test temperature must be decided cautiously. In this study, HWTT test temperature was selected to be 45 ± 1ºC based on experiences with HWTT equipment and local HMA mixtures in Manitoba.

In addition to test temperature, AASHTO T 324 procedure does not specify any HWTT test end criteria. Previous studies have shown that HWTT test output parameters are significantly influenced by several mix design characteristics such as aggregate properties and source, binder grade and source, proportion of RAP/RAS, etc. (Rahman and Hossain, 2014). Therefore, test end criteria should be adjusted to comply with local conditions and demands of highway agencies to correlate better with rutting field performance. According to various agencies, test end criteria relies either on a maximum rut depth value at a certain number of passes/cycles or a minimum number of passes/cycles to reach a specific rut depth value (West et al., 2018). Different termination points of the HWTT test were proved to pose difficulties among the comparison of HWTT test results. As a result, rutting resistance index (RRI) was developed to overcome this difficulty. RRI considers both number of passes and rut depth at the end of the test as well as it was proved to provide a good correlation with field rut depth (Yin et al., 2020). The higher the RRI, the better the rutting resistance of an asphalt mixture and vice versa. RRI can be calculated using Equation 3.2:

$$\text{RRI} = N_{max} * (1 - RD) \quad (3.2)$$

Where N_{max} = number of passes at end of test, and RD = rut depth (inches) at end of test.

Various State DOTs have based their test end criteria mainly on the high temperature performance grade (PG) of asphalt binder used in the mix design. However, research is currently ongoing to establish widely accepted criteria that also consider various design traffic level categories (West et al., 2018). In this study, HWTT test end criteria were selected based on California and Texas State DOTs for similar PG grades of asphalt binder as the ones used in this study. Table 3.10 shows test end criteria for the two high temperature PG grades of asphalt binder considered in this study. The minimum RRI corresponding to each test end criteria was calculated by substituting the number of passes and rut depth value in Equation 3.2.

Table 3.10 HWTT test end criteria

High temperature PG grade of asphalt binder (°C)	HWTT test end criteria	Minimum RRI
58	Minimum 10,000 passes at 12.5 mm rut depth	5,000
64	Minimum 15,000 passes at 12.5 mm rut depth	7,500

During the HWTT test, the wheels apply a constant load over a 230 mm length of travel pass. The maximum rut depth can occur at any point along the full length of travel pass, but the HWTT equipment controls the test according to the rut depth measurement at midpoint only. Therefore, the maximum rut depth criterion of 12.5 mm indicates the measurement at midpoint of the length of travel pass and the HWTT test stops automatically when the maximum rut depth criterion or maximum number of passes by the equipment (i.e., 20,000) is reached.

To fabricate HWTT specimens, laboratory-produced loose asphalt mixtures had to undergo short-term conditioning according to AASHTO R 30 procedure (AASHTO R 30, 2022) prior to the

HWTT test. Fractionated RAP mixtures were short-term conditioned in an oven for 4 hours at 135°C prior to compaction. Plant-produced loose asphalt mixtures had already experienced short-term conditioning during plant mixing; thus, they were compacted directly without further conditioning. After short-term conditioning, two 150 mm diameter Superpave gyratory briquettes compacted to an air void range of 7 ± 0.5% at 150 mm height were prepared for each laboratory and plant-produced mixture. A disc of height 62 ± 2 mm was sawed from each briquette edge (top and bottom) to produce four identical discs. For field specimens, a disc of height 62 ± 2 mm was sawed from the top of four different field cores to test rut resistance of the wearing surface of each in-service mixture. Each disc was then sawed at one edge (approximately 6 mm) to create a contact surface with sufficient width for the back-and-forth motion of the steel wheel. Subsequently, two pairs of discs were aligned together to the same height at the sawed edge. When required, the slightly shorter disc was shimmed up using 1.0 mm galvanized aluminum shims to be level with the other disc during alignment. Finally, the two pairs of aligned discs were fitted in high-density polyethylene moulds and then immersed in the water tank of HWTT equipment to be preconditioned for at least 45 minutes at test temperature. Figure 3.6 shows the HWTT test setup and Figure 3.7 shows the procedure of HWTT specimen preparation.

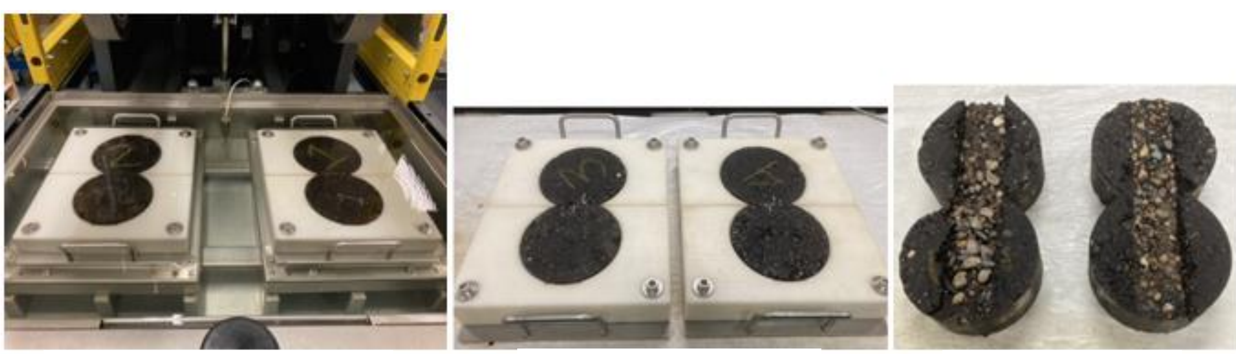

a) Specimens submerged in HWTT water tank

b) Specimens fitted in moulds before test

c) Specimens aligned after test

Figure 3.6 HWTT test setup

a) Sawing the disc from cylinder edge

b) Sawing the edge of disc for specimen alignment

c) Final shape of HWTT specimen

Figure 3.7 Procedure of HWTT specimen preparation

During the HWTT test, the specimen deformation at the center of wheel pass is measured corresponding to the number of wheel passes. The output of HWTT test is a graphical plot of the number of wheel passes versus rut depth at the center of wheel pass as shown in Figure 3.8. This plot is called an HWTT curve and represents six parameters that characterize rutting and moisture performance of an HWTT specimen as follows:

1. Post-compaction consolidation: The deformation that happens to specimens due to repeated loading in the first 1,000 wheel passes. It is caused by densification of an asphalt mixture and significant decrease in air voids.
2. Creep slope: The rate of deformation after post-compaction consolidation and prior to stripping. The resistance to deformation in this phase is mainly dependent on aggregate interlock and binder stiffness. Therefore, this phase indicates rutting potential of specimens due to plastic flow and other mechanisms away from moisture damage. The steeper the creep slope, the higher the rutting potential of a specimen and vice versa.

3. Stripping slope: Rutting resistance during this phase decreases significantly and the failure procedure is accelerated due to rapid growth rate of the rut depth. The rate of deformation during stripping phase is represented by the stripping slope, which indicates moisture susceptibility of specimens. The steeper the stripping slope, the higher the moisture susceptibility of a specimen and vice versa.
4. Stripping inflection point (SIP): The point at which moisture damage starts to take control over the performance of asphalt mixture and is represented by the number of passes at the intercept between creep and stripping slopes. It can be obtained using Equation 3.3 (all parameters are expressed in passes).

   $$\mathrm{SIP} = \frac{\text{Intercept of stripping phase} - \text{Intercept of creep phase}}{\text{Slope of creep phase} - \text{Slope of stripping phase}} \tag{3.3}$$

   According to the outcome of a study by the Iowa Department of Transportation, SIP can only be used to evaluate moisture damage potential of specimens if the ratio of stripping slope to creep slope is greater than or equal to 2 (Schram and Williams, 2012). The greater the number of passes to SIP, the more the specimen is resistant to moisture and vice versa. If the ratio of stripping slope to creep slope is less than 1, stripping is considered negligible, and SIP cannot be used to evaluate moisture damage. However, there were no actions taken if stripping to creep slope ratio is between 1 and 2.
5. Rut depth to SIP: The deformation at the center of wheel pass at SIP. It alone does not evaluate rutting nor moisture potential because the number of passes to SIP can vary significantly between asphalt mixtures.
6. Number of passes to failure: The total number of passes required to reach maximum rut depth criteria at center of wheel pass, which evaluates rutting resistance of specimens. The greater the number of passes to failure, the more rut-resistant the specimen and vice versa.

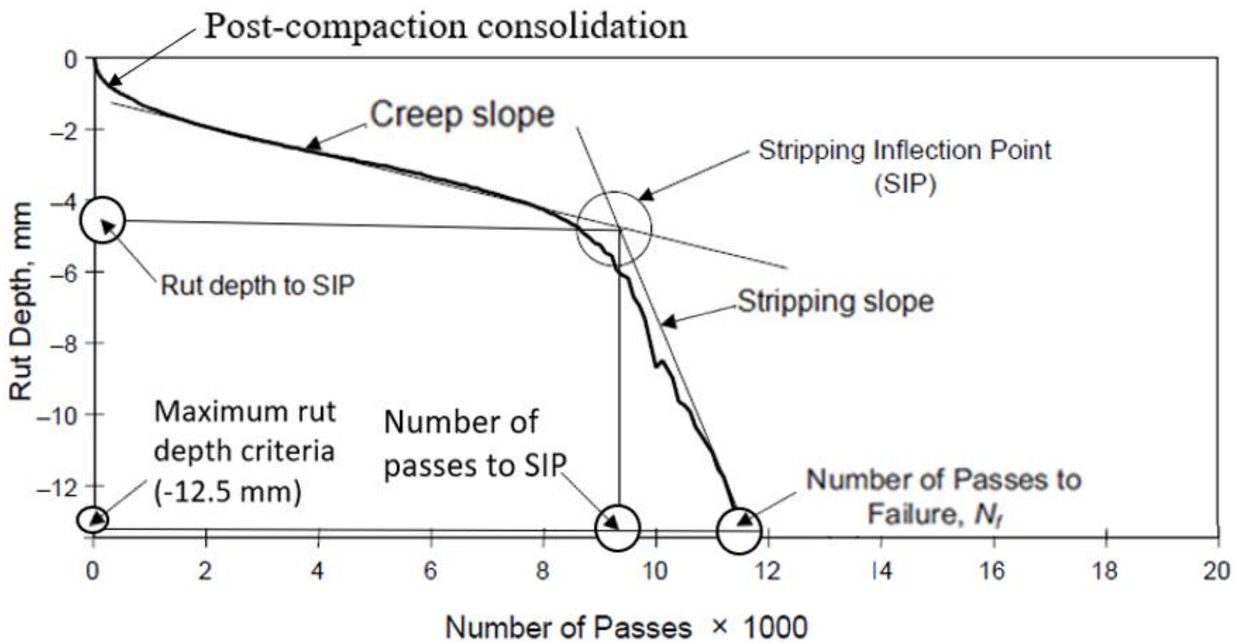

Figure 3.8 Typical HWTT curve (AASHTO T 324, 2023)

3.4.2 Illinois Flexibility Index Test

The Illinois flexibility index test (I-FIT) was used to assess the cracking potential of fractionated RAP and plant-produced mixtures considered in this study. It was conducted according to AASHTO T 393 procedure (AASHTO T 393, 2021). The I-FIT test is a reliable and robust test that was initially proposed by the University of Illinois to rank asphalt mixtures based on their cracking potential. It is derived from the semi-circular bend test where a few alterations were recommended to make the test simpler and more affordable (Ozer et al., 2016). The I-FIT fixture consists of a loading head, a steel base plate and two 25 mm diameter steel rollers. The tip of the loading head has a contact radius of 12.5 ± 0.05 mm. It is also capable of rotating around the vertical loading axis to adjust to slight specimen variations. The two steel rollers are placed on top of two V-shaped steel blocks to maintain a distance of 120 ± 0.1 mm (center to center) throughout the test. The I-FIT test setup is shown in Figure 3.9.

a) Specimen mounted on
test apparatus before test

b) Specimen mounted on
test apparatus after test

Figure 3.9 I-FIT test setup

The I-FIT test is used to evaluate the resistance of asphalt mixtures to intermediate temperature cracking; therefore, the semi-circular test specimen is conditioned at a test temperature of 25 ± 0.5ºC for 2 hours ± 10 min in a water bath or an environmental chamber prior to being mounted on the test apparatus. During the test, the loading machine applies a contact load of 0.1 ± 0.01 KN to the specimen in stroke control at a loading rate of 0.05 KN/s. When the contact load reaches 0.1 KN, the test is performed using load line displacement control at a rate of 50 mm/min. The applied load keeps increasing until the specimen can no longer withstand higher load, so a crack initiates at the tip of the notch and propagates upwards. Accordingly, the applied load starts decreasing and the test stops when the load drops below 0.1 KN.

To fabricate I-FIT specimens, two 150 mm diameter Superpave gyratory briquettes compacted to an air void range of 7 ± 0.5% at 150 mm height were prepared for each laboratory and plant-produced mixture after short-term conditioning. To determine the impact of long-term aging on cracking performance of plant-produced mixtures, half the number of briquettes (i.e., six briquettes out of twelve) did not undergo any forced-draft oven aging procedure. This means that one briquette for each plant-produced mixture was kept in its current condition (i.e., short-term conditioned). The remaining six briquettes of plant-produced mixtures as well as all briquettes of laboratory-produced mixtures were long-term conditioned in an oven at 85 ± 3ºC for 120 ± 0.5 hours according to AASHTO R 30 procedure (AASHTO R 30, 2022). Subsequently, two identical discs of thickness 50 ± 1 mm were sawed from the middle of each briquette and each disc was then split into two identical halves to create semi-circular I-FIT replicates. Finally, a notch of depth 15 ± 1 mm and width 2.25 mm was cut using a tile-saw in the middle of the flat side of each semi-circular specimen. The purpose of the notch is to determine the point of crack initiation during the test. Overall, four identical semi-circular I-FIT specimens were obtained from a single Superpave gyratory compacted asphalt briquette. Figure 3.10 shows the procedure of I-FIT specimen preparation and Figure 3.11 shows cutting locations and dimensions of I-FIT specimens.

a) Cutting into discs

b) Cutting discs into halves

c) Cutting the notch

Figure 3.10 Procedure of I-FIT specimen preparation

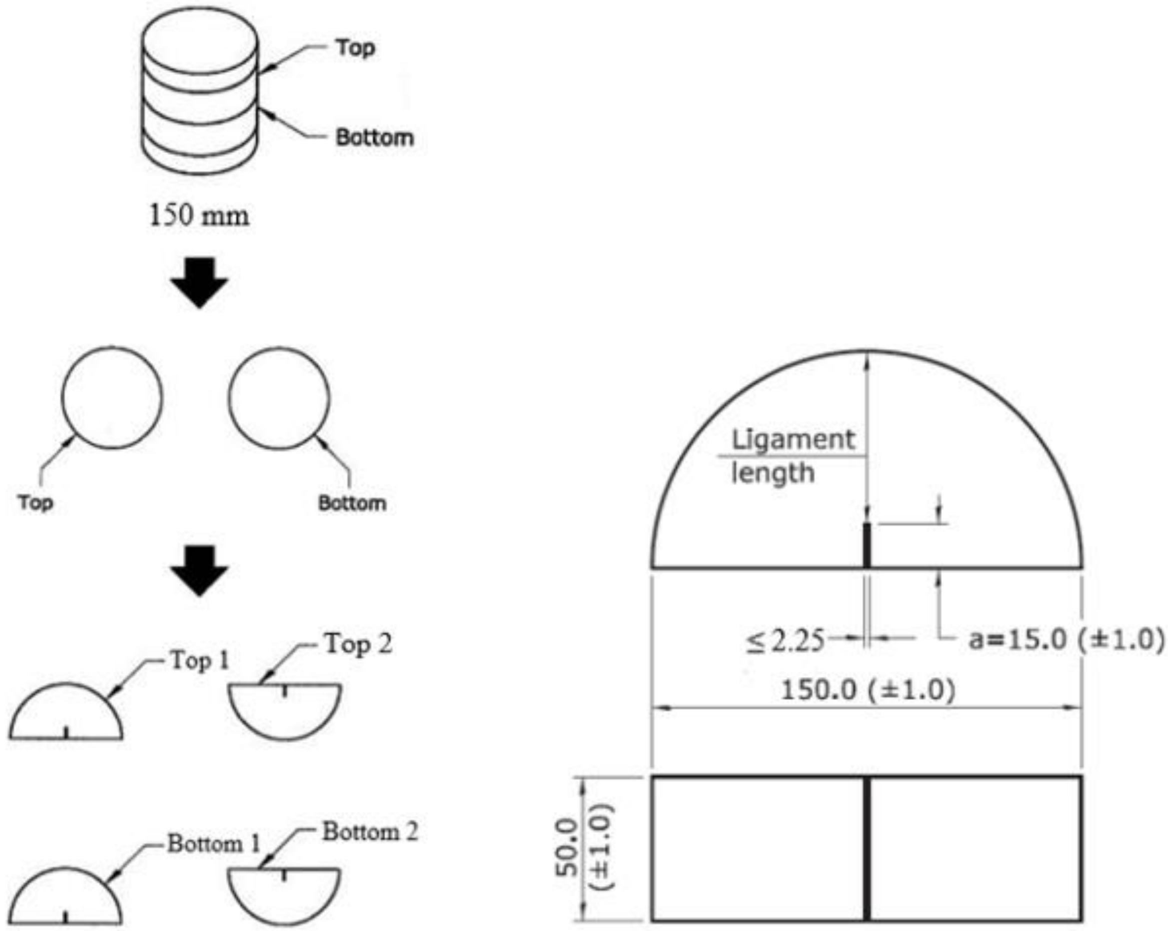

a) Specimen cutting locations

b) Specimen dimensions (mm)

Figure 3.11 I-FIT specimen cutting locations and dimensions (AASHTO T 393, 2021)

During the I-FIT test, the load line displacement is measured corresponding to the load applied to the specimen. The output of the I-FIT test is a graphical plot called load-displacement curve as shown in Figure 3.12. This curve represents six parameters that characterize cracking performance of an I-FIT specimen as follows:

1. Peak load: The maximum load applied to an I-FIT specimen during the test.
2. Tensile strength: The peak load divided by the cross-sectional area of an I-FIT specimen opposite to the curved edge (i.e., the flat side shown at the bottom of Figure 3.11b). Since I-FIT specimens have similar dimensions (thus, cross-sectional area), a higher peak load

always results in a higher tensile strength value. Both peak load and tensile strength can be used to indicate stiffness of an asphalt mixture. The higher the peak load and tensile strength value, the stiffer the asphalt mixture and vice versa. Tensile strength can be obtained using Equation 3.4.

$$\text{Tensile strength (KPa)} = \frac{\text{P}}{2\text{rt}} \tag{3.4}$$

Where P = maximum load (KN), r = radius of specimen (mm), and t = thickness of specimen (mm).

3. Post-peak slope: The slope of the tangential curve at the first inflection point after peak load on the load-displacement curve. It indicates the rate of energy dissipation of a material. The steeper the post-peak slope, the higher the rate of energy dissipation of a material (i.e., brittle material), whereas a low post-peak slope indicates a ductile material. Post-peak slope can be used in conjunction with peak load and tensile strength to predict rutting resistance of an asphalt mixture. A higher post-peak slope as well as peak load and tensile strength value indicates an asphalt mixture with high rutting resistance.
4. Critical displacement: The intercept between post-peak slope and displacement axis. Intuitively, it is inversely related to post-peak slope where a higher post-peak slope yields a lower critical displacement value and vice versa. It can also be used to indicate ductility of a material.
5. Fracture energy: The total energy required to fail an I-FIT specimen completely. It is determined by dividing the total area under load-displacement curve (work of fracture) by the fracture area of an I-FIT specimen. The fracture area is ligament length (Figure 3.11b) multiplied by thickness of specimen. Fracture energy is highly dependent on both peak load and post-peak slope. It can be obtained using Equation 3.5.

$$G_f = \frac{W_f}{(r-a)t} * 10^6 \tag{3.5}$$

Where G_f = fracture energy (J/m^2), W_f = work of fracture (J), and a = notch depth (mm).

6. Flexibility index: The fracture energy divided by post-peak slope of an I-FIT specimen. It is the main indicator of cracking resistance and can be obtained using Equation 3.6. The higher the flexibility index, the better the cracking resistance and vice versa.

$$\text{Flexibility index} = \frac{G_f}{|m|} * A \tag{3.6}$$

Where |m| = absolute value of post-peak slope, and A = unit conversion and scaling factor equal to 0.01.

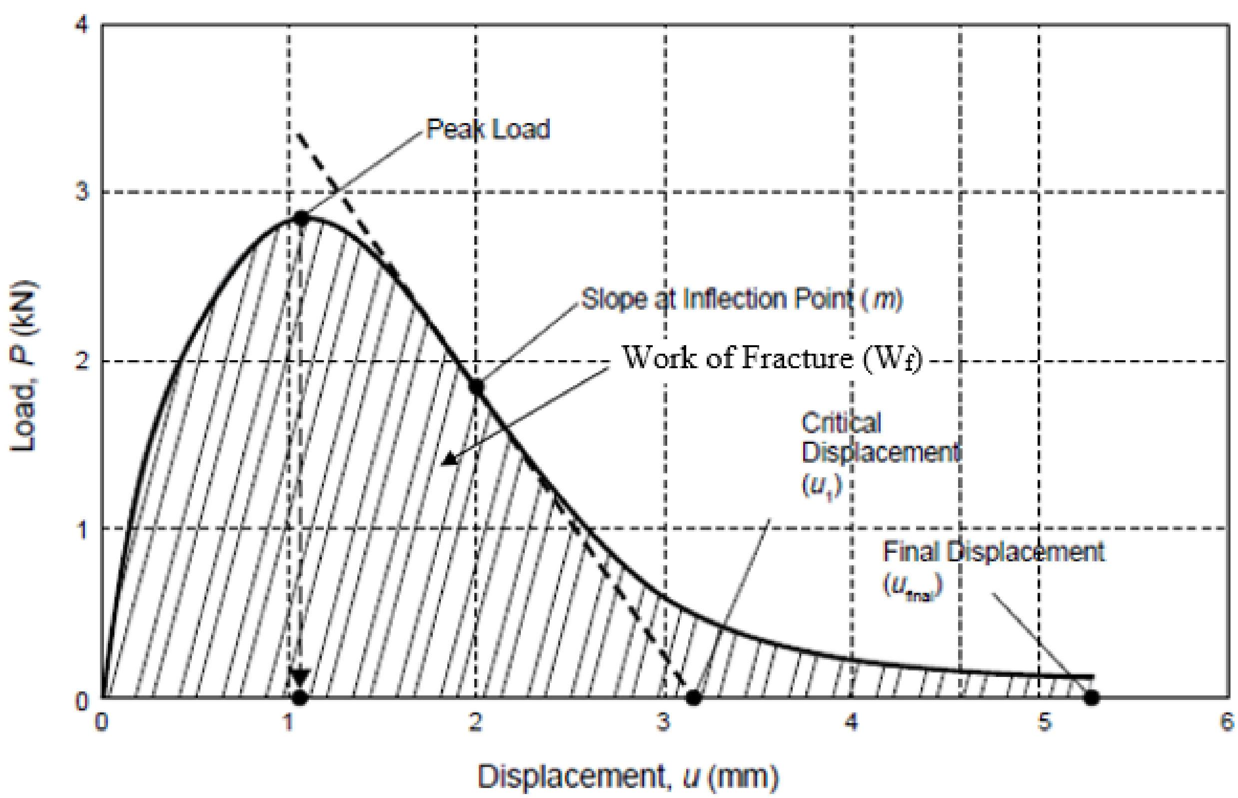

Figure 3.12 Typical load-displacement curve (AASHTO T 393, 2021)

3.4.3 Dynamic Modulus Test

The dynamic modulus test (DMT) was used to evaluate the stiffness of fractionated RAP, plant-produced, and in-service mixtures considered in this study. It was conducted according to

AASHTO T 342 procedure (AASHTO T 342, 2022). The stiffness of an asphalt mixture is represented by its dynamic modulus which is the absolute value of its complex modulus. The complex modulus represents the viscoelastic nature of an asphalt mixture by measuring its resistance to axial deformation under sinusoidal loading. It is determined from the maximum applied stress and the peak recoverable axial strain (Cao et al., 2016). Laboratory testing had proved that the magnitude of recoverable strain varies according to temperature in constant loading conditions (Uzan, 2003). In addition, the presence of a time lag between the applied stress and induced strain (i.e., phase angle) makes the behaviour of asphalt mixtures dependent on time. Both stress and strain are defined by time and angular frequency; therefore, frequency is also time dependent. As a result, the dynamic modulus value of asphalt mixtures is largely dependent on temperature and frequency (Uzan, 2003).

The DMT test was conducted over a range of testing temperatures and loading frequencies. A uniaxial hydraulic machine was used to apply a sinusoidal compressive stress to cylindrical test specimens under six loading frequencies (0.1, 0.5, 1, 5, 10 and 25 Hz). The test was conducted inside an environmental chamber and a liquid nitrogen tank was used to control four testing temperatures (-10, 4.4, 21.1 and 37.8°C). The test specimen was placed in between two loading platens at the top and bottom to ensure that the compressive load applied by the piston is equally distributed over the sample surface area. In addition, a membrane that acts as a friction reducer was placed between the sample surface area and loading platen at both ends. Figure 3.13 shows the DMT test setup for two types of cylindrical test specimens, full-size and small-scale specimens.

a) Full-size specimen

b) Small-scale specimen

Figure 3.13 DMT test setup

In this study, all DMT specimens prepared for assessing the stiffness of fractionated RAP and plant-produced mixtures were full-size specimens as shown in Figure 3.13a. Full-size specimens are asphalt cylinders of diameter 100 mm and height 150 mm extracted from the center of Superpave gyratory compacted briquettes of diameter 150 mm and height 170 mm (Figure 3.15a). After short-term conditioning, loose asphalt mixtures were compacted to an air void range of 7 ± 0.5% at 170 mm height in a Superpave gyratory compactor. AASHTO T 342 procedure does not specify a range of air voids for DMT specimens, since the air void content of a full-size specimen is 1.5 - 2.5% lower than the gyratory compacted briquette. However, loose asphalt mixtures had to be compacted to a constant range of air voids to provide a fair comparison between DM results. Therefore, an air void range of 7 ± 0.5% was selected to conform to other performance tests considered in this study. Subsequently, the gyratory compacted briquette was fixed using a clamp and a full-size specimen was cored from the center using a 100 mm diameter core drill. The cored cylinder was then trimmed by 9 mm from both ends using a saw and another 1 mm was ground at each end using a cylinder end grinder to produce a full-size specimen of height 150 mm with smooth and parallel top and bottom surfaces. Figure 3.14 shows the procedure of full-size DMT specimen preparation.

a) Coring a 100 mm diameter specimen

b) Sawing to trim both ends

c) Grinding to smoothen both ends

Figure 3.14 Procedure of full-size DMT specimen preparation

On the other hand, all DMT specimens prepared for assessing the stiffness of in-service mixtures were small-scale specimens as shown in Figure 3.13b. Due to insufficient thickness of the wearing surface at the top of field core, full-size specimens were not a feasible alternative for conducting the DMT test. Therefore, the field core was fixed using a clamp and a small-scale specimen was cored laterally through the wearing surface using a 50 mm diameter core drill (Figure 3.15b). Similarly, the cored cylinder was sawed and ground equally at both ends to produce a small-scale specimen of height 110 mm with smooth and parallel top and bottom surfaces.

During the DMT test, three vertical extensometers have to be mounted between gauge points at three locations 120 degrees apart on full-size and small-scale specimens to measure axial deformations. Gauge lengths are 100 mm for full-size specimens and 70 mm for small-scale specimens. Consequently, six gauge studs were glued (two at each location) on all specimens to satisfy the gauge lengths stipulated in AASHTO T 342 procedure. Figure 3.15 shows the coring locations and dimensions of final full-size and small-scale specimens prepared for the DMT test.

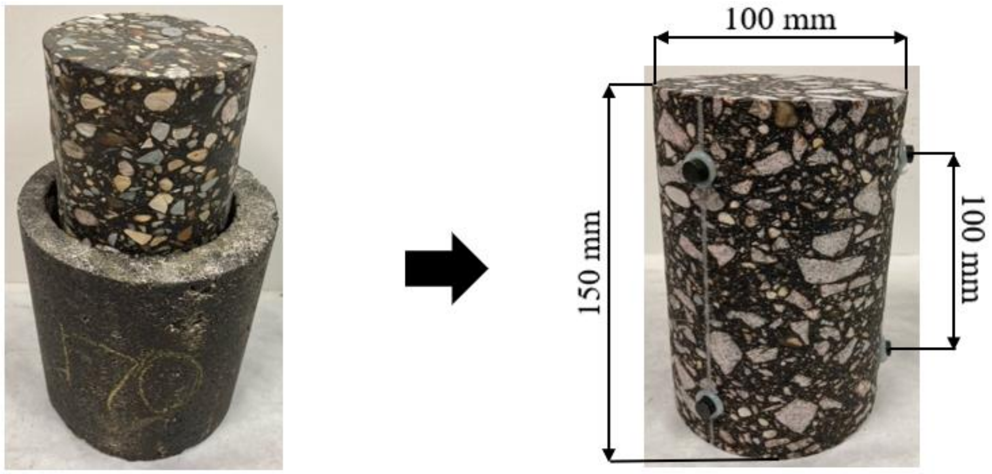

a) Full-size specimen

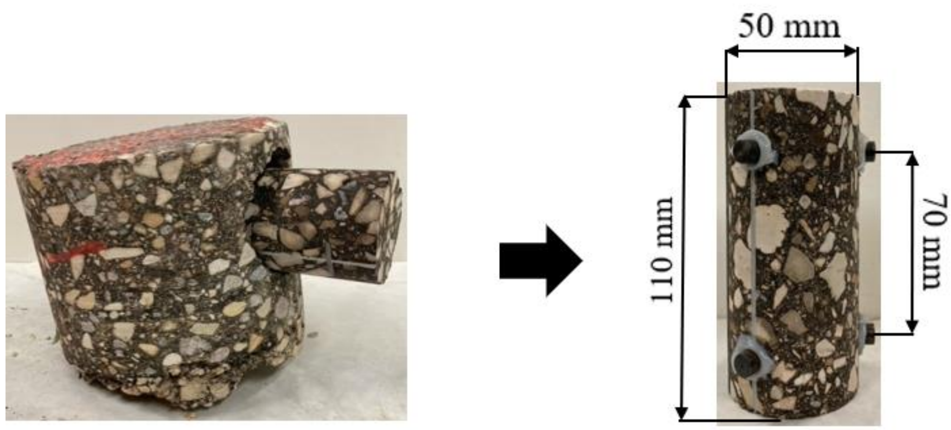

b) Small-scale specimen

Figure 3.15 Coring locations and dimensions of full-size and small-scale DMT specimens

After the DMT test was performed, dynamic modulus values were calculated for each specimen based on the average stresses and strains of the final five cycles at each test temperature and loading frequency. Subsequently, the average dynamic modulus values of specimens in each mixture were combined to construct a dynamic modulus master curve according to AASHTO PP 62 procedure (AASHTO PP 62-10, 2012). As a result, the DMT test results of mixtures were compared over a wider range of temperatures and loading frequencies. Figure 3.16 shows a typical

DM master curve which represents the stiffness of an asphalt mixture on a log-log scale over a range of reduced frequencies.

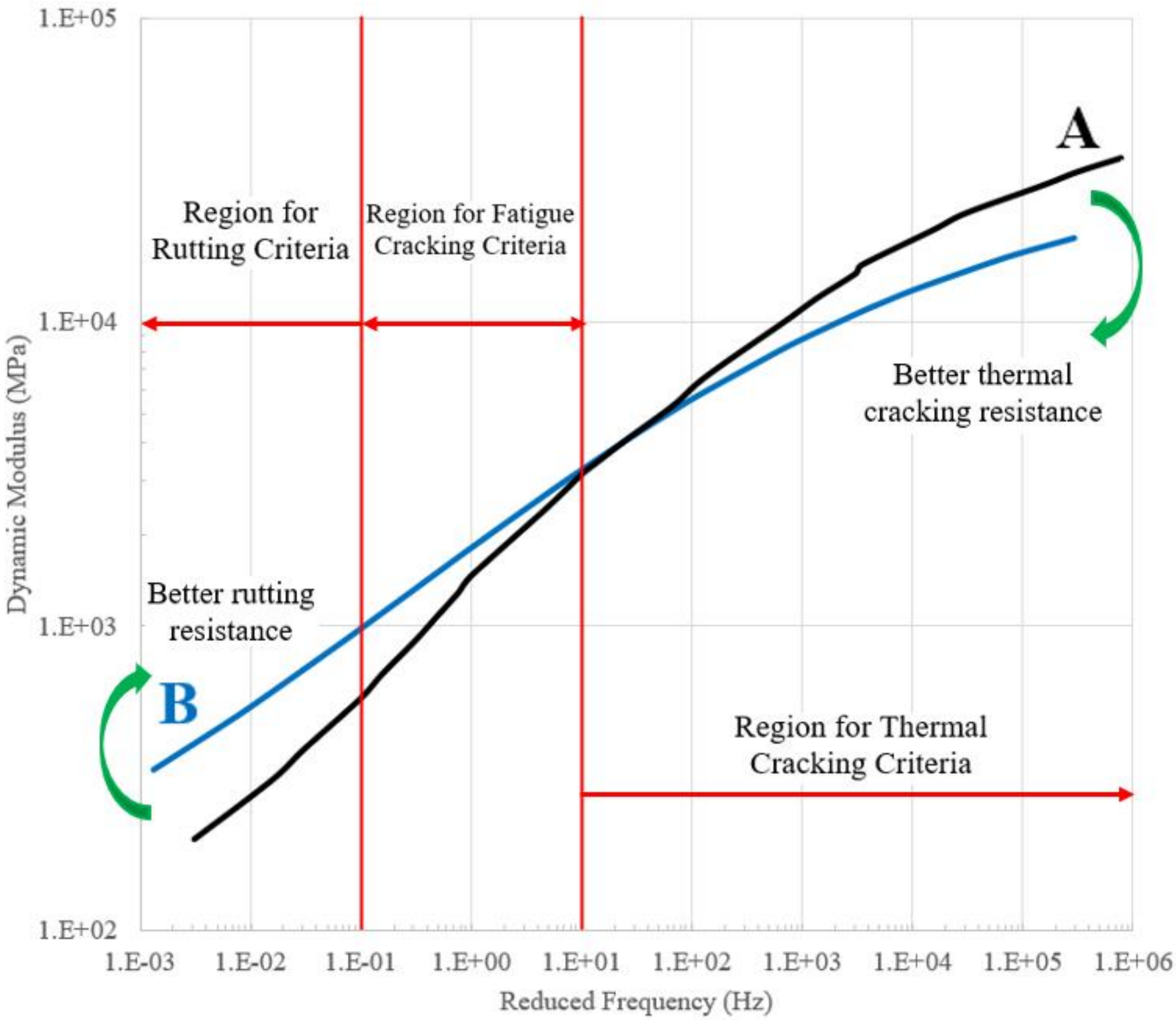

Figure 3.16 Typical dynamic modulus master curve

The right side of DM master curve is the region that represents thermal cracking criteria since it shows stiffness of asphalt mixtures at low temperatures and high frequencies, whereas the left side is the region that represents rutting criteria since it shows stiffness at high temperatures and low frequencies. The middle part is the region that represents fatigue cracking criteria since it shows stiffness at intermediate temperatures and frequencies. Asphalt binders tend to become softer at higher temperatures; hence, it is preferable to have a stiffer pavement to resist deformation due to traffic loads. On the other hand, stiff pavements are not a desirable option at low and intermediate temperatures. Stiff pavements are more brittle; thus, they are more prone to thermal and fatigue cracking at low and intermediate temperatures, respectively. Therefore, it can be concluded from Figure 3.16 that master curve B shows better performance than master curve A at both high and low temperatures. Master curve B has higher dynamic modulus values at high temperatures (i.e., more rut resistant) and lower dynamic modulus values at low temperatures (i.e., more thermal cracking resistant). However, master curve A shows better performance than master curve B at intermediate temperatures due to lower dynamic modulus values (i.e., more fatigue cracking resistant). As a result, it is significant to assess the dynamic modulus of asphalt mixtures at high, low, and intermediate temperatures.

To construct a DM master curve according to AASHTO PP 62 procedure, Equation 3.7 presents the sigmoid function included in the Mechanistic Empirical Pavement Design Guide and the general form for DM master curve.

$$\log|E^*| = \delta + \frac{\alpha}{1+e^{\beta+\gamma\log f_r}} \tag{3.7}$$

Where $|E^*|$ = dynamic modulus (Psi), f_r = reduced frequency (Hz), and α, β, γ, and δ = fitting coefficients.

There are several time-temperature shift functions available in literature to compute the reduced frequency using time-temperature shift factors. In this study, the reduced frequency was calculated using the second-order polynomial shift factor function presented in Equation 3.8. The final form of DM master curve equation can then be attained by substituting the second-order polynomial shift factor function into Equation 3.7.

$$\log f_r = \log f + a_1(T_r - T) + a_2(T_r - T)^2 \tag{3.8}$$

Where f_r = reduced frequency at reference temperature (Hz), f = loading frequency at test temperature (Hz), T_r = reference temperature (°F), T = test temperature (°F), and a_1 and a_2 = fitting coefficients.

In the next step, numerical optimization is performed using “Solver” function in Microsoft Excel to calculate the fitting coefficients that will minimize the sum of squared errors between predicted and measured dynamic modulus values. Then, the DM master curve is fitted and evaluated at a selected reference temperature of 21.1°C (70°F).

3.4.4 Ignition Oven Test

The ignition test method was used to determine the asphalt binder content of each in-service mixture as well as the two RAP fractions of the fractionated RAP study. The test followed AASHTO T 308 procedure (AASHTO T 308, 2022) and was also used to obtain recovered aggregates for gradation analysis of each in-service mixture as well as the two RAP fractions (coarse and fine RAP). Asphalt binder content is a significant property that can impact asphalt mixture performance in terms of cracking, rutting, moisture susceptibility and raveling. Therefore, the ignition test method is a critical experiment for quality assurance and pavement forensic investigations. The ignition oven is equipped with an internal balance to measure weight loss of a sample during the test. In the ignition test method, an oven-dry sample of loose asphalt mixture is heated in a furnace to burn off the asphalt binder. The weight difference between the oven-dry loose asphalt mixture and residual aggregate represents the asphalt binder content within the mixture. It is then expressed as a weight percentage of the oven-dry loose asphalt mixture.

There is no standard practice currently available for using the ignition oven to determine the asphalt binder content of field cores; however, the Ministry of Transportation in Ontario had proposed in their laboratory testing manual (LS-292, 2001) that the outer edges of a field core should be removed prior to conducting the ignition oven test according to AASHTO T 308 procedure. This will help exclude the aggregates damaged due to coring/sawing from the sieve analysis procedure. As a result, the two bulk specific gravity samples of each in-service mixture were softened by heating at 110 ± 5°C to enable trimming of the outer 10 mm thickness of the circumference. Although no trimming depth was specified in LS-292 (2001), 10 mm was found to be a sufficient depth to eliminate all the peripheral sawed aggregate material. Subsequently, the remaining material from the two samples (after trimming) was combined and oven-dried at 110 ± 5°C to produce a 1.5 - 2.5 kg sample of loose asphalt material from each in-service mixture. For the RAP stockpile, a 1.5 - 2.5 kg oven-dry sample of loose coarse and fine RAP material was prepared after fractionation through sieve no. 4 (4.75 mm). The oven-dry sample of loose asphalt mixture was then distributed evenly on two ignition baskets and placed in the ignition furnace heated previously to 538°C.

During the ignition oven test, the temperature, mass loss in grams (g), and percentage mass loss were recorded every minute. The test was completed when the recorded percentage mass loss did not exceed 0.01% for three consecutive minutes. The sample (which is now recovered aggregate) was then removed from the ignition oven and left to cool down at room temperature. Finally, the asphalt binder content was calculated for each in-service mixture and the two RAP fractions using the recorded values of initial and final mass. Figure 3.17 shows the ignition oven as well as a coarse RAP sample before and after the test.

a) Open ignition furnace showing internal balance

b) Coarse RAP sample distributed on ignition basket before test

c) Recovered coarse RAP aggregates on ignition basket after test

Figure 3.17 Ignition oven test setup

Despite the simplicity of conducting the ignition oven test, there is a major limitation associated with this test method. The type of aggregate as well as the ignition furnace may influence the asphalt binder content in the mixture. A small amount of aggregate mass loss has been noticed during the burning process of asphalt binder; hence, the difference between the initial and final mass of sample is not reflected by the asphalt binder content only. Consequently, the asphalt content predicted by the ignition test method will be larger than the actual asphalt content in the mixture. To overcome this issue, a correction factor was assumed to account for the aggregate mass loss and obtain a better estimate of the asphalt binder content. Correction factors typically range from 0 to 0.5% depending on the type of aggregate (Brown et al., 1995). In this study, a correction factor of 0.5% was assumed for all samples to ensure consistency among the calculated asphalt binder contents.

3.4.5 Sieve Analysis

After the ignition oven test, sieve analysis was conducted on the residual aggregate of each in-service mixture as well as coarse and fine RAP fractions according to AASHTO T 27 procedure

(AASHTO T 27, 2023). A set of nine sieves (19 mm, 16 mm, 12.5 mm, 9.5 mm, No. 4, No. 10, No. 40, No. 80, and No. 200) were placed in a mechanical shaker (Figure 3.18b) for 20 minutes to perform the test procedure. Finally, the weight of aggregate retained on each sieve was measured using a balance and the percentages of passing from each sieve were calculated to determine the gradation. Figure 3.18 shows the gradation test setup.

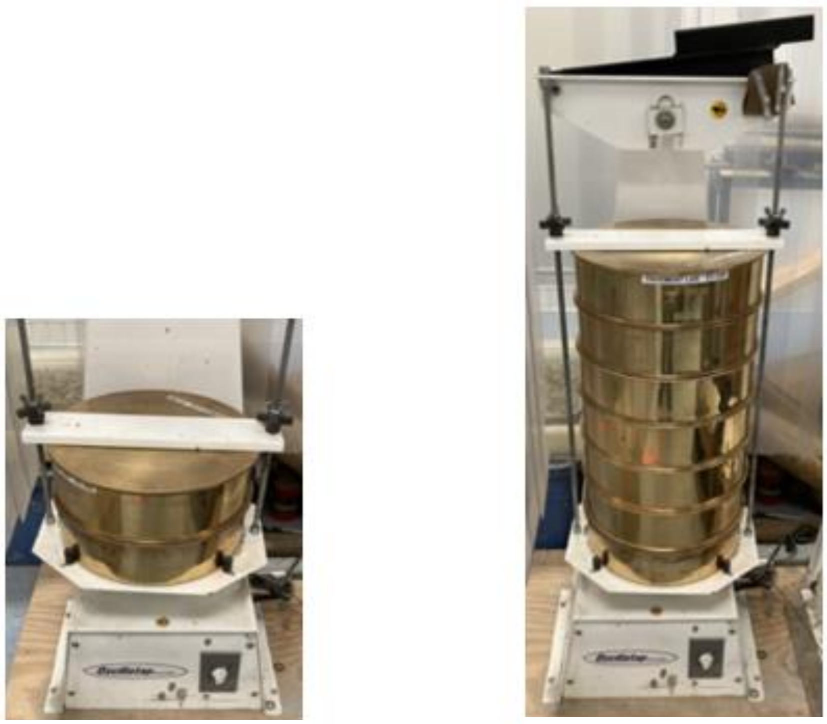

a) RAP fractionation b) Sieve analysis

Figure 3.18 Gradation test setup

Chapter 4. Evaluation of Fractionated RAP Mixtures

4.1 Introduction

This chapter includes a balanced mix design (BMD) framework of five groups of laboratory-produced fractionated HMA-RAP mixtures. The main objective of this study was to utilize RAP fractionation technology to allow for higher RAP consumption as well as to improve the BMD in an effort for moving towards sustainable pavement construction. To fulfill this objective, volumetric properties of the five mix groups were initially explained. Then, their cracking and rutting performance as well as dynamic modulus values were analyzed, discussed, and compared. Moreover, statistical analysis including analysis of variance (ANOVA), Tukey's honestly significant difference (HSD) test, and independent t-test were applied when needed in the analysis.

4.2 Volumetric Properties

The volumetric properties of the five fractionated HMA-RAP mixtures are presented in Table 4.1. The optimum asphalt content (OAC) shows a decreasing trend as RAP proportions increase. The amount of fine material in RAP contributes to a proportion of total air voids in the mix that need to be filled with asphalt binder; hence, lower OAC is observed at higher RAP percentages. Therefore, the 50% coarse RAP mix had the least OAC of all the five mixtures. Furthermore, Table 4.1 shows that asphalt absorption increases as RAP proportions increase. RAP aggregates usually have a small proportion of inactive RAP binder that forms part of the aggregate rock itself; thus, RAP mixes have higher absorption values than the virgin mix (Gottumukkala et al., 2018). Both lower OAC and higher asphalt absorption lead to lower effective asphalt content for RAP mixes.

Table 4.1 also shows that RAP binder contribution to OAC increases at higher RAP proportions, whereas the relationship is reversed for virgin binder contribution to OAC. Moreover, RAP binder ratios can describe RAP content in fractionated RAP mixes differently. The exclusion of fine RAP and low AC of coarse RAP can classify 30% and 40% coarse RAP mixes as mixes with low RAP content in terms of RAP binder ratio. RAP binder ratios were also used to interpolate the blended binder PG grades of the four RAP mixes. The low temperature grade of the four RAP mixes was higher than that of the virgin mix, whereas the high temperature grade experienced an increase in the 50% coarse RAP mix only. Generally, all blended binder PG grades of RAP mixes were stiffer than that of virgin binder.

Table 4.1 Volumetric properties of fractionated HMA-RAP mixtures

Property	Specification limits[1]	Virgin mix	10% RAP	30% Coarse RAP	40% Coarse RAP	50% Coarse RAP
Optimum asphalt content (%)	–	5.50	5.00	5.00	5.00	4.50
Asphalt content from virgin binder (%)	–	5.50	4.55	4.10	3.80	3.00
Asphalt content from RAP (%)	–	0.00	0.45	0.90	1.20	1.50
RAP binder ratio (%)	–	0.00	9.00	18.0	24.0	33.3
Blended binder PG grade	–	58-34	58-28	58-28	58-28	64-22
Air voids (%)	4.0	4.20	4.30	4.10	3.70	4.70
Voids in mineral aggregate (%)	14 Minimum	15.9	14.7	14.3	13.6	13.2
Voids filled with asphalt (%)	65 – 78	73.8	70.6	71.0	73.1	64.6
Asphalt absorption (%)	–	0.36	0.50	0.63	0.72	0.85
Effective asphalt content (%)	–	5.16	4.53	4.40	4.31	3.68
Dust to binder ratio	0.6 – 1.2	0.79	1.06	1.07	1.14	1.38

1. Source: City of Winnipeg, 2020

In Table 4.1, the percentage of air voids for all mix groups comply with the target range of 4 ± 0.5% except the 50% coarse RAP mix which had a higher air void content due to low OAC. In addition, voids in mineral aggregate (VMA) of 40% and 50% coarse RAP mixes did not satisfy minimum requirements. Accurate VMA values rely primarily on accurate determination of specific gravity of aggregates. Nevertheless, it is difficult to accurately determine the specific gravity of RAP aggregates due to modification of aggregate properties (Al-Qadi et al., 2012). Therefore, a tolerance of 1% was given to minimum VMA requirement in this study. The quantity of fine material in RAP led to a reduction in VMA, but an increase in dust to binder ratio of RAP mixes. Intuitively, the decrease in VMA also led to a decrease in voids filled with asphalt (VFA) of RAP mixes. As a result, both VFA and dust to binder ratio of 50% coarse RAP mix did not adhere to specification limits, and no mix with more than 50% RAP content was considered for performance evaluation in this study.

4.3 Hamburg Wheel-Tracking Test Results

The Hamburg wheel-tracking test (HWTT) was conducted according to AASHTO T 324 procedure (AASHTO T 324, 2023) to investigate rutting and moisture potential of the fractionated HMA-RAP mixtures. Two samples of paired laboratory compacted cylinders were tested for each mix simultaneously in one test, and the output from each wheel represented the results of a single sample. Figure 4.1 shows the HWTT test curves and Table 4.2 shows the HWTT test output parameters of the five fractionated HMA-RAP mixture groups.

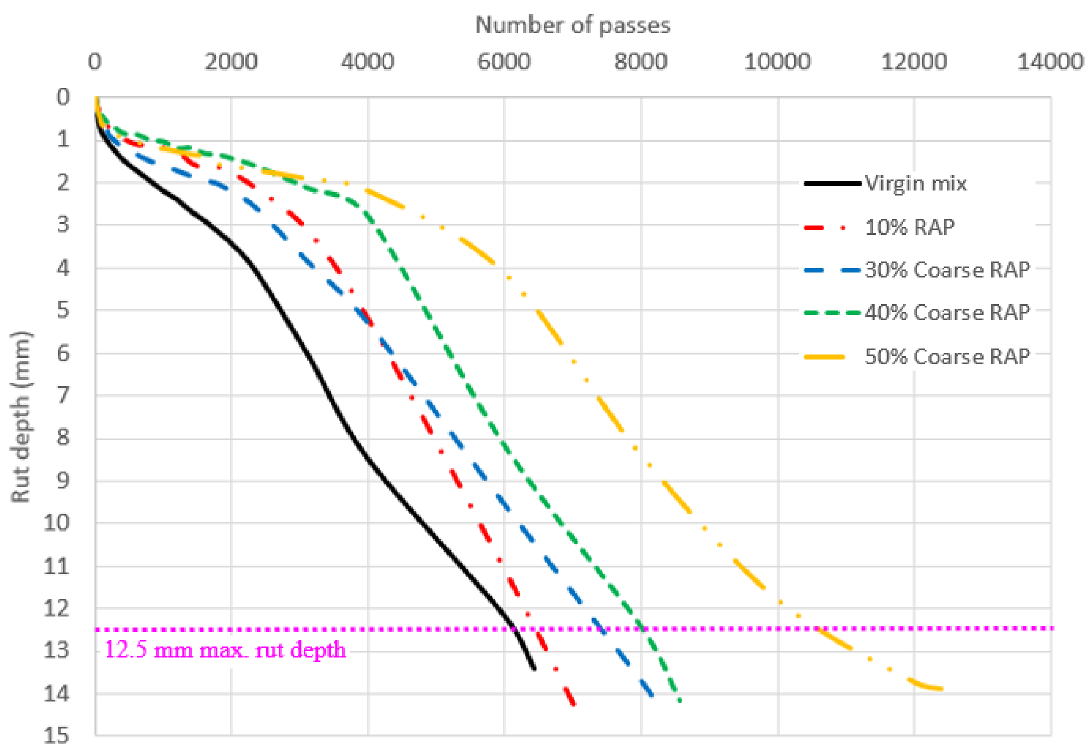

Figure 4.1 HWTT test curves of fractionated HMA-RAP mixtures

Table 4.2 HWTT test results of fractionated HMA-RAP mixtures

Mix	Sample	Creep Slope (mm/pass)	Stripping Slope (mm/pass)	Number of passes to SIP	Rut depth to SIP (mm)	Number of passes to failure (12.5 mm)	Ratio of stripping to creep slope
Virgin mix	1	0.000558	0.004296	3,143	2.73	5,767	7.7
	2	0.001139	0.002817	2,263	3.64	5,941	2.5
	Average	0.000849	0.003557	2,703	3.19	5,854	5.1
10% RAP	1	0.000623	0.003333	3,624	2.67	7,024	5.3
	2	0.000477	0.002959	3,072	2.25	7,043	6.2
	Average	0.000550	0.003146	3,348	2.46	7,034	5.8
30% Coarse RAP	1	0.000510	0.002080	2,597	2.45	8,150	4.1
	2	0.000713	0.002386	2,630	3.00	7,241	3.3
	Average	0.000612	0.002233	2,614	2.73	7,696	3.7
40% Coarse RAP	1	0.000662	0.001833	3,496	3.36	9,301	2.8
	2	0.000419	0.002448	3,711	2.22	8,524	5.8
	Average	0.000541	0.002141	3,604	2.79	8,913	4.3
50% Coarse RAP	1	0.000272	0.002514	5,818	2.60	10,353	9.2
	2	0.000309	0.002480	5,449	2.65	10,026	8.0
	Average	0.000291	0.002497	5,634	2.63	10,190	8.6

Table 4.2 shows that all samples had a ratio of stripping to creep slope greater than 2. This means that all samples had experienced stripping and HWTT results can be used to compare moisture susceptibility of mixes. Table 4.2 also shows that creep and stripping slopes decrease as RAP proportions increase. This means that higher RAP mixtures are more resistant to rutting and moisture damage. Nevertheless, the 30% coarse RAP mix had a higher creep slope than the 10% RAP mix despite being able to withstand greater number of passes to failure. Similarly, the 50% coarse RAP mix had a higher stripping slope than 30% and 40% coarse RAP mixes despite being able to withstand greater number of passes to failure. This deduces that creep and stripping slopes alone cannot be used to identify rutting resistance of a specimen.

Both Figure 4.1 and Table 4.2 clearly show that the five fractionated HMA-RAP mixtures had experienced stripping as well as had reached a maximum rut depth of 12.5 mm at the end of the HWTT test. Due to similar termination points of the HWTT test, the calculation of rutting resistance index (RRI) was not required to compare the HWTT test results. Consequently, Figure 4.2 compares the HWTT test results of the five mixtures in terms of the average number of passes to failure and SIP. The minimum criteria for rutting resistance are also displayed on Figure 4.2, whereas there are still no criteria developed for moisture susceptibility in the HWTT test.

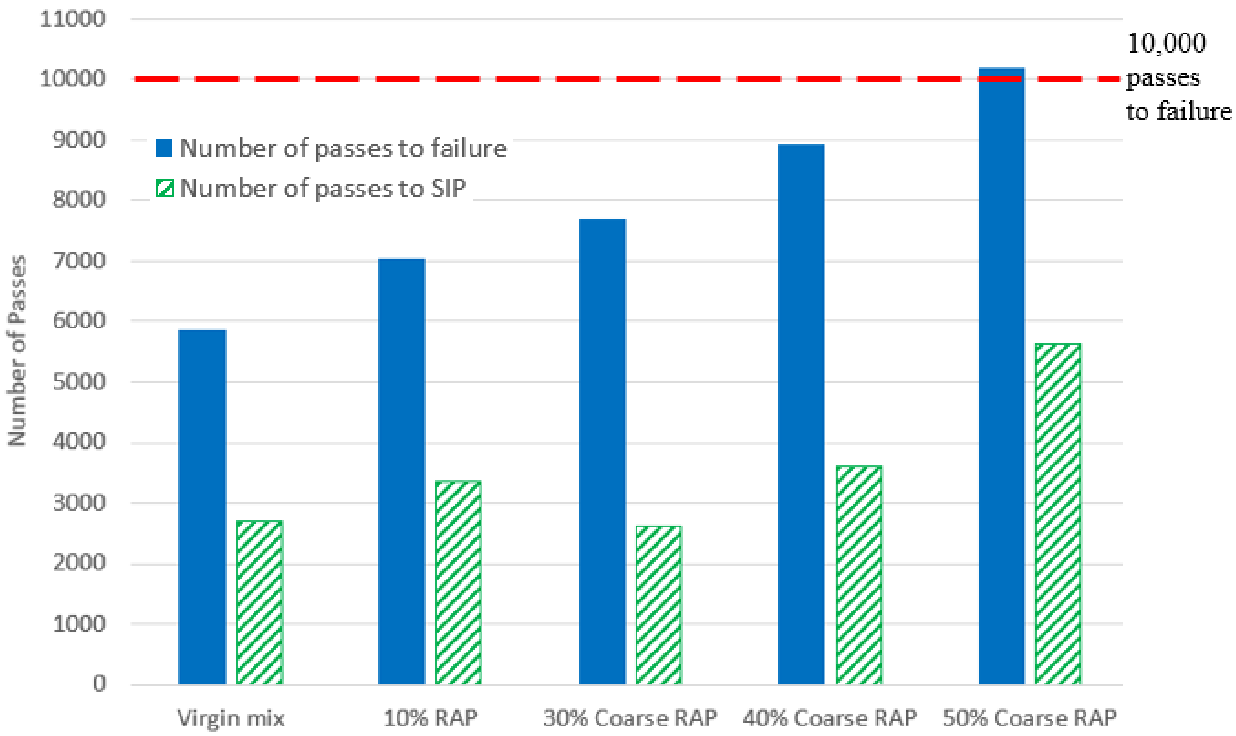

Figure 4.2 Average number of passes to failure and SIP of fractionated HMA-RAP mixtures

Figure 4.2 shows that all mixtures had reached maximum rut depth measurement (i.e., 12.5 mm) at number of passes less than 10,000 except the 50% coarse RAP mix. This means that the 50% coarse RAP mix was the only successful mix in terms of rutting resistance criteria. In addition, rutting resistance showed an increasing trend with higher proportions of RAP. The contribution of RAP binder to total binder content stiffens the mix leading to lower rutting potential. Also, the reduction in total binder content and effective asphalt content with higher RAP proportions leads to better rutting resistance. Consequently, virgin mix (i.e., the mix with highest total binder and effective asphalt content) experienced the least rutting resistance prior to SIP. Figure 4.2 also shows that the number of passes to SIP had an increasing trend with higher proportions of RAP like number of passes to failure. This is mainly due to better adhesion between aggregates and RAP binder which minimizes segregation under action of water. Moreover, RAP aggregates have an inactive layer of RAP binder that makes them act as black rock within the mix (Gottumukkala et al., 2018). This phenomenon is more dominant in fine RAP aggregates which have a higher RAP binder content. Consequently, the 10% RAP mix (which is the only mix containing fine RAP) is more resistant to moisture than the 30% coarse RAP mix.

Table 4.3 shows the independent t-test results at 95% confidence level of the two HWTT test output parameters which represent rutting and moisture resistance. Predominantly, mixture groups with a major difference in RAP content showed a statistically significant difference in terms of number of passes to failure. Moreover, the 50% coarse RAP mixture group had a statistically significant difference in terms of number of passes to SIP with all other mixture groups. These two outcomes suggest that minor changes in RAP content might not be influential on rutting and moisture performance of HMA mixtures as much as major changes in RAP content. This can be attributed to most mixtures falling into one category with weak rutting and moisture resistance; hence, results are not comparable. It is also recommended to use a larger number of specimens in each mixture group to reinforce the outcome of the independent t-test.

Table 4.3 Independent t-test of HWTT test output parameters

Parameter		Number of passes to SIP	Statistically significantly different	Number of passes to failure	Statistically significantly different
Critical T-value[1]		4.303	–	4.303	–
Calculated T-value	Virgin mix and 10% RAP mix	1.242	NO	13.477	YES
	Virgin mix and 30% Coarse RAP mix	0.203	NO	3.979	NO
	Virgin mix and 40% Coarse RAP mix	1.988	NO	7.682	YES
	Virgin mix and 50% Coarse RAP mix	6.142	YES	23.409	YES
	10% RAP mix and 30% Coarse RAP mix	2.656	NO	1.456	NO
	10% RAP mix and 40% Coarse RAP mix	0.863	NO	4.835	YES
	10% RAP mix and 50% Coarse RAP mix	6.884	YES	19.270	YES
	30% and 40% Coarse RAP mix	9.103	YES	2.035	NO
	30% and 50% Coarse RAP mix	16.303	YES	5.163	YES
	40% and 50% Coarse RAP mix	9.507	YES	3.030	NO

1. If Critical T-value < Calculated T-value, groups are statistically significantly different.

4.4 Illinois Flexibility Index Test Results

The Illinois flexibility index test (I-FIT) was conducted according to AASHTO T 393 procedure (AASHTO T 393, 2021) to investigate cracking resistance of the fractionated HMA-RAP mixtures. Eight semi-circular specimens were tested for each mix. Subsequently, the average, standard deviation (S.D.), and coefficient of variation (C.O.V) of the eight samples were determined for each of the six I-FIT test output parameters. Figure 4.3 shows the load-displacement curves and Table 4.4 shows statistical properties of the I-FIT test output parameters for the five fractionated HMA-RAP mixture groups. The values of all I-FIT test output parameters for the eight samples in the five fractionated HMA-RAP mixture groups are represented in Appendix A.

Table 4.4 I-FIT test results of fractionated HMA-RAP mixtures

Parameter	Statistical Property	Mix				
		Virgin mix	10% RAP	30% Coarse RAP	40% Coarse RAP	50% Coarse RAP
Fracture Energy (J/m^2)	Average	1411.46	1119.05	1439.61	1319.10	1301.20
	Minimum	1098.63	753.62	1262.03	745.13	1172.68
	Maximum	1680.11	1256.87	1751.53	1558.24	1515.62
	S.D.	205.29	162.89	154.47	254.27	123.50
	C.O.V (%)	14.54	14.56	10.73	19.28	9.49
Peak Load (KN)	Average	2.70	3.79	3.59	3.49	4.16
	Minimum	2.35	3.48	3.35	3.09	3.84
	Maximum	3.05	4.10	3.96	3.72	4.43
	S.D.	0.21	0.23	0.22	0.25	0.21
	C.O.V (%)	7.89	6.18	6.04	7.05	5.05
Post-Peak Slope	Average	2.60	7.02	5.52	4.72	8.81
	Minimum	2.14	4.92	3.59	3.98	5.97
	Maximum	2.99	9.68	9.22	5.72	11.85
	S.D.	0.31	1.42	1.80	0.69	2.17
	C.O.V (%)	11.90	20.27	32.64	14.62	24.62
Flexibility Index (FI)	Average	5.55	1.64	2.84	2.87	1.58
	Minimum	3.95	1.28	1.58	1.32	1.08
	Maximum	7.51	2.44	4.88	3.61	2.54
	S.D.	1.29	0.38	0.97	0.74	0.51
	C.O.V (%)	23.20	23.14	34.05	25.63	32.54
Tensile Strength (Psi)	Average	53.96	74.82	71.54	69.52	82.58
	Minimum	46.35	67.87	67.01	61.44	75.57
	Maximum	61.07	81.53	79.75	73.88	86.82
	S.D.	4.43	4.90	4.47	4.66	3.85
	C.O.V (%)	8.22	6.55	6.25	6.70	4.66
Critical Displacement (mm)	Average	2.24	1.34	1.73	1.74	1.36
	Minimum	1.90	1.21	1.54	1.59	1.15
	Maximum	2.72	1.55	1.99	1.96	1.63
	S.D.	0.25	0.10	0.16	0.13	0.15
	C.O.V (%)	11.21	7.77	9.18	7.61	11.28

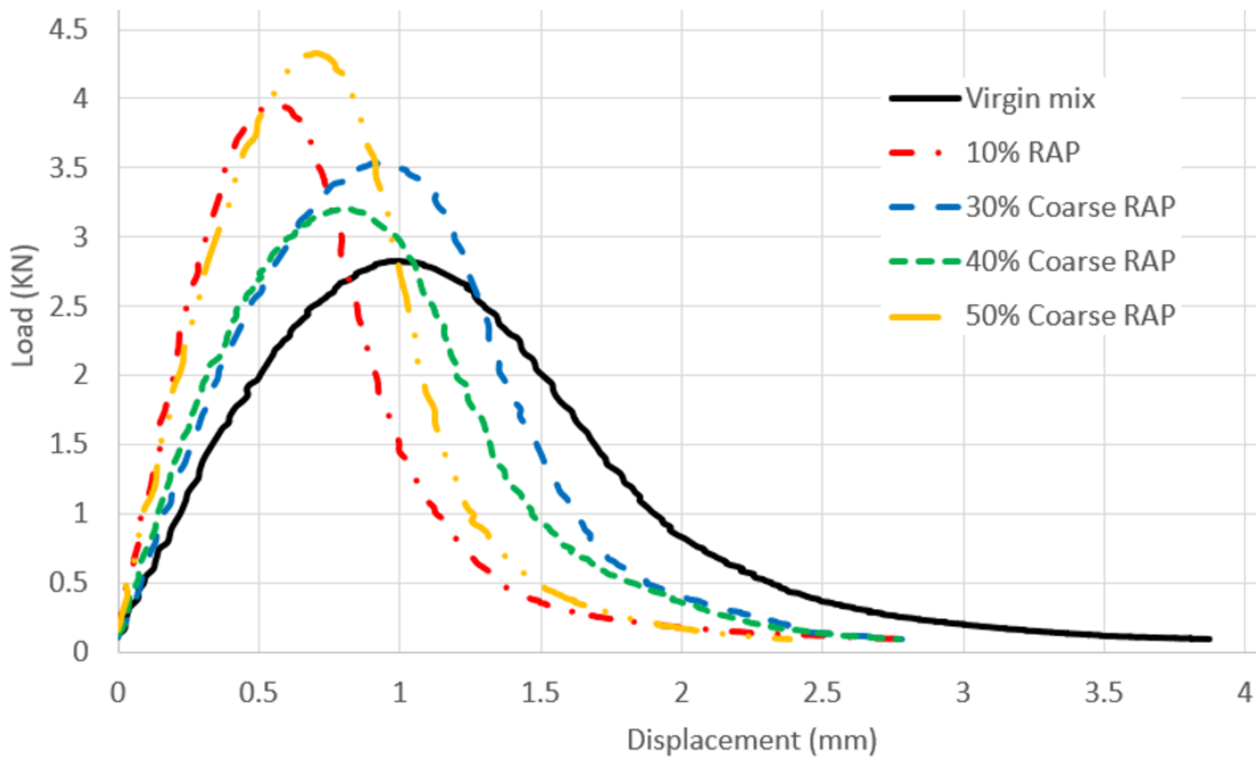

Figure 4.3 Load-displacement curves of fractionated HMA-RAP mixtures

Average peak load and tensile strength values presented in Table 4.4 were plotted in Figure 4.4 to show the similar correlation that these two parameters have with RAP proportions. Since all I-FIT specimens have a very similar cross-sectional area, tensile strength values are directly proportional to peak load values. RAP sample groups have higher peak load and tensile strength values than the virgin mix group due to their greater stiffness. Furthermore, they have higher post-peak slopes and lower critical displacement values than the virgin mix group due to their brittle behaviour. Therefore, RAP sample groups had lower rutting potential than the virgin mix group. This can be clearly observed from Tables 4.2 and 4.4, where the 50% coarse RAP mix had the highest post-peak slope, peak load, and tensile strength value as well as the highest number of wheel passes to failure on the HWTT equipment.

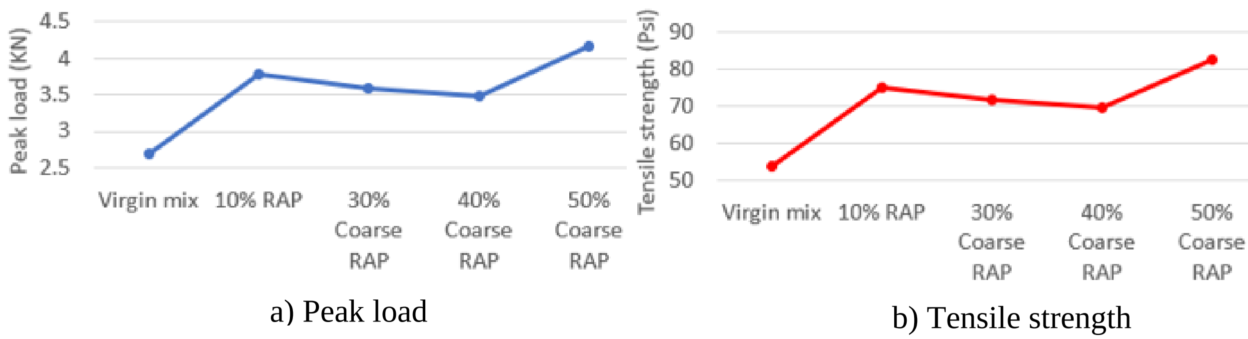

Figure 4.4 Average peak load and tensile strength of fractionated HMA-RAP mixtures

Figure 4.5 compares the average flexibility index and fracture energy values of fractionated HMA-RAP mixtures. The City of Winnipeg public works department and Manitoba Transportation and Infrastructure still do not have acceptance/rejection criteria developed for the assessment of cracking resistance using the I-FIT test. However, the Illinois Department of Transportation had assigned a rudimentary minimum flexibility index value of 8 for the acceptance of cracking performance of asphalt mixtures (West et al., 2018). As a result, a flexibility index value of 8 was selected as a minimum requirement for the initial assessment of cracking resistance of fractionated HMA-RAP mixtures.

Figure 4.5 shows that all mix groups had an average flexibility index value less than 8 indicating a high cracking potential. In addition, all RAP sample groups had a lower average flexibility index value than the virgin mix group, with the 50% coarse RAP mix group having the least average flexibility index value. The contribution of RAP binder to total binder content stiffens the mix and makes it more brittle leading to higher cracking potential. Also, the reduction in total binder content and effective asphalt content with higher RAP proportions leads to higher cracking potential. Nevertheless, 30% and 40% coarse RAP mix groups had better cracking resistance than the 10% RAP mix group, regardless of encompassing a higher RAP proportion. The lower post-peak slopes, peak loads, and tensile strength values indicated a more ductile behaviour for 30%

and 40% coarse RAP mix groups. This can be attributed to variations between RAP binder properties as well as gradations of coarse and fine RAP. In a nutshell, I-FIT test results proved that RAP fractionation can be a successful tool to increase RAP usage in asphalt mixes while mitigating the negative impact of higher RAP proportions on cracking performance.

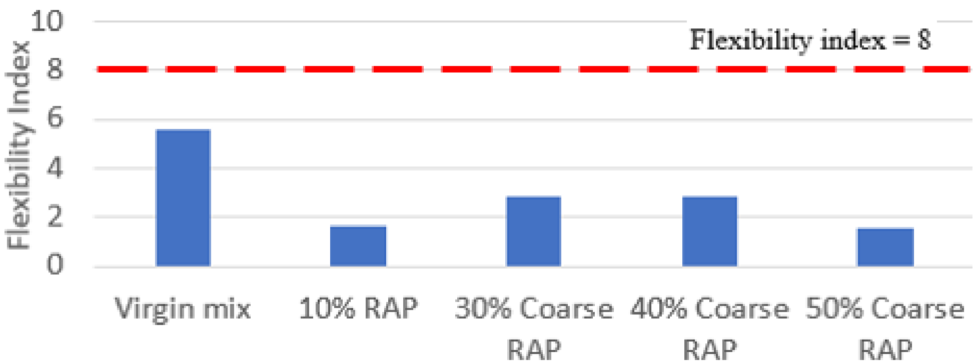

a) Flexibility index

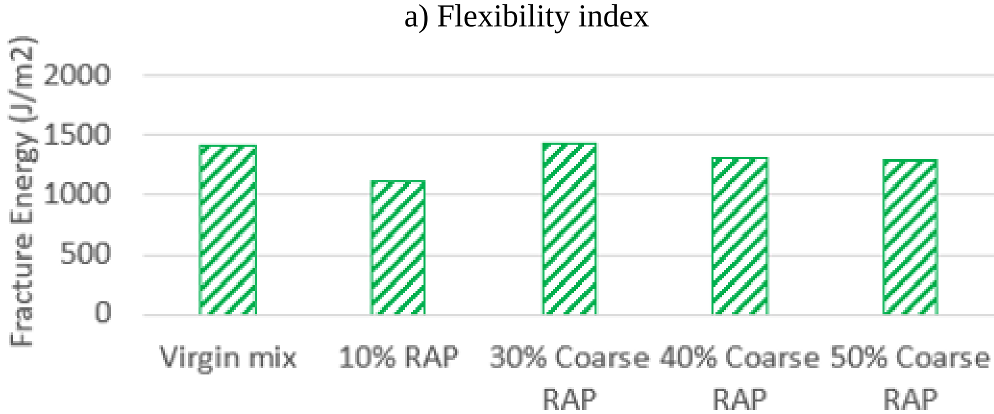

b) Fracture energy

Figure 4.5 Average flexibility index and fracture energy of fractionated HMA-RAP mixtures

Figure 4.5 also shows that average fracture energy values did not have a specific trend with RAP proportions. Although fracture energy is the deciding parameter of cracking performance in several cracking tests, it did not show a correlation like that of flexibility index with the fractionated HMA-RAP mixtures. For instance, the 30% and 50% coarse RAP mix groups had a higher average fracture energy value than the virgin and 10% RAP mix groups, respectively, despite having a lower average flexibility index. This is due to a higher post-peak slope which led to a reduction in their flexibility index. As a result, fracture energy alone cannot represent the cracking performance of an I-FIT specimen, and post-peak slope plays an important role in conjunction with fracture energy to decide the final flexibility index. This phenomenon is reinforced by the results of Tukey's HSD test at 95% confidence level for the three parameters as shown in Table 4.6. Tukey's HSD test showed that most average fracture energy value differences between groups were not statistically significant. Conversely, statistically significant mean differences between groups were identical in the cases of post-peak slope and flexibility index parameters. Therefore, post-peak slope can have a more crucial impact on flexibility index than fracture energy.

Table 4.5 shows one-way ANOVA results at 95% confidence level between the five fractionated HMA-RAP mixture groups for each I-FIT test output parameter. All calculated F-values were greater than critical F-value which indicates that variations between group means are statistically significant for all parameters. This means that a minor change in RAP content (even as low as 10%) is influential on cracking performance of HMA mixtures. In addition, RAP mix groups have higher coefficients of variation than the virgin mix group for flexibility index and post-peak slope parameters (see Table 4.4). This deduces that HMA-RAP mixtures tend to show more variability than virgin mixtures in terms of cracking performance.

Table 4.5 One-way ANOVA of I-FIT test output parameters

Parameter	Flexibility Index	Fracture Energy	Post-Peak Slope	Critical Displacement	Tensile Strength	Peak Load
Calculated F-value	29.30	3.68	20.87	38.66	43.94	46.22
Critical F-value[1]			2.69			

1. If Critical F-value < Calculated F-value, groups are statistically significantly different.

Table 4.6 Tukey's HSD test of I-FIT test output parameters

Parameter		Flexibility Index	Fracture Energy	Post-Peak Slope
Honestly Significant Difference (HSD)[1]		1.21	267.0	2.1
Mean difference between groups[2]	Virgin mix and 10% RAP mix	3.91	292.4	4.4
	Virgin mix and 30% Coarse RAP mix	2.71	28.2	2.9
	Virgin mix and 40% Coarse RAP mix	2.68	92.4	2.1
	Virgin mix and 50% Coarse RAP mix	3.97	110.3	6.2
	10% RAP mix and 30% Coarse RAP mix	1.20	320.6	1.5
	10% RAP mix and 40% Coarse RAP mix	1.23	200.1	2.3
	10% RAP mix and 50% Coarse RAP mix	0.06	182.2	1.8
	30% and 40% Coarse RAP mix	0.03	120.5	0.8
	30% and 50% Coarse RAP mix	1.26	138.4	3.3
	40% and 50% Coarse RAP mix	1.29	17.9	4.1

1. If HSD < Mean difference between groups, groups are statistically significantly different.
2. Red cells indicate groups that are not statistically significantly different.

4.5 Dynamic Modulus Test Results

The dynamic modulus test (DMT) was conducted according to AASHTO T 342 procedure (AASHTO T 342, 2022) to investigate stiffness of the fractionated HMA-RAP mixtures. Two full-size specimens were tested for each mix at four different temperatures (-10, 4.4, 21.1 and 37.8ºC) and six loading frequencies (0.1, 0.5, 1.0, 5.0, 10 and 25 Hz) to determine dynamic modulus. Subsequently, the dynamic modulus values of the two specimens in each mix were averaged and combined to develop a DM master curve according to AASHTO PP 62 procedure (AASHTO PP 62-10, 2012). Figure 4.6 presents the master curves and Table 4.7 shows the average dynamic modulus values of the five fractionated HMA-RAP mixtures groups. The dynamic modulus values of the two specimens in each mixture group are represented in Appendix A.

Table 4.7 Average dynamic modulus of fractionated HMA-RAP mixtures

Temperature	Dynamic Modulus of Virgin mix (MPa)					
(°C)	0.1 Hz	0.5 Hz	1.0 Hz	5.0 Hz	10 Hz	25 Hz
-10	10515.9	13066.5	14035.0	16301.0	17025.5	17629.0
4.4	3958.35	5579.60	6464.05	8782.55	9747.15	10960.0
21.1	1254.60	1831.10	2213.05	3655.65	4264.45	5330.10
37.8	468.090	616.030	738.485	1180.75	1461.35	1850.30
Temperature	Dynamic Modulus of 10% RAP mix (MPa)					
(°C)	0.1 Hz	0.5 Hz	1.0 Hz	5.0 Hz	10 Hz	25 Hz
-10	15239.5	18248.0	19347.5	22020.5	22839.0	23871.5
4.4	6160.85	8465.35	9513.10	12203.5	13283.5	14471.5
21.1	2507.40	3468.45	3806.10	5467.50	6291.60	7711.25
37.8	607.210	914.500	1127.27	1860.40	2305.70	3161.85
Temperature	Dynamic Modulus of 30% Coarse RAP mix (MPa)					
(°C)	0.1 Hz	0.5 Hz	1.0 Hz	5.0 Hz	10 Hz	25 Hz
-10	13545.0	16229.5	17233.5	19688.0	20499.5	21277.0
4.4	5771.05	7940.95	8894.20	11425.5	12444.0	13736.5
21.1	2316.35	3217.30	3772.85	5441.85	6180.95	7242.45
37.8	857.335	1130.63	1282.00	1940.55	2339.85	2950.35
Temperature	Dynamic Modulus of 40% Coarse RAP mix (MPa)					
(°C)	0.1 Hz	0.5 Hz	1.0 Hz	5.0 Hz	10 Hz	25 Hz
-10	13630.5	16424.5	17548.0	20014.5	20935.5	21888.5
4.4	5749.50	7921.10	8968.85	11524.5	12406.0	13330.0
21.1	1955.65	2861.40	3360.30	4942.60	5687.55	6788.70
37.8	522.845	793.465	958.915	1576.85	1940.55	2504.95
Temperature	Dynamic Modulus of 50% Coarse RAP mix (MPa)					
(°C)	0.1 Hz	0.5 Hz	1.0 Hz	5.0 Hz	10 Hz	25 Hz
-10	17952.0	20967.5	22112.5	24030.5	25450.5	26481.0
4.4	8424.35	11091.5	12267.5	15044.0	16165.0	17676.0
21.1	3356.55	4688.70	5347.20	7480.00	8558.40	9789.65
37.8	841.170	1267.35	1587.70	2593.05	3208.15	3915.10

The following observations can be deduced from Figure 4.6:

1. Incorporation of RAP increases stiffness at all testing temperatures. This suggests that RAP mixes may enhance resistance to rutting at warmer temperatures, while reducing fatigue and thermal cracking resistance at intermediate and lower temperatures, respectively.
2. The virgin mix had the least stiffness, and the 50% coarse RAP mix had the highest stiffness at all testing temperatures. This correlates well with HWTT and I-FIT tests results

discussed previously, where the virgin mix had the least rutting resistance but highest cracking resistance and the 50% coarse RAP mix had the highest rutting resistance but least cracking resistance.

3. The 30% and 40% coarse RAP mixes had lower stiffness than the 10% RAP mix at both intermediate and low testing temperatures, whereas only the 30% coarse RAP mix had higher stiffness than the 10% RAP mix at high testing temperatures. This may suggest better fatigue and thermal cracking as well as rutting resistance for the 30% coarse RAP mix over the 10% RAP mix. In addition, it suggests improved fatigue and thermal cracking resistance for the 40% coarse RAP mix over the 10% RAP mix. These observations also correlate well with HWTT and I-FIT tests results discussed previously in Tables 4.2 and 4.4, respectively.

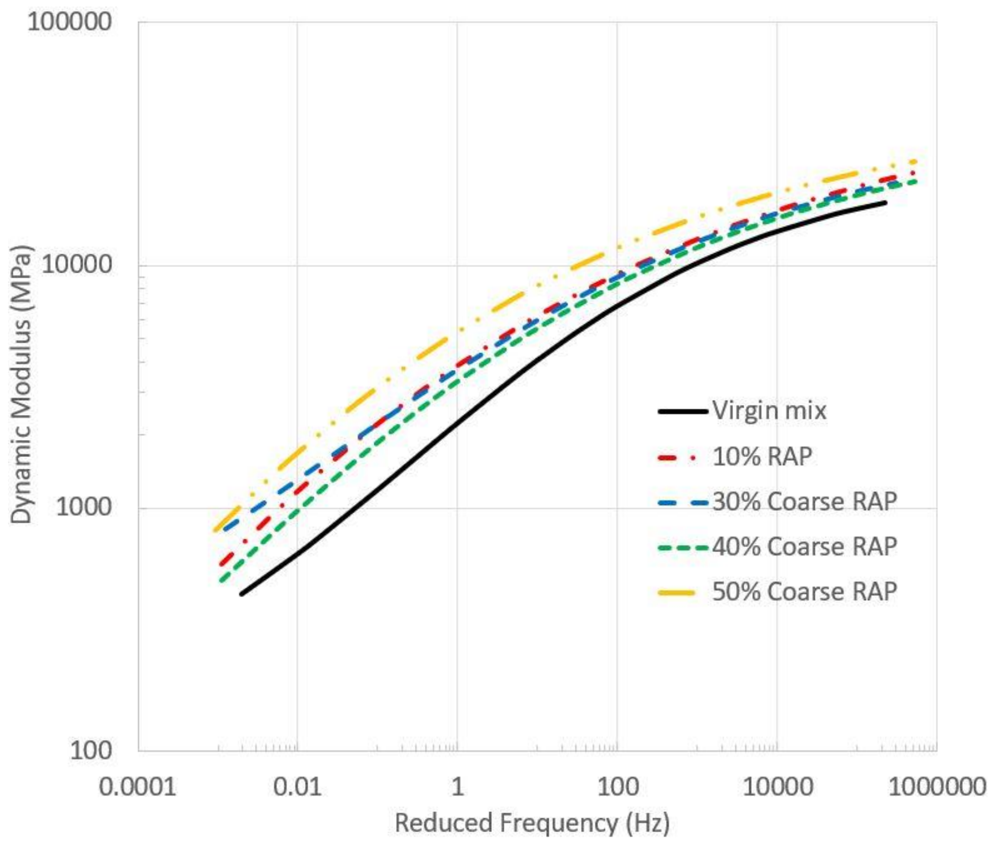

Figure 4.6 Dynamic modulus master curves of fractionated HMA-RAP mixtures

4.6 Correlation Between HWTT, I-FIT and Dynamic Modulus Values

DMT test results can also be used to rank asphalt mixtures with respect to their performance by comparing three dynamic modulus values at testing temperatures and loading frequencies that can be used to indicate three major types of surface distresses (Varamini, 2016). These distresses are thermal cracking at high frequency (25 Hz) and low temperature (-10ºC), fatigue cracking at intermediate frequency (10 Hz) and temperature (21.1ºC), rutting at low frequency (0.1 Hz) and high temperature (37.8ºC). Table 4.8 shows rankings of the five fractionated HMA-RAP mixtures according to their average dynamic modulus ($|E^*|$) values at the three testing temperatures and loading frequencies. HWTT test was conducted at high temperature (45ºC) and I-FIT test was conducted at intermediate temperature (25ºC); therefore, DMT test rutting and fatigue cracking rankings were also compared to HWTT test rankings (based on average number of passes to failure) and I-FIT test rankings (based on average flexibility index), respectively.

Table 4.8 HWTT, I-FIT and DMT tests rankings of fractionated HMA-RAP mixtures

Mix	Thermal cracking (-10ºC, 25 Hz)		Fatigue cracking (21.1ºC, 10 Hz)		I-FIT Rank[1]	Rutting (37.8ºC, 0.1 Hz)		HWTT Rank[1]
	$\lvert E^*\rvert$ (MPa)	Rank[1]	$\lvert E^*\rvert$ (MPa)	Rank[1]		$\lvert E^*\rvert$ (MPa)	Rank[1]	
Virgin mix	17629.0	1	4264.45	1	1	468.09	5	5
10% RAP	23871.5	4	6291.60	4	4	607.21	3	4
30% Coarse RAP	21277.0	2	6180.95	3	3	857.34	1	3
40% Coarse RAP	21888.5	3	5687.55	2	2	522.85	4	2
50% Coarse RAP	26481.0	5	8558.40	5	5	841.17	2	1

1. "1" indicates the best performance and "5" indicates the weakest performance.

Table 4.8 shows that thermal and fatigue cracking rankings were similar according to DMT test results as well as they exhibit a good correlation with I-FIT test rankings. Despite the inverted ranking of 30% and 40% coarse RAP mixes under thermal cracking, statistical analysis of I-FIT test results had proved that cracking resistance of 30% and 40% coarse RAP mixes are not statistically significantly different. On the contrary, rutting rankings according to DMT test do not match with HWTT test rankings. This can be attributed primarily to the different testing conditions between the HWTT test and DMT test. In HWTT test, the asphalt sample is submerged in water as well as the test temperature is relatively higher than 37.8ºC. Additionally, the asphalt sample undergoes permanent deformation in the HWTT test whereas the DMT test only assesses the recoverable strain of a sample. All these variations in testing conditions influence the correlation between HWTT test and DMT test. To reinforce this outcome, the strength of correlation of DM values at intermediate and high temperatures was determined via linear regression analysis with I-FIT and HWTT tests results, respectively. The coefficients of determination (R^2) between $|E^*|_{21.1°C}$ values and all I-FIT test output parameters were measured at all frequencies. Similarly, R^2 values were measured between $|E^*|_{37.8°C}$ values and all HWTT test output parameters at all frequencies. Table 4.9 shows the calculated R^2 values for all conditions.

Table 4.9 Correlation between DM values and output parameters of I-FIT and HWTT tests

Test	Parameter	R^2 at DMT test frequencies					
		0.1 Hz	0.5 Hz	1.0 Hz	5.0 Hz	10 Hz	25 Hz
I-FIT	Flexibility index	0.79	0.79	0.74	0.70	0.70	0.75
	Fracture energy	0.16	0.16	0.10	0.09	0.10	0.15
	Post-peak slope	0.98	0.97	0.93	0.92	0.93	0.96
	Peak load	0.94	0.94	0.92	0.89	0.89	0.91
	Tensile strength	0.94	0.94	0.92	0.90	0.89	0.91
	Critical displacement	0.81	0.80	0.73	0.70	0.70	0.76
HWTT	Number of passes to failure	0.31	0.51	0.58	0.63	0.63	0.56
	Number of passes to SIP	0.17	0.37	0.52	0.63	0.66	0.59
	Creep slope	0.40	0.67	0.77	0.85	0.87	0.86
	Stripping slope	0.30	0.32	0.26	0.23	0.21	0.18
	Rut depth to SIP	0.26	0.43	0.46	0.50	0.50	0.66

Table 4.9 shows that DM values had strong correlation at all frequencies with all I-FIT test output parameters except fracture energy. However, statistical analysis of I-FIT test results proved that fracture energy is not a strong representative of cracking performance. On the other hand, the

correlation between DM values and most HWTT test output parameters varied from weak correlation at lower frequencies to moderate correlation at higher frequencies. An R^2 value of less than 0.5 with all HWTT test output parameters at 0.1 Hz proves the incompatibility of rankings between the DMT and HWTT tests. In Figure 4.7, all coefficient of variation values for DM results at 37.8ºC were higher than at 21.1ºC except for the 50% coarse RAP mix. This means that DM results at higher temperatures tend to show more variability than DM results at lower temperatures. Consequently, DMT test rankings did not match with HWTT test rankings, unlike I-FIT test rankings. In general, DMT test characterizes asphalt mixtures to only predict their cracking and rutting performance. However, it should not be used as a surrogate to reliable cracking and rutting tests such as I-FIT and HWTT tests.

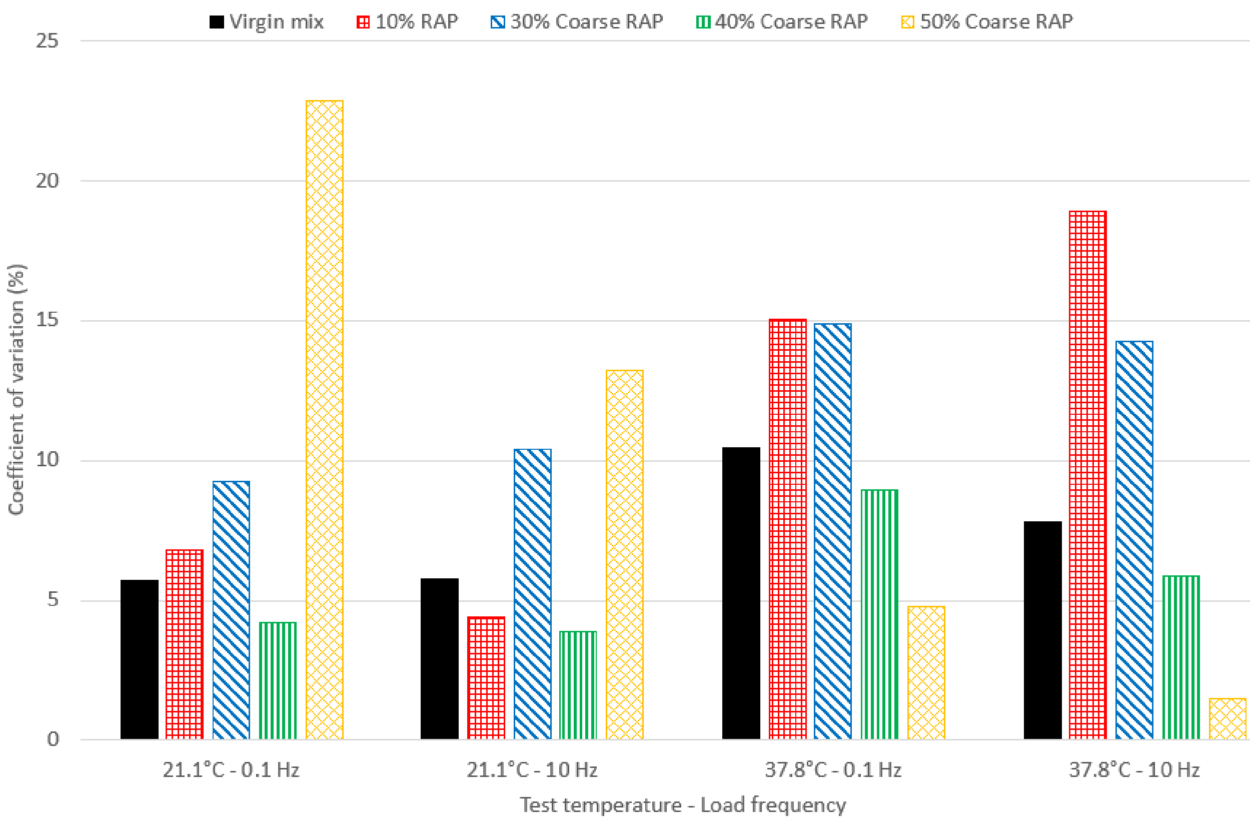

Figure 4.7 Coefficients of variation for dynamic modulus of fractionated HMA-RAP mixtures

4.7 Balanced Mix Design

The performance space diagram (PSD) shown in Figure 4.8 was used to locate the performance tests results of the five fractionated HMA-RAP mixture groups with respect to cracking and rutting tests criteria. Cracking test criteria was based on average flexibility index and rutting test criteria was based on average rut depth at 10,000 passes (N.B.: rut depth at 10,000 passes of mixtures that failed early was extrapolated using the stripping slope).

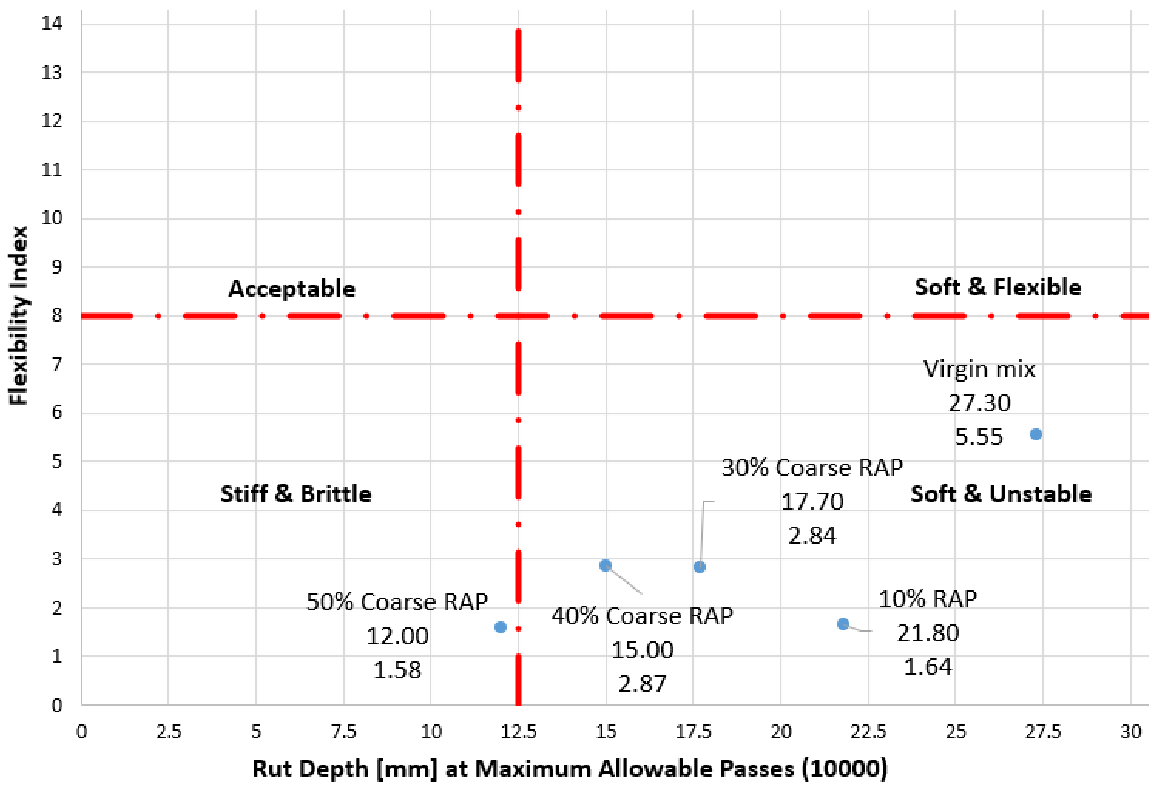

Figure 4.8 Performance space diagram of fractionated HMA-RAP mixtures

A PSD is useful in determining if mixes are present in desirable or unsatisfactory quadrants as well as to decide possible applications for the tested mixes (West et al., 2018). Figure 4.8 shows four performance quadrants based on the minimum criteria of HWTT and I-FIT tests. Mixtures located in the acceptable quadrant will have a high rutting and cracking resistance (i.e., stiff and flexible). Soft and flexible quadrant refers to mixtures with low rutting resistance (soft) and high cracking resistance, whereas stiff and brittle quadrant refers to mixtures with high rutting resistance and low cracking resistance (brittle). Ultimately, mixtures located in the soft and unstable quadrant will have a low rutting and cracking resistance.

Figure 4.8 shows that all fractionated HMA-RAP mixtures are in the soft and unstable quadrant except the 50% coarse RAP mix which is in the stiff and brittle quadrant. This means that all mixtures have a high cracking and rutting potential, but only the 50% coarse RAP mix is slightly more resistant to permanent deformation. Overall, the balanced mix design indicates that all mixtures are poor mixtures that can be used temporarily or on low traffic volume roads only such as residential streets or back lanes, whereas the 50% coarse RAP mix can be a good candidate for the bottom layer (i.e., non-surface mix) of a pavement. Nonetheless, minimum criteria for cracking and rutting resistance should be modified to accommodate Manitoba mix designs and specifications. Additional testing is required on HMA-RAP mixtures to establish acceptable performance testing criteria.

Balanced mix design results proved that incorporation of RAP causes an inverse outcome in terms of cracking and rutting performance. Thus, Table 4.10 takes a closer look at the overall performance of the five fractionated HMA-RAP mixtures via determining their average cracking, rutting and moisture susceptibility rankings. This will help refer to the best performing mixes according to the three performance measures.

Table 4.10 Average performance measures ranking of fractionated HMA-RAP mixtures

Performance measure	Mix				
	Virgin mix	10% RAP	30% Coarse RAP	40% Coarse RAP	50% Coarse RAP
Cracking	1	4	3	2	5
Rutting	5	4	3	2	1
Moisture susceptibility	4	3	5	2	1
Average ranking[1]	3	4	4	2	2

1. "1" indicates the best performance and "5" indicates the weakest performance.

Table 4.10 shows that 40% and 50% coarse RAP mixes demonstrated a higher average performance ranking than virgin, 10% RAP and 30% coarse RAP mixes. This means that fractionated RAP mixtures can obtain overall better performance than virgin and unfractionated RAP mixtures. However, caution should be taken when deciding the suitability of the best performing mixes as one mix can show outstanding ranking for one performance test and poor ranking for the other. But the fact that RAP fractionation had caused improvement in one or more performance measure indicates the significance of considering this technology in pavement design and construction. Therefore, further research is worthwhile to investigate the eligibility of RAP fractionation with various mix types (e.g.: HMA, warm-mix asphalt, stone mastic asphalt, etc.).

4.8 Bailey Method Check of Gradation

Balanced mix design results showed that all five mixture groups had relatively weak cracking and rutting performance. Therefore, the achievement of proper volumetric requirements does not ensure adequate mix performance. This infers that poor performance of these mixtures can be mainly attributed to issues with mix design. Consequently, the gradations of the five mixture groups were evaluated according to the Bailey method. The Bailey method is a tool that evaluates aggregate packing of the coarse and fine aggregate portions of the blend (Vavrik et al., 2002). It relies mainly on the following three ratios to assess the aggregate blend:

1. CA ratio: It describes how the coarse aggregate particles of the total blend pack together.
2. FA_c ratio: It describes how the coarse portion of fine aggregate particles pack together.
3. FA_f ratio: It describes how the fine portion of fine aggregate particles pack together.

Overall, the aggregate blend is divided into three segments depending on NMAS of gradation and the coarse to fine aggregate ratio in each segment is required to fall within a certain range. For fine-graded mixes with NMAS less than 19 mm, the Bailey method evaluation is conducted only on the fine aggregate portion of the total blend. In such cases, the fine aggregate portion is divided into two segments only in which their coarse to fine aggregate ratios are represented by CA and FA_c ratios only (i.e., FA_f ratio is omitted). Table 4.11 shows the recommended ranges of aggregate ratios for fine-graded 12.5 mm NMAS mixtures as well as the general evaluation of Bailey method for the five gradations of fractionated HMA-RAP mixtures. The Bailey method outcome was the same for all mixtures since gradations of the five mixtures were kept very similar.

Table 4.11 Bailey method evaluation of fractionated HMA-RAP mixtures

Aggregate ratio	Recommended range for fine-graded 12.5 mm NMAS mixtures	Bailey method evaluation of all gradations
CA ratio	0.60 – 1.00	> 1.00
FA_c ratio	0.35 – 0.50	< 0.35

Table 4.11 shows that the five mixtures do not satisfy coarse to fine aggregate ratios according to the Bailey method. A CA ratio higher than 1 indicates that the coarse portion of fine aggregate blend is mainly controlled by fine aggregates. In other words, coarse aggregates are only acting as floating aggregates in a matrix of fine aggregates and do not play a significant role in controlling the overall aggregate skeleton. Excessive amount of fine aggregate leads to poor rutting resistance as well as difficulties with field compaction since mixes will have tendency to slide under rollers (Vavrik et al., 2002). Hence, the fine aggregate blend requires more coarse aggregates to result in well-packed mixtures. Percentages passing sieves no. 16 (1.18 mm) and no. 30 (0.60 mm) should decrease to bring coarse to fine aggregate ratios within the recommended ranges and result in a satisfactory Bailey method evaluation.

Poor aggregate interlock of the five fractionated HMA-RAP mixtures might be one reason for inadequate cracking and rutting performance. The gradations of the five mixtures indicate the presence of a significant amount of natural sand. Natural sand is smooth and round which can be another contributing factor to insufficient rutting resistance. Moreover, inadequate compaction of the Superpave gyratory asphalt briquettes might be another reason for poor rutting resistance. Most fractionated RAP briquettes had been subjected only to 10 - 20 gyrations to reach 7 ± 0.5% air voids. The low number of gyrations for laboratory compacted samples is a primary cause of high rutting potential. Furthermore, the use of limestone aggregates might be an encouraging factor of poor mix performance. Limestone aggregates are soft aggregates with limited durability which might be a leading cause of cracking issues. In conclusion, there are several reasons that might have caused unsatisfactory performance of the five fractionated HMA-RAP mixtures and detailed research is required to investigate the actual reason behind the failure of these mixtures.

4.9 Summary

This chapter concludes that the inclusion of RAP in HMA mixtures improves their moisture and rutting resistance but decreases their cracking resistance. This means that RAP reduces the suitability of HMA mixtures to be used as surface layers. In this study, the virgin mix had the highest cracking performance but least rutting performance. Conversely, the 50% coarse RAP mix had the highest rutting performance but least cracking performance. However, fractionated RAP mixtures presented a more ductile behaviour than unfractionated RAP mixtures at a higher RAP content. Fractionated 30% and 40% coarse RAP mixtures had higher flexibility index value than the 10% unfractionated RAP mixture. Overall, fractionated RAP mixtures showed improvement in at least one performance measure in comparison to virgin and unfractionated RAP mixtures which encourages the application of RAP fractionation in pavement design and construction. Statistical analysis of I-FIT and HWTT tests results had proved that RAP content is influential on both cracking and rutting performance of HMA mixtures. Balanced mix design results showed that all HMA-RAP mixtures tested in this study did not achieve the minimum requirements for cracking and rutting, except the 50% coarse RAP mix which showed acceptable rutting resistance. This means that achievement of the desired volumetric properties does not guarantee adequate long-term pavement performance. Issues related to material properties or laboratory mix design process might have led to unacceptable cracking and rutting test results. Therefore, additional testing as well as modifications to current mix design specifications and properties of materials may be required to better understand the behaviour of HMA mixtures. Finally, DMT test results had a stronger correlation with I-FIT test results than with HWTT test results due to higher variability of DM values at higher temperatures as well as the different testing conditions between HWTT test and DMT test.

Chapter 5. Evaluation of Plant-Produced Mixtures

5.1 Introduction

This chapter includes a balanced mix design (BMD) framework of six groups of plant-produced asphalt mixtures that were used to pave different road projects around Manitoba. The main objective of this study was to discover mix design strategies that might improve the BMD as well as to develop preliminary performance-based specifications for cracking and rutting laboratory tests. It has been proved in chapter 4 that there can be several uncertainties related to the mix production process in the laboratory; however, plant-produced mixtures resemble the actual mix production process during construction. Therefore, performance testing of such mixes may better simulate actual performance that road users will encounter in the field. Furthermore, future assessment of field performance for these plant-produced mixtures may help in validating the suggested threshold cracking and rutting test criteria as well as to modify the current BMD developed at the end of this chapter.

To fulfill the objective of this study, volumetric properties of the six plant-produced mixture groups were initially explained. Furthermore, their cracking and rutting performance as well as stiffness modulus values were analyzed and correlated with mix design and volumetric properties. In addition, preliminary threshold criteria were developed based on the database of cracking and rutting performance tests results. Moreover, the impact of long-term aging on cracking test output parameters was discussed and compared with short-term aging. Finally, a balanced mix design (BMD) was developed and statistical analysis including analysis of variance (ANOVA), independent t-test and linear regression correlation matrices were applied when needed in the analysis.

5.2 Volumetric Properties

The volumetric properties of the six plant-produced asphalt mixtures are presented in Table 5.1. These properties were obtained from the mix design documents that were provided by Manitoba Transportation and Infrastructure (MTI) for each mix.

Table 5.1 Volumetric properties of plant-produced mixtures

Property	Mix 1 (19, 58, 0, 0)	Mix 2 (12.5, 58 P, 0, 0)	Mix 3 (12.5, 64 P, 10, 0)	Mix 4 (12.5, 64 P, 10, 3)	Mix 5 (19, 58, 0, 0)	Mix 6 (12.5, 58 P, 0, 0)
Asphalt content – AC (%)	4.70	5.15	5.10	5.80	4.60	5.20
Asphalt content from virgin binder (%)	4.70	5.15	4.64	4.10	4.60	5.20
Asphalt content from RAP and/or RAS (%)	–	–	0.46	1.70	–	–
RAP/RAS binder ratio (%)	–	–	9.02	29.31	–	–
Effective asphalt content – P_{be} (%)	4.38	4.71	4.41	4.64	4.39	4.65
Voids in mineral aggregate – VMA (%)	14.2	15.1	14.2	14.8	14.5	14.8
Voids filled with asphalt – VFA (%)	70.8	71.3	71.7	72.6	70.1	73.7
Dust to binder ratio – P_{200}/P_{be}	0.73	0.66	1.02	1.25	0.91	0.97
Fine aggregate angularity – FAA[1] (%)	43.0	43.7	–	–	43.1	43.2

1. FAA for mixes 3 and 4 were not provided in the mix design documents.

Table 5.1 shows that mixes 1 and 5 had the least AC; thus, they had the least P_{be} and VFA. Mixes 3 and 4 were obtained from the same construction project, but the only difference is that mix 4 had an additional 3% RAS. It can be deduced from RAP/RAS binder ratios in Table 5.1 that 3% RAS accounted for more than 20% of AC in mix 4, while 10% RAP accounted for only 9% of AC in mix 3. RAP consists of 94 – 95% aggregate, whereas aggregates make up only 70 – 80% of RAS. The remaining RAS is stiff binder formulated for roofing standards. Therefore, the higher AC found in RAS caused a significant increase in AC of mix 4. However, most of RAS AC was inactive since mix 4 did not have a much higher P_{be} than mix 3. Table 5.1 also shows that mixes 3 and 4 had the highest dust to binder ratios despite not having the least P_{be}. This can be attributed to higher dust content (i.e., % passing sieve no. 200) found in recycled asphalt material, especially RAS, since P_{200}/P_{be} of mix 4 exceeded the COW specifications maximum limit (i.e., 1.20).

5.3 Hamburg Wheel-Tracking Test Results

5.3.1 Analysis of HWTT Test Output Parameters

The Hamburg wheel-tracking test (HWTT) was conducted according to AASHTO T 324 procedure (AASHTO T 324, 2023) to investigate rutting and moisture potential of the six plant-produced asphalt mixtures. Two samples of paired laboratory compacted cylinders were tested for each mix simultaneously in one test, and the output from each wheel represented the results of a single sample. Table 5.2 shows the HWTT test output parameters of the six plant-produced mixtures. The minimum rutting resistance index (RRI) to pass the HWTT test is 5,000 for mixes 1, 2, 5 and 6 since the high temperature PG grade of the virgin binder used is 58°C. For mixes 3 and 4 with a high temperature PG grade of 64°C for the virgin binder, the minimum RRI to pass the HWTT test is 7,500. For mix 1, rut depth at 20,000 passes was extrapolated by stripping slope.

Table 5.2 shows that all six mixtures had passed the proposed HWTT test criteria according to the type of virgin binder used in the mix design. In addition, Table 5.2 shows that creep slope was a good indicator of rutting resistance. The rutting resistance ranking of the six mixtures according to average creep slope aligns with that according to average RRI. Overall, it can be deduced that HWTT test results were sensitive to several mix design parameters such as NMAS, type of virgin binder as well as amount of RAP and/or RAS. Mixes 1 and 5 had the highest average creep slopes and least average RRI values indicating the highest rutting potential among the six mixtures. This can be attributed primarily to the use of a straight virgin binder in the mix design. Asphalt binders are usually modified with polymers to enhance flexural properties of asphalt pavements and improve their overall performance at both high and low temperature ranges. Therefore, asphalt mixtures designed with straight binders are less resistant to rutting than those designed with polymer-modified binders. Furthermore, mixes 1 and 5 have a higher NMAS which means that their gradations have more coarse aggregates. The presence of fewer fine aggregates in the mix design decreases the interlocking mechanism between aggregate particles which leads to reduced shear strength and mixture stability; thus, higher rutting potential (Ramli et al., 2013). Moreover, mixes 1 and 5 have the least fine aggregate angularity as shown in Table 5.1. Lower angularity of fine aggregates (i.e., increased smoothness of aggregate surfaces) facilitates sliding of fine aggregates against each other under traffic loads which reduces resistance to permanent deflection (Ramli et al., 2013).

Table 5.2 HWTT test results of plant-produced mixtures

Mix	Sample	Creep Slope (mm/pass)	Stripping Slope (mm/pass)	Ratio of stripping to creep slope	Number of passes to SIP	Rut depth to SIP (mm)	Rut depth at 20,000 passes (mm)	RRI
Mix 1 (19, 58, 0, 0)	1	0.000439	0.001143	2.6	8,184	5.13	18.64	5,220
	2	0.000305	0.001906	6.2	14,091	5.80	17.06	7,630
	Avg.	0.000372	0.001525	4.4	11,138	5.47	17.85	6,425
Mix 2 (12.5, 58 P, 0, 0)	1	0.000115	–	–	–	–	4.35	16,576
	2	0.000128	–	–	–	–	4.35	16,575
	Avg.	0.000122	–	–	–	–	4.35	16,576
Mix 3 (12.5, 64 P, 10, 0)	1	0.000087	–	–	–	–	3.79	17,003
	2	0.000068	–	–	–	–	3.26	17,425
	Avg.	0.000078	–	–	–	–	3.53	17,214
Mix 4 (12.5, 64 P, 10, 3)	1	0.000047	–	–	–	–	2.66	17,863
	2	0.000043	–	–	–	–	2.48	18,050
	Avg.	0.000045	–	–	–	–	2.57	17,957
Mix 5 (19, 58, 0, 0)	1	0.000153	0.001101	7.2	18,214	4.30	6.25	15,080
	2	0.000200	0.000682	3.4	12,530	3.64	8.68	13,169
	Avg.	0.000177	0.000892	5.3	15,372	3.97	7.47	14,125
Mix 6 (12.5, 58 P, 0, 0)	1	0.000168	0.000206	1.2	16,443	4.08	4.79	16,227
	2	0.000067	–	–	–	–	2.95	17,675
	Avg.	0.000118	0.000103	0.6	8,222	2.04	3.87	16,951

Table 5.2 also shows that mixes 3 and 4 had the least average creep slopes and highest average RRI values indicating the least rutting potential among the six mixtures. This can be attributed primarily to the presence of a polymer-modified binder having the highest high temperature PG grade (i.e., the stiffest binder found in all mixtures). In addition, mix 3 included RAP, whereas mix 4 included both RAP and RAS. Asphalt binders found in RAP and RAS materials are aged/oxidized binders which lead to stiffer mixes when they contribute to total binder content of the mix design. The higher amount of stiffer binder in RAS caused rutting performance of mix 4 to be better than mix 3. Figure 5.1 shows the HWTT test curves of the six plant-produced mixtures.

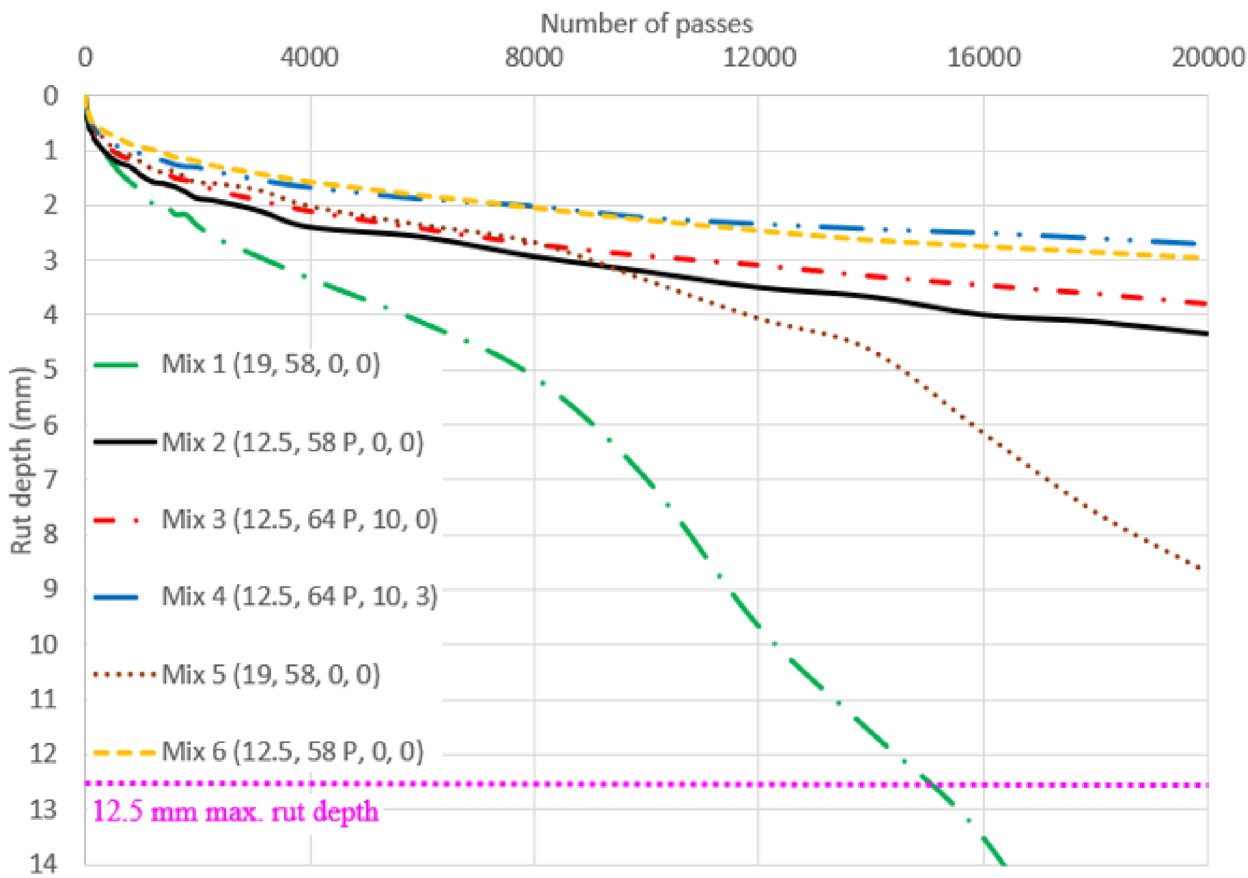

Figure 5.1 HWTT test curves of plant-produced mixtures

Both Table 5.2 and Figure 5.1 show that only mixes 1 and 5 had experienced stripping since both mixes had a ratio of stripping to creep slope greater than 2. Sample 1 of mix 6 also demonstrated a mild stripping behaviour, but it was neglected since the ratio of stripping to creep slope was less than 2. The main reason for having the highest moisture susceptibility can be that mixes 1 and 5 have the least total AC as well as effective AC. Lower AC reduces asphalt film thickness around aggregate particles which accelerates water diffusion. As a result, the adhesive bond between the asphalt film and aggregate particles starts to break down making the mixture prone to moisture damage (Tavassoti and Baaj, 2020). Overall, HWTT test results for moisture performance were compatible with tensile strength ratio (TSR) test results provided in the mix design documents of mixes 1, 2 and 6. Mix 1 had a TSR of 71.8%, whereas mixes 2 and 6 had a TSR of 73%. This means that mix 1 had the weakest moisture performance among the three mixtures which matches with HWTT test results.

5.3.2 Impact of Mix Design Parameters on HWTT Test Results

The six plant-produced asphalt mixtures involved several mix design parameters that can have significant influence on rutting performance. As a result, RRI values of the twelve samples tested in the HWTT equipment were grouped and compared in terms of four mix design parameters, including NMAS (“19 mm” and “12.5 mm”), RAP/RAS (“No RAP/RAS” and “With RAP/RAS”), type of aggregate (“Granite”, “Gravel” and “Limestone”) and type of virgin binder (“58-xx”, “58-xx P” and “64-xx P”). Figure 5.2 shows individual boxplots of RRI values grouped by the aforementioned mix design parameters. However, these boxplots should be interpreted cautiously since interaction between other mix design variables (which might be influential on HWTT test results) is not considered in the analysis. In addition, a database of twelve samples might not be sufficient to explain the interaction between groups of a single mix design parameter because boxplot analysis is highly dependent on sample size of the database.

Figure 5.2a clearly shows higher RRI values for 12.5 mm NMAS mixtures; thus, they exhibit better rutting performance than 19 mm NMAS mixtures. The least RRI value in the 12.5 mm NMAS mixture group is larger than the highest RRI value in the 19 mm NMAS mixture group which indicates the sensitivity of rutting resistance to NMAS. Figure 5.2b shows higher RRI values for RAP/RAS mixtures; thus, they exhibit better rutting performance than mixtures without RAP/RAS. The difference between the two RAP/RAS mixture groups was smaller than the difference between the two NMAS mixture groups. Nevertheless, interquartile ranges of the two RAP/RAS mixture groups still did not overlap with each other indicating that rutting resistance may be sensitive to RAP/RAS.

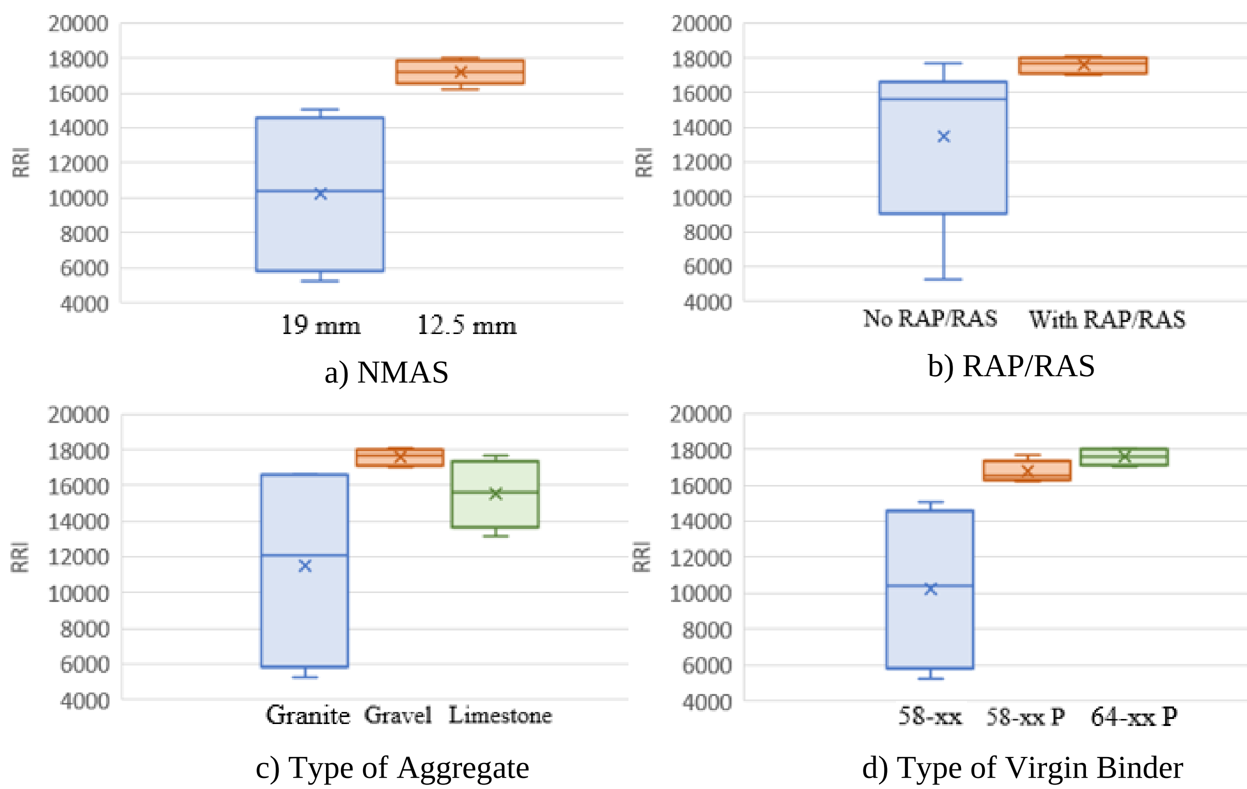

Figure 5.2 Box plots of RRI values by mix design parameter

Figure 5.2c shows that the three aggregate mixture groups demonstrate minor differences in RRI values. Moreover, interquartile ranges of the three mixture groups overlapped with each other which indicates that rutting resistance may not be sensitive to type of aggregate. Figure 5.2d shows a significant difference in RRI values between straight and polymer-modified binder mixture groups. However, the difference was minimal between “58-xx P” and “64-xx P” mixture groups as well as their interquartile ranges overlapped with each other. This means that rutting resistance may be sensitive only to polymer modification of asphalt binder. To verify trends of rutting performance that were observed with the four mix design parameters in the boxplot analysis, one-way ANOVA and independent t-test were conducted on the groups of RRI values at 95% confidence level and the results are presented in Table 5.3.

Table 5.3 Statistical tests results of RRI values by mix design parameter

Mix design parameter	Statistical test	P-value[1]	Statistically significant
NMAS (“19 mm” and “12.5 mm”)	Independent t-test (one-tail)	0.030	YES
RAP/RAS (“No RAP/RAS” and “With RAP/RAS”)	Independent t-test (one-tail)	0.022	YES
Type of aggregate (“Granite”, “Gravel” and “Limestone”)	One-way ANOVA	0.104	NO
Type of virgin binder (“58-xx”, “58-xx P” and “64-xx P”)	One-way ANOVA	0.008	YES
Type of virgin binder (“58-xx” and “58-xx P”)	Independent t-test (one-tail)	0.034	YES
Type of virgin binder (“58-xx” and “64-xx P”)	Independent t-test (one-tail)	0.026	YES
Type of virgin binder (“58-xx P” and “64-xx P”)	Independent t-test (two-tail)	0.081	NO

1. If P-value < 0.05, groups are statistically significantly different.

Table 5.3 shows that one-way ANOVA was conducted to compare three groups of RRI values, whereas independent t-test was conducted to compare only two groups. Additionally, independent t-test was conducted as a follow-up to one-way ANOVA analysis that produced statistically significant differences between group means. Consequently, independent t-test was used to compare individual pairs of RRI groups in terms of type of virgin binder. All independent t-test results were based on one-tail analysis except for the comparison between the two polymer-modified binder mixture groups. According to boxplot analysis, it is uncertain that the difference between "58-xx P" and "64-xx P" mixture groups should happen in a specific direction. In addition, the "64-xx P" mixture group contained RAP/RAS which means that its slight increase in RRI values may be due to another mix design variable (not the type of binder). Therefore, independent t-test compared between these two groups based on two-tail analysis. Overall, Table 5.3 shows that RRI group means had a statistically significant difference in terms of all mix design parameters except type of aggregate and changing the PG grade of a polymer-modified binder which conforms well to the outcome of boxplot analysis. This means that rutting resistance is affected by change in NMAS, inclusion of RAP and/or RAS materials as well as polymer modification of asphalt binder but is not affected by change in aggregate type or binder type without polymer modification.

5.3.3 Correlation Between Asphalt Mixture Properties and HWTT Test Results

In this section, correlation matrices were developed to determine the relations between RRI values and typical asphalt mixture properties including asphalt content (AC), effective asphalt content (P_{be}), voids in mineral aggregate (VMA), voids filled with asphalt (VFA) and dust to binder ratio (P_{200}/P_{be}). Correlation values represent the coefficient of correlation (R) of a linear relationship between two variables. A range of R values from -1 to +1 is used to represent the strength as well as direction of the linear relationship. A negative R value indicates an inverse relation between two variables meaning an increase in one variable will lead to a decrease in the other. A positive R value indicates a direct relation between two variables meaning an increase in one variable will also lead to an increase in the other. An absolute R value closer to 1 (either on positive or negative side) indicates a stronger correlation between two variables. In general, R value greater than 0.5 is considered moderate to strong correlation, whereas R value less than 0.5 is considered weak correlation. Table 5.4 shows the coefficients of correlation between RRI values and asphalt mixture properties for three different conditions.

Table 5.4 Coefficients of correlation between RRI values and asphalt mixture properties

	AC	P_{be}	VMA	VFA	P_{200}/P_{be}
RRI (All mixtures included)	0.66	0.59	0.55	0.53	0.54
RRI (Without RAP/RAS mixtures)	0.66	0.75	0.86	0.47	0.33
RRI (Without 19 mm NMAS mixtures)	0.69	-0.18	-0.25	0.21	0.76

Correlation values between RRI and asphalt mixture properties were initially evaluated when all six plant-produced mixtures were included in the analysis to explore the strength and directions of the relations. For this condition, Table 5.4 shows that RRI had direct moderate relations with all asphalt mixture properties. Nevertheless, this is unreasonable as higher AC usually results in weaker rutting performance. Moreover, higher VMA and VFA are indicators of higher AC; thus, they should have an inverse relation with RRI. The only reasonable correlation was noticed with P_{200}/P_{be} since higher P_{200}/P_{be} indicates a lower effective AC. Consequently, correlation values between RRI and asphalt mixture properties were re-evaluated under two conditions. The first condition was to omit mixtures that included RAP/RAS from the analysis and the second condition was to omit mixtures that had 19 mm NMAS and straight binder from the analysis. The purpose of this step was to find out the set of mixtures that will adjust the correlation values between RRI and asphalt mixture properties to the most reasonable relations. Table 5.4 shows that correlation values maintained a direct relation between RRI and all asphalt mixture properties after omitting RAP/RAS mixtures from the analysis which means that no significant difference had happened under this condition. On the other hand, negative correlation values of RRI with P_{be} and VMA as well as a closer R value to the inverse direction with VFA means that neglection of 19 mm NMAS mixtures containing straight binder from the analysis led to the most reasonable correlation values.

Overall, it can be inferred that HWTT test may not be the ideal test for implementing a BMD and developing performance-based specifications. The weak correlation of RRI with P_{be}, VMA and VFA as well as an illogical direct strong relation with AC proves that RRI parameter is incapable of capturing the impact of asphalt mixture properties on rutting performance. As a result, other rutting performance tests such as Asphalt Pavement Analyzer, Flow Number Test and Superpave Shear Tester should be taken into consideration and tested for their eligibility to become part of the BMD.

5.3.4 Development of Preliminary HWTT Test Criteria

Based on HWTT test results of the six plant-produced asphalt mixtures, local preliminary HWTT test criteria were developed for the application of BMD. HWTT test criteria were distinguished based on the most influential mix design parameters on rutting resistance. Based on boxplot analysis and correlation values between RRI and asphalt mixture properties, NMAS and use of polymer-modified binders were the two most significant parameters affecting HWTT test results. In addition to having weakest rutting and moisture performance as well as highest variability in HWTT test results (interpreted by largest interquartile ranges in boxplot analysis), mixes 1 and 5 caused coefficients of correlation between RRI values and asphalt mixture properties to deviate from the expected trend. Consequently, preliminary HWTT test criteria developed for mixtures with 19 mm NMAS and/or straight binders were different from mixtures with 12.5 mm NMAS and/or polymer-modified binders as shown in Table 5.5.

Table 5.5 Suggested preliminary HWTT test criteria

Mix design parameter		Preliminary HWTT test criteria
NMAS	19 mm	Maximum 10.0 mm rut depth at 15,000 passes
	12.5 mm	Maximum 10.0 mm rut depth at 20,000 passes
Type of virgin binder	Straight binder	Maximum 10.0 mm rut depth at 15,000 passes
	Polymer-modified binder	Maximum 10.0 mm rut depth at 20,000 passes

Since all mixes showed relatively adequate rutting performance, preliminary HWTT test criteria were selected such that majority of the tested samples must pass the proposed criteria. Thus, a database of rut depth values at 20,000 passes for all twelve samples was used to plot the cumulative distribution curve shown in Figure 5.3, and the rut depth corresponding to actual frequency of 85% (i.e., 10 mm) was selected to be the HWTT test criteria for rutting resistance. This means that 85% of the tested samples will have a maximum rut depth value of 10 mm at 20,000 passes. For HWTT test criteria of mixtures with 19 mm NMAS and/or straight binders, the same 10 mm maximum rut depth was selected but at fewer number of passes (i.e., 15,000) since these mixtures are expected to possess weaker rutting resistance. According to the suggested preliminary HWTT test criteria, only sample 1 of mix 1 would fail the rutting requirement. However, it cannot be deduced that mix 1 will require mix design modifications for improving its rutting performance, since a larger number of samples should be tested and analyzed to support this decision.

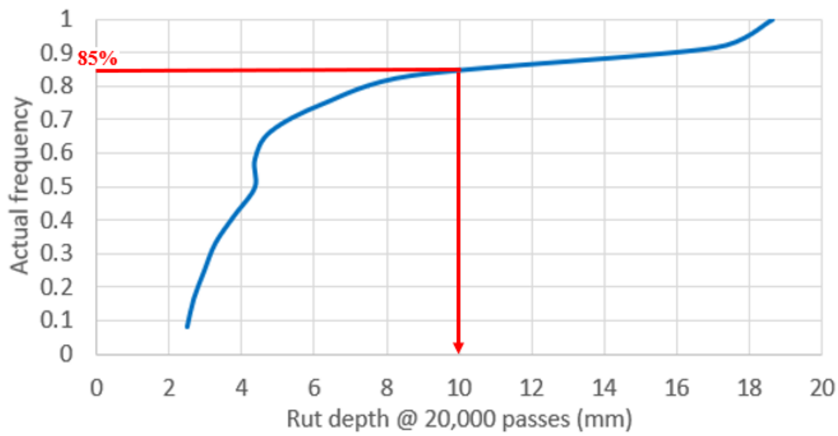

Figure 5.3 Cumulative distribution plot for rut depth at 20,000 passes

In conclusion, the proposed HWTT test criteria are not more than preliminary criteria based on the set of plant-produced asphalt mixtures included in this study. In other words, these criteria are subject to change if a greater database of HWTT test results was included (i.e., if a larger number of samples and/or mixtures were tested). Additionally, other types of mixtures such as warm-mix asphalt mixtures or mixtures encompassing high RAP contents might have their own criteria if tested and analyzed. Moreover, field evaluation of rutting performance for these six plant-produced mixtures is necessary after construction to verify the suggested HWTT test criteria. Finally, future studies are recommended to develop HWTT test criteria for moisture resistance. Despite that 19 mm NMAS mixtures and/or use of straight binder can also be correlated to weaker moisture resistance, the HWTT test results of the current six plant-produced mixtures cannot be used to develop moisture criteria since only one-third of the tested samples had experienced stripping. Therefore, a wider variety of asphalt mixtures should be evaluated to determine mix design parameters that would trigger poor moisture performance.

5.4 Illinois Flexibility Index Test Results

5.4.1 Analysis of I-FIT Test Output Parameters

The Illinois flexibility index test (I-FIT) was conducted according to AASHTO T 393 procedure (AASHTO T 393, 2021) to investigate cracking potential of the six plant-produced asphalt mixtures. Four semi-circular specimens were tested for each mix after a long-term aging protocol of 120 hours at 85°C. Subsequently, the average, standard deviation (S.D.), and coefficient of variation (C.O.V) of the four samples were determined for each of the six I-FIT test output parameters. Table 5.6 shows statistical properties of I-FIT test output parameters for the six plant-produced mixtures. The minimum flexibility index (FI) to pass the I-FIT test is 8 for all mixes as recommended primitively by Illinois Department of Transportation. The values of all I-FIT test output parameters for the four samples of each plant-produced mixture are represented in Appendix B.

Table 5.6 I-FIT test results of plant-produced mixtures

Parameter	Statistical Property	Mix Mix 1 (19, 58, 0, 0)	Mix 2 (12.5, 58 P, 0, 0)	Mix 3 (12.5, 64 P, 10, 0)	Mix 4 (12.5, 64 P, 10, 3)	Mix 5 (19, 58, 0, 0)	Mix 6 (12.5, 58 P, 0, 0)
Fracture Energy (J/m^2)	Average	1433.8	1423.7	1933.8	1890.0	1230.4	1454.4
	Minimum	1176.5	1340.8	1831.8	1772.3	1144.0	1240.5
	Maximum	1594.6	1491.8	2090.3	2088.1	1359.0	1653.2
	S.D.	180.48	74.70	115.73	139.11	99.80	122.91
	C.O.V (%)	12.59	5.25	5.98	7.36	8.11	8.45
Peak Load (KN)	Average	2.54	2.16	2.96	3.82	3.75	3.80
	Minimum	2.40	2.03	2.82	3.72	3.70	3.73
	Maximum	2.83	2.32	3.03	3.95	3.77	3.87
	S.D.	0.20	0.14	0.10	0.12	0.03	0.07
	C.O.V (%)	7.97	6.60	3.25	3.14	0.85	1.87
Post-Peak Slope	Average	2.54	1.68	2.23	4.76	7.04	5.90
	Minimum	2.25	1.44	1.77	4.04	5.85	4.48
	Maximum	3.19	1.94	2.72	6.00	9.73	9.24
	S.D.	0.44	0.23	0.39	0.90	1.82	0.35
	C.O.V (%)	17.23	13.50	17.38	18.83	25.87	5.85
Flexibility Index (FI)	Average	5.73	8.60	8.93	4.08	1.83	2.73
	Minimum	4.72	7.49	6.73	3.13	1.19	1.34
	Maximum	6.64	10.36	11.81	5.01	2.15	3.50
	S.D.	0.98	1.34	2.12	0.81	0.44	0.28
	C.O.V (%)	17.04	15.52	23.72	19.79	23.88	10.40
Tensile Strength (Psi)	Average	50.50	42.46	58.93	74.39	73.03	74.80
	Minimum	46.17	39.74	56.73	71.09	72.42	73.08
	Maximum	54.99	46.44	60.70	77.45	73.43	77.07
	S.D.	3.77	2.98	1.65	2.73	0.44	2.07
	C.O.V (%)	7.46	7.02	2.80	3.67	0.61	2.77
Critical Displacement (mm)	Average	2.36	2.94	2.85	2.22	1.45	1.69
	Minimum	2.21	2.73	2.58	2.12	1.26	1.40
	Maximum	2.64	3.06	3.22	2.51	1.61	1.86
	S.D.	0.19	0.15	0.27	0.19	0.15	0.07
	C.O.V (%)	8.10	4.95	9.55	8.63	10.03	3.87

Table 5.6 shows that mixes 5 and 6 have the least average FI values indicating highest cracking potential. This can be attributed mainly to the use of limestone aggregates which are soft

aggregates that can easily break if subjected to pressure. By comparing between mixtures of different NMAS that were obtained from the same construction project (i.e., mixes 1 and 2 as well as mixes 5 and 6), it can also be investigated from Table 5.6 that 12.5 mm NMAS mixtures have better cracking resistance than 19 mm NMAS mixtures. This can be attributed to difference in AC between the two gradation groups where 19 mm NMAS mixtures have average AC less than 5% and 12.5 mm NMAS mixtures have average AC more than 5%. Reducing NMAS is one method that can be applied to indirectly increase the design AC of asphalt mixtures because smaller aggregate sizes have higher surface-to-volume ratio. As a result, relatively more asphalt binder is required to coat these aggregate surfaces leading to higher AC which is directly proportional to cracking resistance. Moreover, smaller NMAS is a main reason for better aggregate interlock and decreased segregation issues which also contribute to better cracking performance.

Table 5.6 demonstrates the negative impact of RAS content on cracking resistance since the average FI of mix 4 dropped by more than 50% in comparison to mix 3 due to only 3% RAS. RAS binders are usually air-blown asphalt; thus, they are highly oxidized and very stiff binders. RAS binders have an average high temperature PG grade above 140°C and an average low temperature PG grade above 0°C (Zhou et al., 2012). Therefore, the highest average peak load value of mix 4 can be due to the stiffening effect caused by RAS binder. Table 5.6 also proves that type of virgin binder might not have a significant effect on cracking performance. Mix 2, with a polymer-modified binder, had a higher average FI than mixes 1 and 5 with straight binders. In addition, mix 3 demonstrated the best cracking performance despite having the stiffest type of virgin binder. This can be due to the I-FIT test being conducted at an intermediate temperature of 25°C. Low temperatures tend to expose brittle behaviour of asphalt binders more than intermediate temperatures. In conclusion, it can be deduced from Table 5.6 that reducing NMAS and/or increasing AC as well as avoiding the use of limestone aggregates and/or RAS are all strategies that can improve cracking performance. Consequently, mixes 2 and 3 were the only two mixtures that passed the proposed FI threshold. Figure 5.4 shows load-displacement curves of the six plant-produced mixtures.

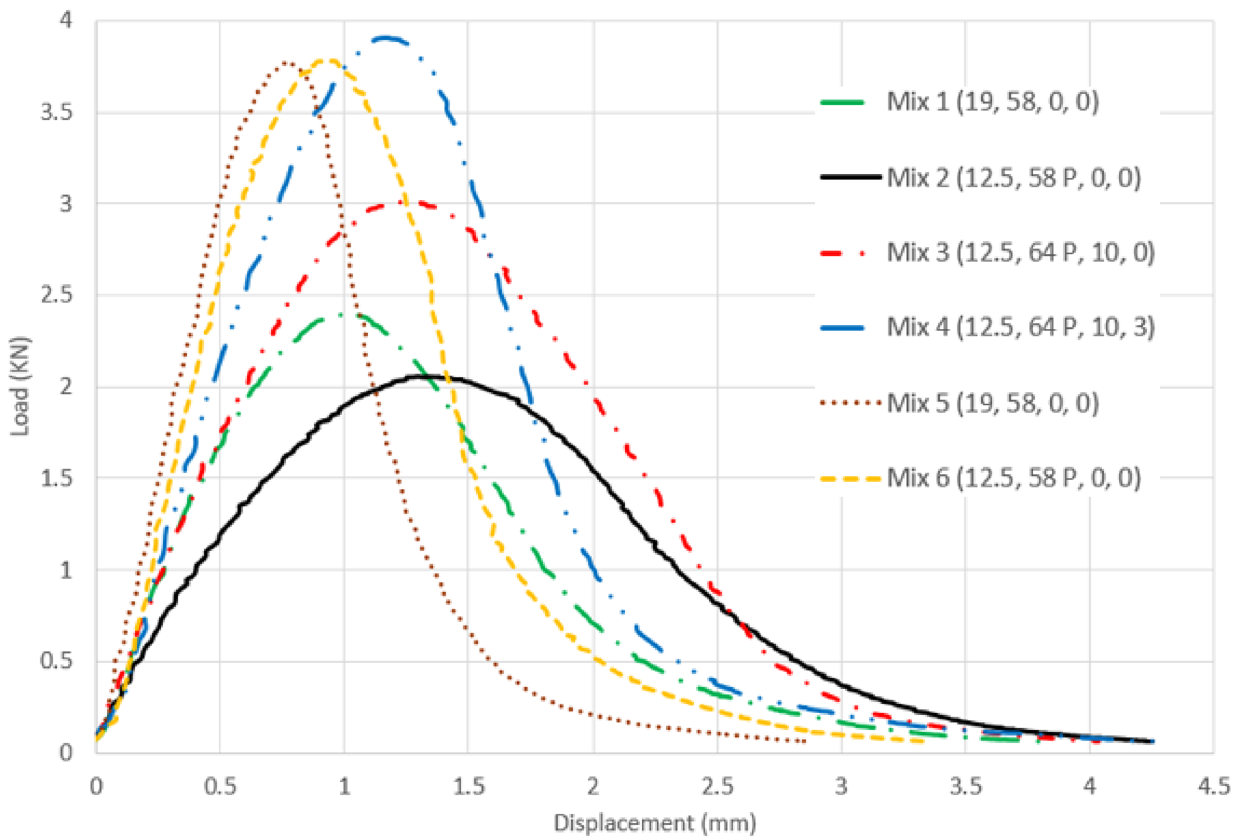

Figure 5.4 Load-displacement curves of plant-produced mixtures

Table 5.6 shows that fracture energy alone does not represent cracking performance of an I-FIT specimen. For instance, mix 4 had considerably higher average fracture energy value than mixes 1 and 2 despite having lower average FI. This means that higher fracture energy does not necessarily indicate better cracking resistance. On the contrary, post-peak slopes correlated well with average FI values. Mixes 2 and 3 (i.e., the only two mixtures that fulfilled minimum cracking requirements) had the least average post-peak slopes among the six mixtures. This illustrates the significance of post-peak slope in evaluating cracking resistance in conjunction with fracture energy. Finally, Table 5.6 proves that higher peak loads and tensile strength values do not always indicate lower cracking performance. Mix 3 demonstrated the best cracking performance while having higher average peak load and tensile strength than mix 1. Mixes 1 and 3 had relatively similar ductile behaviour (i.e., rate of crack propagation) since they both had close average post-peak slopes to each other. This means that the ability of mix 3 to resist higher stresses prior to crack initiation improved its FI in comparison to mix 1.

5.4.2 Impact of Mix Design Parameters on I-FIT Test Results

The six plant-produced asphalt mixtures involved several mix design parameters that can have significant influence on cracking performance. As a result, FI values of the 24 semi-circular specimens were grouped and compared in terms of four mix design parameters, including NMAS ("19 mm" and "12.5 mm"), RAP/RAS ("No RAP/RAS" and "With RAP/RAS"), type of aggregate ("Granite", "Gravel" and "Limestone") and type of virgin binder ("58-xx", "58-xx P" and "64-xx P"). The NMAS parameter also divided mixtures based on AC. 19 mm NMAS mixture group represented mixtures with AC less than 5% (< 5.0%) and 12.5 mm NMAS mixture group represented mixtures with AC more than 5% (> 5.0%). Figure 5.5 shows individual boxplots of FI values grouped by the aforementioned mix design parameters. Similar to HWTT test analysis, these boxplots should be interpreted cautiously since interaction between other mix design variables (which might be influential on I-FIT test results) is not considered in the analysis. According to AASHTO T 393 procedure (AASHTO T 393, 2021), a minimum of three semi-circular specimens are required to represent the I-FIT test result of one mix. Therefore, a database of 24 samples should be sufficient to explain the interaction between groups of a single mix design parameter since four samples were tested for each mix. However, accuracy of boxplot analysis will still increase if a larger database of FI values was included.

Figure 5.5a shows higher FI values for 12.5 mm NMAS mixtures with higher AC; thus, they exhibit better cracking performance than 19 mm NMAS mixtures with lower AC. Although interquartile ranges of the two mixture groups overlapped with each other, the mean FI values were relatively far from each other. Hence, it is unclear from the boxplot whether cracking resistance is sensitive to NMAS and/or AC. Figure 5.5b shows higher FI values for RAP/RAS mixtures; thus, they exhibit better cracking performance than mixtures without RAP/RAS. Nevertheless, this is an irrational outcome since RAP and RAS materials tend to make asphalt mixtures stiffer and more brittle. In addition, interquartile ranges of the two mixture groups overlapped with each other as well as mean FI values were relatively close to each other which means that cracking resistance may not be sensitive to RAP/RAS according to the boxplot.

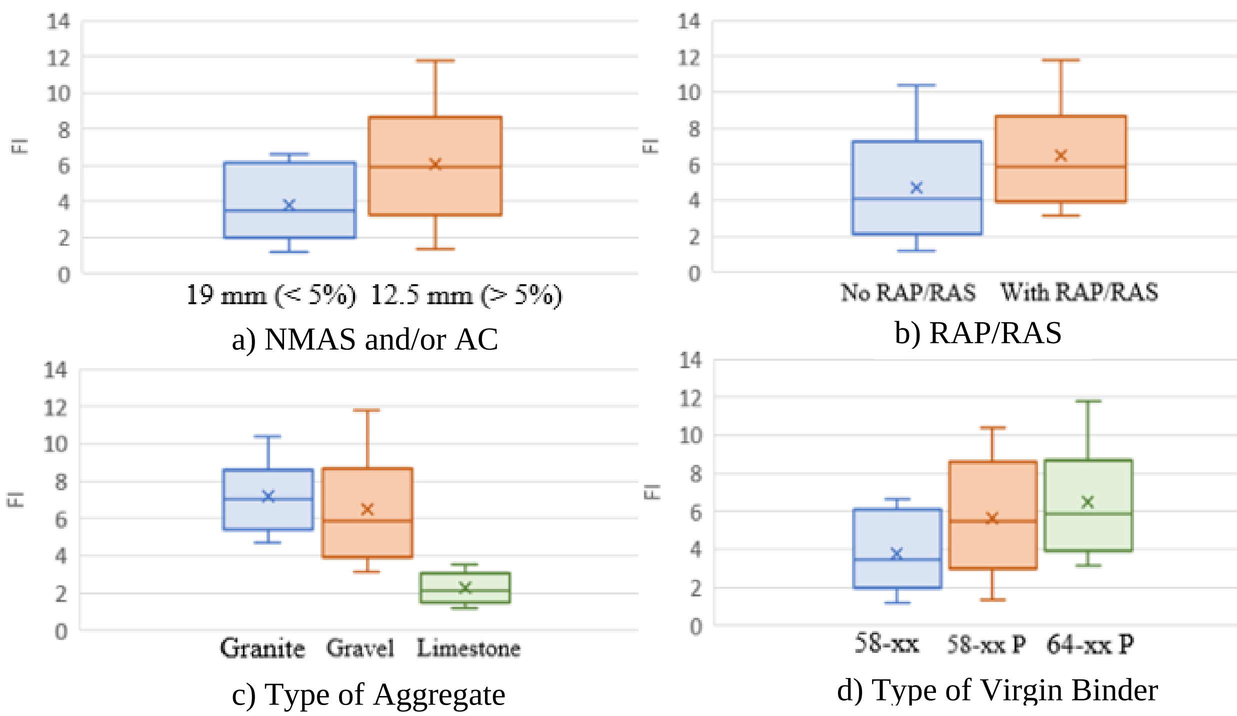

Figure 5.5 Box plots of FI values by mix design parameter

Figure 5.5c shows a significant difference in FI values when limestone aggregate mixture group was compared with other two aggregate mixture groups. However, the difference was minimal between granite and gravel aggregate mixture groups as well as their interquartile ranges overlapped with each other. This means that cracking resistance may be sensitive to type of aggregate only if limestone aggregates are used in the mix design. Figure 5.5d shows that the three asphalt binder mixture groups demonstrate minor differences in FI values. Moreover, interquartile ranges of the three mixture groups overlapped with each other which indicates that cracking resistance may not be sensitive to type of asphalt binder. To verify trends of cracking performance that were observed with the four mix design parameters in the boxplot analysis, one-way ANOVA and independent t-test were conducted on the groups of FI values at 95% confidence level and the results are presented in Table 5.7.

Table 5.7 Statistical tests results of FI values by mix design parameter

Mix design parameter	Statistical test	P-value[1]	Statistically significant
NMAS (“19 mm” and “12.5 mm”) and/or AC (“< 5.0%” and “> 5.0%”)	Independent t-test (two-tail)	0.04873	YES
RAP/RAS (“No RAP/RAS” and “With RAP/RAS”)	Independent t-test (two-tail)	0.18566	NO
Type of virgin binder (“58-xx”, “58-xx P” and “64-xx P”)	One-way ANOVA	0.17642	NO
Type of aggregate (“Granite”, “Gravel” and “Limestone”)	One-way ANOVA	0.00023	YES
Type of aggregate (“Granite” and “Gravel”)	Independent t-test (two-tail)	0.60502	NO
Type of aggregate (“Granite” and “Limestone”)	Independent t-test (one-tail)	0.00003	YES
Type of aggregate (“Gravel” and “Limestone”)	Independent t-test (one-tail)	0.00244	YES

1. If P-value < 0.05, groups are statistically significantly different.

Table 5.7 shows that FI group means did not have a statistically significant difference in terms of type of virgin binder as well as inclusion of RAP and/or RAS materials. Although inclusion of RAS was proved in section 5.4.1 to have a significant negative effect on cracking performance, a low RAP content of 10% in mix 3 did not cause a considerable drop in cracking resistance.

Therefore, mean FI values of RAP/RAS mixture group were comparable to the mixture group without RAP/RAS. In other words, the outcome of independent t-test might change if mixtures with higher RAP contents were included in the analysis. However, this does not deny that RAS is an influential mix design parameter on cracking performance. Overall, it can be deduced from Table 5.7 that cracking performance is mainly affected by change in NMAS and/or AC as well as use of limestone aggregates in asphalt mix design. In addition to the least FI values for mixes 5 and 6, application of one-tail independent t-test to compare between FI group means with a limestone aggregate mixture group indicates that the impact of limestone aggregates on cracking performance is certain to happen in the negative trend. As a result, the fragility of limestone aggregates was visually proved by comparing the shapes of three semi-circular specimens after the I-FIT test in Figure 5.6. Figure 5.6a shows a specimen from mix 1 with granite aggregates, whereas Figure 5.6b shows a specimen from mix 3 with gravel aggregates. Figure 5.6c shows a specimen from mix 5 with limestone aggregates.

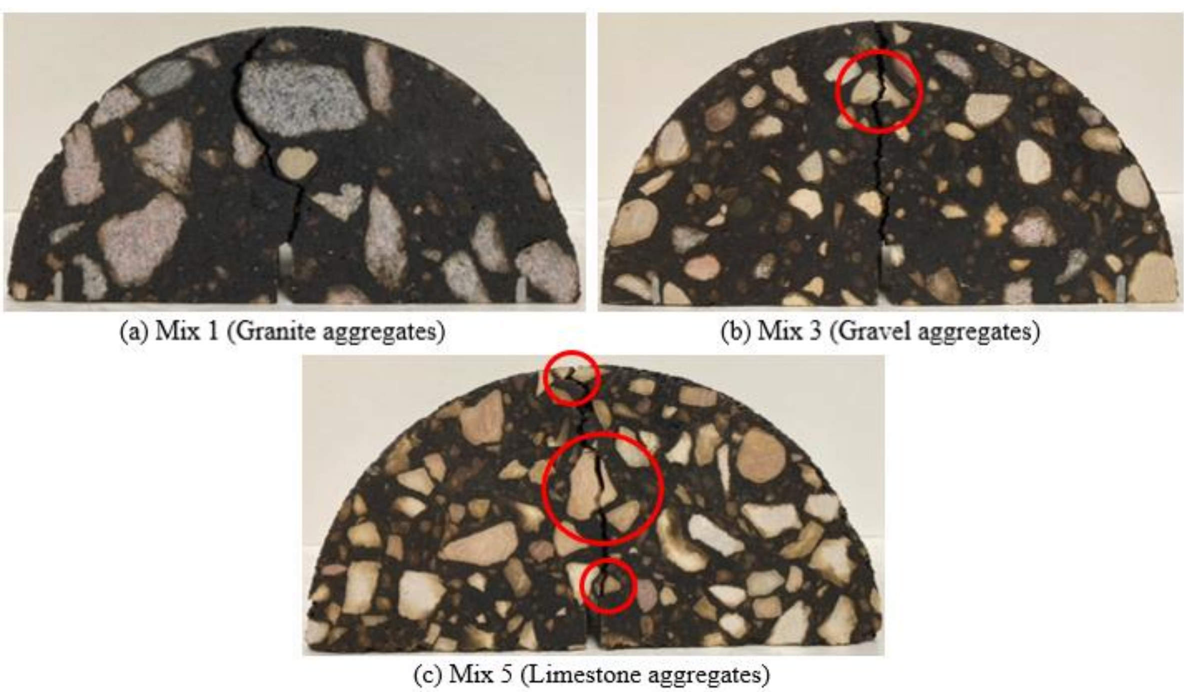

Figure 5.6 Semi-circular specimens after I-FIT test by type of aggregate

Figure 5.6a clearly shows that crack propagation happened between aggregate particles and eventually all aggregates remained intact which proves the stiffness of granite aggregates. Figure 5.6b shows that crack propagation happened through only one aggregate particle while other aggregates remained intact. This means that gravel aggregates may be softer than granite aggregates, but still they cannot be confirmed to be a main reason for poor cracking performance since mix 3 had highest average FI. Finally, Figure 5.6c shows that all aggregates that came across the crack trajectory broke and failed to resist any force which may indicate a rapid rate of crack propagation. This correlates well with highest post-peak slopes as well as least FI values for mixtures with limestone aggregates (i.e., mixes 5 and 6).

5.4.3 Impact of Long-Term Aging on I-FIT Test Results

Cracking is a type of pavement defect that is expected to happen in late service life of a pavement. Thus, long-term aging methods should be applied to all specimens expected to undergo any cracking test. To date, there is no fixed long-term aging protocol assigned for all cracking tests, but AASHTO R 30 standard (AASHTO R 30, 2022) had specified forced-draft oven aging on specimens at 85°C for five days. This long-term aging method has been of importance for industry due to its availability and practicability; however, several research is ongoing to reduce the time of oven aging to increase its feasibility. In this section, I-FIT test results of specimens that experienced long-term aging were compared with specimens that did not undergo any long-term aging protocol. The objective of this comparison is to understand the effect of standard AASHTO R 30 long-term aging procedure on cracking potential of plant-produced asphalt mixtures.

Preparation of unaged semi-circular specimens was identical to that of long-term aged specimens. Four I-FIT specimens were sawed from one Superpave gyratory compacted briquette for each mix to create a total of 24 specimens for the six plant-produced mixtures. Then, the I-FIT test was conducted on these specimens directly according to AASHTO T 393 procedure (AASHTO T 393, 2021). Nevertheless, these 24 specimens still experienced short-term aging during plant mixing; therefore, they were referred to as short-term aged specimens. Figure 5.7 shows three histograms that compare averages of FI values, fracture energy values and post-peak slopes between short-term and long-term aged I-FIT specimens for the six plant-produced mixtures. The statistical significance between the means of the two aging groups was determined by independent t-test at 95% confidence level. The drop in average FI due to long-term aging was calculated using Equation 5.1 and was denoted as aging rate. The values of all I-FIT test output parameters for the 24 short-term aged specimens are represented in Appendix B.

$$\text{Aging Rate (\%)} = \frac{Average\ FI_{Short-term} - Average\ FI_{Long-term}}{Average\ FI_{Short-term}} * 100 \qquad (5.1)$$

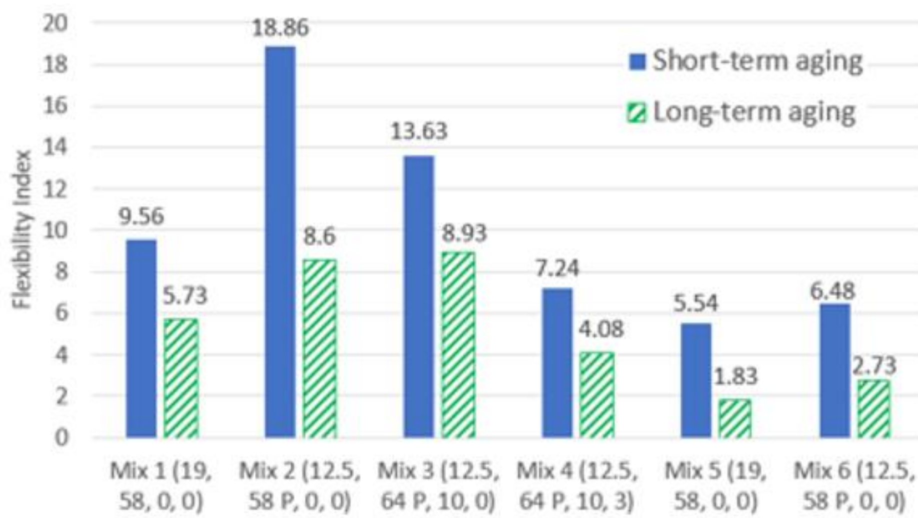

Aging rate (%)	40.1	54.4	34.5	43.7	67.0	57.9
Statistically significant	YES	YES	YES	YES	YES	NO

a) Flexibility index

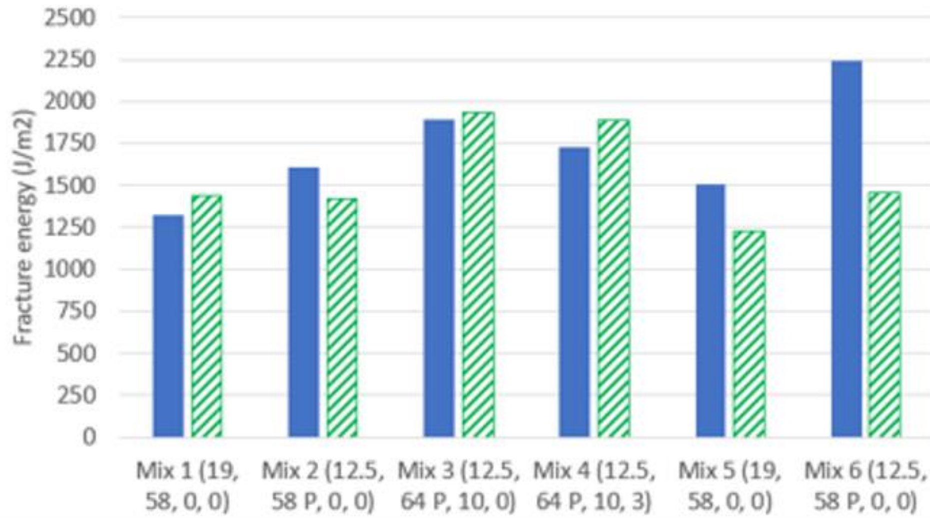

Statistically significant	NO	YES	NO	NO	YES	NO

b) Fracture energy

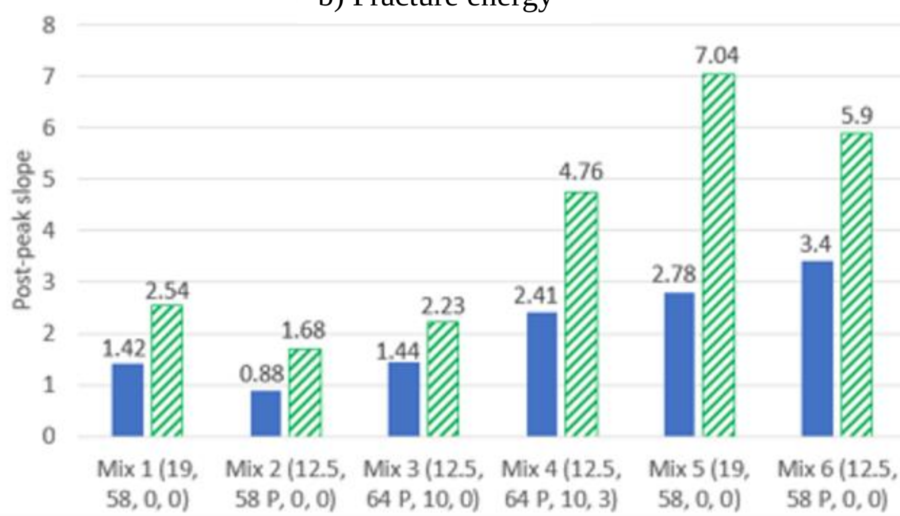

Statistically significant	YES	YES	YES	YES	YES	NO

c) Post-peak slope

Figure 5.7 Averages of I-FIT test results under short-term and long-term aging conditions

Figure 5.7a shows that long-term aging caused average FI values of the six mixtures to decrease considerably. This can be attributed to higher average post-peak slopes of long-term aged specimens as represented in Figure 5.7c. Aging increases asphaltene concentration which makes asphalt binders stiffer; thus, crack growth rate is higher in aged specimens and asphalt mixtures are more brittle. Additionally, means of FI values and post-peak slopes between the two aging groups are statistically significant for all mixtures except mix 6. This indicates the significant impact of aging on crack growth rate and on cracking potential. Furthermore, mixes 5 and 6 had the highest aging rate whereas mixes 3 and 4 had relatively the least aging rate. This means that the use of limestone aggregates not only had led to the least cracking resistance, but also had led to least aging resistance. On the contrary, the presence of already aged binders in mixes 3 and 4 increased aging resistance because recycled binders are less likely to undergo additional aging in comparison to virgin binders. Table 5.8 compares averages of critical displacement values, peak loads, and tensile strength values between short-term and long-term aged I-FIT specimens for the six plant-produced mixtures. Similarly, independent t-test was used to determine the statistical significance between the means of the two aging groups at 95% confidence level.

Table 5.8 Averages of I-FIT test results under short-term and long-term aging conditions

Parameter	Mix	Aging condition		Statistically significant
		Short-term	Long-term	
Critical Displacement (mm)	Mix 1 (19, 58, 0, 0)	2.99	2.36	YES
	Mix 2 (12.5, 58 P, 0, 0)	3.96	2.94	
	Mix 3 (12.5, 64 P, 10, 0)	3.50	2.85	
	Mix 4 (12.5, 64 P, 10, 3)	2.70	2.22	
	Mix 5 (19, 58, 0, 0)	2.21	1.45	
	Mix 6 (12.5, 58 P, 0, 0)	2.02	1.69	
Peak Load (KN)	Mix 1 (19, 58, 0, 0)	1.89	2.54	YES
	Mix 2 (12.5, 58 P, 0, 0)	1.70	2.16	
	Mix 3 (12.5, 64 P, 10, 0)	2.29	2.96	
	Mix 4 (12.5, 64 P, 10, 3)	2.81	3.82	
	Mix 5 (19, 58, 0, 0)	2.88	3.75	
	Mix 6 (12.5, 58 P, 0, 0)	3.15	3.80	
Tensile Strength (Psi)	Mix 1 (19, 58, 0, 0)	36.92	50.50	YES
	Mix 2 (12.5, 58 P, 0, 0)	34.23	42.46	
	Mix 3 (12.5, 64 P, 10, 0)	45.45	58.93	
	Mix 4 (12.5, 64 P, 10, 3)	55.29	74.39	
	Mix 5 (19, 58, 0, 0)	57.31	73.03	
	Mix 6 (12.5, 58 P, 0, 0)	61.00	74.80	

Figure 5.7b shows that long-term aging caused the average fracture energy values of three mixtures to increase slightly. Although this is an unexpected trend, the increase in fracture energy can be due to stiffer (i.e., aged) mixes having higher peak loads which may increase the area under load-displacement curves. On the other hand, aged mixes have higher post-peak slopes which may reduce the area under load-displacement curves. It is the ratio between increase in peak load and increase in post-peak slope that decides whether fracture energy will increase or decrease. Figure 5.8 compares typical load-displacement curves of short-term and long-term aged I-FIT specimens.

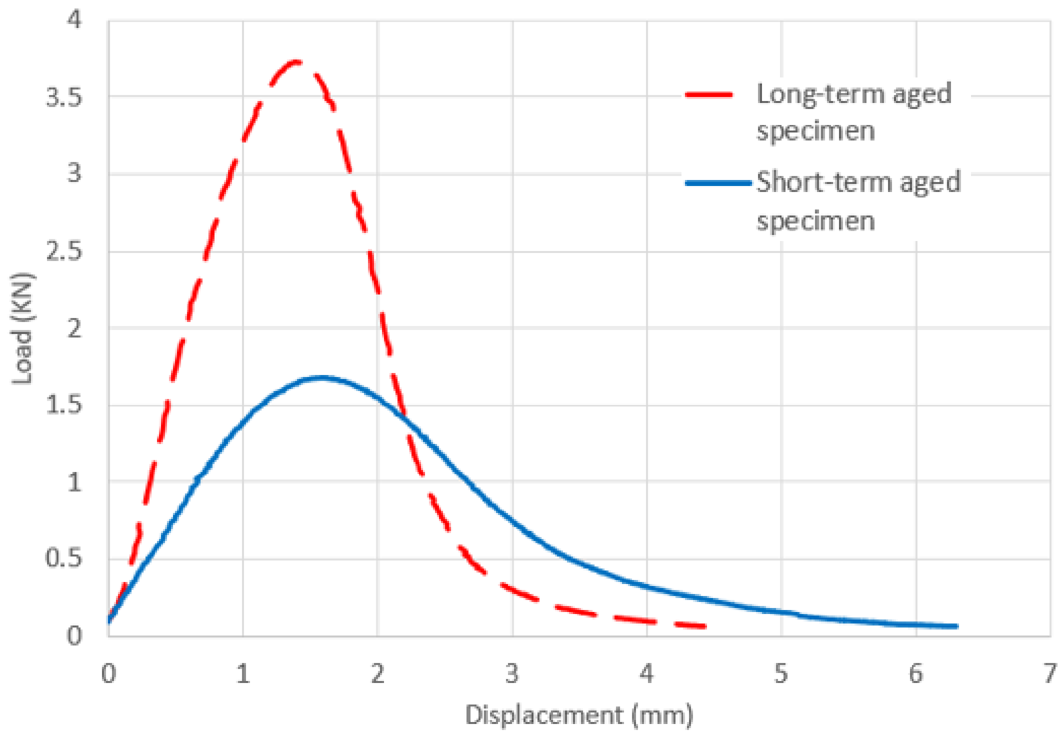

Figure 5.8 Typical load-displacement curves of short-term and long-term aged I-FIT specimens

Ultimately, Table 5.8 shows that long-term aging caused average peak loads and tensile strength values to increase for the six mixtures. Since these two I-FIT test output parameters are the main representatives of asphalt mixture stiffness, statistically significant means between the two aging groups for all mixtures indicate the influence of age hardening on stiffness of asphalt mixtures. Conversely, statistically insignificant means of fracture energy values between the two aging groups for four mixtures (out of a total of six mixtures) indicate that this I-FIT test output parameter cannot explain aging rate of asphalt mixtures.

5.4.4 Impact of Mix Design Parameters on Aging Rate

The six plant-produced asphalt mixtures involved several mix design parameters that can have significant influence on aging rate. Four aging rate values were calculated for each mixture according to the ascending order of FI values in the two aging sample groups. Although FI values of short-term and long-term aged specimens are not related, it was still a feasible method of representing average aging rates for each mixture. Subsequently, the 24 aging rate values were grouped and compared in terms of four mix design parameters, including NMAS (“19 mm” and “12.5 mm”), RAP/RAS (“No RAP/RAS” and “With RAP/RAS”), type of aggregate (“Granite”, “Gravel” and “Limestone”) and type of virgin binder (“58-xx”, “58-xx P” and “64-xx P”). Figure 5.9 shows individual boxplots of aging rate values grouped by the aforementioned mix design parameters. Similar to HWTT and I-FIT tests analysis, these boxplots should be interpreted cautiously since interaction between other mix design variables (which might be influential on aging rates) is not considered in the analysis. Aging rate values based on ascending order of FI values for short-term and long-term aged specimens are represented in Appendix B.

Figure 5.9a shows lower aging rates for 12.5 mm NMAS mixtures; thus, they are more aging resistant than 19 mm NMAS mixtures. However, interquartile ranges of the two mixture groups overlapped with each other and the mean aging rates were relatively close to each other. Hence, aging rate may not be sensitive to NMAS. Figure 5.9b clearly shows lower aging rates for RAP/RAS mixtures; thus, they are more aging resistant than mixtures without RAP/RAS. Despite a minor overlap between interquartile ranges of the two mixture groups, the mean aging rates were far away from each other which means that aging rate may be sensitive to RAP/RAS.

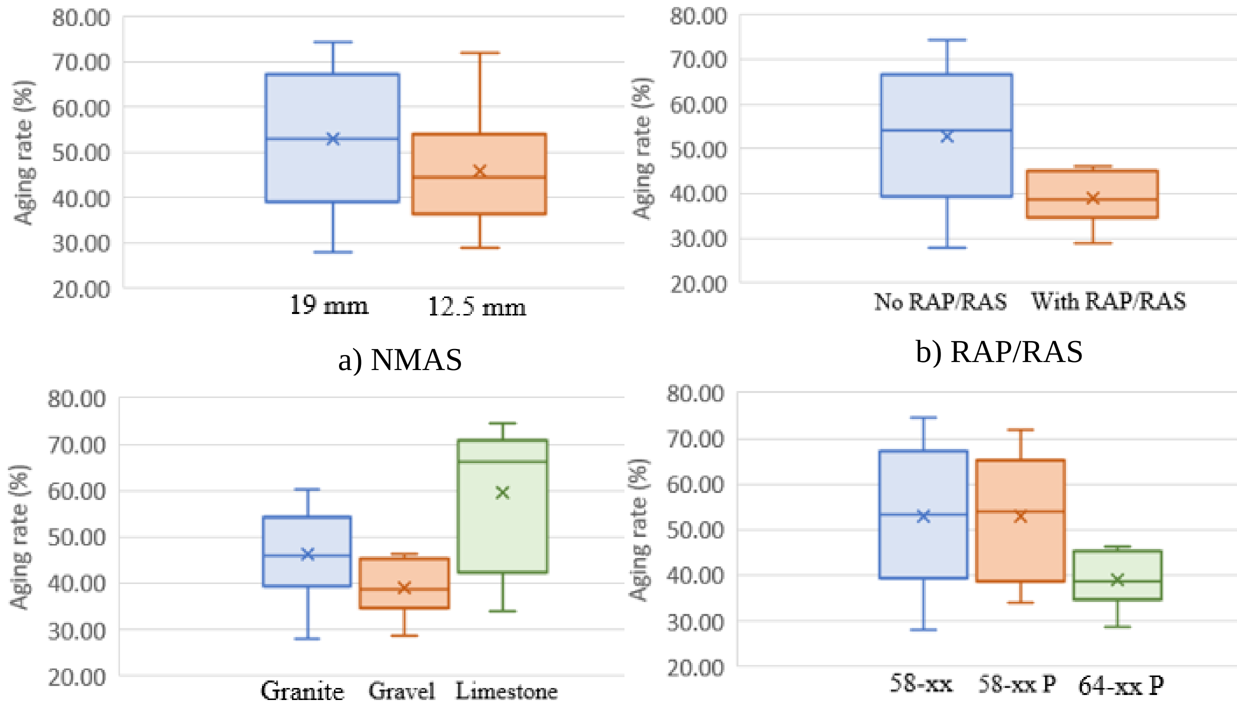

a) NMAS

b) RAP/RAS

c) Type of Aggregate

d) Type of Virgin Binder

Figure 5.9 Box plots of aging rate values by mix design parameter

Figure 5.9c shows clear differences in aging rate among the three aggregate mixture groups. Despite the lower aging rate of gravel aggregate mixture group can also be attributed to presence of RAP/RAS, limestone aggregate mixture group had much lower resistance to aging than the other two aggregate mixture groups. This means that the aging rate may be sensitive to type of aggregate especially limestone aggregates. Figure 5.9d shows a significant difference in aging rate when “64-xx P” binder mixture group was compared with the other two binder mixture groups. However, the difference was minimal between “58-xx” and “58-xx P” binder mixture groups as well as their interquartile ranges overlapped with each other. This means that aging rate may be sensitive to type of virgin binder only if stiffer binders with higher temperature PG grades are used in the mix design. To verify trends of aging rate that were observed with the four mix design parameters in the boxplot analysis, independent t-test was conducted on the groups of aging rate values at 95% confidence level and the results are presented in Table 5.9.

Table 5.9 shows that aging rate values had a statistically significant difference in terms of inclusion of RAP and/or RAS materials as well as use of limestone aggregates and stiffer virgin binders with higher temperature PG grades which conforms well to the outcome of boxplot analysis. Limestone aggregates mitigate aging resistance; hence, they are not good candidates to maintain serviceability of asphalt mixtures. On the other hand, incorporation of RAP/RAS materials and/or use of stiffer virgin binders are useful strategies to improve aging resistance. However, they might not be a reliable approach to produce aging resistant mixtures because recycled materials and stiffer asphalt binders generally result in brittle asphalt mixtures with low flexibility.

Table 5.9 Independent t-test results of aging rate values by mix design parameter

Mix design parameter	Independent t-test	P-value[1]	Statistically significant
NMAS (“19 mm” and “12.5 mm”)	two-tail	0.310	NO
RAP/RAS (“No RAP/RAS” and “With RAP/RAS”)	one-tail	0.002	YES
Type of aggregate (“Granite” and “Gravel”)	two-tail	0.114	NO
Type of aggregate (“Granite” and “Limestone”)	one-tail	0.033	YES
Type of aggregate (“Gravel” and “Limestone”)	one-tail	0.004	YES
Type of virgin binder (“58-xx” and “58-xx P”)	two-tail	0.992	NO
Type of virgin binder (“58-xx” and “64-xx P”)	one-tail	0.025	YES
Type of virgin binder (“58-xx P” and “64-xx P”)	one-tail	0.013	YES

1. If P-value < 0.05, groups are statistically significantly different.

5.4.5 Development of Preliminary I-FIT Test Criteria

Based on I-FIT test results of the six plant-produced asphalt mixtures, local preliminary I-FIT test criteria were developed for both short-term and long-term aging conditions. The suggested threshold FI values for the two aging conditions are presented in Table 5.10.

Table 5.10 Suggested local preliminary I-FIT test criteria

Aging condition	Minimum Flexibility Index
Short-term	10.5
Long-term	7.0

The threshold FI values in Table 5.10 had been selected based on the influence of mix design properties on cracking performance. According to boxplot analysis, use of limestone aggregates in mix design was the most significant parameter affecting I-FIT test results. In addition to having the highest cracking potential, mixes 5 and 6 were least resistant to aging. Therefore, mixes 5 and 6 were classified as brittle mixes that cannot pass I-FIT test criteria. Furthermore, comparing between average FI values of mixes obtained from the same construction project helped in deciding the preliminary criteria. The 3% RAS in mix 4 had led to approximately 50% reduction in average FI value in comparison to mix 3 for both aging conditions. Moreover, the higher NMAS and/or lower AC in mix 1 had led to 50% and 35% reduction in average FI value in comparison to mix 2 for short-term and long-term aging conditions, respectively. As a result, mixes 1 and 4 were also classified as brittle mixes that cannot pass I-FIT test criteria. Ultimately, it was decided that only mixes 2 and 3 are eligible to pass I-FIT test criteria and the threshold FI values in Table 5.10 were selected such that nearly all samples in the two mixture groups should pass the criteria for both aging conditions.

In conclusion, the proposed I-FIT test criteria are preliminary criteria based only on the set of plant-produced asphalt mixtures included in this study. Nevertheless, these criteria still provide a meaningful separation between acceptable and unacceptable cracking performance for asphalt mixtures in Manitoba. Similar to HWTT test criteria, I-FIT test criteria are subject to change if other types of mixtures such as high RAP mixtures or warm-mix asphalt mixtures were included in this study. In addition, evaluation of field performance is necessary to validate any proposed criteria for any performance test. Therefore, field cracking performance of these six plant-produced mixtures should be monitored after construction to verify the suggested I-FIT test criteria especially for long-term aging condition.

5.5 Dynamic Modulus Test Results

The dynamic modulus test (DMT) was conducted according to AASHTO T 342 procedure (AASHTO T 342, 2022) to investigate stiffness of the six plant-produced asphalt mixtures. Three full-size specimens were tested for each mix at four different temperatures (-10, 4.4, 21.1 and 37.8ºC) and six loading frequencies (0.1, 0.5, 1.0, 5.0, 10 and 25 Hz) to determine dynamic modulus. Subsequently, dynamic modulus values of the three specimens in each mix were averaged and combined to develop a DM master curve according to AASHTO PP 62 procedure (AASHTO PP 62-10, 2012). Figure 5.10 presents the master curves and Table 5.11 shows the average dynamic modulus values of the six plant-produced mixture groups. The dynamic modulus values of the three specimens in each mixture group are represented in Appendix B.

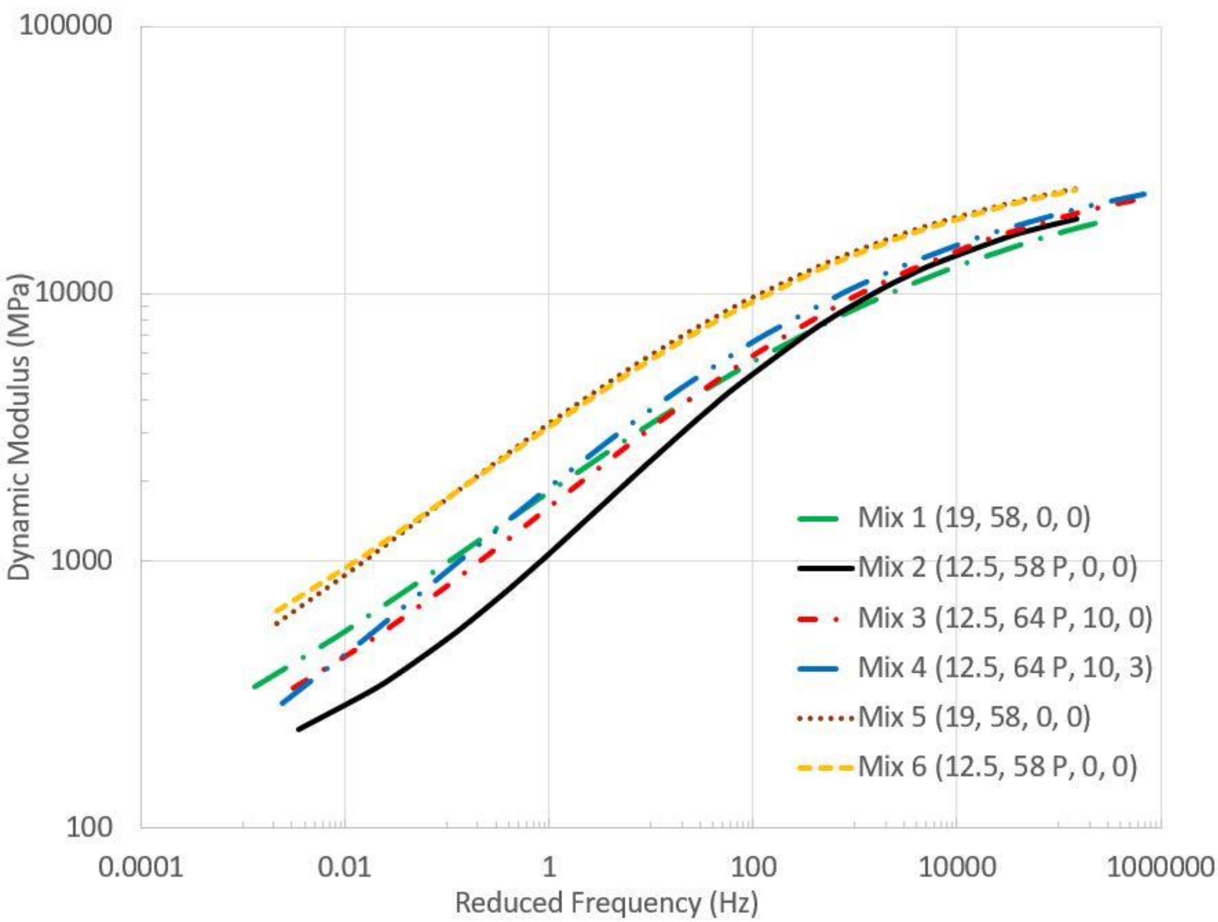

Figure 5.10 Dynamic modulus master curves of plant-produced mixtures

Table 5.11 Average dynamic modulus of plant-produced mixtures

Temperature (°C)	Dynamic Modulus of Mix 1 (19, 58, 0, 0) - MPa					
	0.1 Hz	0.5 Hz	1.0 Hz	5.0 Hz	10 Hz	25 Hz
-10	8902.00	11721.3	12986.3	15980.7	17163.7	18754.7
4.4	3527.63	4966.87	5753.33	8005.93	9202.93	10639.5
21.1	1040.95	1490.77	1768.13	2731.40	3240.63	4049.53
37.8	354.853	473.410	551.283	844.993	1084.77	1456.90
Temperature (°C)	**Dynamic Modulus of Mix 2 (12.5, 58 P, 0, 0) - MPa**					
	0.1 Hz	0.5 Hz	1.0 Hz	5.0 Hz	10 Hz	25 Hz
-10	8057.57	11116.4	12562.0	16342.0	17887.7	19723.3
4.4	2289.17	3666.80	4520.10	7099.73	8438.90	10047.2
21.1	512.733	813.350	1018.47	1820.60	2382.90	3382.17
37.8	243.597	324.140	370.727	551.730	750.737	1109.30
Temperature (°C)	**Dynamic Modulus of Mix 3 (12.5, 64 P, 10, 0) - MPa**					
	0.1 Hz	0.5 Hz	1.0 Hz	5.0 Hz	10 Hz	25 Hz
-10	11704.7	15317.3	16842.3	20439.0	21866.3	23395.3
4.4	3669.87	5367.37	6295.63	9070.43	10233.0	11713.7
21.1	839.650	1228.10	1503.60	2553.43	3203.30	4153.53
37.8	353.980	468.760	548.713	875.643	1138.00	1588.07
Temperature (°C)	**Dynamic Modulus of Mix 4 (12.5, 64 P, 10, 3) - MPa**					
	0.1 Hz	0.5 Hz	1.0 Hz	5.0 Hz	10 Hz	25 Hz
-10	12355.3	15834.0	17356.3	20772.3	22246.3	24047.7
4.4	4287.70	6084.73	7084.10	9805.20	11011.7	12474.7
21.1	931.170	1484.03	1847.63	3063.87	3777.70	4849.67
37.8	310.610	450.053	554.770	963.033	1252.33	1657.27
Temperature (°C)	**Dynamic Modulus of Mix 5 (19, 58, 0, 0) - MPa**					
	0.1 Hz	0.5 Hz	1.0 Hz	5.0 Hz	10 Hz	25 Hz
-10	13487.7	16974.0	18554.0	22313.0	23746.7	25465.0
4.4	6010.83	8323.17	9555.00	12768.7	14194.0	16041.0
21.1	1781.00	2677.10	3221.13	4997.37	5943.30	7256.67
37.8	615.797	868.383	1039.09	1706.13	2192.90	2954.80
Temperature (°C)	**Dynamic Modulus of Mix 6 (12.5, 58 P, 0, 0) - MPa**					
	0.1 Hz	0.5 Hz	1.0 Hz	5.0 Hz	10 Hz	25 Hz
-10	12585.7	15937.0	17462.0	21206.7	22791.0	24764.3
4.4	5694.27	7850.80	9014.00	12131.0	13597.0	15499.7
21.1	1763.93	2576.90	3095.47	4767.97	5645.50	6974.00
37.8	668.027	944.507	1104.62	1712.70	2120.27	2841.43

The master curves in Figure 5.10 show that mixes 5 and 6 had higher dynamic modulus values than mixes 1, 2, 3 and 4 at all testing temperatures. This suggests that mixes 5 and 6 may enhance rutting resistance at warmer temperatures, while reducing fatigue and thermal cracking resistance at intermediate and lower temperatures, respectively. At intermediate temperatures, mixes 2 and 3 had lower dynamic modulus values than mixes 1 and 4. This suggests that mixes 2 and 3 may enhance fatigue cracking resistance which correlates well with I-FIT test results discussed previously in Table 5.6, where mixes 2 and 3 had highest average FI values. At low temperatures, comparison was more challenging because mixes 1, 2, 3 and 4 had relatively close dynamic modulus values to each other. However, mixes 3 and 4 tend to show higher dynamic modulus values than mixes 1 and 2 indicating higher thermal cracking potential. Mixes 3 and 4 include the stiffest type of virgin binder as well as RAP and RAS. This conforms well to the concept that low temperatures tend to expose brittle behaviour of stiffer asphalt binders more than intermediate temperatures. Finally, Figure 5.10 shows that dynamic modulus values at high temperatures do not correlate well with HWTT test results discussed previously in Table 5.2. Mixes 1 and 5, that had the least average RRI values, showed higher dynamic modulus values than mixes 2, 3 and 4. Despite that comparison between the two tests might be unnecessary because all mixtures had acceptable rutting performance, reasons for incompatible rankings between HWTT test results and dynamic modulus values at high temperatures are mentioned in the following section.

5.6 Correlation Between HWTT, I-FIT and Dynamic Modulus Values

DMT test results were used to rank the six plant-produced asphalt mixtures with respect to their resistance to thermal cracking, fatigue cracking and rutting. Thermal cracking resistance was ranked by comparing average dynamic modulus values at low temperature (-10°C) and high frequency (25 Hz). Fatigue cracking resistance was ranked by comparing average dynamic modulus values at intermediate temperature (21.1°C) and frequency (10 Hz). Rutting resistance was ranked by comparing average dynamic modulus values at high temperature (37.8°C) and low frequency (0.1 Hz). Table 5.12 shows rankings of the six plant-produced mixtures. Since HWTT test was conducted at high temperature (45ºC) and I-FIT test was conducted at intermediate temperature (25ºC), DMT test rutting and fatigue cracking rankings were also compared to HWTT test rankings (based on average RRI) and I-FIT test rankings (based on average FI), respectively.

Table 5.12 HWTT, I-FIT and DMT tests rankings of plant-produced mixtures

Mix	Thermal cracking (-10ºC, 25 Hz)		Fatigue cracking (21.1ºC, 10 Hz)		I-FIT Rank[1]		Rutting (37.8ºC, 0.1 Hz)		HWTT Rank[1]
	$\lvert E^* \rvert$ (MPa)	Rank[1]	$\lvert E^* \rvert$ (MPa)	Rank[1]	Short-term	Long-term	$\lvert E^* \rvert$ (MPa)	Rank[1]	
Mix 1 (19, 58, 0, 0)	18754.7	1	3240.63	3	3	3	354.85	3	6
Mix 2 (12.5, 58 P, 0, 0)	19723.3	2	2382.90	1	1	2	243.60	6	4
Mix 3 (12.5, 64 P, 10, 0)	23395.3	3	3203.30	2	2	1	353.98	4	2
Mix 4 (12.5, 64 P, 10, 3)	24047.7	4	3777.70	4	4	4	310.61	5	1
Mix 5 (19, 58, 0, 0)	25465.0	6	5943.30	6	6	6	615.80	2	5
Mix 6 (12.5, 58 P, 0, 0)	24764.3	5	5645.50	5	5	5	668.03	1	3

1. “1” indicates the best performance and “6” indicates the weakest performance.

Table 5.12 shows that fatigue cracking rankings according to DMT test correlate well with I-FIT test rankings for both short-term and long-term aging conditions. Average FI values of mixes 2 and 3 are relatively similar for long-term aging condition; thus, their inverted I-FIT test ranking could be considered insignificant. In addition, Table 5.12 shows that thermal cracking rankings according to DMT test correlate well with I-FIT test rankings only for mixes 4, 5 and 6. This means that these three mixes are also expected to have weak thermal cracking resistance. For the other three mixes, mix 3 had higher thermal cracking potential than mixes 1 and 2. Mix 3 has the stiffest type of virgin binder as well as 10% RAP proportion. This reveals the sensitivity of thermal cracking resistance to stiffer asphalt binders since mixes 1 and 2 are virgin mixes.

On the other hand, Table 5.12 shows that rutting rankings according to DMT test do not match with HWTT test rankings. As mentioned previously in chapter 4, this can be attributed primarily to different testing conditions between HWTT test and DMT test. Different testing temperatures as well as immersion of samples in water in the HWTT test might be a reason for incompatible rankings. Moreover, HWTT test assesses permanent deformation whereas DMT test assesses recoverable strain of samples which might be another variation that had led to incompatible rankings. To reinforce this outcome, the strength of correlation of DM values at intermediate and high temperatures was determined via linear regression analysis with I-FIT and HWTT tests results, respectively. The coefficients of determination (R^2) between $|E^*|_{21.1°C}$ values and FI values were measured at all frequencies for both short-term and long-term aging conditions. Similarly, R^2 values were measured between $|E^*|_{37.8°C}$ values and RRI, rut depth at 20,000 passes as well as creep slope at all frequencies. Table 5.13 shows the calculated R^2 values for all conditions.

Table 5.13 Correlation between DM values and output parameters of I-FIT and HWTT tests

Test	Parameter	R^2 at DMT test frequencies					
		0.1 Hz	0.5 Hz	1.0 Hz	5.0 Hz	10 Hz	25 Hz
I-FIT	Flexibility index (short-term)	0.70	0.72	0.72	0.71	0.70	0.66
	Flexibility index (long-term)	0.77	0.82	0.83	0.82	0.81	0.79
HWTT	Rutting Resistance Index	0.0010	0.0040	0.0050	0.0110	0.0120	0.0160
	Rut depth at 20,000 passes	0.0020	0.0050	0.0060	0.0120	0.0130	0.0170
	Creep slope	0.0020	0.0001	0.0001	0.0025	0.0030	0.0050

Table 5.13 shows that DM values had strong correlation with FI values at all frequencies for both short-term and long-term aging conditions. Conversely, DM values had very weak correlation with the three HWTT test output parameters at all frequencies. Therefore, DMT test rankings did not match with HWTT test rankings, unlike I-FIT test rankings. This means that the I-FIT test may be an ideal test for implementing a BMD as well as developing performance-based specifications.

Overall, DMT test cannot replace reliable tests, such as I-FIT and HWTT tests, to rank cracking and rutting performance. This is because the DMT test characterizes asphalt mixtures to only predict their cracking and rutting performance. In a nutshell, it is ranking according to HWTT test that should be used to classify rutting performance of the six plant-produced asphalt mixtures.

5.7 Balanced Mix Design

A performance space diagram (PSD) is a visual tool that helps mix designers to identify whether performance measures of asphalt mixtures are balanced or not. Figure 5.11 shows two PSD's, each consisting of four quadrants divided according to preliminary I-FIT and HWTT tests criteria. The six plant-produced asphalt mixtures are located within the quadrants based on their I-FIT and HWTT tests results to aid in deciding possible applications for these mixtures. Figure 5.11a represents a PSD with threshold FI value for short-term aging condition. Figure 5.11b represents a PSD with threshold FI value for long-term aging condition. HWTT test results are displayed based on average rut depth (mm) at 20,000 passes for mixes 2, 3, 4 and 6. For mixes 1 and 5, HWTT test results are displayed based on average rut depth (mm) at 15,000 passes. I-FIT test results are displayed based on minimum, average and maximum FI values for each mixture. Range of FI combined between two performance quadrants for multiple mixtures; hence, it would better represent cracking performance on PSD. Ranges of rut depths were in one performance quadrant for all mixtures except mix 1; thus, mix 1 was eventually assessed based on its average value.

Figure 5.11 shows that mixes 2 and 3 are entirely located in the acceptable quadrant for both aging conditions. This means that these two mixtures are the best performing mixtures with outstanding cracking and rutting resistance; therefore, they can be good candidates for high traffic volume roads such as urban arterials or freeways. Mix 1 is predominantly located in the soft and unstable quadrant for short-term aging condition, whereas it is entirely located in the same quadrant for long-term aging condition. This means that mix 1 is a poor mix that does not accept both cracking and rutting criteria. Consequently, mix 1 can be a good candidate for roads with temporary use only such as back lanes or driveways. Although mix 1 is a binder course layer (i.e., non-surface mix), it might suit its function only for low traffic volume roads such as local roads in residential areas. However, the use of mix 1 as a non-surface mix for high traffic volume roads is not recommended.

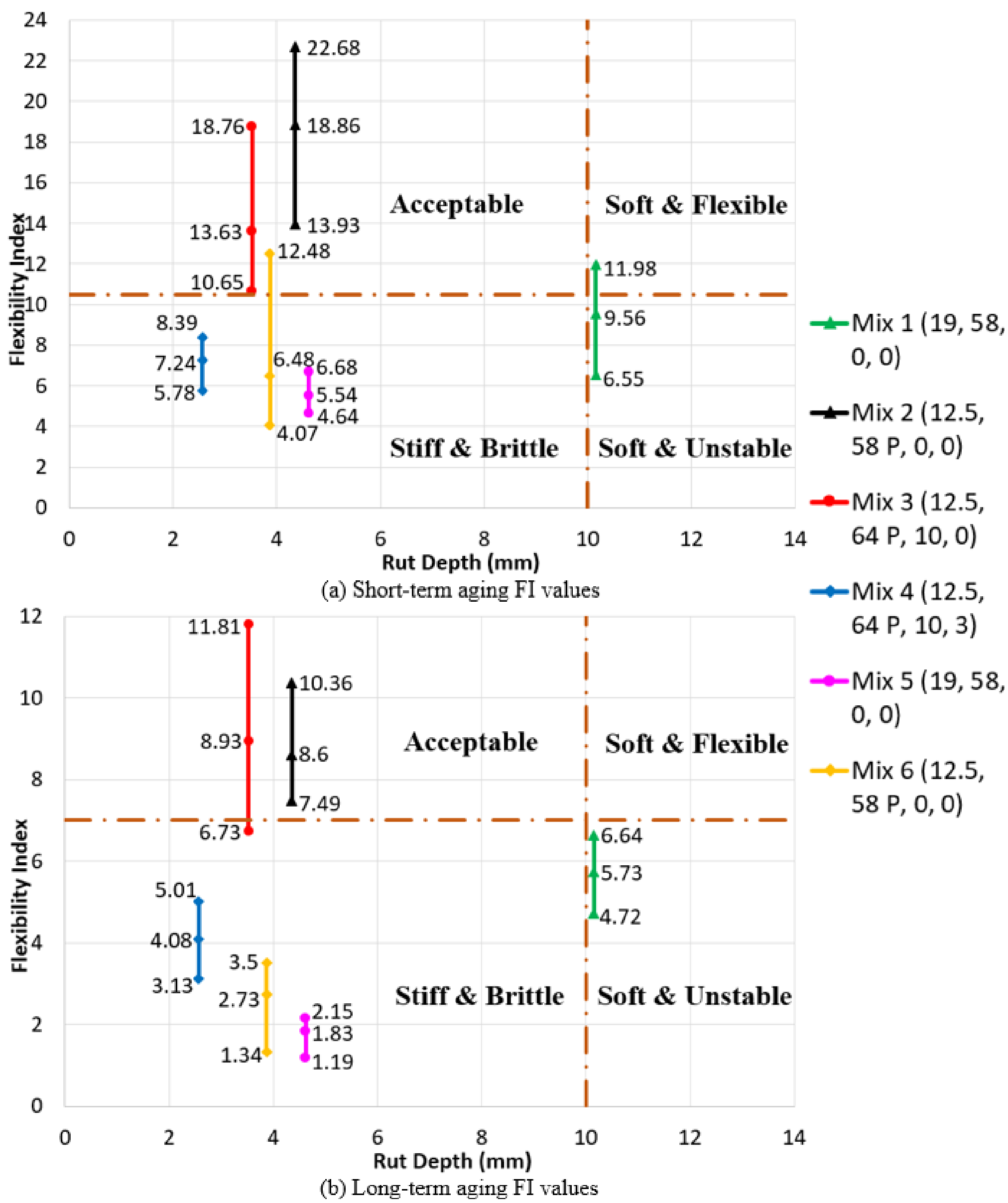

Figure 5.11 Performance space diagrams of plant-produced mixtures

On the other hand, mixes 4 and 5 are found in the stiff and brittle quadrant for both aging conditions. This means that these two mixtures have high rutting resistance but poor cracking resistance; therefore, they can be good candidates as bottom layers of a full-depth pavement (i.e., non-surface mixes) since they cannot be exposed to direct vehicle loads due to their low flexibility. This already complies to the function of mix 5 which is a binder coarse layer. Mix 6 is entirely located in the stiff and brittle quadrant for long-term aging condition, whereas it is combined with the acceptable quadrant for short-term aging condition. Mix 6 had one crack-resistant sample with a considerably higher FI value than average for short-term aging condition. This sample could be considered as an outlier and mix 6 would be classified as a brittle mix like mixes 4 and 5 for both aging conditions.

5.8 Summary

This chapter presented cracking and rutting performance tests results of six plant-produced asphalt mixtures consisting of various mix design parameters. Cracking performance test was conducted for both short-term and long-term aging conditions. HWTT test results concluded that mixes 1 and 5 had the least rutting resistance as well as they were the only two mixtures that experienced stripping. This was mainly attributed to higher NMAS and use of straight asphalt binder; thus, these two mixtures were assigned lower rutting criteria in the HWTT test. I-FIT test results concluded that mixes 1, 4, 5 and 6 had the least cracking resistance due to incorporation of RAS, higher NMAS, lower AC, and use of limestone aggregates in asphalt mix design. Comparison between short-term and long-term aging I-FIT test results proved that use of limestone aggregates had led to the least aging resistance. On the contrary, incorporation of RAP and RAS materials improved aging resistance. Table 5.14 summarizes the impact of the most influential mix design parameters on cracking, rutting and aging resistance.

Table 5.14 Impact of influential mix design parameters on cracking, rutting and aging resistance

Performance measure	Mix design parameter	Correlation
Rutting resistance	Nominal Maximum Aggregate Size	Inverse
	Proportion of RAP/RAS	Direct
	Polymer modification of asphalt binder	Direct
Cracking resistance	Nominal Maximum Aggregate Size	Inverse
	Asphalt Content	Direct
	Proportion of RAS	Inverse
	Proportion of limestone aggregates	Inverse
Aging resistance	Proportion of RAP/RAS	Direct
	Proportion of limestone aggregates	Inverse
	High temperature PG grade of asphalt binder	Direct

Table 5.14 involves strategies that can be implemented to optimize the BMD. However, these strategies should be implemented cautiously as steps taken to mitigate cracking issues may cause rutting issues. Overall, the best strategies to optimize the BMD based on the results of this study would be designing virgin mixtures with 12.5 mm NMAS and polymer-modified binders. Moreover, inclusion of low RAP content (≤ 20%) may enhance rutting performance without significantly reducing cracking performance which supports a BMD. On the other hand, inclusion of RAS, increasing NMAS, decreasing AC, and use of limestone aggregates significantly reduce cracking performance; therefore, these four strategies do not lead to a successful BMD. Finally, the presence of only two plant-produced mixtures in the acceptable quadrant of the PSD indicates that relying solely on volumetric properties as End Results Specification does not guarantee adequate long-term performance of the final mix design. Therefore, combining performance testing with current volumetric mix design procedures and integrating performance tests criteria to End Results Specification is recommended to construct durable asphalt mixtures.

Chapter 6. Evaluation of In-Service Mixtures

6.1 Introduction

Several rutted wheel paths have been investigated on recently constructed roads in the city of Winnipeg (COW). As part of forensic investigations, field cores were extracted from four regional streets and experimental tests were conducted on in-service surface layers to investigate reasons for premature failure of these streets. The main objective of this study was to determine via advanced laboratory tests whether surface mixtures meet the specified standards of quality and performance. Initially, bulk densities of the field cores are discussed and asphalt contents of the four groups are compared. Then, the four mix gradations are determined to confirm whether they meet COW specification limits (City of Winnipeg, 2020). In addition, rutting performance and stiffness of the field samples are analyzed and linear regression analysis was applied to correlate between dynamic modulus values and HWTT test results.

6.2 Bulk Densities

The bulk specific gravity (BSG) of field cores extracted from four regional streets was determined according to AASHTO T 166 procedure (AASHTO T 166, 2022). The average BSG value of two cores was determined for each street except for street 3. The second core of street 3 could not be used for representing the density of the wearing surface because it had some visible surface cracks; therefore, only one core was tested. Detailed calculations of BSG are presented in Appendix C. The BSG values were 2.215, 2.280, 2.226, and 2.249 for streets 1, 2, 3, and 4, respectively. Street 1 had the least density which could be a reason for why rutting was observed on street 1. On the other hand, street 2 did not experience rutting and had the highest density. This means that BSG values correlate well with the outcome of field inspection; however, other properties (not only density) might also contribute to the same conclusion.

6.3 Ignition Oven Test Analysis

The ignition test method was used to determine asphalt content (AC) of the four in-service asphalt mixtures according to AASHTO T 308 procedure (AASHTO T 308, 2022). Table 6.1 shows AC values of each mixture after the deduction of 0.5% to account for the correction factor. Detailed calculations of AC are presented in Appendix C. AC values from the job mix formula (JMF) were obtained from Marshall mix design reports for each street. Table 6.1 shows the range of AC values from minimum to maximum found in these reports. The middle AC in each range (i.e., 5.5%) was used to calculate the difference between AC measurements from the JMF and ignition oven test.

Table 6.1 Ignition oven test results and comparison with job mix formula

Street number	Range of AC from JMF (%)	AC from ignition oven test (%)	Average difference between two AC measurements (%)
Street 1	5.0 – 6.0	6.23	0.70
Street 2	5.0 – 6.0	6.60	1.10
Street 3	5.2 – 5.8	6.44	0.95
Street 4	N/A[1]	7.05	–

1. N/A: Data not available.

Table 6.1 shows that mixtures from streets 1, 2, and 3 had roughly the same range of AC according to JMF. Furthermore, AC values obtained via ignition oven test were approximately 0.5 – 1.0% higher than those from the JMF. During the ignition test method, flammable mix components (such as organic matters) are removed, and fine aggregate particles are lost in the ventilation which leads to higher estimated values of AC. Figure 6.1 shows the time-temperature profiles of the four in-service asphalt mixtures during ignition.

Figure 6.1 does not show much variability between time-temperature profiles of the four mixtures since all peak temperatures were achieved in a short timeframe (between 12 – 15 minutes). Moreover, the profiles were closely aligned with each other in the post-peak zone as well as a constant temperature of 538°C was reached at 44 minutes for the four profiles. The lack of variability in time-temperature series of these in-service mixtures can be attributed to similar aggregate type and asphalt binder grade as well as only one sample of uniform size being tested for each mix. Therefore, testing a larger number of samples with different sizes as well as mixtures with varying gradations and binder types can aid in producing time-temperature profiles having a better correlation with AC results.

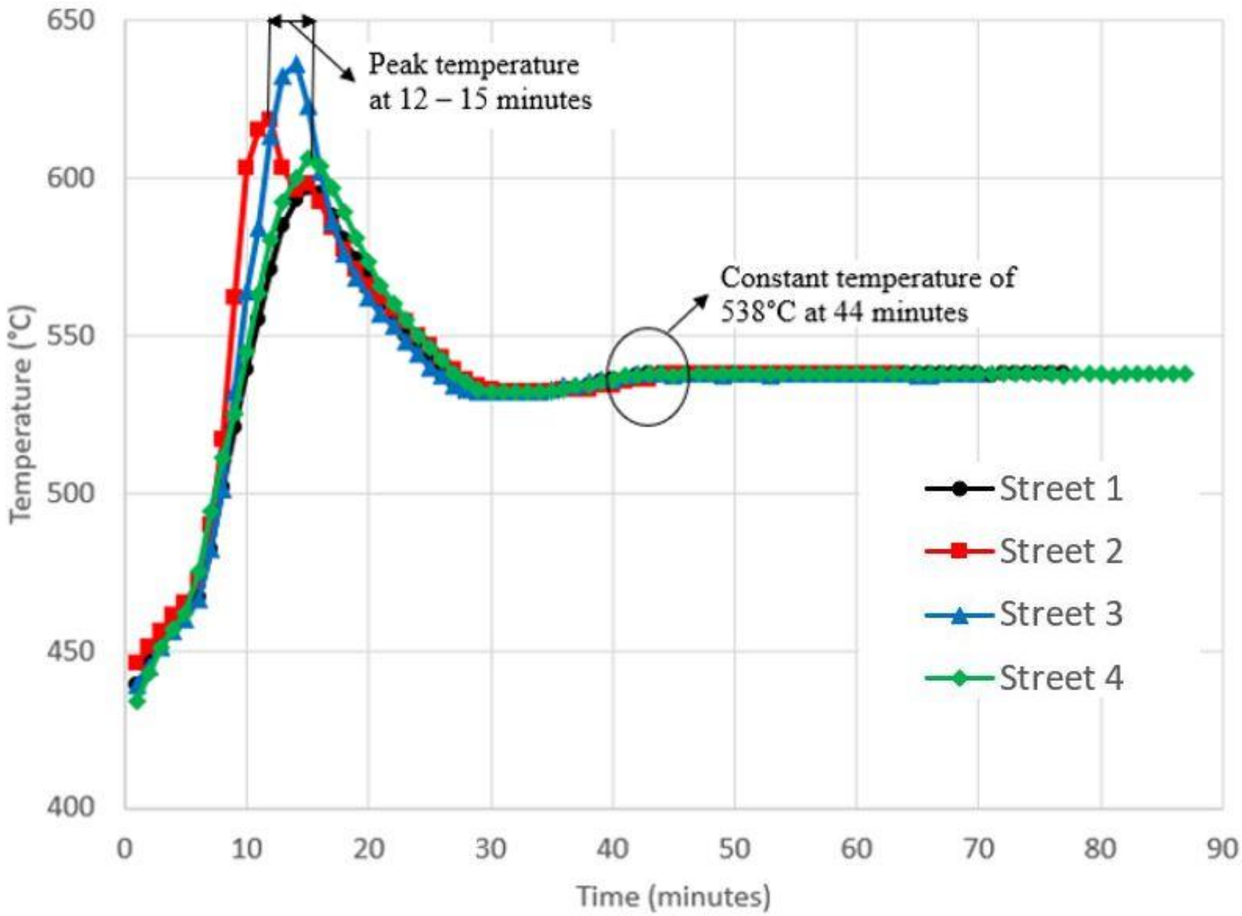

Figure 6.1 Time-temperature profiles of in-service asphalt mixtures

After the ignition oven test, the gradation of extracted aggregates of each in-service asphalt mixture was determined using Marshall set of sieves in COW specifications (City of Winnipeg, 2020). Table 6.2 shows gradations of the four in-service asphalt mixtures as well as gradation limits according to COW specifications (City of Winnipeg, 2020). Detailed calculations of sieve analysis procedure are presented in Appendix C.

Table 6.2 Aggregate gradations of in-service asphalt mixtures

Sieve size (mm)	Percent passing				Specification limits (%)
	Street 1	Street 2	Street 3	Street 4	
19	100.0	100.0	100.0	100.0	100
16	99.6	100.0	100.0	100.0	90 – 100
12.5	93.1	92.9	95.0	93.7	75 – 95
9.5	78.0	82.0	80.8	84.5	70 – 90
4.75	60.2	63.0	65.4	65.0	55 – 70
2.00	42.8	51.1	52.7	52.8	35 – 55
0.425	15.9	23.6	19.7	25.0	17 – 32
0.180	8.0	8.3	8.2	9.7	4 – 12
0.075	5.0	5.0	4.9	5.7	3 – 7

Table 6.2 shows that all four mixtures have a maximum aggregate size of 16 mm and a NMAS of 12.5 mm which is typical for wearing surface gradations in the city of Winnipeg. Furthermore, the four gradations fall within the required specification limits at all sieves except for the mixture from street 1 which had a 1% deviation from the minimum limit at sieve no. 40 (0.425 mm). Nevertheless, this minor deviation can be attributed to the changes in gradation resulting from the ignition test method, particularly that it is in the fine portion of the mix. Hence, this deviation can be neglected and the mixture from street 1 can be considered to accept the specification limits for gradation. Figure 6.2 shows the 0.45 power gradation curves of the four in-service asphalt mixtures as well as the maximum and minimum specification limits.

Both Table 6.1 and Figure 6.2 show that the mixture from street 1 had the least AC and the least amount of fine aggregates, whereas the mixture from street 4 had the highest AC and the most amount of fine aggregates. Moreover, the mixture from street 2 had higher AC as well as more fine aggregates than the mixture from street 3. This means that the amount of AC resulting from the ignition test method correlates well with the fine fraction of gradation passing sieve no. 10 for all four mixtures which proves the sensitivity of the ignition test method to the fine portion of mix gradation. Therefore, there is a need for determining an accurate aggregate correction factor according to the individual mix design to increase the reliability of AC results from the ignition oven test.

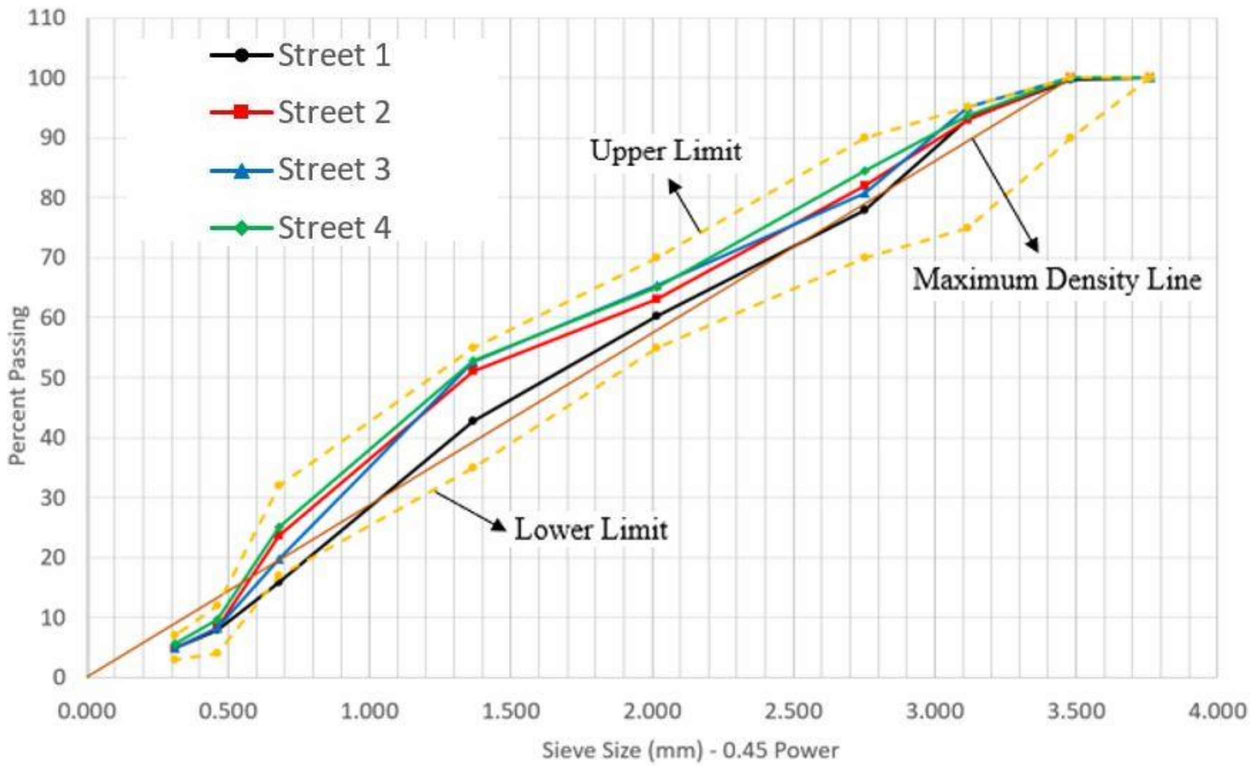

Figure 6.2 0.45 power gradation curves of in-service asphalt mixtures

6.4 Hamburg Wheel-Tracking Test Results

The Hamburg wheel-tracking test (HWTT) was conducted according to AASHTO T 324 procedure (AASHTO T 324, 2023) to investigate rutting and moisture potential of the four in-service asphalt mixtures. Two samples of paired field compacted wearing surface cylinders were tested for each in-service mixture simultaneously in one test except for the mixture from street 2. Rutting was not observed on street 2; therefore, only one sample was tested to examine rutting performance. Table 6.3 shows the HWTT test output parameters of seven samples obtained from the four streets.

As previously mentioned in chapter 5, performance test results of field samples could be used to check the reliability of preliminary performance test criteria developed in the BMD framework.

The suggested HWTT test criteria of plant-produced mixtures were developed according to mix design guidelines and production conditions in Manitoba. Since the four streets of this study are in the city of Winnipeg, asphalt mixtures are expected to maintain similar design and construction conditions as in Manitoba. Therefore, rutting test results of the four in-service asphalt mixtures were used to validate the preliminary HWTT test criteria developed for plant-produced mixtures in chapter 5. All in-service mixtures have a straight asphalt binder; thus, Table 6.3 shows the rut depth at 15,000 passes for the seven samples to compare with the maximum 10 mm rut depth criterion required at the same number of passes.

Table 6.3 shows that the sample from street 2 had the least creep slope as well as the highest RRI indicating the best rutting performance. This conforms well to the absence of rutted wheel paths on street 2. On the contrary, several rutted wheel paths were investigated on street 1, while the two samples collected from that street showed adequate rutting performance. One reason can be that the HWTT test had assessed the remaining rutting resistance of these field samples after some had already been consumed by traffic loads. Thus, the HWTT result might not represent the total rutting resistance of the tested samples. Another reason can be that visible rutting on the pavement surface does not necessarily indicate improper mix design of the HMA layer. Rutting may occur due to several reasons including inadequate compaction or replacement of the subgrade layer. This deduces the significance of examining severely rutted pavements and carefully identifying the root cause of rutting to decide the appropriate action of repair.

Table 6.3 HWTT test results of in-service asphalt mixtures

Parameter	Street 1		Street 2	Street 3		Street 4	
	Sample-01	Sample-02	Sample-01	Sample-01	Sample-02	Sample-01	Sample-02
Creep Slope (mm/pass)	0.000204	0.000215	0.000163	0.000235	0.000393	0.000923	0.000211
Stripping Slope (mm/pass)	0.000400	-	0.000200	0.000358	-	0.001681	-
Number of passes to SIP	17,997	-	16,806	13,440	-	8,885	-
Rut depth to SIP (mm)	8.96	-	4.79	6.38	-	14.04	-
Rut depth at 15,000 passes (mm)	8.47	6.26	4.58	6.67	8.12	23.81	4.79
Ratio of stripping to creep slope	1.96	-	1.23	1.52	-	1.82	-
RRI	12,449	14,276	15,717	10,458	12,150	1,359	15,426
Result of rutting potential	Pass	Pass	Pass	Pass	Pass	Fail	Pass
Result of moisture potential[1]	N/A	Pass	N/A	N/A	Pass	N/A	Pass

1. N/A: Data not available.

Table 6.3 also shows inconsistent HWTT test results for the two samples obtained from a single street. In addition to one pass and one fail rutting test result on street 4, one sample from streets 1 and 3 did not experience stripping (unlike the other sample) indicating a superior moisture performance. However, all samples from streets 1, 2, and 3 that encountered stripping had a number of passes to SIP greater than 10,000 which also indicates adequate moisture performance, but a ratio of stripping to creep slope less than 2 for all samples identifies that SIP cannot be used as an indicator of moisture susceptibility (Tavassoti and Baaj, 2020). As a result, relying on two samples only might be insufficient to represent HWTT test results of one street and a larger number of samples from various locations should be tested to better illustrate HWTT test results of an in-service mixture as well as to provide better comparison and ranking of rutting and moisture performance for multiple field projects. Figure 6.3 shows the HWTT curves of the seven field samples.

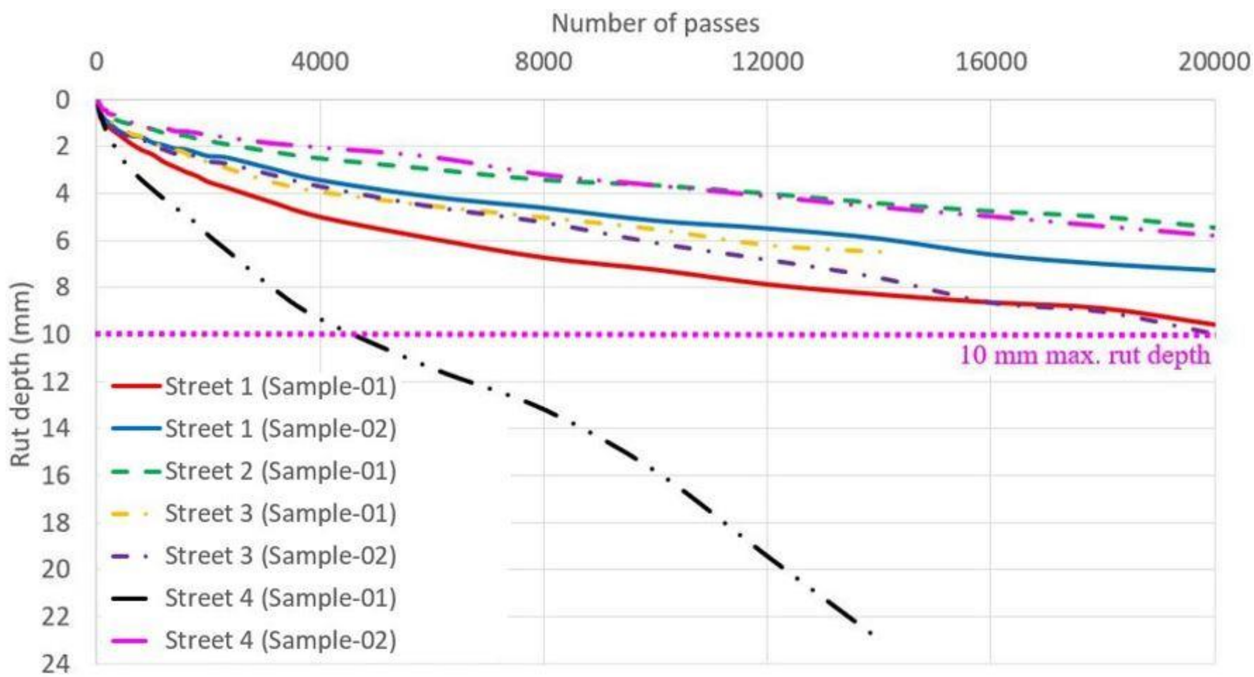

Figure 6.3 HWTT test curves of in-service asphalt mixtures

It is logical to conclude from both Table 6.3 and Figure 6.3 that all samples had adequate rutting performance except for one sample collected from street 4 which was unable to reach 20,000 passes at the end of the test. This proves the reliability of the preliminary HWTT test criteria developed in chapter 5 since all samples had rut depth less than 10 mm at 15,000 passes except for sample-01 from street 4. In other words, the preliminary HWTT test criteria were able to distinguish between acceptable and unacceptable rutting performance of in-service asphalt mixtures which validates these criteria to be used in Manitoba.

Overall, field samples that passed rutting criteria did not show significant differences among their creep slopes. Moreover, the stripping potential cannot be identified for all samples that experienced stripping. One main reason for this outcome is the similarity in mix design constituents for the four in-service asphalt mixtures such as type of aggregate and binder. Additionally, these field samples were collected from streets that are in the same city and fall within the same category of road functional classification (i.e., regional roads). Hence, they were subjected to approximately similar traffic levels and climatic conditions. Therefore, a collection of samples from streets of different locations and functional class as well as mixture components and/or proportions is required to produce HWTT test results with greater variability.

6.5 Dynamic Modulus Test Results

The dynamic modulus test (DMT) was conducted according to AASHTO T 342 procedure (AASHTO T 342, 2022) to investigate stiffness of the four in-service asphalt mixtures. Two small-scale specimens cored laterally from the wearing surface were tested for each mixture at four different temperatures (-10, 4.4, 21.1 and 37.8ºC) and six loading frequencies (0.1, 0.5, 1.0, 5.0, 10 and 25 Hz) to determine dynamic modulus. Subsequently, dynamic modulus values of the two specimens in each mixture were averaged and combined to develop a DM master curve according to AASHTO PP 62 procedure (AASHTO PP 62-10, 2012). Table 6.4 shows average dynamic modulus values of the four in-service asphalt mixture groups and Figure 6.4 represents their master curves. Dynamic modulus values of the two specimens in each mixture group are presented in Appendix C.

The master curves in Figure 6.4 show that samples from streets 1 and 2 had higher dynamic modulus values than samples from streets 3 and 4 at all testing temperatures. This suggests that streets 1 and 2 samples may enhance resistance to rutting at warmer temperatures, while reducing fatigue and thermal cracking resistance at intermediate and lower temperatures, respectively. This correlates well with HWTT test results discussed previously in Table 6.3, where samples from streets 1 and 2 had higher RRI (thus, rutting resistance) than samples from streets 3 and 4. Overall, the master curves of the four mixtures represent a rational outcome of field performance in which streets demonstrating better rutting resistance are expected to have lower cracking resistance. This can also be attributed to mix design similarities between samples as well as exposure to steady field conditions mainly traffic levels and climate.

Table 6.4 Average dynamic modulus values of in-service asphalt mixtures

Temperature	Dynamic Modulus of Street 1 (MPa)					
(°C)	0.1 Hz	0.5 Hz	1.0 Hz	5.0 Hz	10 Hz	25 Hz
-10	12828.5	15321.5	16367.5	18720.5	19478.5	20601.5
4.4	5867.30	7963.65	8949.30	11433.7	12302.5	13755.5
21.1	1673.70	2540.85	3078.50	4668.10	5490.20	6540.20
37.8	438.310	671.400	878.455	1512.30	1970.35	2609.90
Temperature	Dynamic Modulus of Street 2 (MPa)					
(°C)	0.1 Hz	0.5 Hz	1.0 Hz	5.0 Hz	10 Hz	25 Hz
-10	10710.1	13169.5	14198.0	16794.5	17746.5	18768.0
4.4	4525.20	6212.25	7071.00	9476.20	10435.1	11680.0
21.1	1367.15	2069.40	2492.40	3901.90	4643.95	5648.00
37.8	452.395	667.895	792.955	1322.80	1719.15	2318.90
Temperature	Dynamic Modulus of Street 3 (MPa)					
(°C)	0.1 Hz	0.5 Hz	1.0 Hz	5.0 Hz	10 Hz	25 Hz
-10	9558.80	11520.0	12533.0	14999.0	15904.5	17096.5
4.4	4073.00	5679.20	6491.90	8627.95	9515.15	10583.8
21.1	1113.82	1758.35	2160.55	3457.95	4093.10	5020.10
37.8	271.080	422.680	553.890	949.310	1285.85	1790.40
Temperature	Dynamic Modulus of Street 4 (MPa)					
(°C)	0.1 Hz	0.5 Hz	1.0 Hz	5.0 Hz	10 Hz	25 Hz
-10	9254.95	11387.8	12311.8	14658.5	15501.0	16499.5
4.4	3578.85	5040.10	5789.40	7823.50	8739.75	9748.20
21.1	965.510	1509.90	1857.90	2993.90	3583.70	4367.65
37.8	275.310	431.005	520.550	875.900	1181.99	1633.60

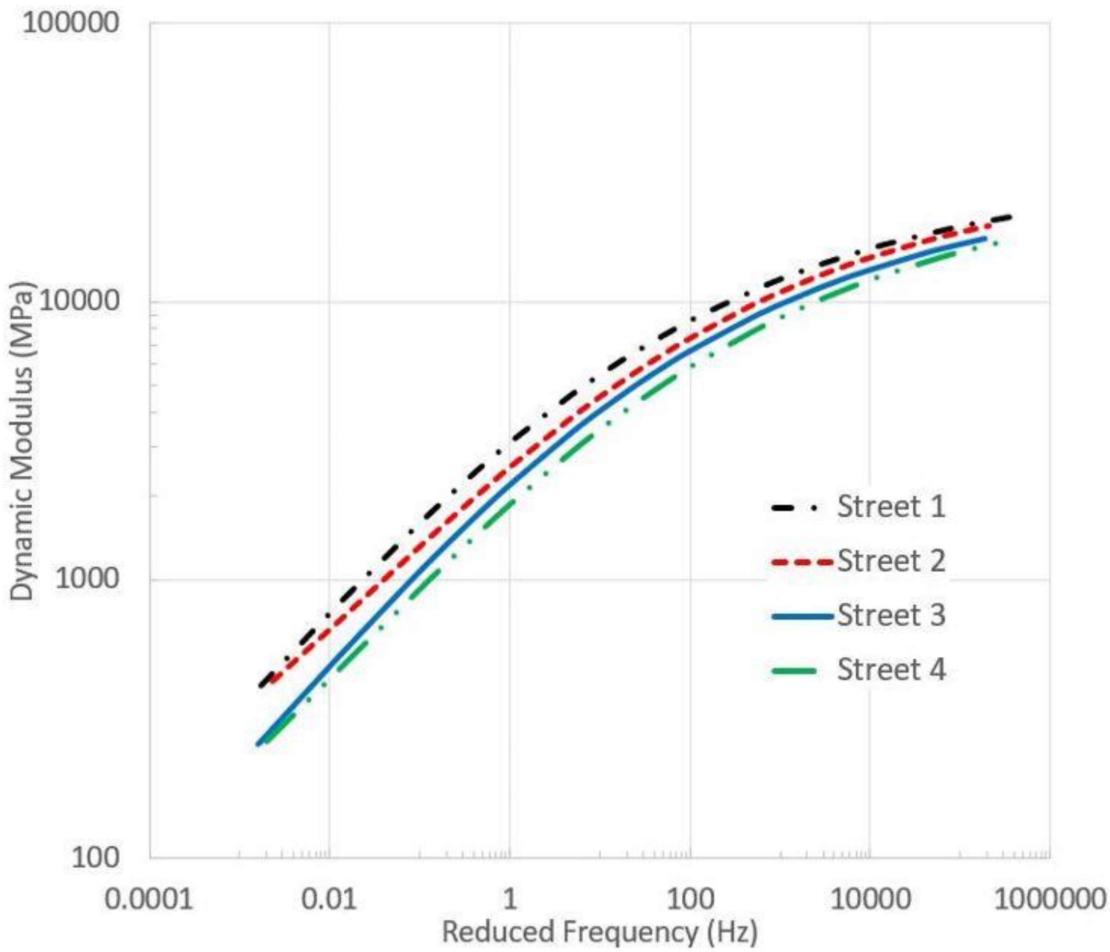

Figure 6.4 Dynamic modulus master curves of in-service asphalt mixtures

6.6 Correlation Between HWTT and Dynamic Modulus Values

DMT test results were used to rank the four in-service asphalt mixtures with respect to their rutting performance by comparing their average dynamic modulus values at high temperature (37.8°C) and low frequency (0.1 Hz). Since HWTT test was conducted at high temperature (45°C), DMT test rankings were also compared with HWTT test rankings according to the average value of three test output parameters including RRI, number of passes to failure and creep slope. Other HWTT test output parameters including stripping slope and number of passes to SIP were omitted because not all samples had experienced moisture damage. Table 6.5 compares four rankings of the in-service asphalt mixture groups (N.B.: the average value of RRI, number of passes to failure, and creep slope for street 2 is the value of an individual sample tested in the HWTT test).

Table 6.5 HWTT and DMT tests rankings of in-service asphalt mixtures

Street number	Rutting (37.8ºC, 0.1 Hz)		Rutting Resistance Index (RRI)		Number of passes to failure		Creep Slope	
	$\lvert E^*\rvert$ (MPa)	Rank[1]	Average	Rank[1]	Average	Rank[1]	Average (mm/pass)	Rank[1]
Street 1	438.31	2	13,363	2	35,844	2	0.000210	2
Street 2	452.40	1	15,717	1	55,350	1	0.000163	1
Street 3	271.08	4	11,304	3	28,459	3	0.000314	3
Street 4	275.31	3	8,393	4	30,363	4	0.000567	4

1. "1" indicates the best performance and "4" indicates the weakest performance.

Table 6.5 shows same rankings among the three HWTT test output parameters as well as they exhibit a good correlation with DMT test rankings. This encourages the application of small-scale specimens to predict rutting performance of in-service asphalt mixtures. Despite the inverted ranking of streets 3 and 4 under DMT test, the average dynamic modulus values of streets 3 and 4 are similar to a high degree which suggests that rutting performance using the DMT test can only be distinguished if mixtures have significant differences between their dynamic modulus values. In other words, the ranking of these two streets can readily change if the dynamic modulus values of more than two samples were averaged in each mixture group. Moreover, the sample that failed the rutting test imposed the weakest performance for street 4 among the three HWTT test output parameters. Nevertheless, if a larger number of samples from street 4 were tested in the HWTT test, the results might prove anomaly of the sample that had poor rutting performance and alter the ranking of streets 3 and 4. In conclusion, HWTT and DMT tests rankings had a good correlation regardless of the exact ranking of streets 3 and 4. To confirm this outcome, the strength of correlation of dynamic modulus values at high temperature was determined via linear regression analysis with the three HWTT test output parameters. The coefficients of determination (R^2) between $\lvert E^*\rvert_{37.8°C}$ values and RRI, number of passes to failure as well as creep slope were measured at all frequencies. Table 6.6 shows the calculated R^2 values for the three conditions.

Table 6.6 Correlation between DM values and HWTT test output parameters

Parameter	R^2 at DMT test frequencies of 37.8°C					
	0.1 Hz	0.5 Hz	1.0 Hz	5.0 Hz	10 Hz	25 Hz
Rutting Resistance Index	0.78	0.74	0.67	0.64	0.62	0.65
Number of passes to failure	0.64	0.57	0.37	0.31	0.29	0.30
Creep Slope	0.65	0.64	0.67	0.66	0.66	0.69

Table 6.6 shows that R^2 values for RRI and creep slope parameters are greater than 0.5 indicating a medium to strong correlation at all frequencies. This means that creep slope showed good potential in predicting rutting performance prior to stripping. R^2 values for number of passes to failure showed medium correlation at 0.1 Hz and 0.5 Hz only, while it showed weak correlation at higher frequencies between 1.0 Hz and 25 Hz. Both RRI and number of passes to failure are the two most critical parameters in determining rutting performance of asphalt mixtures in the HWTT test and both parameters had stronger correlation with DMT test results at lower frequencies with the highest R^2 value observed at 0.1 Hz. This suggests that $|E^*|_{37.8°C}$ values at lower frequencies (particularly 0.1 Hz) have good potential to assess rutting susceptibility of asphalt mixtures. The HWTT test has a frequency of 0.87 Hz since its wheels travel at a constant speed of 52 passes per 60 seconds. This frequency is closer to lower frequencies in the DMT test; therefore, number of passes to failure and RRI parameters had stronger correlation with $|E^*|_{37.8°C}$ values at lower frequencies (0.1 and 0.5 Hz) in comparison to higher frequencies (5, 10 and 25 Hz). Other studies have also reported a similar trend between $|E^*|_{37.8°C}$ values and the flow number (FN) test (Apeagyei, 2016). The FN test has identical sample size (i.e., a cylinder of 100 mm diameter and 150 mm height) as well as similar test conditions (i.e., applies axial compression to the sample) to DMT test; therefore, it has reported stronger correlations with dynamic modulus values than HWTT test.

6.7 Summary

This chapter concludes that field samples extracted from four different streets in the city of Winnipeg did not produce a specific trend of results in the HWTT and ignition oven tests. The similarities in mix design procedure and properties of materials for road construction projects in the same city as well as exposure to uniform traffic levels and climatic conditions are all factors that did not allow for a diverse outcome. Moreover, rutting is expected to happen early in the pavement service life since asphalt binder oxidizes and stiffens as the pavement ages. Hence, the tested samples might have not represented the actual rutting resistance of the wearing surface as the cores were extracted after 1 – 2 years of service life (i.e., after the pavement surface already became more rut-resistant). In other words, HWTT test results might have showed better rutting performance than that experienced in the field for the initial 1 – 2 years. However, important relationships concerning field samples had still been proved such as strong correlation between HWTT and DMT test results at low frequencies for small-scale specimens. Moreover, performance testing of field samples was proved to be an effective procedure to endorse performance-based specifications developed via laboratory testing on plant-produced mixtures within the same region.

In general, testing in-service mixtures did not show a promising outcome in this study. A collection of field samples extracted from road projects with different mix design properties and materials as well as exposed to variable traffic levels and climatic conditions is recommended to produce a more comparable outcome of field performance testing. Also, rut testing of field cores extracted shortly after the pavement has been opened to traffic might aid in producing test results that are better correlated with field performance.

Chapter 7. Summary, Conclusions, and Recommendations

The main objective of this thesis was to evaluate cracking and rutting performance of asphalt mixtures to validate current volumetric mix design methods as well as to develop strategies for moving towards a more efficient balanced mix design (BMD). To fulfill this objective, the thesis was divided into three separate studies. The summary, objectives, major findings, and conclusions of each study are explained in the following section.

7.1 Summary, Findings and Conclusions

7.1.1 Fractionated RAP Mixtures

The objective of this study was to evaluate cracking and rutting performance of fractionated RAP mixtures that meet current Superpave mix design requirements as well as to assess the eligibility of the method of RAP fractionation in contributing to a more successful BMD. To fulfill this objective, five laboratory-produced asphalt mixtures containing RAP were tested and analyzed. The mixtures consisted of a virgin mix and 10% RAP mix with unprocessed RAP as well as three mixtures with 30%, 40% and 50% coarse RAP. Rutting resistance was evaluated using Hamburg wheel-tracking test (HWTT), cracking resistance was evaluated using Illinois flexibility index test (I-FIT), and stiffness was evaluated using dynamic modulus test (DMT). The findings and conclusions of this study are as follows:

1. All fractionated RAP mixtures did not fulfill the desired rutting test criteria (i.e., minimum 10,000 passes at 12.5 mm rut depth) except the 50% coarse RAP mix. In addition, the 50% coarse RAP mix demonstrated the best moisture performance.
2. Both rutting and moisture resistance showed an increasing trend with higher proportions of RAP.

3. All fractionated RAP mixtures did not fulfill the desired cracking test criteria (i.e., minimum flexibility index of 8). Furthermore, RAP mixtures had higher cracking potential than the virgin mix and the 50% coarse RAP mix demonstrated the least cracking resistance.
4. Both 30% and 40% coarse RAP mixes had better cracking performance than the 10% unprocessed RAP mix which proves that RAP fractionation can be a successful tool to increase RAP usage in hot-mix asphalt mixtures while mitigating the negative impact of higher RAP proportions on cracking performance.
5. DMT test results had stronger correlation with I-FIT test results than with HWTT test results due to higher variability of DM values at higher temperatures as well as different testing conditions between HWTT test and DMT test.
6. Fractionated RAP mixtures showed improvements in at least one performance measure in comparison to virgin and unprocessed RAP mixtures. Therefore, it is worthwhile to consider RAP fractionation in hot-mix asphalt design and construction.

7.1.2 Plant-Produced Mixtures

The objective of this study was to evaluate cracking and rutting performance as well as aging resistance of plant-produced asphalt mixtures and to develop local preliminary threshold criteria for cracking and rutting performance tests. To fulfill this objective, six plant-produced mixtures containing different mix design properties were tested and analyzed. The mixtures included virgin materials, RAP and RAS, straight and polymer-modified binders as well as gradations with different nominal maximum aggregate size (NMAS). Rutting resistance was evaluated using the HWTT test, cracking resistance was evaluated using the I-FIT test, and stiffness was evaluated using the DMT test. HWTT and I-FIT test results were plotted on a performance space diagram to investigate parameters that optimized both cracking and rutting performance. The findings and conclusions of this study are as follows:

1. HWTT test results proved that reduction of NMAS, incorporation of RAP and/or RAS as well as use of polymer-modified binders are all significant strategies that improve rutting performance.
2. HWTT test criteria were divided based on NMAS and use of straight or polymer-modified asphalt binder. Mixtures with 19 mm NMAS and/or straight binder were assigned a preliminary criteria of maximum 10 mm rut depth at 15,000 passes, whereas mixtures with 12.5 mm NMAS and/or polymer-modified binder were assigned a preliminary criteria of maximum 10 mm rut depth at 20,000 passes. According to these criteria, only one mix with 19 mm NMAS failed to fulfill the minimum requirements.
3. I-FIT test results proved that increase in NMAS, decrease in asphalt content, incorporation of RAS, and use of limestone aggregate are all significant strategies that reduce cracking performance.
4. I-FIT test results of short-term and long-term aged specimens proved that incorporation of RAP and/or RAS as well as use of stiffer virgin binders with higher temperature PG grade are two significant strategies that improve aging resistance, whereas use of limestone aggregate mitigates aging resistance.
5. Preliminary I-FIT test criteria for short-term aged specimens was minimum flexibility index of 10.5, whereas preliminary I-FIT test criteria for long-term aged specimens was minimum flexibility index of 7.0. According to these criteria, four mixtures failed to fulfill the minimum requirements. These mixtures were either 19 mm NMAS mixtures or mixtures containing limestone aggregates and/or RAS.

6. DMT test results had stronger correlation with I-FIT test results than with HWTT test results due to different testing conditions between HWTT test and DMT test.
7. The performance space diagram proved that designing 12.5 mm NMAS mixtures with low or no RAP content is the best strategy to optimize the BMD. On the other hand, including RAS or limestone aggregates in the asphalt mix design as well as increasing NMAS or decreasing asphalt content might not lead to a successful BMD.

7.1.3 In-Service Mixtures

The objective of this study was to evaluate performance of in-service asphalt mixtures to investigate the probable causes of early-age deterioration in the city of Winnipeg. To fulfill this objective, in-service asphalt cores were extracted from four regional streets near pavement defect areas and their performance was tested and analyzed. Rutting resistance was evaluated using the HWTT test and stiffness was evaluated using the DMT test. The findings and conclusions of this study are as follows:

1. Bulk specific gravity values correlated well with the outcome of field inspection, where the street that experienced most rutting had the least density value and vice versa.
2. Ignition oven test results were sensitive to the fine portion of mix gradation; however, similarities in material properties (such as type of aggregate and asphalt binder) for the four in-service mixtures had led to lack of variability in time-temperature series of ignition oven test.
3. HWTT test results did not correlate well with the outcome of field inspection which means that visible rutting on the pavement surface does not necessarily indicate improper mix design of the hot-mix asphalt layer. Other reasons including inadequate compaction or replacement of the subgrade layer should also be taken into consideration. In addition,

exposure of the four in-service mixtures to consistent field conditions (such as traffic volume and climate) did not allow for a diverse outcome among HWTT test results.

4. HWTT test results of in-service mixtures validated the local preliminary HWTT test criteria developed for plant-produced mixtures since the criteria was capable of distinguishing between acceptable and unacceptable rutting performance in the field.
5. DMT test results of the four in-service mixtures represented a rational outcome of field performance in which streets demonstrating better rutting resistance were expected to have lower cracking resistance.
6. Small-scale specimens showed a high capability of evaluating dynamic modulus and rutting resistance of in-service mixtures since DMT test results had strong correlation with HWTT test results.

7.2 Recommendations

Based on the results of the three studies included in this thesis, the following are recommendations for future research and practical applications:

1. Most of the mixtures included in the fractionated RAP and plant-produced mixtures studies did not fulfill both acceptable cracking and rutting requirements simultaneously. This shows the limitations that the volumetric mix design procedure has in evaluating performance of asphalt mixtures. Therefore, it is recommended to implement practical and appropriate performance tests in current mix design procedures as well as quality control (QC) and quality assurance (QA) activities. Also, it is recommended to integrate suitable performance tests criteria to End Results Specification for acceptance of various asphalt mix designs.

2. It is recommended to consider RAP fractionation as a suitable practice for all hot-mix asphalt mixtures that include high proportions of RAP.
3. It is recommended to evaluate in-service (i.e., field) performance of roadways constructed by plant-produced mixtures investigated in this study. This will help to compare laboratory and field performance of these mixtures as well as to validate preliminary performance tests criteria established in this study.
4. Plant-produced mixtures were investigated to establish preliminary performance tests criteria. Also, it is recommended to investigate laboratory-produced mixtures to establish preliminary performance tests criteria. This will help to determine the impact of production variability on volumetric mix design procedure as well as performance test results.
5. Fractionated RAP study deduced that inability of mixtures to fulfill cracking and rutting requirements could be attributed to unsatisfactory Bailey method evaluation. In addition, plant-produced mixtures study deduced that NMAS is an influential mix design parameter on both cracking and rutting performance. Consequently, it is recommended to conduct further research to investigate the impact of gradation on performance test results of asphalt mixtures.
6. It is recommended to conduct further research to investigate the impact of other types of asphalt mixtures on performance test results. Other types of mixtures include warm-mix asphalt and stone mastic asphalt mixtures as well as mixtures with high RAP contents, fibers, recycling agents and/or anti-stripping additives. This will help acquire knowledge about other parameters that are susceptible to mix performance and to modify preliminary cracking and rutting tests criteria for BMD application.

7. Asphalt pavements in Manitoba might be susceptible to thermal cracking since low temperatures may reach -30°C during winter months. Therefore, it is recommended to assess thermal cracking performance of mixes using practical and feasible thermal cracking tests (such as disc-shaped compact tension test and creep compliance test) as well as to develop criteria for these tests and include them in BMD applications.
8. It is recommended to include other cracking and rutting tests (such as semi-circular bend test, flow number test, etc.) in the performance assessment of asphalt mixtures as well as to verify correlations between these tests results. This will help identify ideal cracking and rutting tests for establishment of the BMD approach.
9. It is recommended to investigate the influence of other lab-simulated aging conditions on cracking performance of asphalt mixtures and correlate the results with actual in-service cracking performance. Other lab-simulated aging conditions include aging loose mixes instead of compacted specimens or using a different combination of time and temperature during oven-heating. This will help integrate the ideal long-term aging protocol to cracking tests in BMD applications.
10. During inspection of in-service performance, it is recommended to carefully identify the root cause of rutting of severely rutted pavements to decide the appropriate action of repair. Also, it is recommended to extract field cores from streets with variable materials and mix design properties as well as exposed to inconsistent traffic volumes and climatic conditions to verify and expand the findings of in-service performance testing.

References

AASHTO PP 62-10 (2012). Developing Dynamic Modulus Master Curves for Hot Mix Asphalt (HMA). American Association of State Highway and Transportation Officials, Washington, D.C.

AASHTO R 30 (2022). Standard Practice for Laboratory Conditioning of Asphalt Mixtures. American Association of State Highway and Transportation Officials, Washington, D.C.

AASHTO R 35 (2022). Standard Practice for Superpave Volumetric Design for Asphalt Mixtures. American Association of State Highway and Transportation Officials, Washington, D.C.

AASHTO T 27 (2023). Standard Method of Test for Sieve Analysis of Fine and Coarse Aggregates. American Association of State Highway and Transportation Officials, Washington, D.C.

AASHTO T 84 (2022). Standard Method of Test for Specific Gravity and Absorption of Fine Aggregate. American Association of State Highway and Transportation Officials, Washington, D.C.

AASHTO T 85 (2022). Standard Method of Test for Specific Gravity and Absorption of Coarse Aggregate. American Association of State Highway and Transportation Officials, Washington, D.C.

AASHTO T 166 (2022). Standard Method of Test for Bulk Specific Gravity (Gmb) of Compacted Asphalt Mixtures Using Saturated Surface-Dry Specimens. American Association of State Highway and Transportation Officials, Washington, D.C.

AASHTO T 308 (2022). Standard Method of Test for Determining the Asphalt Binder Content of Asphalt Mixtures by the Ignition Method. American Association of State Highway and Transportation Officials, Washington, D.C.

AASHTO T 312 (2019). Standard Method of Test for Preparing and Determining the Density of Asphalt Mixture Specimens by Means of the Superpave Gyratory Compactor. American Association of State Highway and Transportation Officials, Washington, D.C.

AASHTO T 324 (2023). Standard Method of Test for Hamburg Wheel-Track Testing of Compacted Asphalt Mixtures. American Association of State Highway and Transportation Officials, Washington, D.C.

AASHTO T 342 (2022). Standard Method of Test for Determining Dynamic Modulus of Hot Mix Asphalt (HMA). American Association of State Highway and Transportation Officials, Washington, D.C.

AASHTO T 393 (2021). Determining the Fracture Potential of Asphalt Mixtures Using the Illinois Flexibility Index Test (I-FIT). American Association of State Highway and Transportation Officials, Washington, D.C.

Al-Qadi, I. L., Aurangzeb, Q., Carpenter, S. H., Pine, W. J., and Trepanier, J. (2012). Impact of High RAP Content on Structural and Performance Properties of Asphalt Mixtures. Research Report FHWA-ICT-12-002, Illinois Center for Transportation, Rantoul, IL.

Al-Qadi, I. L., Carpenter, S. H., Roberts, G. L., Ozer, H., and Aurangzeb, Q. (2009). Investigation of Working Binder in Hot-Mix Asphalt Containing Recycled Asphalt Pavements. Paper No. 09-1262, presented at the 88th Annual Meeting of the Transportation Research Board, Washington, D.C.

Al-Qadi, I. L., Ozer, H., Lambros, J., El Khatib, A., Singhvi, P., Khan, T., Rivera-Perez, J., and Doll, B. (2015). Testing Protocols to Ensure Performance of High Asphalt Binder Replacement Mixes Using RAP and RAS. Research Report FHWA-ICT-15-017, Illinois Center for Transportation, Rantoul, IL.

Apeagyei, A. K. (2016). Correlating Rutting with Dynamic Modulus of Asphalt Concrete. Proceedings of the Institution of Civil Engineers - Transport, Volume 164, Issue 4, 241–249. https://doi.org/10.1680/tran.9.00056

Arshad, A. K., Awang, H., Shaffie, E., Hashim, W., and Abd Rahman, Z. (2018). Performance Evaluation of Hot Mix Asphalt with Different Proportions of RAP Content. International Conference on Civil & Environmental Engineering, E3S Web of Conferences, Article No. 01026, Volume 34. https://doi.org/10.1051/e3sconf/20183401026

Baghaee Moghaddam, T. (2019). Development of High Modulus Asphalt Concrete Mix Design Technology for Use on Ontario's Highways. UWSpace. http://hdl.handle.net/10012/14323

Brown, E. R., Kandhal, P. S., Roberts, F. L., Kim, Y. R., Lee, D. Y., and Kennedy, T. W. (2009). Hot Mix Asphalt Materials, Mixture Design, and Construction. NAPA Research and Education Foundation. 3rd edition, Lanham, Maryland, 318-321.

Brown, E. R., Murphy, N. E., Yu, L., and Mager, S. (1995). Historical Development of Asphalt Content Determination by the Ignition Method. National Center for Asphalt Technology (NCAT) Report No. 95-2.

Cao, P., Jin, F., Zhou, C., Feng, D., and Song, W. (2016). Steady-State Dynamic Method: An Efficient and Effective Way to Predict Dynamic Modulus of Asphalt Concrete. Construction and Building Materials, 111, 54-62. https://doi.org/10.1016/j.conbuildmat.2016.02.071

City of Winnipeg (2020). Asphaltic Concrete Pavement Works. Specification CW 3410 – R12, December.

Coleri, E., Sreedhar, S., and Obaid, I. A. (2020). Development of a Balanced Mix Design Method in Oregon. Research Report FHWA-OR-RD-21-03, Oregon State University, Corvallis, OR.

Copeland, A. (2011). Reclaimed Asphalt Pavement in Asphalt Mixtures: State of the Practice. Research Report FHWA-HRT-11-021, Office of Infrastructure Research and Development, McLean, VA.

Faheem, A., Abboud, B., Coe, J., and Alsalihi, M. (2018). Effect of Warm Mix Asphalt (WMA) Low Mixing and Compaction Temperatures on Recycled Asphalt Pavement (RAP) Binder Replacement. Research Report FHWA-PA-2018-002-TEM WO 008, Temple University, Philadelphia, PA.

Federal Highway Administration (2016). Balanced Mix Design Task Force Update of Activities. Slide presentation at Asphalt Expert Task Group Meeting, Salt Lake City, UT.

Gottumukkala, B., Kusam, S. R., Tandon, V., and Muppireddy, A. R. (2018). Estimation of Blending of Rap Binder in a Recycled Asphalt Pavement Mix. Journal of Materials in Civil Engineering, Volume 30, Issue 8. https://doi.org/10.1061/(ASCE)MT.1943-5533.0002403

Grobler, J., Rebbechi, J., and Denneman, E. (2018). National Performance-Based Asphalt Specification Framework, Austroads.

Han, S., Cheng, X., Liu, Y., and Zhang, Y. (2019). Laboratory Performance of Hot Mix Asphalt with High Reclaimed Asphalt Pavement (RAP) and Fine Reclaimed Asphalt Pavement (FRAP) Content. Materials, 12, 2536. DOI: 10.3390/ma12162536

Hill, B. (2011). Performance Evaluation of Warm Mix Asphalt Mixtures Incorporating Reclaimed Asphalt Pavement. M.Sc. Thesis, University of Illinois at Urbana-Champaign, Urbana, IL.

Hossain, M., Musty, H. Y., and Sabahfer, N. (2012). Use of High-Volume Reclaimed Asphalt Pavement for Asphalt Pavement Rehabilitation Due to Increased Highway Truck Traffic from Freight Transportation. Research Report 25-1121-0001-452, Mid-America

Transportation Center, University of Nebraska, Lincoln, NE.

Huang, B., Li, G., Vukosavljevic, D., Shu, X., and Egan, B. K. (2005). Laboratory Investigation of Mixing Hot-Mix Asphalt with Reclaimed Asphalt Pavement. Transportation Research Record: Journal of the Transportation Research Board, Volume 1929, Issue 1, 37-45. https://doi.org/10.1177/0361198105192900105

Kadhim, H. (2019). Improving Durability of Asphalt Mixes Produced with Reclaimed Asphalt Pavement (RAP) by Enhancing Binder Blending. Ph.D. Thesis, University of Waterloo, Waterloo, Ontario, Canada.

Kafi Farashah, M. (2023). Development of Sustainable Asphalt Mix Solution for Use in Approach Intersection Pavements in Southern Ontario. Ph.D. Thesis, University of Waterloo, Waterloo, Ontario, Canada.

Kalcheff, I. V., and Tunnicliff, D. G. (1982). Effects of Crushed Stone Aggregate Size and Shape on Properties of Asphalt Concrete. Proceedings of Association of Asphalt Paving Technologists, Volume 51, pp. 453-483.

Kandhal, S. P., and Mallick, B. R. (1997). Pavement Recycling Guidelines for State and Local Governments: Participant's Reference Book. Research Report FHWA-SA-98-042, National Center for Asphalt Technology at Auburn University, Auburn, AL.

Kandhal, S. P., and Mallick, B. R. (2001). Effect of Mix Gradation on Rutting Potential of Dense-Graded Asphalt Mixtures. Transportation Research Record: Journal of the Transportation Research Board, Volume 1767, Issue 1, 146-151. https://doi.org/10.3141/1767-18

Kim, S., Sholar, G. A., Byron, T., and Kim, J. (2009). Performance of Polymer-Modified Asphalt Mixture with Reclaimed Asphalt Pavement. Transportation Research Record: Journal of the Transportation Research Board, Volume 2126, Issue 1, 109-114.

https://doi.org/10.3141/2126-13

Lachance, A. M. (2006). Properties of Asphalt Mixtures Containing RAP. M.Sc. Thesis, University of New Hampshire, Durham, NH.

Li, X., Marasteanu, M. O., Williams, R. C., and Clyne, T. R. (2008). Effect of Reclaimed Asphalt Pavement (Proportion and Type) and Binder Grade on Asphalt Mixtures. Transportation Research Record: Journal of the Transportation Research Board, Volume 2051, Issue 1, 90-97. https://doi.org/10.3141/2051-11

LS-292 (2001). Method of Test for Quantitative Determination of Asphalt Cement Content by Ignition and Analysis of Remaining Aggregate from Bituminous Paving Mixtures. Laboratory Testing Manual, Rev. No. 24, Ministry of Transportation, Ontario, Canada.

Lu, D. X., Saleh, M., and Nguyen, N. H. T. (2019). Effect of Rejuvenator and Mixing Methods on Behaviour of Warm Mix Asphalt Containing High RAP Content. Construction and Building Materials, 197, 792-802. https://doi.org/10.1016/j.conbuildmat.2018.11.205

Mahboub, K., and Little, D. N. (1988). Improved Asphalt Concrete Design Procedure. Research Report 474-1F, Texas Transportation Institute, Texas A&M University, College Station, TX.

McDaniel, R. (2011). Blending Charts and High RAP Mixes. Slide presentation at Kansas Asphalt Forum, Topeka, KS.

McDaniel, R., and Anderson, R. M. (2001). Recommended Use of Reclaimed Asphalt Pavement in the Superpave Mix Design Method: Technician’s Manual. NCHRP Report 452, Transportation Research Board, National Research Council, National Academy Press, Washington, D.C.

Mohammad, L. N., Kim, M., and Challa, H. (2016). Development of Performance-based

Specifications for Louisiana Asphalt Mixtures. Research Report FHWA/LA.14/558, Louisiana State University, Baton Rouge, LA.

Newcomb, D., and Zhou, F. (2018). Balanced Design of Asphalt Mixtures. Research Report MN/RC 2018-22, Texas A&M Transportation Institute, College Station, TX.

Noorvand, H., Brockman, S. C., Mamlouk, M., and Kaloush, K. (2021). Effect of Aramid Fibers on Balanced Mix Design of Asphalt Concrete. CivilEng, 3(1), 21-34. https://doi.org/10.3390/civileng3010002

Ozer, H., Al-Qadi, I. L., Lambros, J., El-Khatib, A., Singhvi, P., and Doll, B. (2016). Development of the Fracture-Based Flexibility Index for Asphalt Concrete Cracking Potential Using Modified Semi-Circle Bending Test Parameters. Construction and Building Materials, 115, 390-401. https://doi.org/10.1016/j.conbuildmat.2016.03.144

Rahman, F., and Hossain, M. (2014). Review and Analysis of Hamburg Wheel Tracking Device Test Data. Research Report KS-14-1, Kansas State University Transportation Center, Manhattan, KS.

Ramli, I., Yaacob, H., Abdul Hassan, N., Ismail, C. R., and Hainin, M. R. (2013). Fine Aggregate Angularity Effects on Rutting Resistance of Asphalt Mixture. Jurnal Teknologi (Science & Engineering), 65(3), 105-109. DOI: 10.11113/jt.v65.2154

Salehi-Ashani, S. (2021). Development of Performance-Related Specifications for Asphalt Mixtures in Ontario. Ph.D. Thesis, University of Waterloo, Waterloo, Ontario, Canada.

Saliani, S. S., Carter, A., Baaj, H., and Tavassoti, P. (2019). Characterization of Asphalt Mixtures Produced with Coarse and Fine Recycled Asphalt Particles. Infrastructures, Volume 4, 67. https://doi.org/10.3390/infrastructures4040067

Schram, S., and Williams, R. C. (2012). Ranking of HMA Moisture Sensitivity Tests in Iowa.

Research Report RB00-012, Iowa Department of Transportation, Ames, IA.

Shah, A., McDaniel, R., Huber, G. A., and Gallivan, V. L. (2007). Investigation of Properties of Plant-Produced Reclaimed Asphalt Pavement Mixtures. Transportation Research Record: Journal of the Transportation Research Board, Volume 1998, Issue 1, 103-111. https://doi.org/10.3141/1998-13

Shannon, C. P. (2012). Fractionation of Recycled Asphalt Pavement Materials: Improvement of Volumetric Mix Design Criteria for High-RAP Content Surface Mixtures. M.Sc. Thesis, The University of Iowa, Iowa City, IA. DOI: 10.17077/etd.cr5iux3w

Solaimanian, M., and Tahmoressi, M. (1996). Variability Analysis of Hot-Mix Asphalt Concrete Containing High Percentage of Reclaimed Asphalt Pavement. Transportation Research Record: Journal of the Transportation Research Board, Volume 1543, Issue 1, 89–96. https://doi.org/10.1177/0361198196154300111

Soleymani, H. R., McDaniel, R., and Abdelrahman, M. (2000). Investigation of the Black Rock Issue for Recycled Asphalt Mixtures. Proceedings of the Association of Asphalt Paving Technologists Annual Meeting, Volume 69, 366-390, Association of Asphalt Paving Technologists (AAPT), Reno, NV.

Tavassoti, P., and Baaj, H. (2020). Moisture Damage in Asphalt Concrete Mixtures: State of the Art and Critical Review of the Test Methods. Soils and Materials Session, Transportation Association of Canada (TAC) Conference.

Uzan, J. (2003). Characterization of Asphalt Concrete Materials for Permanent Deformation. International Journal of Pavement Engineering, Volume 4, Issue 2, 77–86. https://doi.org/10.1080/10298430310001593272

Varamini, S. (2016). Technical, Economic, and Environmental Evaluation of Warm Mix Asphalt and Coloured Asphalt for Usage in Canada. Ph.D. Thesis, University of Waterloo, Waterloo, Ontario, Canada.

Vavrik, W. R., Huber, G., Pine, W. J., Carpenter, S. H., and Bailey, R. (2002). Bailey Method for Gradation Selection in Hot-Mix Asphalt Mixture Design. Research Report Number E-C044, Transportation Research Circular, Transportation Research Board of the National Academies.

West, R. (2015). Best Practices for RAP and RAS Management. Research Report QIP 129, National Asphalt Pavement Association, Lanham, MD.

West, R., Kvasnak, A., Tran, N., Powell, B., and Turner, P. (2009). Testing of Moderate and High Reclaimed Asphalt Pavement Content Mixes: Laboratory and Accelerated Field Performance Testing at the National Center for Asphalt Technology Test Track. Transportation Research Record: Journal of the Transportation Research Board, Volume 2126, Issue 1, 100-108. https://doi.org/10.3141/2126-12

West, R., Rodezno, C., Leiva, F., and Taylor, A. (2018). Regressing Air Voids for Balanced HMA Mix Design. Research Report WHRP 0092-16-06, National Center for Asphalt Technology at Auburn University, Auburn, AL.

West, R., Rodezno, C., Leiva, F., and Yin, F. (2018). Development of a Framework for Balanced Mix Design. Final Report to the National Cooperative Highway Research Program (NCHRP), Project 20-07, Task 406.

West, R., Willis, J. R., and Marasteanu, M. (2013). Improved Mix Design, Evaluation, and Materials Management Practices for Hot Mix Asphalt with High Reclaimed Asphalt Pavement Content. NCHRP Report 752, Transportation Research Board, Washington, D.C.

Willis, J. R., Turner, P., Padula, F., Tran, N., and Julian, G. (2013). Effects of Changing Virgin Binder Grade and Content on High Reclaimed Asphalt Pavement Mixture Properties. Transportation Research Record: Journal of the Transportation Research Board, Volume 2371, Issue 1, 66-73. https://doi.org/10.3141/2371-08

Xiao, F., Amirkhanian, S., and Juang, C. H. (2007). Rutting Resistance of Rubberized Asphalt Concrete Pavements Containing Reclaimed Asphalt Pavement Mixtures. Journal of Materials in Civil Engineering, Volume 19, Issue 6, pp. 475–483. https://doi.org/10.1061/(ASCE)0899-1561(2007)19:6(475)

Yin, F., Chen, C., West, R., Martin, A. E., and Arambula-Mercado, E. (2020). Determining the Relationship among Hamburg Wheel-Tracking Test Parameters and Correlation to Field Performance of Asphalt Pavements. Transportation Research Record: Journal of the Transportation Research Board, Volume 2674, Issue 4, 281-291. https://doi.org/10.1177/0361198120912430

Zaumanis, M., and Mallick, R. B. (2015). Review of Very High-Content Reclaimed Asphalt Use in Plant-Produced Pavements: State of the Art. International Journal of Pavement Engineering, Volume 16, Issue 1, 39-55. https://doi.org/10.1080/10298436.2014.893331

Zhao, S., Huang, B., Shu, X., and Woods, M. E. (2015). Quantitative Characterization of Binder Blending: How Much Recycled Binder is Mobilized During Mixing? Transportation Research Record: Journal of the Transportation Research Board, Volume 2506, Issue 1, 72-80. https://doi.org/10.3141/2506-08

Zhou, F. (2017). Development of an IDEAL Cracking Test for Asphalt Mix Design and QC/QA. The Association of Asphalt Pavement Technologists, 86, 549-578.

Zhou, F., Button, J. W., and Epps, J. A. (2012). Best Practice of Using RAS in HMA. Research

Report FHWA/TX-12/0-6614-1, Texas Transportation Institute, Texas A&M University, College Station, TX.

Zhou, F., Sheng, H., and Scullion, T. (2006). Integrated Asphalt (Overlay) Mixture Design, Balancing Rutting and Cracking Requirements. Research Report FHWA/TX-06/0-5123-1, Texas Transportation Institute, Texas A&M University, College Station, TX.

Appendix A

Table A-1 I-FIT test output parameters of specimens in virgin mix group

Specimen	I-FIT test output parameter					
	Flexibility Index	Fracture Energy (J/m^2)	Post-Peak Slope	Critical Displacement (mm)	Tensile Strength (Psi)	Peak Load (KN)
1	5.93	1422.20	2.40	2.72	46.35	2.35
2	6.18	1680.11	2.72	2.18	61.07	3.05
3	6.73	1499.89	2.23	2.33	53.73	2.64
4	4.51	1348.04	2.99	2.03	57.32	2.82
5	5.53	1486.59	2.69	2.25	55.51	2.83
6	3.95	1148.81	2.91	2.12	53.85	2.67
7	7.51	1607.40	2.14	2.40	53.79	2.69
8	4.07	1098.63	2.70	1.90	50.04	2.51

Table A-2 I-FIT test output parameters of specimens in 10% RAP mix group

Specimen	I-FIT test output parameter					
	Flexibility Index	Fracture Energy (J/m^2)	Post-Peak Slope	Critical Displacement (mm)	Tensile Strength (Psi)	Peak Load (KN)
1	1.42	1018.59	7.17	1.26	67.87	3.48
2	1.54	1198.88	7.80	1.32	77.96	3.99
3	1.30	1256.87	9.68	1.29	81.53	4.10
4	2.44	1201.31	4.92	1.55	69.24	3.51
5	1.87	1191.07	6.36	1.41	71.54	3.61
6	1.56	1179.70	7.56	1.35	77.31	3.89
7	1.28	753.62	5.90	1.32	74.23	3.75
8	1.70	1152.32	6.76	1.21	78.91	3.96

Table A-3 I-FIT test output parameters of specimens in 30% coarse RAP mix group

Specimen	I-FIT test output parameter					
	Flexibility Index	Fracture Energy (J/m^2)	Post-Peak Slope	Critical Displacement (mm)	Tensile Strength (Psi)	Peak Load (KN)
1	2.79	1351.06	4.85	1.80	69.80	3.54
2	4.88	1751.53	3.59	1.99	69.89	3.49
3	2.72	1262.03	4.64	1.63	67.01	3.35
4	2.95	1388.60	4.70	1.68	68.63	3.40
5	1.58	1452.36	9.22	1.54	79.75	3.96
6	2.61	1568.47	6.01	1.91	76.09	3.80
7	2.05	1400.52	6.84	1.58	73.33	3.73
8	3.11	1342.34	4.32	1.71	67.84	3.44

Table A-4 I-FIT test output parameters of specimens in 40% coarse RAP mix group

Specimen	I-FIT test output parameter					
	Flexibility Index	Fracture Energy (J/m^2)	Post-Peak Slope	Critical Displacement (mm)	Tensile Strength (Psi)	Peak Load (KN)
1	3.07	1223.42	3.99	1.96	61.44	3.09
2	3.30	1448.00	4.39	1.78	71.43	3.66
3	3.49	1388.99	3.98	1.74	67.89	3.38
4	2.40	1375.29	5.72	1.61	73.13	3.71
5	2.82	1315.35	4.66	1.65	63.94	3.20
6	1.32	745.13	5.65	1.59	71.09	3.46
7	2.96	1498.35	5.06	1.72	73.35	3.72
8	3.61	1558.24	4.32	1.90	73.88	3.68

Table A-5 I-FIT test output parameters of specimens in 50% coarse RAP mix group

Specimen	I-FIT test output parameter					
	Flexibility Index	Fracture Energy (J/m^2)	Post-Peak Slope	Critical Displacement (mm)	Tensile Strength (Psi)	Peak Load (KN)
1	1.16	1172.68	10.08	1.27	79.47	3.98
2	1.15	1361.89	11.85	1.34	86.82	4.43
3	1.08	1222.29	11.30	1.15	86.41	4.34
4	1.27	1197.78	9.46	1.27	82.97	4.05
5	1.71	1319.10	7.70	1.35	84.24	4.32
6	1.71	1202.46	7.05	1.32	75.57	3.84
7	2.54	1515.62	5.97	1.63	84.76	4.28
8	2.01	1417.78	7.06	1.53	80.40	4.03

Table A-6 Dynamic modulus values of samples in virgin mix group

Temperature (°C)	Dynamic Modulus of Sample 1 (MPa)					
	0.1 Hz	0.5 Hz	1.0 Hz	5.0 Hz	10 Hz	25 Hz
-10	11611.0	14403.0	15482.0	17771.0	18384.0	18865.0
4.4	4218.00	5970.70	6933.60	9438.60	10481.0	11716.0
21.1	1305.20	1910.00	2309.80	3816.30	4437.50	5696.60
37.8	502.660	651.610	783.000	1270.80	1541.60	1864.70
Temperature (°C)	Dynamic Modulus of Sample 2 (MPa)					
	0.1 Hz	0.5 Hz	1.0 Hz	5.0 Hz	10 Hz	25 Hz
-10	9420.70	11730.0	12588.0	14831.0	15667.0	16393.0
4.4	3698.70	5188.50	5994.50	8126.50	9013.30	10204.0
21.1	1204.00	1752.20	2116.30	3495.00	4091.40	4963.60
37.8	433.520	580.450	693.970	1090.70	1381.10	1835.90

Table A-7 Dynamic modulus values of samples in 10% RAP mix group

Temperature (°C)	Dynamic Modulus of Sample 1 (MPa)					
	0.1 Hz	0.5 Hz	1.0 Hz	5.0 Hz	10 Hz	25 Hz
-10	17185.0	20274.0	21409.0	24088.0	24978.0	26089.0
4.4	6714.60	9157.20	10270.0	13110.0	14199.0	15487.0
21.1	2628.20	3605.20	4019.00	5763.00	6486.40	7899.50
37.8	671.750	1030.10	1283.50	2115.70	2613.90	3612.20
Temperature (°C)	Dynamic Modulus of Sample 2 (MPa)					
	0.1 Hz	0.5 Hz	1.0 Hz	5.0 Hz	10 Hz	25 Hz
-10	13294.0	16222.0	17286.0	19953.0	20700.0	21654.0
4.4	5607.10	7773.50	8756.20	11297.0	12368.0	13456.0
21.1	2386.60	3331.70	3593.20	5172.00	6096.80	7523.00
37.8	542.670	798.900	971.030	1605.10	1997.50	2711.50

Table A-8 Dynamic modulus values of samples in 30% coarse RAP mix group

Temperature (°C)	Dynamic Modulus of Sample 1 (MPa)					
	0.1 Hz	0.5 Hz	1.0 Hz	5.0 Hz	10 Hz	25 Hz
-10	15390.0	18514.0	19717.0	22513.0	23376.0	24248.0
4.4	6129.40	8417.00	9501.10	12227.0	13330.0	14748.0
21.1	2468.00	3463.60	4063.80	5837.60	6636.30	7716.30
37.8	947.590	1269.50	1392.50	2121.00	2575.40	3220.50
Temperature (°C)	Dynamic Modulus of Sample 2 (MPa)					
	0.1 Hz	0.5 Hz	1.0 Hz	5.0 Hz	10 Hz	25 Hz
-10	11700.0	13945.0	14750.0	16863.0	17623.0	18306.0
4.4	5412.70	7464.90	8287.30	10624.0	11558.0	12725.0
21.1	2164.70	2971.00	3481.90	5046.10	5725.60	6768.60
37.8	767.080	991.750	1171.50	1760.10	2104.30	2680.20

Table A-9 Dynamic modulus values of samples in 40% coarse RAP mix group

Temperature (°C)	Dynamic Modulus of Sample 1 (MPa)					
	0.1 Hz	0.5 Hz	1.0 Hz	5.0 Hz	10 Hz	25 Hz
-10	14178.0	16998.0	18085.0	20536.0	21231.0	22249.0
4.4	5730.70	7944.60	9044.10	11673.0	12732.0	14161.0
21.1	2013.60	2846.80	3349.00	4942.90	5842.70	6882.10
37.8	555.850	838.120	1009.00	1632.00	2020.90	2689.00
Temperature (°C)	Dynamic Modulus of Sample 2 (MPa)					
	0.1 Hz	0.5 Hz	1.0 Hz	5.0 Hz	10 Hz	25 Hz
-10	13083.0	15851.0	17011.0	19493.0	20640.0	21528.0
4.4	5768.30	7897.60	8893.60	11376.0	12080.0	12499.0
21.1	1897.70	2876.00	3371.60	4942.30	5532.40	6695.30
37.8	489.840	748.810	908.830	1521.70	1860.20	2320.90

Table A-10 Dynamic modulus values of samples in 50% coarse RAP mix group

Temperature (°C)	Dynamic Modulus of Sample 1 (MPa)					
	0.1 Hz	0.5 Hz	1.0 Hz	5.0 Hz	10 Hz	25 Hz
-10	19447.0	22798.0	23967.0	25271.0	27156.0	28589.0
4.4	8569.20	11274.0	12497.0	15293.0	16524.0	18031.0
21.1	3898.60	5347.00	5968.00	8247.20	9358.40	10662.0
37.8	812.820	1256.70	1587.10	2552.60	3175.00	3848.90
Temperature (°C)	Dynamic Modulus of Sample 2 (MPa)					
	0.1 Hz	0.5 Hz	1.0 Hz	5.0 Hz	10 Hz	25 Hz
-10	16457.0	19137.0	20258.0	22790.0	23745.0	24373.0
4.4	8279.50	10909.0	12038.0	14795.0	15806.0	17321.0
21.1	2814.50	4030.40	4726.40	6712.80	7758.40	8917.30
37.8	869.520	1278.00	1588.30	2633.50	3241.30	3981.30

Appendix B

Table B-1 I-FIT test output parameters of long-term aged samples of Mix 1 (19, 58, 0, 0)

Specimen	I-FIT test output parameter					
	Flexibility Index	Fracture Energy (J/m^2)	Post-Peak Slope	Critical Displacement (mm)	Tensile Strength (Psi)	Peak Load (KN)
1	6.64	1594.59	2.40	2.64	51.77	2.54
2	6.49	1459.52	2.25	2.33	49.06	2.40
3	5.07	1176.47	2.32	2.21	46.17	2.40
4	4.72	1504.42	3.19	2.27	54.99	2.83

Table B-2 I-FIT test output parameters of long-term aged samples of Mix 2 (12.5, 58 P, 0, 0)

Specimen	I-FIT test output parameter					
	Flexibility Index	Fracture Energy (J/m^2)	Post-Peak Slope	Critical Displacement (mm)	Tensile Strength (Psi)	Peak Load (KN)
1	10.36	1491.79	1.44	3.00	40.69	2.03
2	7.64	1481.77	1.94	3.06	46.44	2.32
3	8.91	1380.63	1.55	2.98	39.74	2.05
4	7.49	1340.77	1.79	2.73	42.96	2.24

Table B-3 I-FIT test output parameters of long-term aged samples of Mix 3 (12.5, 64 P, 10, 0)

Specimen	I-FIT test output parameter					
	Flexibility Index	Fracture Energy (J/m^2)	Post-Peak Slope	Critical Displacement (mm)	Tensile Strength (Psi)	Peak Load (KN)
1	11.81	2090.30	1.77	3.22	56.73	2.82
2	8.39	1862.98	2.22	2.74	58.92	2.99
3	8.78	1950.13	2.22	2.86	60.70	3.01
4	6.73	1831.80	2.72	2.58	59.37	3.03

Table B-4 I-FIT test output parameters of long-term aged samples of Mix 4 (12.5, 64 P, 10, 3)

Specimen	I-FIT test output parameter					
	Flexibility Index	Fracture Energy (J/m^2)	Post-Peak Slope	Critical Displacement (mm)	Tensile Strength (Psi)	Peak Load (KN)
1	4.39	1772.33	4.04	2.12	71.09	3.72
2	3.78	1820.25	4.82	2.14	75.52	3.90
3	3.13	1879.27	6.00	2.12	77.45	3.95
4	5.01	2088.06	4.17	2.51	73.49	3.72

Table B-5 I-FIT test output parameters of long-term aged samples of Mix 5 (19, 58, 0, 0)

Specimen	I-FIT test output parameter					
	Flexibility Index	Fracture Energy (J/m^2)	Post-Peak Slope	Critical Displacement (mm)	Tensile Strength (Psi)	Peak Load (KN)
1	2.06	1358.96	6.61	1.61	73.00	3.76
2	1.91	1143.97	5.98	1.44	72.42	3.77
3	2.15	1259.27	5.85	1.49	73.43	3.70
4	1.19	1159.35	9.73	1.26	73.26	3.76

Table B-6 I-FIT test output parameters of long-term aged samples of Mix 6 (12.5, 58 P, 0, 0)

Specimen	I-FIT test output parameter					
	Flexibility Index	Fracture Energy (J/m^2)	Post-Peak Slope	Critical Displacement (mm)	Tensile Strength (Psi)	Peak Load (KN)
1	3.14	1407.98	4.48	1.73	73.08	3.73
2	3.50	1653.22	4.72	1.86	77.07	3.87
3	2.94	1515.98	5.16	1.78	74.09	3.78
4	1.34	1240.54	9.24	1.40	74.97	3.80

Table B-7 I-FIT test output parameters of short-term aged samples of Mix 1 (19, 58, 0, 0)

Specimen	I-FIT test output parameter					
	Flexibility Index	Fracture Energy (J/m^2)	Post-Peak Slope	Critical Displacement (mm)	Tensile Strength (Psi)	Peak Load (KN)
1	6.55	1145.83	1.75	2.66	35.80	1.86
2	10.37	1379.23	1.33	3.19	36.43	1.88
3	11.98	1617.02	1.35	3.21	42.14	2.13
4	9.34	1167.04	1.25	2.88	33.30	1.68

Table B-8 I-FIT test output parameters of short-term aged samples of Mix 2 (12.5, 58 P, 0, 0)

Specimen	I-FIT test output parameter					
	Flexibility Index	Fracture Energy (J/m^2)	Post-Peak Slope	Critical Displacement (mm)	Tensile Strength (Psi)	Peak Load (KN)
1	13.93	1574.31	1.13	3.75	35.48	1.79
2	22.32	1740.72	0.78	4.17	34.01	1.65
3	16.51	1469.15	0.89	3.78	33.33	1.68
4	22.68	1655.60	0.73	4.13	34.09	1.67

Table B-9 I-FIT test output parameters of short-term aged samples of Mix 3 (12.5, 64 P, 10, 0)

Specimen	I-FIT test output parameter					
	Flexibility Index	Fracture Energy (J/m^2)	Post-Peak Slope	Critical Displacement (mm)	Tensile Strength (Psi)	Peak Load (KN)
1	18.76	1970.14	1.05	3.87	42.98	2.12
2	11.79	1897.41	1.61	3.42	45.31	2.32
3	10.65	1799.46	1.69	3.32	46.50	2.32
4	13.32	1892.10	1.42	3.40	47.00	2.39

Table B-10 I-FIT test output parameters of short-term aged samples of Mix 4 (12.5, 64 P, 10, 3)

Specimen	I-FIT test output parameter					
	Flexibility Index	Fracture Energy (J/m^2)	Post-Peak Slope	Critical Displacement (mm)	Tensile Strength (Psi)	Peak Load (KN)
1	7.75	1875.04	2.42	2.86	56.02	2.83
2	8.39	1752.66	2.09	2.89	54.80	2.77
3	5.78	1571.79	2.72	2.40	55.68	2.85
4	7.03	1701.91	2.42	2.63	54.64	2.78

Table B-11 I-FIT test output parameters of short-term aged samples of Mix 5 (19, 58, 0, 0)

Specimen	I-FIT test output parameter					
	Flexibility Index	Fracture Energy (J/m^2)	Post-Peak Slope	Critical Displacement (mm)	Tensile Strength (Psi)	Peak Load (KN)
1	6.68	1517.26	2.27	2.41	53.77	2.71
2	4.85	1674.54	3.45	2.24	61.08	3.08
3	4.64	1364.49	2.94	1.94	58.90	2.93
4	5.98	1476.45	2.47	2.23	55.47	2.79

Table B-12 I-FIT test output parameters of short-term aged samples of Mix 6 (12.5, 58 P, 0, 0)

Specimen	I-FIT test output parameter					
	Flexibility Index	Fracture Energy (J/m^2)	Post-Peak Slope	Critical Displacement (mm)	Tensile Strength (Psi)	Peak Load (KN)
1	4.75	1367.84	2.88	2.06	54.25	2.81
2	4.07	1517.80	3.73	1.98	67.46	3.45
3	4.60	1541.90	3.35	2.17	63.30	3.28
4	12.48	4543.06	3.64	1.87	58.97	3.06

Table B-13 Aging rates based on ascending order of flexibility index values

Mix	Flexibility Index (FI) in ascending order		Aging rate (%)
	Short-term aging	Long-term aging	
Mix 1 (19, 58, 0, 0)	6.55	4.72	27.94
	9.34	5.07	45.72
	10.37	6.49	37.42
	11.98	6.64	44.57
Mix 2 (12.5, 58 P, 0, 0)	13.93	7.49	46.23
	16.51	7.64	53.73
	22.32	8.91	60.08
	22.68	10.36	54.32
Mix 3 (12.5, 64 P, 10, 0)	10.65	6.73	36.81
	11.79	8.39	28.84
	13.32	8.78	34.08
	18.76	11.81	37.05
Mix 4 (12.5, 64 P, 10, 3)	5.78	3.13	45.85
	7.03	3.78	46.23
	7.75	4.39	43.35
	8.39	5.01	40.29
Mix 5 (19, 58, 0, 0)	4.64	1.19	74.35
	4.85	1.91	60.62
	5.98	2.06	65.55
	6.68	2.15	67.81
Mix 6 (12.5, 58 P, 0, 0)	4.07	1.34	67.08
	4.60	2.94	36.09
	4.75	3.14	33.89
	12.48	3.50	71.96

Table B-14 Dynamic modulus values of samples of Mix 1 (19, 58, 0, 0)

Temperature	Dynamic Modulus of Sample 1 (MPa)					
(°C)	0.1 Hz	0.5 Hz	1.0 Hz	5.0 Hz	10 Hz	25 Hz
-10	8521.40	11112.0	12272.0	15056.0	16027.0	17411.0
4.4	3342.70	4643.50	5351.90	7447.00	8679.50	10005.0
21.1	1020.70	1472.00	1713.50	2665.40	3186.80	3967.90
37.8	338.080	450.990	522.810	801.360	1007.30	1320.50
Temperature	Dynamic Modulus of Sample 2 (MPa)					
(°C)	0.1 Hz	0.5 Hz	1.0 Hz	5.0 Hz	10 Hz	25 Hz
-10	8491.10	11260.0	12476.0	15445.0	16475.0	18000.0
4.4	3302.10	4642.50	5381.80	7533.20	8539.30	9893.60
21.1	994.950	1416.80	1694.10	2597.60	3093.90	3932.50
37.8	343.250	458.210	533.380	818.030	1042.90	1428.20
Temperature	Dynamic Modulus of Sample 3 (MPa)					
(°C)	0.1 Hz	0.5 Hz	1.0 Hz	5.0 Hz	10 Hz	25 Hz
-10	9693.50	12792.0	14211.0	17441.0	18989.0	20853.0
4.4	3938.10	5614.60	6526.30	9037.60	10390.0	12020.0
21.1	1107.20	1583.50	1896.80	2931.20	3441.20	4248.20
37.8	383.230	511.030	597.660	915.590	1204.10	1622.00

Table B-15 Dynamic modulus values of samples of Mix 2 (12.5, 58 P, 0, 0)

Temperature	Dynamic Modulus of Sample 1 (MPa)					
(°C)	0.1 Hz	0.5 Hz	1.0 Hz	5.0 Hz	10 Hz	25 Hz
-10	7170.30	9913.10	11242.0	14752.0	16301.0	18145.0
4.4	1964.40	3129.60	3843.10	6152.50	7369.50	8961.40
21.1	449.900	711.900	890.910	1575.70	2071.40	3035.30
37.8	220.510	293.710	337.750	505.940	685.720	1018.20
Temperature	Dynamic Modulus of Sample 2 (MPa)					
(°C)	0.1 Hz	0.5 Hz	1.0 Hz	5.0 Hz	10 Hz	25 Hz
-10	8079.60	11122.0	12506.0	16252.0	17748.0	19358.0
4.4	2313.30	3675.20	4543.40	7134.60	8441.10	9917.10
21.1	507.830	803.200	995.090	1768.10	2271.60	3253.30
37.8	245.610	324.670	368.990	540.570	734.510	1086.90
Temperature	Dynamic Modulus of Sample 3 (MPa)					
(°C)	0.1 Hz	0.5 Hz	1.0 Hz	5.0 Hz	10 Hz	25 Hz
-10	8922.80	12314.0	13938.0	18022.0	19614.0	21667.0
4.4	2589.80	4195.60	5173.80	8012.10	9506.10	11263.0
21.1	580.470	924.950	1169.40	2118.00	2805.70	3857.90
37.8	264.670	354.040	405.440	608.680	831.980	1222.80

Table B-16 Dynamic modulus values of samples of Mix 3 (12.5, 64 P, 10, 0)

Temperature (°C)	Dynamic Modulus of Sample 1 (MPa)					
	0.1 Hz	0.5 Hz	1.0 Hz	5.0 Hz	10 Hz	25 Hz
-10	11011.0	14517.0	15841.0	19261.0	20697.0	21637.0
4.4	3439.30	5056.70	5935.30	8668.10	9747.00	11193.0
21.1	838.800	1226.20	1496.50	2534.60	3124.80	4240.70
37.8	311.620	415.570	487.640	798.320	1032.10	1416.60
Temperature (°C)	Dynamic Modulus of Sample 2 (MPa)					
	0.1 Hz	0.5 Hz	1.0 Hz	5.0 Hz	10 Hz	25 Hz
-10	12424.0	16200.0	17913.0	21678.0	23144.0	24970.0
4.4	3902.70	5632.20	6577.60	9418.40	10671.0	11946.0
21.1	865.020	1291.90	1595.90	2736.90	3517.90	4553.60
37.8	397.750	525.740	608.060	955.000	1247.10	1715.80
Temperature (°C)	Dynamic Modulus of Sample 3 (MPa)					
	0.1 Hz	0.5 Hz	1.0 Hz	5.0 Hz	10 Hz	25 Hz
-10	11679.0	15235.0	16773.0	20378.0	21758.0	23579.0
4.4	3667.60	5413.20	6374.00	9124.80	10281.0	12002.0
21.1	815.130	1166.20	1418.40	2388.80	2967.20	3666.30
37.8	352.570	464.970	550.440	873.610	1134.80	1631.80

Table B-17 Dynamic modulus values of samples of Mix 4 (12.5, 64 P, 10, 3)

Temperature (°C)	Dynamic Modulus of Sample 1 (MPa)					
	0.1 Hz	0.5 Hz	1.0 Hz	5.0 Hz	10 Hz	25 Hz
-10	12606.0	16151.0	17761.0	21202.0	22751.0	24586.0
4.4	4383.40	6273.00	7305.90	10155.0	11388.0	12930.0
21.1	910.260	1402.70	1741.50	2957.10	3753.90	4860.20
37.8	310.490	449.310	553.510	952.750	1210.10	1636.90
Temperature (°C)	Dynamic Modulus of Sample 2 (MPa)					
	0.1 Hz	0.5 Hz	1.0 Hz	5.0 Hz	10 Hz	25 Hz
-10	12999.0	16486.0	17975.0	21439.0	22885.0	24894.0
4.4	4505.40	6333.60	7334.60	10037.0	11170.0	12838.0
21.1	1022.80	1731.00	2128.30	3442.70	4138.10	5108.50
37.8	334.160	482.340	592.070	1032.30	1361.40	1718.20
Temperature (°C)	Dynamic Modulus of Sample 3 (MPa)					
	0.1 Hz	0.5 Hz	1.0 Hz	5.0 Hz	10 Hz	25 Hz
-10	11461.0	14865.0	16333.0	19676.0	21103.0	22663.0
4.4	3974.30	5647.60	6611.80	9223.60	10477.0	11656.0
21.1	860.450	1318.40	1673.10	2791.80	3441.10	4580.30
37.8	287.180	418.510	518.730	904.050	1185.50	1616.70

Table B-18 Dynamic modulus values of samples of Mix 5 (19, 58, 0, 0)

Temperature	Dynamic Modulus of Sample 1 (MPa)					
(°C)	0.1 Hz	0.5 Hz	1.0 Hz	5.0 Hz	10 Hz	25 Hz
-10	13192.0	16494.0	17983.0	21597.0	22881.0	24112.0
4.4	5876.00	8113.50	9275.30	12349.0	13656.0	15483.0
21.1	1648.10	2437.80	2882.20	4393.00	5083.40	5980.70
37.8	595.630	838.130	979.870	1621.20	2092.00	2781.70
Temperature	Dynamic Modulus of Sample 2 (MPa)					
(°C)	0.1 Hz	0.5 Hz	1.0 Hz	5.0 Hz	10 Hz	25 Hz
-10	13943.0	17410.0	18991.0	22737.0	24114.0	26000.0
4.4	6200.60	8594.40	9870.40	13188.0	14611.0	16585.0
21.1	1858.80	2814.20	3413.60	5311.80	6329.40	7876.60
37.8	637.990	915.950	1118.10	1841.10	2378.60	3168.10
Temperature	Dynamic Modulus of Sample 3 (MPa)					
(°C)	0.1 Hz	0.5 Hz	1.0 Hz	5.0 Hz	10 Hz	25 Hz
-10	13328.0	17018.0	18688.0	22605.0	24245.0	26283.0
4.4	5955.90	8261.60	9519.30	12769.0	14315.0	16055.0
21.1	1836.10	2779.30	3367.60	5287.30	6417.10	7912.70
37.8	613.770	851.070	1019.30	1656.10	2108.10	2914.60

Table B-19 Dynamic modulus values of samples of Mix 6 (12.5, 58 P, 0, 0)

Temperature	Dynamic Modulus of Sample 1 (MPa)					
(°C)	0.1 Hz	0.5 Hz	1.0 Hz	5.0 Hz	10 Hz	25 Hz
-10	11704.0	14950.0	16476.0	20124.0	21642.0	23513.0
4.4	5220.10	7255.40	8365.90	11366.0	12794.0	14603.0
21.1	1634.30	2393.20	2877.40	4450.00	5309.90	6664.90
37.8	534.430	768.570	911.050	1426.50	1815.80	2436.30
Temperature	Dynamic Modulus of Sample 2 (MPa)					
(°C)	0.1 Hz	0.5 Hz	1.0 Hz	5.0 Hz	10 Hz	25 Hz
-10	13711.0	17224.0	18796.0	22715.0	24436.0	26636.0
4.4	6374.60	8818.00	10131.0	13524.0	15113.0	17457.0
21.1	1982.50	2866.50	3402.20	5179.20	6091.00	7347.70
37.8	790.710	1095.90	1260.60	1931.30	2342.10	3128.90
Temperature	Dynamic Modulus of Sample 3 (MPa)					
(°C)	0.1 Hz	0.5 Hz	1.0 Hz	5.0 Hz	10 Hz	25 Hz
-10	12342.0	15637.0	17114.0	20781.0	22295.0	24144.0
4.4	5488.10	7479.00	8545.10	11503.0	12884.0	14439.0
21.1	1675.00	2471.00	3006.80	4674.70	5535.60	6909.40
37.8	678.940	969.050	1142.20	1780.30	2202.90	2959.10

Appendix C

Table C-1 Bulk specific gravity procedure of field cores from street 1

Parameter	Core 1	Core 2
Oven-dry weight (g)	1763.3	1809.0
Saturated surface-dry weight (g)	1766.3	1823.9
Submerged weight in water (g)	1000.0	973.80
Bulk specific gravity (G_{sb})	2.301	2.128

Table C-2 Bulk specific gravity procedure of field cores from street 2

Parameter	Core 1	Core 2
Oven-dry weight (g)	1630.7	2032.0
Saturated surface-dry weight (g)	1633.5	2037.5
Submerged weight in water (g)	914.50	1150.9
Bulk specific gravity (G_{sb})	2.268	2.292

Table C-3 Bulk specific gravity procedure of field core from street 3

Parameter	Core 1
Oven-dry weight (g)	2088.0
Saturated surface-dry weight (g)	2090.0
Submerged weight in water (g)	1152.0
Bulk specific gravity (G_{sb})	2.226

Table C-4 Bulk specific gravity procedure of field cores from street 4

Parameter	Core 1	Core 2
Oven-dry weight (g)	1816.7	1771.3
Saturated surface-dry weight (g)	1823.5	1774.9
Submerged weight in water (g)	999.00	1003.0
Bulk specific gravity (G_{sb})	2.203	2.295

Table C-5 Ignition oven test procedure of sample from street 1

Parameter	Sample 1
Weight of empty ignition basket (g)	3008.0
Weight of ignition basket + initial sample (g)	5408.0
Weight of initial sample (g)	2400.0
Weight of ignition basket + remaining sample (g)	5246.4
Weight of remaining sample (g)	2238.4
Asphalt content (%)	6.73

Table C-6 Ignition oven test procedure of sample from street 2

Parameter	Sample 1
Weight of empty ignition basket (g)	3007.4
Weight of ignition basket + initial sample (g)	5407.4
Weight of initial sample (g)	2400.0
Weight of ignition basket + remaining sample (g)	5237.0
Weight of remaining sample (g)	2229.6
Asphalt content (%)	7.10

Table C-7 Ignition oven test procedure of sample from street 3

Parameter	Sample 1
Weight of empty ignition basket (g)	3064.6
Weight of ignition basket + initial sample (g)	5464.6
Weight of initial sample (g)	2400.0
Weight of ignition basket + remaining sample (g)	5298.0
Weight of remaining sample (g)	2233.4
Asphalt content (%)	6.94

Table C-8 Ignition oven test procedure of sample from street 4

Parameter	Sample 1
Weight of empty ignition basket (g)	3064.9
Weight of ignition basket + initial sample (g)	5464.9
Weight of initial sample (g)	2400.0
Weight of ignition basket + remaining sample (g)	5283.6
Weight of remaining sample (g)	2218.7
Asphalt content (%)	7.55

Table C-9 Sieve analysis procedure of sample from street 1

Sieve size (mm)	Weight of sieve + aggregate retained (g)	Weight of empty sieve (g)	Aggregate retained (g)	Aggregate retained (%)	Cumulative aggregate retained (%)	Percent passing
19	1396.20	1396.20	0	0	0	100
16	1373.10	1364.10	9.00	0.40	0.40	99.60
12.5	1490.20	1345.50	144.70	6.48	6.89	93.11
9.5	1678.90	1340.80	338.10	15.15	22.03	77.97
4.75	1678.60	1280.90	397.70	17.82	39.85	60.15
2.00	1585.70	1197.50	388.20	17.39	57.24	42.76
0.425	1586.30	986.20	600.10	26.88	84.12	15.88
0.180	1081.20	904.30	176.90	7.92	92.04	7.96
0.075	963.50	897.90	65.60	2.94	94.98	5.02
Pan	985.90	873.90	112.00	5.02	100	0
Total	–	–	2232.30	–	–	–

Table C-10 Sieve analysis procedure of sample from street 2

Sieve size (mm)	Weight of sieve + aggregate retained (g)	Weight of empty sieve (g)	Aggregate retained (g)	Aggregate retained (%)	Cumulative aggregate retained (%)	Percent passing
19	1396.30	1396.30	0	0	0	100
16	1365.50	1365.50	0	0	0	100
12.5	1504.10	1346.10	158.00	7.10	7.10	92.90
9.5	1582.90	1340.40	242.50	10.90	18.01	81.99
4.75	1705.20	12820	423.20	19.03	37.04	62.96
2.00	1460.80	1196.70	264.10	11.88	48.91	51.09
0.425	1598.10	986.70	611.40	27.49	76.41	23.59
0.180	1245.10	905.40	339.70	15.27	91.68	8.32
0.075	971.80	898.20	73.60	3.31	94.99	5.01
Pan	984.80	873.40	111.40	5.01	100	0
Total	–	–	2223.90	–	–	–

Table C-11 Sieve analysis procedure of sample from street 3

Sieve size (mm)	Weight of sieve + aggregate retained (g)	Weight of empty sieve (g)	Aggregate retained (g)	Aggregate retained (%)	Cumulative aggregate retained (%)	Percent passing
19	1395.70	1395.70	0	0	0	100
16	1365.30	1365.30	0	0	0	100
12.5	1456.70	1347.00	109.70	4.92	4.92	95.08
9.5	1658.90	1341.20	317.70	14.25	19.17	80.83
4.75	1624.30	1280.90	343.40	15.40	34.57	65.43
2.00	1482.70	1198.40	284.30	12.75	47.32	52.68
0.425	1723.30	986.90	736.40	33.03	80.34	19.66
0.180	1160.70	905.30	255.40	11.45	91.80	8.20
0.075	970.50	897.50	73.00	3.27	95.07	4.93
Pan	983.00	873.10	109.90	4.93	100	0
Total	–	–	2229.80	–	–	–

Table C-12 Sieve analysis procedure of sample from street 4

Sieve size (mm)	Weight of sieve + aggregate retained (g)	Weight of empty sieve (g)	Aggregate retained (g)	Aggregate retained (%)	Cumulative aggregate retained (%)	Percent passing
19	1396.80	1396.80	0	0	0	100
16	1365.60	1365.60	0	0	0	100
12.5	1485.30	1346.30	139.00	6.27	6.27	93.73
9.5	1545.30	1341.20	204.10	9.21	15.47	84.53
4.75	1715.10	1281.30	433.80	19.57	35.04	64.96
2.00	1467.60	1198.80	268.80	12.12	47.16	52.84
0.425	1604.70	987.30	617.40	27.85	75.01	24.99
0.180	1245.40	905.70	339.70	15.32	90.33	9.67
0.075	986.10	898.20	87.90	3.96	94.29	5.71
Pan	1000.50	874.00	126.50	5.71	100	0
Total	–	–	2217.20	–	–	–

Table C-13 Dynamic modulus values of samples from street 1

Temperature	Dynamic Modulus of Sample 1 (MPa)					
(°C)	0.1 Hz	0.5 Hz	1.0 Hz	5.0 Hz	10 Hz	25 Hz
-10	14635.0	17282.0	18415.0	20921.0	21772.0	22984.0
4.4	7026.70	9427.30	10512.0	13212.0	14003.0	15734.0
21.1	2089.80	3128.30	3761.90	5595.50	6545.50	7716.90
37.8	558.980	878.470	1138.90	1909.50	2491.00	3233.20
Temperature	Dynamic Modulus of Sample 2 (MPa)					
(°C)	0.1 Hz	0.5 Hz	1.0 Hz	5.0 Hz	10 Hz	25 Hz
-10	11022.0	13361.0	14320.0	16520.0	17185.0	18219.0
4.4	4707.90	6500.00	7386.60	9655.40	10602.0	11777.0
21.1	1257.60	1953.40	2395.10	3740.70	4434.90	5363.50
37.8	317.640	464.330	618.010	1115.10	1449.70	1986.60

Table C-14 Dynamic modulus values of samples from street 2

Temperature	Dynamic Modulus of Sample 1 (MPa)					
(°C)	0.1 Hz	0.5 Hz	1.0 Hz	5.0 Hz	10 Hz	25 Hz
-10	9774.10	12142.0	13118.0	15606.0	16588.0	17446.0
4.4	4462.20	6004.40	6763.30	9076.30	9909.20	11004.0
21.1	1469.80	2164.00	2565.80	3971.20	4694.70	5591.60
37.8	539.940	774.300	890.850	1471.10	1867.50	2434.30
Temperature	Dynamic Modulus of Sample 2 (MPa)					
(°C)	0.1 Hz	0.5 Hz	1.0 Hz	5.0 Hz	10 Hz	25 Hz
-10	11646.0	14197.0	15278.0	17983.0	18905.0	20090.0
4.4	4588.20	6420.10	7378.70	9876.10	10961.0	12356.0
21.1	1264.50	1974.80	2419.00	3832.60	4593.20	5704.40
37.8	364.850	561.490	695.060	1174.50	1570.80	2203.50

Table C-15 Dynamic modulus values of samples from street 3

Temperature	Dynamic Modulus of Sample 1 (MPa)					
(°C)	0.1 Hz	0.5 Hz	1.0 Hz	5.0 Hz	10 Hz	25 Hz
-10	9512.20	11624.0	12444.0	14478.0	15170.0	16010.0
4.4	3552.00	5000.60	5727.20	7710.50	8506.30	9445.60
21.1	974.730	1535.50	1895.00	3033.00	3562.30	4380.00
37.8	233.060	367.480	507.180	876.720	1188.10	1678.30
Temperature	Dynamic Modulus of Sample 2 (MPa)					
(°C)	0.1 Hz	0.5 Hz	1.0 Hz	5.0 Hz	10 Hz	25 Hz
-10	9605.40	11416.0	12622.0	15520.0	16639.0	18183.0
4.4	4594.00	6357.80	7256.60	9545.40	10524.0	11722.0
21.1	1252.90	1981.20	2426.10	3882.90	4623.90	5660.20
37.8	309.100	477.880	600.600	1021.90	1383.60	1902.50

Table C-16 Dynamic modulus values of samples from street 4

Temperature (°C)	Dynamic Modulus of Sample 1 (MPa)					
	0.1 Hz	0.5 Hz	1.0 Hz	5.0 Hz	10 Hz	25 Hz
-10	6750.90	8422.60	9242.60	11264.0	12018.0	12941.0
4.4	2319.20	3254.40	3766.10	5277.00	5922.50	6644.40
21.1	693.920	1063.10	1314.40	2068.30	2476.90	3074.90
37.8	210.230	334.600	394.230	650.900	876.270	1296.30

Temperature (°C)	Dynamic Modulus of Sample 2 (MPa)					
	0.1 Hz	0.5 Hz	1.0 Hz	5.0 Hz	10 Hz	25 Hz
-10	11759.0	14353.0	15381.0	18053.0	18984.0	20058.0
4.4	4838.50	6825.80	7812.70	10370.0	11557.0	12852.0
21.1	1237.10	1956.70	2401.40	3919.50	4690.50	5660.40
37.8	340.390	527.410	646.870	1100.90	1487.70	1970.90